RICE UNIVERSITY

Re-Engineering the alkanolamine absorption process to economize carbon capture

by

Sumedh Warudkar

A Thesis Submitted
in Partial Fulfillment of the
Requirements for the Degree

Doctor of Philosophy

Approved, Thesis Committee:

George J. Hirasaki, Chair
A J. Hartsook Professor in Chemical and Biomolecular Engineering

Michael S. Wong
Professor of Chemical and Biomolecular Engineering and Chemistry

Kenneth R. Cox
Professor in the Practice at Chemical and Biomolecular Engineering

Walter G. Chapman
William W. Akers Professor of Chemical and Biomolecular Engineering

W. Edward Billups
Professor of Chemistry

Houston, Texas
April, 2013

ABSTRACT

Re-Engineering the alkanolamine absorption process to economize carbon capture

by

Sumedh Warudkar

Power plants that burn coal and natural gas to produce electricity generate more than half of global carbon dioxide (CO_2) emissions. Separating the carbon dioxide (CO_2) emitted at these large sources of emission, followed by long term storage has been proposed as short to medium term solution to mitigate climate change. Implementation of this strategy called 'Carbon Capture and Storage' will allow the continued use of fossil fuels while simultaneously reduce our carbon dioxide (CO_2) emissions. Technologies such as the alkanolamine absorption process, used to separate carbon dioxide (CO_2) from gas mixtures already exist and are widely used in the natural gas industry. However, it is presently infeasible to apply them for Carbon Capture and Storage due to their relatively large energy consumption and the associated cost penalties. It is estimated that even with the use of state-of-the-art technology, the cost of electricity will increase by around 90%. The research presented in this thesis is focused on developing strategies to limit the increase in the cost of electricity due to implementation of Carbon Capture and Storage. Specifically, three different approaches have been explored as a part of this research effort. In the first, a process simulation software; ProMax has been used to optimize the alkanolamine absorption process to suit Carbon Capture application. The second approach involves exploring the idea of adding a co-solvent such as an alcohol to reduce the energy consumption of the carbon dioxide (CO_2) removal process. Finally, a novel carbon dioxide (CO_2) separation process involving a combined absorber/desorber unit has been proposed

and demonstrated to work. Combining the absorber and stripper columns can aid in building a more compact process in addition to providing opportunities for heat integration and capital savings.

Acknowledgments

It would be untruthful of me to think or feel that the journey over the past five and half years towards earning my doctorate would have been possible without anyone's help or support. Thus, first and foremost; I would like to express my sincere gratitude to everyone who has been involved with me in any capacity during my time at Rice University.

Several individuals made sacrifices to make it possible for me to attend graduate school. I am deeply indebted to my family; my father, Mr. Shripad Warudkar; my mother, Mrs. Vidya Warudkar; my brother, Mr. Himanshu Warudkar and my sister-in-law, Mrs. Abha Warudkar. I am particularly thankful to my wife, Pooja who has provided me incredible support through this entire journey. She has been the calming influence in my life and backed me to navigate the difficult periods in my research. She has helped me stay firmly rooted to reality through both, the successful and the not-so-successful phases in graduate school.

I have been privileged to be able to learn to conduct scientific research under the guidance of Dr. George J. Hirasaki. His approach to research relies on a careful understanding of the fundamental processes that are responsible for observed phenomena. I have come to realize that this is the *single most important* transferable skill that any graduate student can learn while conducting doctoral research. In addition, Dr. Hirasaki's work ethics and dedication has always motivated me to step out of my comfort zone and take up challenges, be it technical, organizational or physical. I will always be grateful to Dr. Hirasaki for *teaching me to think*.

I would like to acknowledge Dr. Michael S. Wong for co-advising my research.

He has supported me through difficult times, especially during the initial phases of my research. It was he who motivated me to take up the challenge of writing and submitting the research proposal to the US Department of Energy. This eventually resulted in our project being awarded a $1 million award in August 2011.

I would like to thank Dr. Walter G. Chapman, Dr. Kenneth R. Cox and Dr. W. Edward Billups for serving on my doctoral thesis committee.

I would like to sincerely thank every teacher and educator, who in a formal or informal role has taught me something useful and helped me improve myself over the past 27 odd years.

Several students - undergraduate and graduate as well as staff members have been very helpful during the course of my research at Rice University. Ms. Maura Puerto has been of immense help in resolving any technical challenges concerning the design and fabrication of my experimental setups. Dr. Jerimiah Forsythe was helpful in the setup and commissioning of my experimental prototypes. His insights based on his knowledge of chemistry were always useful during technical discussions. Mr. Sriram Chandrasekhar, the Rice University undergraduate student who was doing exploratory research on this project when I joined it, provided a enthusiastic companion in the search for the right materials for this research project. Dr. Michael Rauschhuber, Dr. Neeraj Rohilla, Dr. Sayantan Chatterjee, Dr. Jose Lopez and other members of Dr. Hirasaki and Dr. Wong's research groups have been great individuals for both technical and non-technical discussions concerning research.

Finally, I would like to thank Rice University for offering me the Chemical and Biomolecular Engineering graduate fellowship and the Loewenstern graduate fellowship in Engineering; to the Energy and Environmental Systems Institute at Rice University, Rice University consortium for processes in porous media, Schlumberger Ltd. and the US Department of Energy grant # DE0007531 for funding support.

Contents

Abstract ii

Acknowledgments iv

1 Introduction 1

1.1 Background 1

1.2 Organization 5

2 Climate change and carbon capture and storage 8

2.1 Fossil fuels and climate change 8

2.2 Carbon Capture and Storage 11

2.3 Technologies for Carbon Capture 14

2.3.1 Adsorption 15

2.3.2 Cryogenic separation 17

2.3.3 Membrane separation 18

2.3.4 Absorption 20

2.4 Carbon dioxide (CO_2), compression, storage and monitoring 22

2.5 Challenges with Carbon Capture and Storage 23

3 Amine absorption technology: technical description and current research 26

3.1 Amine absorption technology 26

3.1.1 Original development 26

3.1.2 Modifications for use in carbon capture 34

3.1.3 Remaining challenges 35
3.2 Current research and development 36
3.2.1 Better absorbents 37
3.2.2 Process intensification 40
3.3 Scope for advancing carbon capture research 43
3.4 Direction of our research work 46

4 Effects of variation in stripper operating pressure on the performance of the amine absorption process for carbon capture: a technical perspective 48
4.1 Motivation 48
4.2 Research approach 49
4.2.1 ProMax and amine systems modeling 49
4.2.2 Flowsheet development 52
4.2.3 Evaluating parasitic power loss 57
4.2.4 Process and simulation parameters 61
4.3 Results and analysis 65
4.3.1 Effect of stripper operating pressure on reboiler heat duty . . 65
4.3.2 Effect of stripper operating pressure on column sizing 70
4.3.3 Effect of stripper operating pressure on heat exchanger sizing . 72
4.3.4 Effect of stripper operating pressure on compression duty . . . 74
4.3.5 Effect of stripper operating pressure on parasitic power losses 76
4.4 Concluding Remarks 80

5 Effects of variation in stripper operating pressure on the performance of the amine absorption process for carbon capture: an economic perspective 84
5.1 Motivation 84
5.2 Research approach 85

5.3 Sizing and rating methodology 86
5.3.1 Sizing separation columns 86
5.3.2 Sizing separator vessels 88
5.3.3 Rating heat exchangers 90
5.3.4 Rating Fluid Drivers 94
5.3.5 Generic simulation parameters employed for economic evaluation 96
5.4 Effects of variation in stripper pressure on cost of carbon capture . . 96
5.4.1 Effect of variation in stripper pressure on the cost of amine absorber and stripper 98
5.4.2 Effect of variation in stripper pressure on the cost of lean/rich amine heat exchanger 102
5.4.3 Effect of variation in stripper pressure on the cost of amine reboiler 103
5.4.4 Effect of variation in stripper pressure on the cost of carbon dioxide (CO_2) compression train 105
5.4.5 Effect of variation in stripper pressure on the overall cost of carbon capture plant 106
5.5 Concluding Remarks 111

6 Development of superior absorbents for carbon dioxide (CO_2) removal: emphasizing the role of the solvent 113

6.1 Motivation 113
6.2 Research Approach 115
6.3 Contribution of various constituent physiochemical processes to reboiler duty 117
6.4 Role of the alkanolamine solvent 123
6.5 Estimating the effect of addition of alcohol to alkanolamines on energy consumption 126
6.5.1 A brief review of published literature 126

6.5.2 Approach to estimating reboiler duty 129
6.5.3 General framework for evaluating reboiler duty using equilibrium approach 133
6.5.4 Evaluating reboiler duty for aqueous diethanolamine (DEA) systems 138
6.5.5 Evaluating reboiler duty for aqueous diethanolamine (DEA) blended with methanol 146
6.6 Effect of addition of alcohol on carbon dioxide (CO_2) absorption kinetics 155
6.6.1 Experimental setup for studying reaction kinetics 156
6.6.2 Results and analysis of flow experiments to study carbon dioxide (CO_2) absorption kinetics 158
6.7 Implications of replacing conventional absorbents with alcohol blended aqueous alkanolamines 162
6.8 Concluding Remarks 167

7 Combined pressure and temperature contrast separation of carbon dioxide (CO_2): key concepts & process development 170
7.1 Motivation 170
7.2 Combining the absorber and stripper columns: developing the concept of an integrated unit 171
7.3 Selecting the right material: ceramic foams 174
7.4 Characterizing the hydrodynamic behavior of ceramic foams 181
7.4.1 Experimental setup 182
7.4.2 Experimental procedure 184
7.4.3 Experimental results 185
7.5 Characterizing the mass transfer behavior of ceramic foams 190
7.5.1 Experimental setup 191
7.5.2 Experimental method 193
7.5.3 Experimental results 194

7.6 Experiments to determine design parameters for proof-of-concept demonstration 200
7.6.1 Experimental procedure 201
7.6.2 Experimental results 202
7.7 Concluding Remarks 205
7.7.1 Hydrodynamic studies 205
7.7.2 Mass transfer studies 207

8 Integrating the absorber and stripper units for the separation of carbon dioxide (CO_2): proof of concept demonstration 208
8.1 Development of the experimental prototype 209
8.1.1 Choice of materials 209
8.1.2 Design considerations 211
8.1.3 Setup of experimental prototype 213
8.2 Proof-of-concept demonstration 221
8.2.1 Choice of operating parameters 221
8.2.2 Experimental procedure 225
8.2.3 Experimental results and analysis 228
8.3 Concluding Remarks 238

9 Recommendations for future work 240
9.1 Calibrating the economic feasibility of using waste heat with coal-fired power plant operational data 241
9.2 Development of novel absorbents 241
9.3 Generating thermodynamic data and modeling 242
9.4 Exploring the potential for side reactions between alcohols and amines 244
9.5 Modeling of combined absorber stripper system 246

Appendix A Design sheets for stainless steel prototype and miniature boiler 248

Bibliography **272**

List of Figures

2.1 World energy consumption in Million tonnes of oil equivalent (Mtoe) (2011) [1] 9
2.2 Growth of atmospheric carbon dioxide (CO_2) concentration and global temperature anomaly over roughly the same time period [2, 3, 4] 10
2.3 Global Greenhouse Gas (GHG) abatement cost curve [5] 12
2.4 Schematic representation of Carbon Capture and Storage (CCS) [6] . 13
2.5 Schematic representation of adsorption process for carbon dioxide (CO_2) separation from flue gas [7] 16
2.6 Schematic representation of cryogenic separation process for carbon dioxide (CO_2) separation from flue gas [7] 18
2.7 Schematic representation of membrane separation process for carbon dioxide (CO_2) separation from flue gas [7] 19
2.8 Schematic representation of gas absorption (alkanolamine) separation process for carbon dioxide (CO_2) separation from flue gas [7] 21

3.1 Chemical structure of various commercial alkanolamines 27
3.2 Schematic representation of amine absorption process for natural gas sweetening [8] 28
3.3 Temperature and acid gas removal profiles in an absorber column . . 30
3.4 Temperature and absorbent regeneration profiles in a desorber column 31
3.5 Heat of reaction for 4 different alkanolamines [9, 10] 32
3.6 Reaction rate at 25°C for different alkanolamines [11, 12] 33

4.1 Graphic explanation of model complexity [13] 51
4.2 Flowsheet for the amine absorption process for CO_2 separation with high pressure strippers 53
4.3 Flowsheet for the amine absorption process for CO_2 separation with vacuum strippers 54
4.4 Schematic representation of a steam jet ejector [14] 57
4.5 Flowsheet for the compression of CO_2 separated with amine absorption trains using high pressure strippers 58
4.6 Flowsheet for the compression of CO_2 separated with amine absorption trains using vacuum strippers 58
4.7 Flowsheet for the glycol dehydration unit for conditioning CO_2 before transportation 59
4.8 Electric power equivalence of low pressure steam 60
4.9 Dependence of reboiler energy duty on stripper operating pressure . . 68
4.10 Dependence of absorber diameter on stripper operating pressure . . . 71
4.11 Dependence of stripper diameter on stripper operating pressure . . . 73
4.12 Dependence of CO_2 compression duty on stripper operating pressure . 75
4.13 Dependence of parasitic power losses on stripper operating pressure . 77
4.14 Dependence of parasitic power loss for vacuum strippers on waste heat availability 79

5.1 Dependence of absorber costs on stripper operating pressure 99
5.2 Dependence of stripper costs on stripper operating pressure 100
5.3 Dependence of amine heat exchanger costs on stripper operating pressure 103
5.4 Dependence of amine reboiler costs on stripper operating pressure . . 104
5.5 Dependence of carbon dioxide (CO_2) compression train costs on stripper operating pressure 105

5.6 Dependence of the overall cost of carbon capture plants on stripper operating pressure 107

6.1 Contribution of stripping vapor energy consumption to reboiler heat duty 119
6.2 Lumped contribution of heat of reaction and sensible heating duty to the reboiler heat duty 119
6.3 Ratio of CO_2 to H_2O partial pressures in equilibrium with different alkanolamines ($\alpha = 0.5$ moles-CO_2/mole-amine) 121
6.4 Contribution of physiochemical processes to reboiler duty - (MEA 20 wt%) 121
6.5 Contribution of physiochemical processes to reboiler duty - (DEA 40 wt%) 122
6.6 Contribution of physiochemical processes to reboiler duty - (DGA 60 wt%) 122
6.7 A comparison of the specific heat capacity of water and various alcohols 125
6.8 A comparison of the heat of vaporization of water and various alcohols 125
6.9 A comparison of the equilibrium partial pressure of carbon dioxide (CO_2) above two diethanolamine (DEA) based absorbent formulations at 100°C 128
6.10 Simplified schematic representation of a typical amine absorption unit 133
6.11 Vapor liquid equilibrium data for aqueous diethanolamine (DEA) 34.8 wt% 139
6.12 Vapor liquid equilibrium data for aqueous diethanolamine (DEA) blended with methanol (40:40:20 - wt%) 147
6.13 Experimental setup used to studying the effect of diglycolamine (DGA) solvent on CO_2 absorption kinetics 157

6.14 Degree of CO_2 removal taking place in absorber column with various diglycolamine (DGA) solvents 159
6.15 Dielectric constant of different solvents - water, methanol and ethanol 160
6.16 CO_2 solubility in different solvents - water, methanol and ethanol . . 160
6.17 Kinematic viscosity of various diglycolamine (DGA) absorbents with water, methanol and ethanol as solvents 161
6.18 A comparison of reboiler duty for common aqueous alkanolamines and methanol blended diethanolamine (DEA) 165
6.19 A comparison of parasitic power loss for various amine absorption plant configurations using aqueous diethanolamine (DEA) - with and without methanol 165

7.1 Schematic representation of the novel process with an integrated absorber and stripper 172
7.2 A commercial sample of alumina foam 176
7.3 Different routes to manufacturing ceramic foams [15] 177
7.4 Scanning electron micrographs of a 45 pores per inch (ppi) sample of alumina foam 178
7.5 Pore size distribution in a 45 pore per inch (ppi) sample of alumina foam 179
7.6 Pore size distribution in a 45 pore per inch (ppi) sample of alumina foam 179
7.7 Schematic representation of experimental setup developed for studying hydrodynamic behavior of ceramic foams 182
7.8 Experimental setup for studying the hydrodynamic behavior of ceramic foams 186
7.9 Pressure drop in 45 pores per inch (ppi) ceramic foam at varying gas and liquid flow-rates 187

7.10 Pressure drop in 30 pores per inch (ppi) ceramic foam at varying gas and liquid flow-rates 187
7.11 Pressure drop in 20 pores per inch (ppi) ceramic foam at varying gas and liquid flow-rates 189
7.12 Schematic representation of experimental setup developed for studying mass transfer performance of ceramic foams 192
7.13 Degree of CO_2 pickup with different tower packing (30 wt% DGA, gas at 3 SLPM, liquid at 0.02 LPM) 196
7.14 Degree of CO_2 pickup with different tower packing (30 wt% DGA, gas at 5 SLPM, liquid at 0.04 LPM) 198
7.15 Degree of CO_2 pickup with different tower packing (60 wt% DGA, gas at 3 & 5 SLPM, liquid at 0.02 & 0.04 LPM) 198
7.16 Comparison of CO_2 removal performance under different gas and liquid flow conditions (10.2 cm long ceramic foam column) 203
7.17 Comparison of CO_2 removal performance under different gas and liquid flow conditions (15.2 cm long ceramic foam column) 203
7.18 Comparison of CO_2 removal performance under different gas and liquid flow conditions (20.3 cm long ceramic foam column) 205
7.19 Comparison of CO_2 removal performance under different gas and liquid flow conditions (25.4 cm long ceramic foam column) 206

8.1 Rendering of the stainless steel prototype 214
8.2 An assembly view of the stainless steel prototype 215
8.3 An assembly cross-section view of the stainless steel prototype 216
8.4 Rendering of the miniature steam generator 217
8.5 An assembly view of the miniature steam generator 218
8.6 An assembly cross-section view of the miniature steam generator . . . 219

8.7 Schematic representation of the experimental setup developed for the proof-of-concept demonstration 222
8.8 Photograph of the experimental setup developed for the proof-of-concept demonstration 223
8.9 Degree of CO_2 removal at variable gas flow-rates and absorbent flow-rate of 0.01 liters per minute (LPM) 230
8.10 Dependence of maximum lateral flow-rate of absorbent on pressure difference across absorption and stripping chambers 231
8.11 Degree of CO_2 removal at variable gas flow-rates and absorbent flow-rate of 0.02 liters per minute (LPM) 232
8.12 Degree of CO_2 removal at variable gas flow-rates and absorbent flow-rate of 0.03 liters per minute (LPM) 233
8.13 Degree of CO_2 removal at variable gas flow-rates, absorbent flow-rate of 0.01 liters per minute (LPM) and pressure differential (Δ P) of 20.7 kPa - with and without steam 234
8.14 A schematic representation of the experimental setup used for the proof-of-concept demonstration - with experimental measurements and observations 235
8.15 Temporal dependence of absorption side external surface temperatures 236
8.16 Temporal dependence of stripping side external surface temperatures 236

List of Tables

3.1 Typical concentration and amine loading limits practiced in commercial operation of amine absorption systems [16] 34

4.1 Parameters for Evaluation of Equivalent Power Losses [17, 18] 62
4.2 Composition of flue gas used in simulation studies [19] 63
4.3 System parameters used in ProMax simulations 66
4.4 Heat exchanger parameters in the amine absorption system simulations 67
4.5 Absorbent flowrates under different stripper operating conditions . . . 75
4.6 Absorbent flowrates under different stripper operating conditions . . . 79

5.1 Parameters used for economic evaluation of equipment cost 87
5.2 Dimensions of various separation columns in the carbon capture plant 89
5.3 Dimensions of various separation vessels in the carbon capture plant . 91
5.4 Overall heat transfer coefficients for various heat exchangers (U) . . . 92
5.5 Heat transfer surface areas for different heat exchangers in the carbon capture plant 93
5.6 Parameters used for rate the various fluid drivers in the carbon capture plant 95
5.7 Generic parameters used in evaluation of equipment costs [20, 21, 22, 23] 97
5.8 Individual cost of carbon capture plant equipment 108
5.9 Individual cost of carbon capture plant equipment (contd..) 109

5.10 Individual cost of carbon capture plant equipment (contd..) 110

6.1 Antoine equation parameters for water and methanol 140
6.2 Parameters used for reboiler duty calculations 141
6.3 Properties and composition of material streams exiting the absorber . 142
6.4 Properties and composition of rich absorbent: aqueous diethanolamine (DEA), before and after entering stripper 143
6.5 Comparison of stripper operational parameters evaluated using equilibrium approach and ProMax 144
6.6 Parameters used for reboiler duty calculations 149
6.7 Properties and composition of material streams exiting the absorber . 150
6.8 Properties and composition of rich absorbent: methanol blended aqueous diethanolamine (DEA), before and after entering stripper . . 151
6.9 Stripper and reboiler operational parameters for methanol blended aqueous diethanolamine (DEA) 152

7.1 Comparison of geometric surface area of ceramic foam and various tower packings 180

8.1 Properties of porous alumina membrane 210
8.2 Properties of polyethersulfone membrane 211
8.3 Diglycolamine (DGA) concentration in stripping chamber effluent . . 237

9.1 Amine degradation products 245

Chapter 1

Introduction

1.1 Background

World energy consumption is increasing at a rapid pace. Between 1990 and 2008, global energy consumption increased by 42.6% and it is projected to rise by roughly the same amount between 2008 and 2030. As of 2012, fossil fuels - coal, natural gas and crude oil provide 83% of our primary energy and while there is a steady investment in renewable sources of energy such as solar, wind and biomass; it is projected that fossil fuels would continue to supply around 79% of global energy in 2030 [24]. The combustion of fossil fuels, however, produces carbon dioxide (CO_2) - a greenhouse gas. The enormous quantity of carbon dioxide (CO_2) emitted into the atmosphere by our fossil fuel consumption thus far has resulted in an increase in the atmospheric carbon dioxide (CO_2) concentration from 298 parts per million (ppm) in 1905 to 395 parts per million (ppm) in 2012 [25]. This increased carbon dioxide (CO_2) concentration has been linked to a rise in worldwide temperatures - one of the many consequences of the global phenomenon of climate change. Other more destructive

results of climate change include a rise in sea level, melting of polar ice-caps, increase in the frequency and severity of extreme events such as hurricanes, tornadoes, etc. and a change in global precipitation patterns which will quite likely result in severe droughts in some regions while flooding in others [26]. These effects are expected to cause unprecedented economic losses in the future, which provides a strong motivation to mitigate climate change by limiting our carbon dioxide (CO_2) emissions. Various strategies have been proposed to mitigate the disastrous consequences of climate change. These include short term, low-cost-low-impact options like boosting the use of energy efficient technology; long term, high-cost-high-impact-options such as reducing or completely eliminating fossil fuels from the global energy mix and medium term, moderate-cost-high-impact choices like the switch from coal to natural gas as well as carbon capture and storage [27].

About 41% of all carbon dioxide (CO_2) released by fossil fuel combustion comes from the generation of electricity. Worldwide, coal and natural gas fired power plants emit around 12 Gigatons (Gt) of carbon dioxide (CO_2) annually [28]. From an economic and logistical standpoint, these power plants are an easier emission source to decarbonize as compared to the tiny carbon dioxide (CO_2) emissions from the tailpipe of individual motor vehicles. Carbon capture and storage (CCS), thus, is the removal and long term storage of the carbon dioxide (CO_2) exhaust from these point sources of emission. Carbon dioxide (CO_2) from power plant exhaust is first separated from other components of flue gas, compressed to a pipeline pressures of between 8 Mega-

pascals (MPa) and 16 Megapascals (MPa) and stored in suitable geolocical locations such as saline aquifers, depleted oil and gas fields and deep unmineable coal seams [29]. US Department of Energy's (DOE) National Energy Technology Laboratory (NETL) estimates that North America alone has enough geological storage capacity for 900 years long carbon dioxide (CO_2) emissions at current emission rates [30].

Flue gas from power plants is a mixture of several gases in varying proportions. Combustion of natural gas produces flue gas containing between 3% - 5% carbon dioxide (CO_2), a majority of nitrogen (N_2)),excess oxygen (O_2), argon (Ar), minute quantities of nitrogen oxides (NO_x)) and water vapor (H_2O). Flue gas from coal fired power plants is composed of between 13% - 15% carbon dioxide (CO_2), nitrogen (N_2)),excess oxygen (O_2), argon (Ar), minute quantities of nitrogen oxides (NO_x)), sulfur oxides (SO_x) as well as water vapor (H_2O) [31]. Several methods can be employed to remove carbon dioxide (CO_2) from flue gas. These include physical or chemical gas absorption using liquid solvents, selective physical or chemical adsorption on solid adsorbents, membrane separation and cryogenic distillation. Amongst these, gas absorption using chemical agents like alkanolamines is the most advanced and commercially preferred method for separating carbon dioxide (CO_2) from gas mixtures. Amine absorption has been used since the 1950s for removal of hydrogen sulfide (H_2S) and carbon dioxide (CO_2) from natural gas as a part of a process called *natural gas sweetening*. Amine absorption has a favorable performance with both - feedstocks like natural gas which is supplied at a high pressures of upto 8 Megapascals

(MPa) and those at a much lower pressure such as flue gas, which is at atmospheric pressure [9].

With all its favorable characteristics, a major disadvantage of amine absorption is the energy intensive nature of this process. In particular, absorbent regeneration in conventional amine absorption process requires large quantities of low pressure steam between 350 kilopascal (kPa) - 450 kilopascal (kPa). This energy consumption is justified in case of natural gas sweetening due to the favorable economics of natural gas sale. However, the only tangible product of carbon capture is high pressure carbon dioxide (CO_2) - a chemical which will likely command a low market value due to its large supply and low demand. Thus, it is estimated that when retrofitted with amine absorption technology for carbon capture; the cost of electricity from conventional power plants will increase by 21% - 91% [32]. Thus, to make carbon capture and storage (CCS) economically feasible; significant advances must be made to improve or modify the amine absorption technology to make it more suitable for carbon capture.

The research presented in this thesis is motivated by a need to optimize the amine absorption technology to better employ the resources available at a coal-fired power plant. As discussed above, the conventional amine absorption process requires a large supply of low pressure steam for carbon dioxide (CO_2) desorption. The most convenient option at a coal-fired power plant is to draw the steam upstream of the low pressure (LP) turbine or at one of the suitable steam vent ports along the length of the turbine. This however, results in the unreasonably large (21%-91%) increase in

the cost of electricity (COE) [32]. To overcome this challenge, we have explored the option of operating the amine absorption process under conditions beyond current practice. Specifically, we study the effects of varying the operating pressure and temperature in a stripper unit. We have also considered in this study, vacuum strippers, which make it feasible to use waste heat - very low pressure steam that cannot be used for electricity generation. Modifications to the operating conditions inevitably affect other system parameters such as equipment sizing. We have conducted an economic evaluation to reasonably account for these effects and to determine the most economical process operating configuration. Finally, we have developed a novel process for separating carbon dioxide (CO_2) from flue gas. The most innovative feature of this process is its use of a single integrated unit for absorption and stripping instead of two separate columns. We make use of novel materials called 'ceramic foams' for gas-liquid contacting. The latter part of this thesis will be dedicated to elucidating the research involved in taking the conceptual idea for this process and developing it to the point of a bench-scale proof-of-concept demonstration.

1.2 Organization

This thesis is divided into *seven* chapters to clearly organize the work conducted as a part this dissertation. We begin with a brief discussion of carbon capture and storage (CCS) in Chapter 2. We address the concept of retrofitting existing coal fired power plants with this technology. We then expand upon our discussion of existing

technologies for carbon dioxide (CO_2) separation and report the status of current research towards improving gas absorption technology in Chapter 3. In Chapter 4, we describe the basis for the amine process simulations that were developed to study the effects of changes in operating conditions. We will also discourse about our simulation results, comment on system performance under different conditions and identify the most promising process configurations that are of interest of from an economics perspective. These research results have been presented at the American Institute for Chemical Engineers (AIChE) conferences and have been published in the International Journal for Greenhouse Gas Control [33, 34]. Chapter 5 examines the promising process configurations shortlisted in Chapter 4 by evaluating the capital and operating costs for the processes. These results have also been presented at the American Institute for Chemical Engineers (AIChE) conferences and a manuscript to be submitted to the International Journal of Greenhouse Gas Control is in the works. In Chapter 6, we will discuss our research on the development of novel absorbent formulations for carbon dioxide (CO_2) removal. These results have produced a provisional patent application which was filed in October 2012 with the full application due in late 2013 [35]. Studies conducted to estimate reboiler duty for aqueous alkanolamine systems blended with alcohol are being written up into a manuscript. We will elaborate upon the concept of the novel process developed as a part of this research work in Chapter 7. We discuss the properties of the materials that have been selected to carry out a bench-scale, proof-of-concept demonstration

of this process. Chapter 7 also includes the results of the 2-phase hydrodynamic and mass transfer studies conducted in a 1-D glass column containing the mass gas-liquid contacting medium. Details about the design and operation of a plexiglas prototype developed to conduct 2-phase flow experiments with air and water are listed in Chapter 8. We discuss the design and operation of the stainless steel prototype developed for a fully functional proof-of-concept demonstration of the process. The results of this are also described in Chapter 8. Finally, Chapter 9 will contain the scope and recommendations for future work in this project.

Chapter 2

Climate change and carbon capture and storage

2.1 Fossil fuels and climate change

World population has grown exponentially in the 20^{th} century. This has been fueled by and has resulted in a massive boom in energy consumption, supplied mainly through the consumption of fossil fuels; namely - coal, crude oil and natural gas. Figure 2.1 shows the global energy supply from various sources expressed in Million tonnes of oil equivalent (Mtoe). The dominance of fossil fuels in our present energy mix is clearly observable in Figure 2.1 - with more than 85% being provided by them. We are almost completely dependent on petroleum and natural gas for our heating and transportation needs. Natural gas and coal based power-plants provide as much as 65% of the total electricity generated worldwide.

The combustion of these fossil fuels produces carbon dioxide (CO_2), the concentrations of which have risen by almost 25% from in the past 50 years - a rate faster than ever before in the history of our planet. United Nations estimated that in 2009, global carbon dioxide (CO_2) emissions were around 29 Gigatons [36]. With develop-

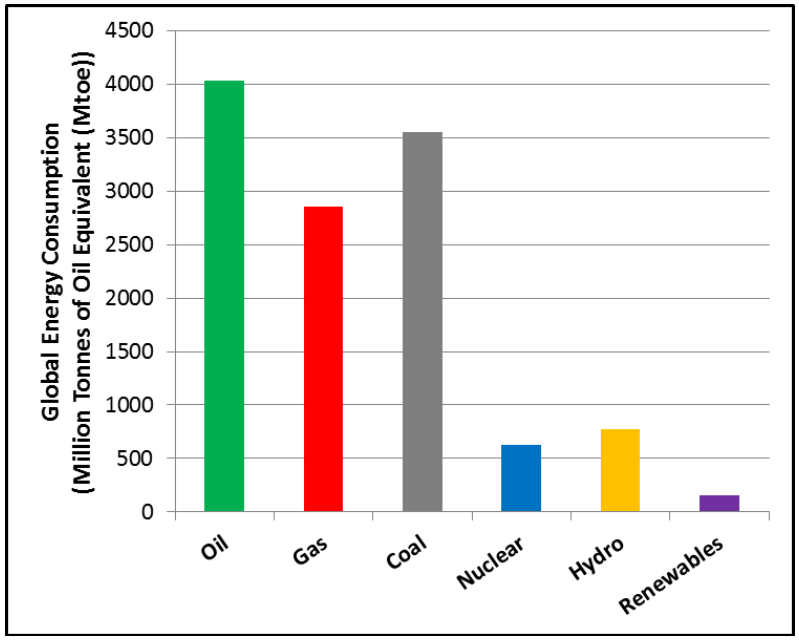

Figure 2.1 : World energy consumption in Million tonnes of oil equivalent (Mtoe) (2011) [1]

ing nations like India, China and Brazil developing economically at a rapid pace, in the absence of a purposeful change in course; carbon dioxide (CO_2) emissions will only rise further. It is well known that carbon dioxide (CO_2) is a *greenhouse gas* - meaning, it traps a part of incident solar infrared radiation and prevents it from reflecting back into space. An increase in atmospheric carbon dioxide (CO_2) concentration invariably results in a rise in global temperatures, which is what has been recorded over the past 50+ years. This phenomenon, along with several associated perturbations in global weather patterns are collectively termed as 'global climate change'. Figure 2.2 shows the rise in atmospheric carbon dioxide (CO_2) concentrations along with the global temperature anomaly - a scientific measure of the departure of global temperatures

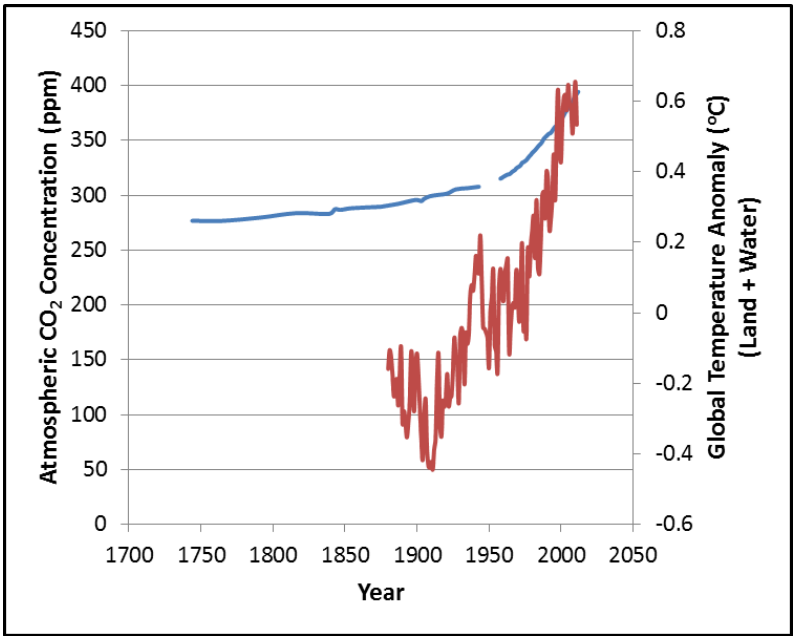

Figure 2.2 : Growth of atmospheric carbon dioxide (CO_2) concentration and global temperature anomaly over roughly the same time period [2, 3, 4]

from the long-term average.

As seen in Figure 2.2, global temperatures have risen by 0.74°C ± 0.18°C in the last century and according to the Intergovernmental Panel on Climate Change (IPCC), they are projected to increase by a further 1.1°C to 2.9 °C over the next century [4]. While this increase *seems* minimal and one might even argue that a slightly warmer world would perhaps be more favorable, the predicted consequences of this increase are terrifying. Climate change is already resulting in the loss of ice from our glaciers and polar ice-caps at a faster rate than at which is is replenished each year. The melting of polar, glacier and sea ice is estimated to contribute to a rise in sea-level between 18 cm and 59 cm in the 21st century which will result in difficulties

at huge coastal settlements which includes world cities like New York,USA; Tokoyo, Japan and Mumbai, India [26]. The destabilization of polar permafrost is capable of releasing the massive reserves of methane (CH_4) (estimated at 1900 Gigatons) that are presently trapped as clathrate compounds. Methane (CH_4) has 25 times as much greenhouse effect potential as carbon dioxide (CO_2) and studies show that thawing of permafrost alone could risk a sudden release of upto 50 Gigatons of methane (CH_4) [37].

Rise in temperature is already being linked to an alteration in the global precipitation patterns and the increasing instances of flooding and drought conditions in populated areas of the world. Erratic precipitation behavior will likely have massive consequences globally since the stability of food production is largely dependent on the predictable behavior of rainfall. Higher temperatures also favor the formation of more intense extreme weather phenomena like hurricanes and tornadoes, and at a greater frequency. They also result in more arid summers and winters, resulting in higher risk of wildfires; the likes of which are being witnessed all over United States already. All these outcomes will have adverse effects on human life and the scale of global economic activity.

2.2 Carbon Capture and Storage

Concerned governments, businesses and agencies have thoroughly studied their options to mitigate climate change. Figure 2.3 shows one such analysis that shows the

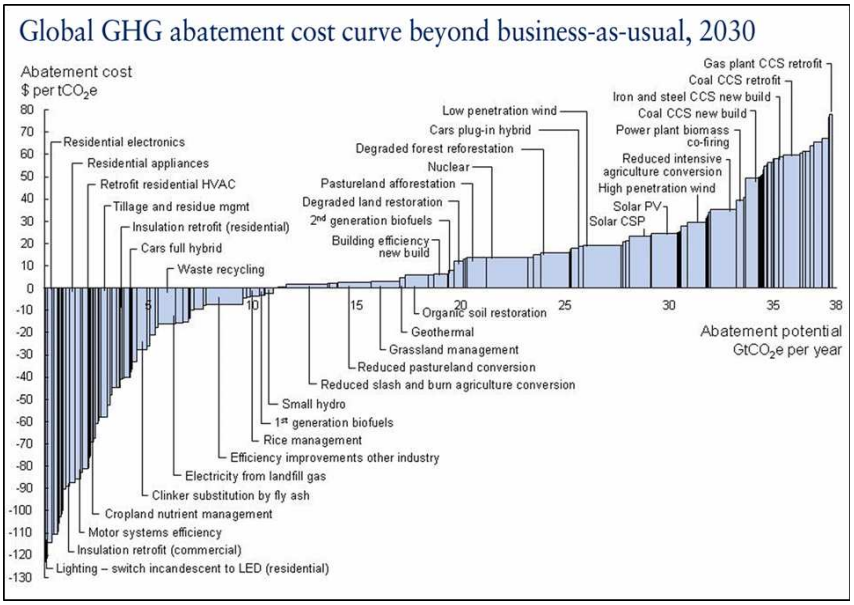

Figure 2.3 : Global Greenhouse Gas (GHG) abatement cost curve [5]

estimated cost of reducing carbon dioxide (CO_2) emissions by a ton. It shows that clearly some reduction in the carbon dioxide (CO_2) emissions can be achieved by focusing on better energy efficiency, reforming agricultural and industrial practices and recycling waste. However, to achieve the target of stabilizing our atmospheric carbon dioxide (CO_2) concentration at 500 ppm by mid-century, before gradually reducing it; more aggressive strategies need to be adopted. All analysis points towards an inevitable, continued dependence on fossil fuels; at least for the next few decades. Large commercial projects involving alternative energy technologies like *biofuels*, *wind* and *solar* are currently being initiated, however, it will take more than a few decades for them to make significant market penetration. This leaves all but one practical option on the table to shrink our carbon dioxide (CO_2) emissions in the short and medium term - Carbon Capture and Storage (CCS) [5, 32].

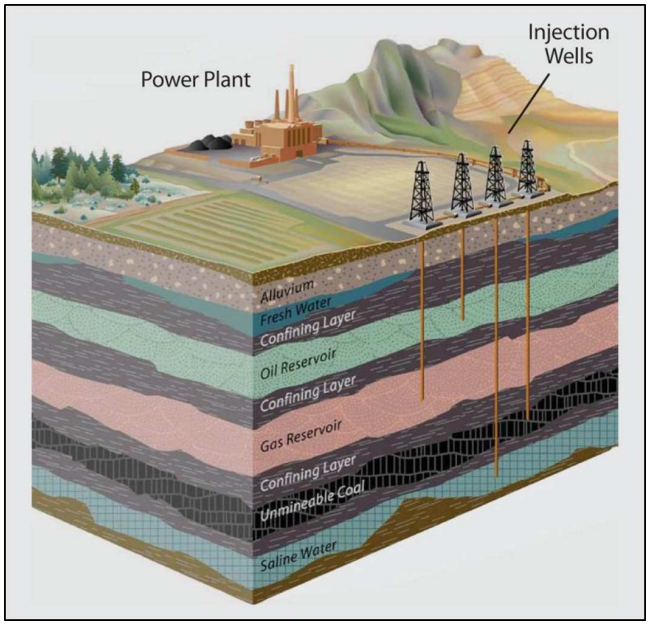

Figure 2.4 : Schematic representation of Carbon Capture and Storage (CCS) [6]

Carbon Capture and Storage (CCS) is an approach to mitigate climate change that has generated strong interest in the scientific community and has received the support of policymakers, as a promising idea. Carbon Capture and Storage (CCS) involves the 'capture' (i.e. removal) of carbon dioxide (CO_2) at point sources of emission, followed by compression and safe, long-term storage in suitable geological reservoirs like depleted oil and gas fields and deep saline aquifers. The most viable candidates for the application of Carbon Capture and Storage (CCS) are power generation utilities such as coal and natural gas fired power plants which emit around 50% of carbon dioxide (CO_2) released in the United States. Figure 2.4 shows a schematic representation of the concept of Carbon Capture and Storage (CCS).

Globally, coal and natural gas based power plants contribute in excess of 40% to annual CO_2 emissions. Carbon Capture and Storage (CCS) at power plants is

expected to scale down their emissions by as much as 90%; thus contributing significantly towards the goal of limiting atmospheric carbon dioxide (CO_2) concentration goals. Carbon Capture and Storage (CCS) is considered favorably primarily because it will allow us to continue using fossil fuels while alternative sources gain greater market share and yet, minimize the impact of the carbon dioxide (CO_2) emissions.

As discussed above, Carbon Capture and Storage (CCS) consists of three stages:

- *Carbon dioxide (CO_2) capture*: Separation of carbon dioxide (CO_2) from the flue gas emissions at power plants
- *Compression*: Compression of carbon dioxide (CO_2) to a pipeline pressure of between 8 and 16 Megapascals (MPa)
- *Transport, storage and monitoring (TSM)*: Transport of compressed carbon dioxide (CO_2) to storage site followed by injection into geological formation and monitoring for any leaks

We discuss the various aspects of Carbon Capture and Storage in the following sections.

2.3 Technologies for Carbon Capture

Coal and natural gas are the most common feedstocks used to generate electricity at thermal power plants. At existing power plants, these fuels undergo combustion in the presence of excess air to release heat which is used to produce steam and finally, generate electricity. The combustion of coal and natural gas generates flue

gas which typically has a composition of 5–15% carbon dioxide (CO_2), 65–75 % nitrogen (N_2), 2–12% oxygen (O_2) and 5–15% water vapor (H_2O). In addition, there are small amounts of pollutants like carbon monoxide (CO), oxides of nitrogen and sulfur (NO_x, SO_x) and trace quantities of heavy metals like Mercury (Hg) [38]. In carbon capture, carbon dioxide (CO_2) in the flue gas is separated using suitable technology and the 'decarbonized' flue gas, consisting mainly of N_2 is released into the atmosphere. Several methods to separate carbon dioxide (CO_2) from gas mixtures, based on different physical and chemical principles have been developed. These are discussed in detail in the sections below.

2.3.1 Adsorption

The phenomenon of adhesion of gases, liquids or dissolved solids to a surface is called 'adsorption'. Adsorbents can be naturally occurring materials like coal, charcoal and certain zeolites or can be synthetically manufactured complex ones like molecular sieves and metal organic frameworks (MOFs). Gases can be adsorbed physically (i.e. surface adhesion is supported only by molecular interactions and surface forces) or chemically (i.e. the adsorbed molecules form chemical bonds with the surface) on solids to form a film of molecules on the surface. Since the amount of gas adsorbed on a solid is proportional to the available surface area; highly porous materials with high specific surface areas act as good adsorbents. Adsorbents can be chemically treated to increase their capacity as well as their specificity towards a particular com-

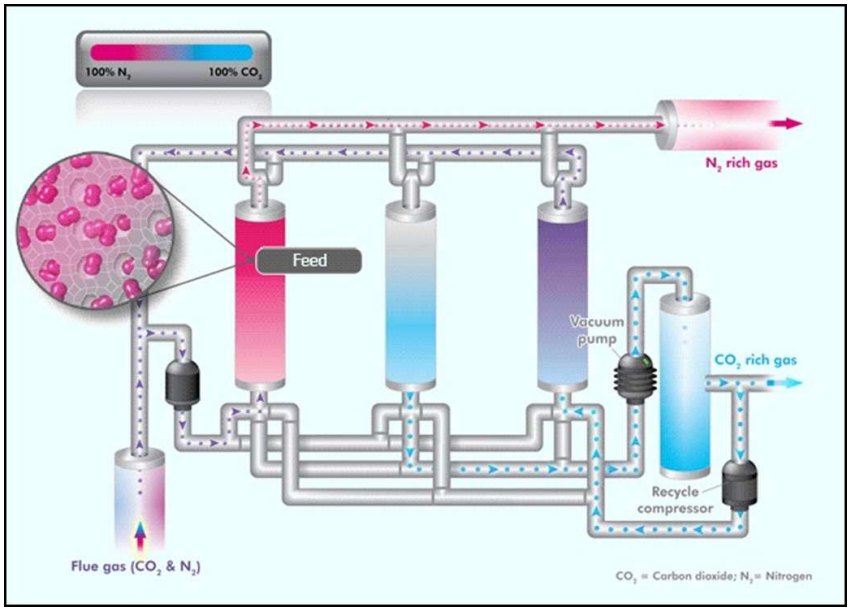

Figure 2.5 : Schematic representation of adsorption process for carbon dioxide (CO_2) separation from flue gas [7]

ponent that may be present in a gas mixture. In case of carbon capture, carbon dioxide (CO_2) is present in a dilute mixture containing with a ratio of CO_2/N_2 of between 1:5 - 1:15. Thus, an adsorbent suitable for carbon capture must possess very high selectivity towards carbon dioxide (CO_2) adsorption. Certain materials like specially treated activated carbon, some molecular sieves and metal organic frameworks (MOFs) selectively adsorb carbon dioxide (CO_2) on their surface. Such adsorbents are potential candidates for use in carbon dioxide (CO_2) separation. Figure 2.5 shows a schematic of an adsorptive CO_2 separation process.

In a typical adsorptive separation process as represented in Figure 2.5; the gas mixture is first contacted with the adsorbent in an adsorption column. Operating conditions for the adsorption column are selected on the basis of the inlet gas composition,

adsorbent material and the degree of carbon dioxide (CO_2) removal desired. After the adsorbent material is sufficiently saturated with the gas component of interest, it is regenerated. For adsorptive gas separation, two operational configurations have been commercialized and are commonly used. These are *pressure swing adsorption (PSA)* - saturated adsorbent is regenerated by reducing the system pressure which results in desorption of gases and *temperature swing adsorption (TSA)* - saturated adsorbent is regenerated by providing thermal energy to destabilize the adsorbate-surface bonds and release it. Adsorption is considered the technology of choice to recover trace amounts of contaminants or high-value components of gas streams. It is also favored when the feed gas stream is available at a high pressure.

2.3.2 Cryogenic separation

Distillation is an unit operation commonly performed to separate liquid mixtures based on differences in the volatility of their components. By liquefying flue gas through cooling and condensation, it is possible to separate carbon dioxide (CO_2) from other components of the flue gas. This process is called cryogenic distillation. The scientific basis of cryogenic separation is that when a gas mixture composed primarily of carbon dioxide (CO_2) and nitrogen (N_2)is steadily cooled, the CO_2 condenses to form a liquid while N_2 remains a gas. The vapor phase consisting mainly of nitrogen (N_2) can be allowed to escape and the liquid carbon dioxide (CO_2) transported for compression and storage. Cryogenic distillation is quite popular for separating carbon

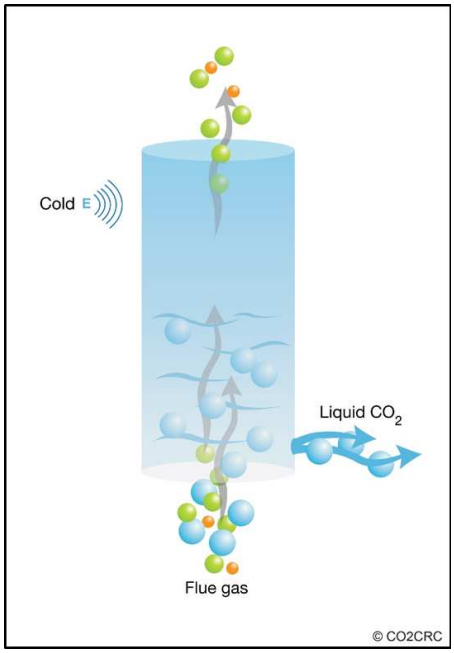

Figure 2.6 : Schematic representation of cryogenic separation process for carbon dioxide (CO_2) separation from flue gas [7]

dioxide (CO_2) from concentrated feed gas streams ((CO_2) concentration: 90% and above). A schematic representation of cryogenic distillation process is shown in Figure 2.6.

2.3.3 Membrane separation

Membrane separation has been successfully established as an approach for separating single components of interest from gas mixtures. The petroleum industry has been using polymeric membranes for separation of carbon dioxide (CO_2) from light hydrocarbons in natural gas. Metallic membranes have been used for recovering unreacted hydrogen (H_2) from ammonia (NH_3) produced in Haber's process. A variety

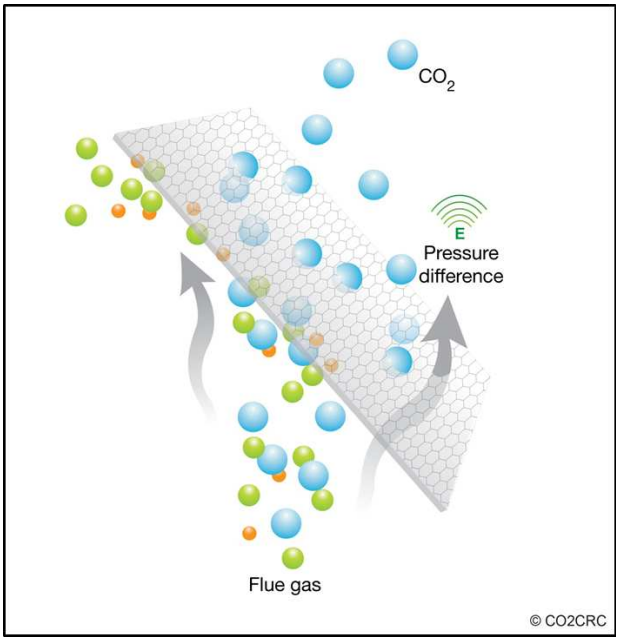

Figure 2.7 : Schematic representation of membrane separation process for carbon dioxide (CO_2) separation from flue gas [7]

of membranes like ceramic, inorganic, metallic, polymeric and liquid membranes have been developed for the purpose of gas separation. The actual physical mechanism responsible for gas separation varies and is dependent on the type of membrane used. Polymeric membranes are made from different types of materials like cellulose acetate (CA), polysulfone (PS), polyethylene (PE), Teflon (PTFE), polypropylene (PP) and others. The ability of polymeric membranes to separate gases depends on their selective interaction with the target gas molecules. Target gas molecules are typically soluble in the membrane matrix and transport across the membrane by diffusion. This transport is explained by the solution-diffusion mechanism of transport. A schematic of polymeric membrane separation is shown in Figure 2.7.

Unlike polymeric membranes, ceramic and metallic membranes are typically porous. Ceramic membranes are commonly manufactured from oxides of metals like aluminum (e.g., Al_2O_3), silicon (e.g., SiO_2), titanium (e.g., TiO_2) and zirconium (e.g., ZrO_2). Metallic membranes are commonly made of noble metals like platinum (Pt) and palladium (Pd). Depending on the sizes of pores in the membrane, the gas molecules either permeate through the membrane or get blocked. Thus, in principle the membranes act like sieves to separate the gas molecules based on their sizes. Both metallic and ceramic membranes are stable at high temperatures. In addition, ceramic membranes are chemically inert and can be used in extreme environments of high acidity or basicity, where polymeric or metal membranes fail to function efficiently. Due to the inherent nature of the process which relies on the differences in the physical properties of the gases being separated, membrane separation is favored in systems where there is a large contrast in the properties of the components of the mixture. As with adsorption, high feed gas pressure is a requirement for membrane separation in order to handle realistic gas flow rates (since diffusion mechanisms are slow).

2.3.4 Absorption

Absorptive separation processes rely on the affinity of liquid absorbents for one component over others in a gas mixture. Gas absorption is by far the most widely used method for carbon dioxide (CO_2) separation from gas mixtures. Gases can be absorbed into liquids by two different mechanisms, namely - physical and chemical

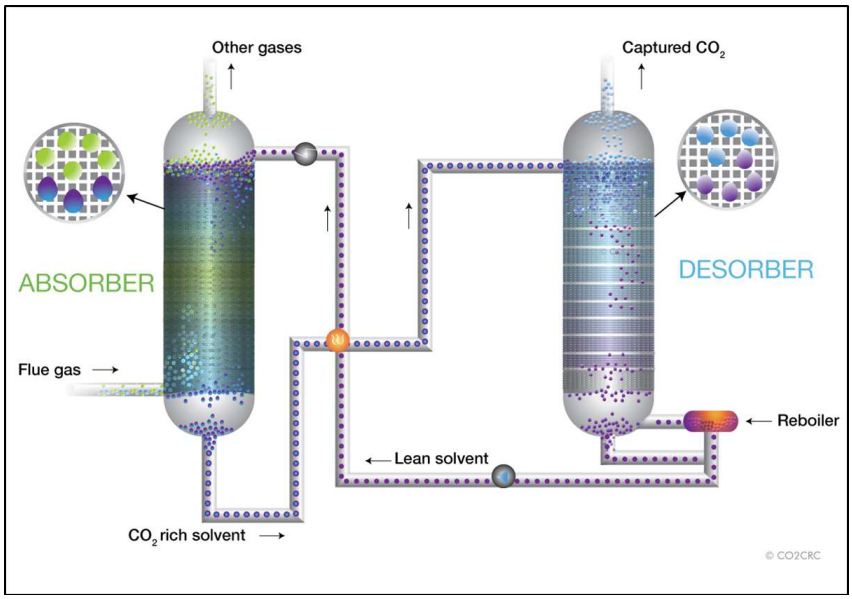

Figure 2.8 : Schematic representation of gas absorption (alkanolamine) separation process for carbon dioxide (CO_2) separation from flue gas [7]

absorption. Physical absorption involves the dissolution of gases into liquids without an accompanying chemical reaction. Chemical absorption on the contrary involves binding of the absorbed gas molecules into the liquid by the formation of reaction products between the gas and the absorbent chemical. Physical and chemical absorbents are used extensively in the chemical industry. Selexol® - a proprietary mixture of dimethyl ethers of polyethylene glycol and Rectisol® - essentially refrigerated methanol are two *physical absorption* processes have been used to separate carbon dioxide (CO_2) from syngas produced by coal and biomass gasification. The petroleum industry has used *alkanolamines* for a long time in natural gas sweetening by removal of carbon dioxide (CO_2) and hydrogen sulfide (H_2S). Figure 2.8 is a schematic representation of a typical alkanolamine absorption process.

Physical absorption processes are typically operated at high pressures (300 - 2000 psia) as the amount of gas dissolved in liquids is proportional to the partial pressure of the component of interest in the gas phase (i.e. Henry's law). Solvents with high dissolution capacity for the gas components of interest are ideal choices for physical absorption processes. Chemical absorption on the contrary is a favored process when the feed stream is at a relatively low pressure. Thus, the alkanolamine process using aqueous monoethanolamine (MEA, C_2H_7NO), diethanolamine (DEA, $C_4H_{11}NO_2$), diglycolamine (DGA, $C_4H_{11}NO_2$)and other chemicals is the preferred technology for removal of carbon dioxide (CO_2)and hydrogen sulfide (H_2S)from natural gas.

2.4 Carbon dioxide (CO_2), compression, storage and monitoring

Carbon dioxide (CO_2) separated from flue gases is compressed to a pipeline pressure between 8 and 16 Megapascals (MPa) and transported to the storage site [29]. The compressed carbon dioxide (CO_2) is injected into suitable geological formations either for storage or applications such as enhanced oil recovery (EOR). Different geological formations have been identified and their carbon dioxide (CO_2) storage capacity evaluated. Depleted oil and gas fields are considered as the primary storage sites. The storage capacity for these reservoirs is estimated at between 675 and 900 Gigatons (Gt) of carbon dioxide (CO_2) [29]. In addition to their substantial storage capacity, the petroleum industry has also developed detailed understanding of petroleum

reservoirs geology. This is critical towards analyzing and monitoring the risk associated with the storage of enormous quantities of carbon dioxide (CO_2) into geological formations. An application of captured carbon dioxide (CO_2) which is gaining appreciable support from all quarters is enhanced oil recovery (EOR) which will help recover greater amounts of oil from depleted oil fields and partly offset the involved costs.

Other potential reservoirs for captured carbon dioxide (CO_2) include coal deposits that are either too thin or lie too deep to be mined economically. These are collectively classified as unminaeble coal seams. The storage capacity of unmineable coal seams is expected to be between 15 and 200 Gigatons (Gt) of carbon dioxide (CO_2). Saline aquifers - formations that contain highly mineralized brine and are considered of no benefit to humans are considered to be another massive potential carbon dioxide (CO_2) sink. However, a better understanding of the geology of such formations needs to be developed first.

2.5 Challenges with Carbon Capture and Storage

Carbon capture and storage (CCS) presents a unique opportunity to make a smooth transition from carbon-based energy to alternative energy sources like nuclear, solar and wind while minimizing the impact of the associated carbon dioxide (CO_2) emissions. Several gas separation methods and technologies are available for the removal of carbon dioxide (CO_2) from gas mixtures. However, amongst these; the

alkanolamine absorption process is the closest to a ready-to-deploy method for carbon dioxide (CO_2) capture. However, while it is the closest in terms of scale and the gas conditions to be handled; it isn't optimized for post-combustion carbon capture. The alkanolamine absorption process is very energy intensive, requiring massive quantities of low pressure steam (60-75 psia) to regenerate the chemical absorbent. This makes the existing process extremely costly to implement for carbon dioxide (CO_2) removal at fossil fuel based power plants.

A typical 500 Megawatt (MW) power plant emits around 10,000 tonnes/day of carbon dioxide (CO_2) and around 70,000 tonnes/day of flue gas [39]. Even with the use of state-of-the-art amine absorption technology to for carbon capture; the cost of electricity is projected to increase by between 43%–88% [29]. Other untested technologies are projected to result in an even higher increase the cost of electricity. Application of alkanolamine absorption technology for carbon capture will result in the consumption of a part of the steam produced and the electricity generated at the power plant to regenerate the absorbent and operate the process auxilliaries. The cumulative loss in the power plant output due to carbon capture is called 'parasitic power load'. It is estimated that application of current amine absorption process to a 500 MW plant would a parasitic load of around 115 MW, resulting in almost 23% reduction in the net electricity output of the power plant [40]. This reduction in energy output, along with the capital expenditure involved in the design and construction of the carbon capture and compression units results in an increase in the

cost of electricity produced. Carbon dioxide (CO_2) absorption and compression together account for between 90%–95% of the carbon capture and storage (CCS) cost. The share of the absorption process is the dominant one and accounts for 85%–90% of the total cost increase [40].

The National Energy Technology Laboratory (NETL), a science, technology and energy laboratory owned and operated by US Department of Energy (DoE) is coordinating the US government's carbon capture and sequestration (CCS) program. The targets set for the NETL program on post-combustion carbon capture and storage (CCS) are 90% CO_2 capture with no more than 35% increase in the cost of electricity (CoE) as compared to an existing coal-based power plant without carbon capture [40]. For NETL targets for carbon capture and storage (CCS) to be realized; immediate breakthroughs in technology will be required so that the energy penalties in separation processes can be reduced significantly.

Chapter 3

Amine absorption technology: technical description and current research

3.1 Amine absorption technology

3.1.1 Original development

Alkanolamine (amine) absorption is an old technology. Triethanolamine (TEA), the first alkanolamine to become commercially available; was used in early gas-treating plants in the 1930s [9]. As other alkanolamines like monoethanolamine (MEA), diethanolamine (DEA), methyldiethanoamine (MDEA) and diglycolamine (DGA) became commercially available; the slower reacting triethanolamine (TEA) was gradually displaced from commercial operation. Even after 80+ years, amine absorption continues to be the technology of choice for natural gas sweetening in large parts due to the extensive amounts of design and operational data available for the process and due to its effectiveness in removing carbon dioxide (CO_2) and hydrogen sulfide (H_2S) under a wide range of feed conditions. Figure 3.1 shows the chemical structure for four different alkanolamines.

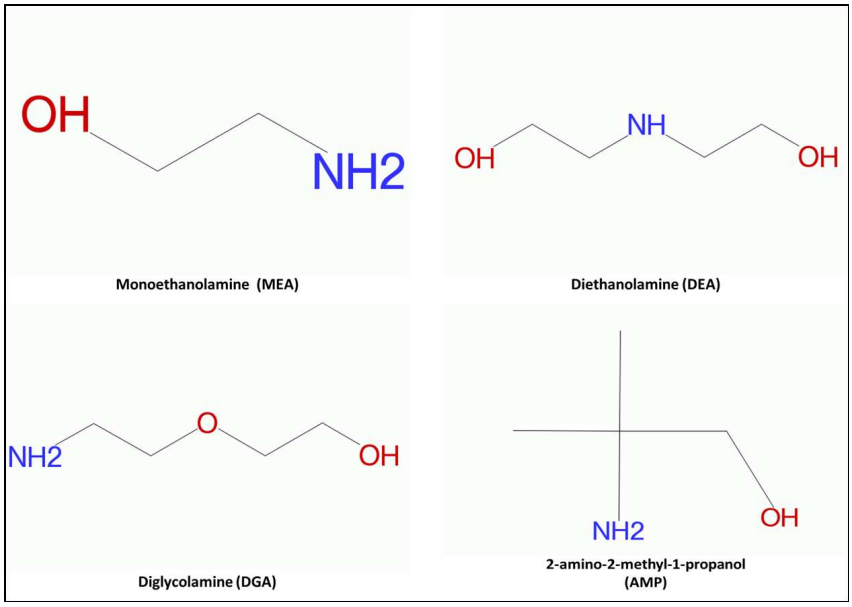

Figure 3.1 : Chemical structure of various commercial alkanolamines

Figure 3.2 shows a schematic of the amine absorption process used for natural gas sweetening. A typical amine absorption plant consists of the following essential equipment:

- An absorber column
- A desorber column
- A rich amine/lean amine heat exchanger
- Booster pump(s)
- A reboiler
- A partial condenser
- An amine cooler

Additional equipment like amine reclaimers and flash tanks are also present as a part of the system when required.

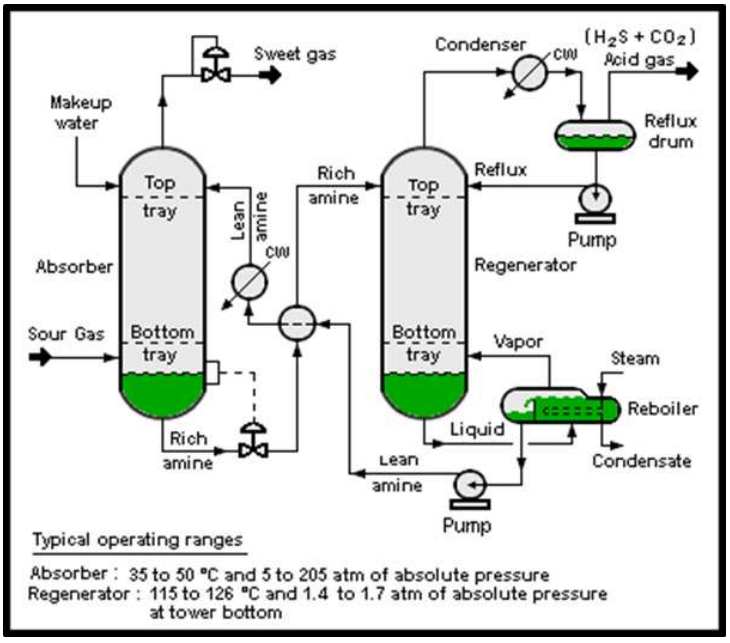

Figure 3.2 : Schematic representation of amine absorption process for natural gas sweetening [8]

In the amine absorption process for natural gas sweetening, sour gas *first* enters the absorber column. The absorber is operated under counter-current flow conditions. The operational pressure of the absorber varies between 500 kilopascals (kPa) and 20,000 kilopascals (kPa) and is largely a function of the sour gas pressure. Aqueous amine solution, which functions as the absorbent for carbon dioxide (CO_2) and hydrogen sulfide (H_2S) is introduced into the absorber at the top. As the absorbent flows down, it absorbs the acidic gases from the sour gas and gets saturated. Reaction schemes 3.1 - 3.5 show the reactions between alkanolamines and carbon dioxide (CO_2) and hydrogen sulfide (H_2S) [9].

$$H_2O \rightleftharpoons H^+ + OH^- \tag{3.1}$$

$$H_2S \rightleftharpoons H^+ + HS^- \tag{3.2}$$

$$CO_2 + H_2O \rightleftharpoons HCO_3^- + H^+ \tag{3.3}$$

$$RNH_2 + H^+ \rightleftharpoons RNH_3^+ \tag{3.4}$$

$$RNH_2 + CO_2 \rightleftharpoons RNHCOO^- + H^+ \tag{3.5}$$

When amines react with hydrogen sulfide (H_2S), they form a salt with the bisulfide ion (HS^-) - a product of hydrogen sulfide (H_2S) dissociation. The reaction between amines and carbon dioxide (CO_2) is more complex. Primary and secondary amines react with carbon dioxide (CO_2) to form a carbamate as explained in reaction 3.5. At higher carbamate saturations, a significantly slower reaction takes place which results in the formation of a bicarbonate. Tertiary amines cannot form carbamates and thus, undergo the slower bicarbonate formation reaction.

The reaction between amines and carbon dioxide (CO_2) and hydrogen sulfide (H_2S) is exothermic, which results in a constant change in the temperature of the absorbent throughout its flow in the column. Figure 3.3 shows the temperature and carbon dioxide (CO_2) removal profile in a column operating at 7000 kilopascals (kPa) with 22 wt% monoethanolamine (MEA) as the absorbent. The aqueous amine solution, loaded with acidic gases exits the absorber column at the bottom; at a temperature of around 65°C. This amine solution with high acid gas saturation (henceforth referred as 'rich amine solution') flows to a heat exchanger unit commonly referred to as the lean/rich amine heat exchanger. The heat exchanger contacts the hot regenerated amine solution coming from the reboiler and the cold rich amine from the

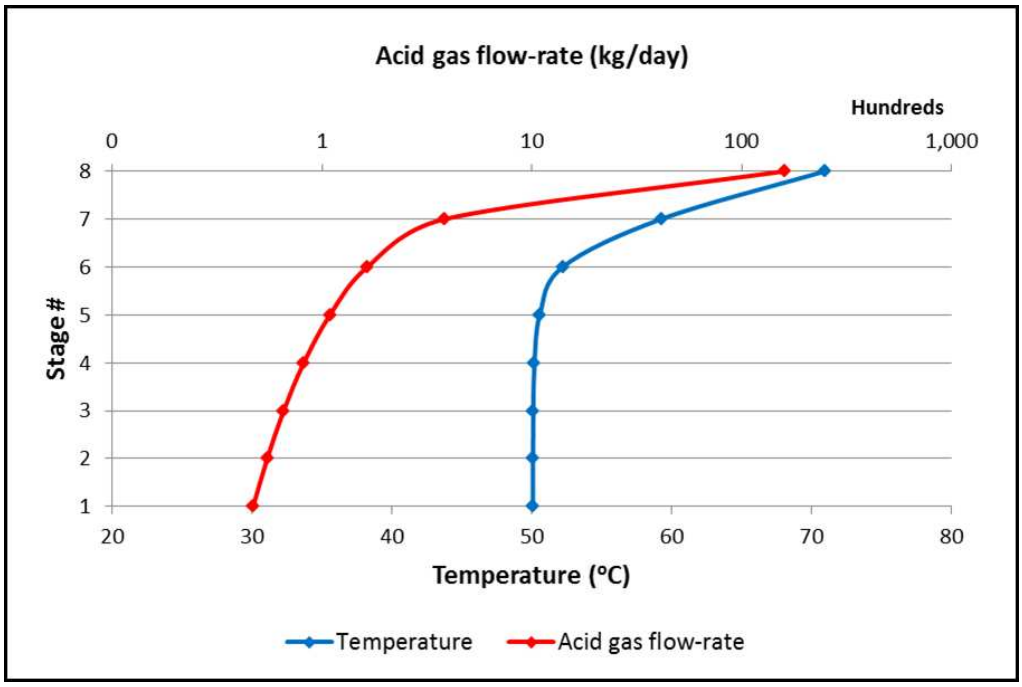

Figure 3.3 : Temperature and acid gas removal profiles in an absorber column

absorber. The heated rich amine solution subsequently flows to the desorber column. Desorbers are typically operated at a pressure ranging between 150 kilopascals (kPa) and 200 kilopascals (kPa) and a temperature ranging between 105°C and 120°C. The heated rich amine solution enters the desorber at temperatures close to 100°C and undergoes heating after entering it. In order to regenerate the absorbent, it must be stripped of the absorbed acid gases by breaking the amine - acid gas complexes. The energy required to heat the rich amine and drive the endothermic desorption reactions is provided by low pressure steam provided to a reboiler located at the base of the desorber. Supplied steam is typically in a pressure range of 400 kilopascals (kPa) - 500 kilopascals (kPa) and a temperature of 200°C and 250°C. The actual carrier for thermal energy in the desorber is the stripping vapor - primarily steam; generated by

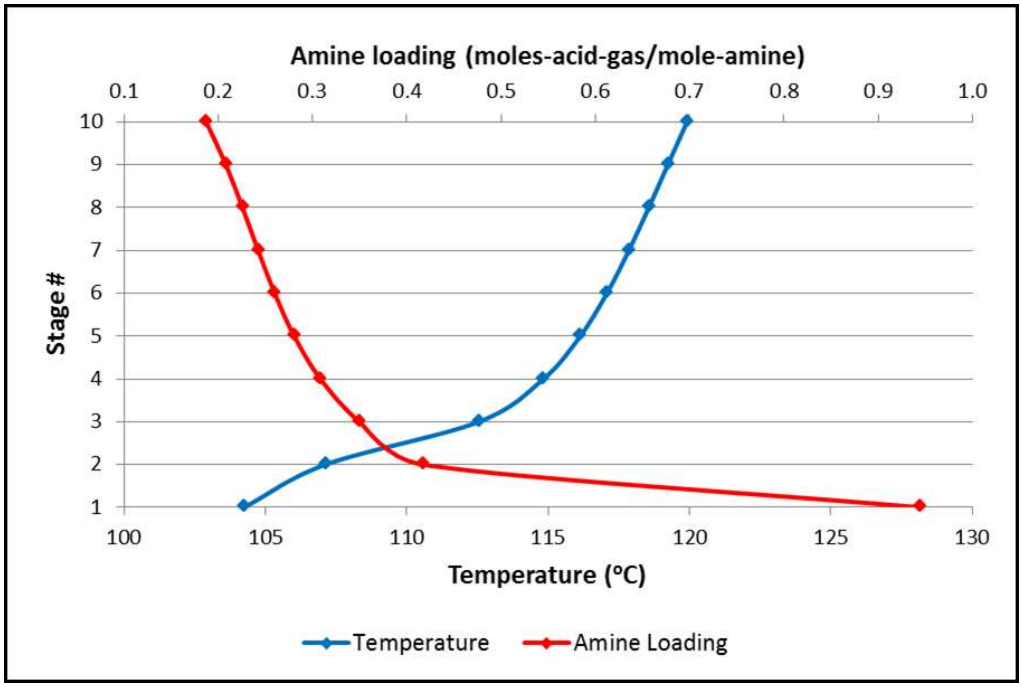

Figure 3.4 : Temperature and absorbent regeneration profiles in a desorber column

evaporating a fraction of the amine solution. The stripping vapor exits the desorber at the top, along with the liberated acid gases and enters a partial condenser where the stripping vapor is condensed and returned to the desorber column as a reflux stream. The acid gases maybe released into the atmosphere or sent to a Claus process plant for desulfurization of the hydrogen sulfide (H_2S). Figure 3.3 shows the temperature profile and the gradual regeneration of acid gas loaded monoethanolamine in a desorber column operating at 190 kilopascals (kPa). The regenerated amine leaves the lean/rich amine heat exchanger in the vicinity of 60°C and undergoes further cooling in an amine cooler to bring down its temperature to around 40°C, which is the optimum inlet temperature for the process.

Several alkanolamines are considered practical in today's commercial operations.

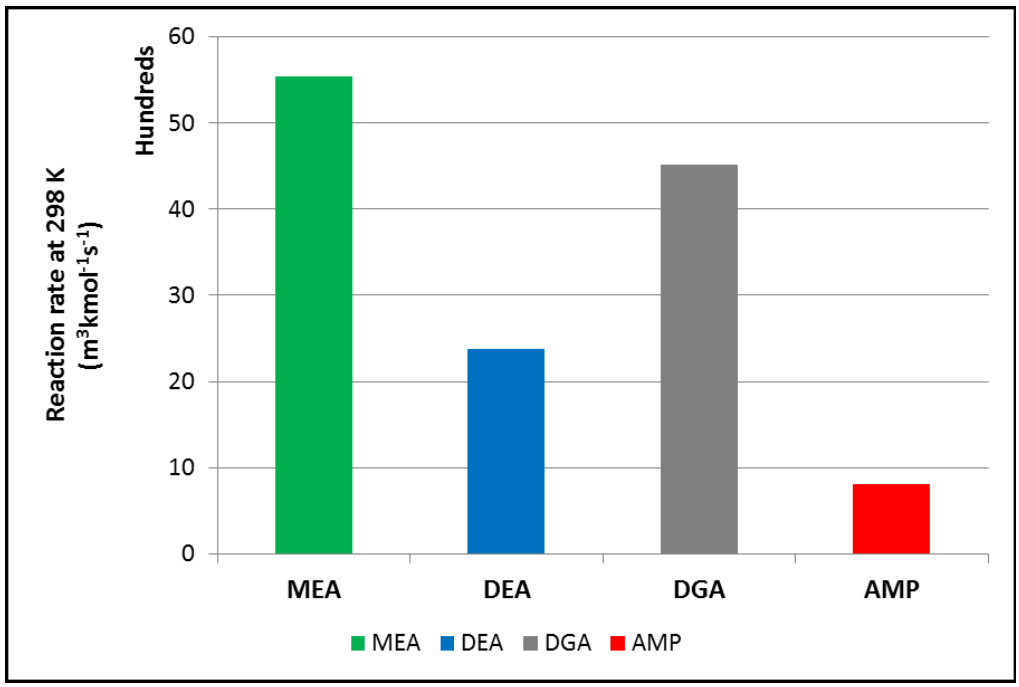

Figure 3.5 : Heat of reaction for 4 different alkanolamines [9, 10]

These include but are not limited to monoethanolamine (MEA), diethanolamine (DEA), diglycolamine (DGA), methyldiethanolamine (MDEA) and diisopropylamine (DIPA). In addition, several commercial operators prefer to operate blended alkanolamines; wherein, a secondary amine such as diethanolamine (DEA) - a slower reacting amine with a low heat of reaction is 'activated' with a faster reacting primary amine such as monoethanolamine (MEA) or piperazine (PZ). Studies have shown that blended amines may have advantages in reducing reboiler energy duty as compared to single amines [41].

Figure 3.5 and 3.6 show the heat of reaction and the reaction rate for 4 different alkanolamines. Monoethanolamine (MEA) and diglycolamine (DGA) are primary amines, diethanolamine (DEA) is a secondary amine and 2-amino-2-methyl-1-

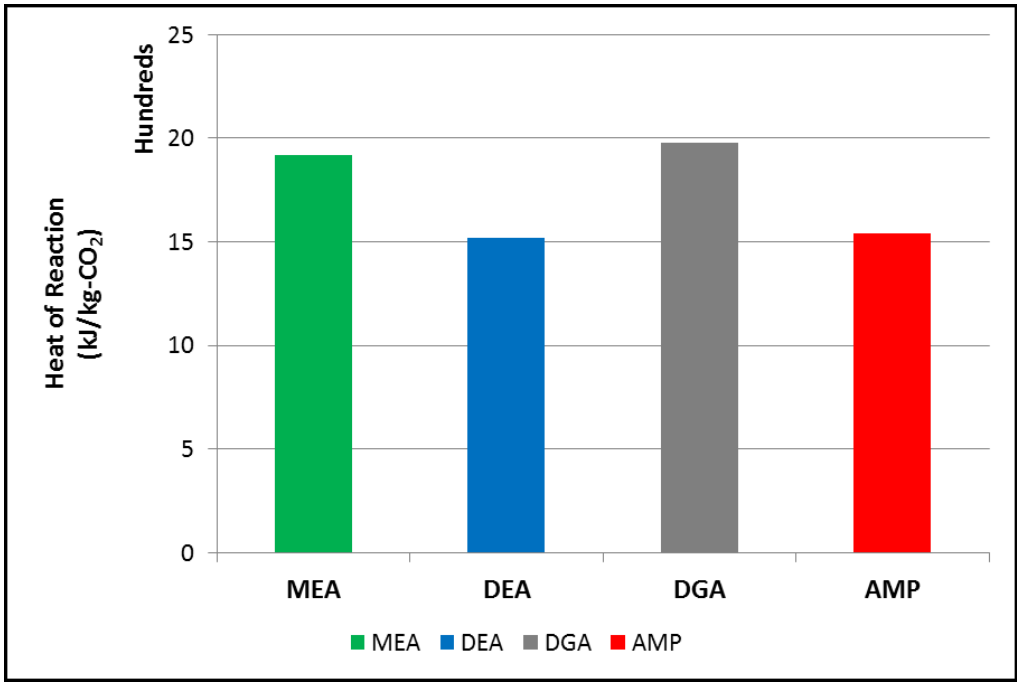

Figure 3.6 : Reaction rate at 25°C for different alkanolamines [11, 12]

propanol (AMP) is a primary amine, albeit with a bulky side group which results in steric hindrance that destabilizes the carbamate. Comparing figures 3.5 and 3.6 shows a clear trend that faster reacting amines also have higher heat of reaction. An interesting feature revealed in this comparison, however, is that whereas diethanolamine (DEA) and 2-amino-2-methyl-1-propanol (AMP) have a reaction rate less than half that of monoethanolamine (MEA) and diglycolamine (DGA), their heats of reaction are not proportionally smaller. The heat of reaction for diethanolamine (DEA) is only 20% smaller than that of monoethanolamine (MEA). Thus, when selecting the absorbent; careful consideration is typically given to the composition and properties of the feed gas, particularly the ratio of the acidic gases and the economics of constructing and operating the gas processing unit.

Almost all columns used in gas sweetening operation are constructed with carbon steel. Alkanolamine systems, particularly those which involve the handling of natural gas rich in carbon dioxide (CO_2) are particularly susceptible to corrosion problems. These problems are known to become more severe with an increase in the amine concentration, the acid gas loading of the amine solution and the temperature. The use of corrosion inhibitor chemicals is common practice to prevent or reduce the rate of equipment corrosion. It is however, standard practice to operate the amine absorption systems with strict operational limits. The range of permissible concentrations and rich amine loadings maintained in current commercial operation are described in Table 3.1.

Table 3.1 : Typical concentration and amine loading limits practiced in commercial operation of amine absorption systems [16]

Amine	**Concentration (wt %)**	**Rich amine loading (mol/mol)**
MEA	15 - 40	0.30 - 0.40
DEA	25 - 40	0.35 - 0.40
MDEA	50 - 55	0.45 - 0.50
DGA	30 - 70	0.35 - 0.40

3.1.2 Modifications for use in carbon capture

State-of-the-art amine absorption technology described in §§3.1.2 has to be suitably modified to be used for carbon capture. Unlike natural gas sweetening, where the sour gas is delivered to the absorber at high pressures; the feed to the amine absorber

in a carbon capture system is power plant exhaust - flue gas, at atmospheric pressure. In order to provide sufficient fluid head to overcome the pressure drop in the absorber column, a flue gas blower is installed upstream of the absorber. Even with the additional pressure, it is only economical to operate the absorber at around 150 kilopascals (kPa). The low operating pressure has another significant consequence - a low partial pressure for carbon dioxide (CO_2); the effects of which can be observed in the reaction rates, especially for the slower reacting amines like methyldiethanolamine (MDEA) and 2-amino-2-methyl-1-propanol (AMP). A more important difference gas sweetening and carbon capture though is the nature of the application itself. Natural gas sweetening is an essential step before any sour natural gas can be sold to industrial or residential consumers. Thus, the output of the gas sweetening operation is a value-added product which attracts revenue. Carbon capture on the contrary, in the current regulatory environment is similar to a tax; one that is an economic burden on the energy producers. For this reason, carbon capture demands a much tighter optimization of all available resources - capital, space, materials and energy than gas sweetening.

3.1.3 Remaining challenges

As discussed in §§3.1.2, the amine absorption process is energy intensive; requiring low pressure steam at 400 - 500 kilopascals (kPa) for continuous operation. At an existing pulverized coal (PC) power plant, the most convenient source of steam under current

setup is located upstream of the low pressure (LP) turbine. Drawing steam from the turbine system, however, will result in a decrease in the power plant electricity output. This loss of generation capacity along with the parasitic electric load of the process auxillaries like pumps, blowers and compressors will result in a net increase in the cost of electricity (CoE). It is estimated that the use of current technology at an existing coal-fired power plant will result in a 42 - 66 % increase in the cost of electricity (CoE) [42]. This includes the contributions of both the capital and operating expenses of the carbon capture process. This extent of increase in cost of electricity is considered unacceptable for economic reasons. Hence, researchers across the globe are engaged in developing solutions aimed at minimizing or eliminate any increase in cost of electricity (CoE) associated with carbon capture. In §3.2, we discuss the scope and development of current research work.

3.2 Current research and development

Current research on amine absorption technology for carbon capture can be classified to be focusing on two broad themes as described below:

- Developing better absorbents
- Process intensification

In the following subsections, we discuss some of the research developments that are most relevant to the research conducted as a part of this dissertation research.

3.2.1 Better absorbents

Several physical and chemical properties are of importance when selecting an absorbent for the amine absorption process. Desirable characteristics include a low molecular weight, high reaction rate and a low heat of reaction; whereas the undesirable ones are high cost, high volatility, corrosivity and toxicity. Primary amines such as monoethanolamine (MEA) and diglycolamine (DGA) have high reaction rates - significantly higher than those for secondary amines like diethanolamine (DEA). However, primary amines also have a higher heat of reaction as compared to secondary amines; which adversely affects the reboiler duty. Monoethanolamine (MEA) has a significantly higher volatility than other amines, which, in addition to its corrosivity; limits the absorbent concentration used in commercial operation. One of the main focal points for research on carbon capture has been to develop absorbents with reasonably fast reaction kinetics while maintaining a low heat of reaction [9].

Mitsubishi Heavy Industries (MHI) have developed their proprietary hindered amines (KS-1, KS-2 and KS-3), which are claimed to result in a significantly lower reboiler duty than monoethanolamine (MEA). Hindered amines are primary amines with bulky side groups which lead to substantial destabilization of the amine carbamate, resulting in a closer approach to the 1:1 stoichiometry which results in the formation of the amine bicarbonate. Carbamate instability results in a lower heat of reaction than the comparable primary amines - a favorable characteristic. However, the large side groups and unstable intermediates also result in thermodynamic con-

ditions which cause slower reactivity between the amine and carbon dioxide (CO_2). Mitsubishi Heavy Industries have reported a steam consumption for KS-1 that is 30% lower than that for monoethanolamine (MEA) [43].

Researchers at the University of Texas at Austin have been actively studying the use of piperazine to increase the reactivity of slower reacting amines and bicarbonates. Piperazine ($C_4H_{10}N_2$) is a cyclic diamine. Although a weak base itself, piperazine has a reactivity that is orders of magnitude higher than that of primary amines such as monoethanolamine (MEA) and diglycolamine (DGA) [44]. One approach adopted by the researchers involves the use of potassium carbonate (K_2CO_3) solutions blended with small quantities of piperazine. Potassium carbonate reacts with carbon dioxide (CO_2) to form potassium bicarbonate ($KHCO_3$). The reaction between potassium carbonate and carbon dioxide (CO_2) is slow, which makes it infeasible to use aqueous solutions of this salt by itself. However, the addition of piperazine promotes the reaction and depending on the conditions, can result in rates that are 2x - 3x higher than those for 30 wt% monoethanolamine (MEA) [45, 46]. One of the more recent efforts by the group involves the use of aqueous piperazine for carbon dioxide (CO_2) absorption. As discussed above, reaction kinetics studies with 0.6 M and 2.0 M solutions of piperazine have shown it to react significantly faster than commonly used primary amines. Although the use of aqueous piperazine hasn't yet progressed beyond pilot plant studies, it is estimated that the reboiler energy duty for piperazine is around 10% lower than for 30 wt% monoethanolamine (MEA) [47].

A very novel alternative to conventional absorbents has been presented with the invention of ionic liquids. Ionic liquids are salts that exist in a molten state at room temperature and thus have a very different set of physiochemical properties than conventional absorbents like alkanolamines which are all organic compounds with covalent bonds. Ionic liquids possess some very favorable features, the most notable ones being low volatility, high conductivity, high thermal stability and favorable solvating properties for a wide range of both polar and non-polar compounds. Carbon dioxide (CO_2) exhibits an exceptional solubility in numerous ionic liquids (ILs) and hence they are potential absorbents for its removal from flue gases. Several research groups in both academic and industrial settings are active in ionic liquid research. Researchers at Clarkson University, University of Tennessee and Oak Ridge National Laboratory (ORNL) investigated the use of ionic liquids for separation of carbon dioxide (CO_2)/ nitrogen (N_2) mixtures. Amongst the ionic liquids (ILs) examined, 1-butyl-3-methyl imidazolium bis[trifluoromethylsulfonyl] amide had the highest selectivity of 127 and a Henry's law constant (H) of 35 bar [48]. Researchers at Queen's University in Canbada and Georgia Institute of Technology synthesized a novel solvent which could be switched between a non-polar, non-ionic liquid and a polar ionic liquid by changing the atmosphere composition. They reported that a 1:1 mixture of 1,8-diazabicyclo-[5.4.0]-undec-7-ene (DBU) and 1-hexanol could be switched between a non-ionic and ionic liquid by addition and removal of carbon dioxide (CO_2) from its atmosphere. Thus, in an atmosphere composed mainly of carbon dioxide (CO_2);

the ionic liquid existed while under an atmosphere of nitrogen (N_2) it reverted back to the non-ionic form. This absorbent thus introduced a different class of absorbents which don't require heat to be supplied for regeneration [49]. Much research has been conducted in the field of ionic liquids since then with a focus on developing ionic liquids consisting of single salts, high carbon dioxide (CO_2) uptake capacity and low energy requirement for regeneration [50].

3.2.2 Process intensification

While selection of a good absorbent is of critical importance to the success of a gas separation process based on physical or chemical absorption, process configuration, operation and resource utilization are of equal importance. As discussed before, amine absorption technology has been in use for a long time. However, carbon capture as a target application is significantly different both in terms of resource availability and separation challenges. Thus, researchers have concentrated their focus on themes like process intensification, optimization and developing novel separation processes.

Researchers at University of Texas at Austin conducted simulation studies using AspenPlus to explore the performance of the amine absorption process using novel stripper configurations and operating conditions. As discussed in §§3.1.1, conventionally stripper columns have been operated between 150 kilopascals (kPa) and 200 kilopascals (kPa). The limiting factor in operating stripper columns at higher pressures is the thermal degradation of absorbents as well as equipment corrosion; both

of which worsen with an increase in the pressure and thus, the temperature. Development of novel absorbent formulations that are thermally stable at higher temperatures and use of corrosion inhibitors could potentially make it feasible to operate stripper columns at higher pressures than today. Based on this rationale, researchers explored system performance for stripper units operating at a higher pressure of 300 kilopascals (kPa). They found that operating at higher stripper pressures resulted in a reduced reboiler duty. In addition to high pressure strippers, they studied the viability of using vacuum strippers for carbon capture application. Vacuum strippers are an interesting possibility since they operate at lower temperatures than conventional strippers and open the possibility of using alternative energy sources such as waste heat, for absorbent regeneration. The team of researchers at University of Texas studied the performance of a vacuum stripper at 30 kilopascals (kPa) and found that although the stripping operation itself was feasible; under the selected operating conditions, the compression costs were infeasible [51, 52, 53].

Ammonia can be considered the simplest of all amines and thus, the most basic and most reactive. It has been long considered a theoritically superior substitute to the conventional alkanolamines used for carbon dioxide (CO_2) absorption. However, the use of ammonia in an absorption process poses very unique cchallenges; the most important of which is its extremely high volatility even at room temperature and potential problems with the solubility of ammonium bicarbonate formed by the reaction between ammonia and carbon dioxide (CO_2). Researchers at Alstom, how-

ever, were able to make a breakthrough into the use of aqueous ammonia solution as an absorbent with the development of their patented 'chilled ammonia process'. Like the conventional alkanolamine process, the chilled ammonia process has an absorber and a stripper column. However, to minimize the loss of ammonia through vaporization; the absorber is operated at a low temperature - between 2°C - 10°C. These below atmospheric temperatures are maintained with the use of a dedicated refrigeration unit which cools the absorber column. In addition, the process requires the use of additional equipment to reclaim ammonia escaping with the decarbonized flue gas [54, 55]. The reboiler steam requirement for the chilled ammonia process has been found to be comparable to that for monoethanolamine (MEA). However, due to higher reactivity and a reaction stoichiometry of 1:1 for the ammonia - carbon dioxide (CO_2) reaction; Alstom researchers believe that cost savings are achievable through smaller equipment and requirements for lesser absorbent chemicals.

Amidst efforts to modify the amine absorption process to make it more suitable for carbon capture application have been attempts to develop novel processes aimed at achieving cost savings by challenging conventional process configurations. One such notable effort was advanced by researchers at the Research Institute of Innovative Technology for the Earth (RITE) in Kyoto, Japan. They challenged the conventional setup of the amine absorption process which involves a separate absorber and stripper column and instead used a porous polymeric membrane such as a hollow fiber as the support to achieve both absorption and desorption. Early iterations of the the

'membrane flash process' involved co-current gas and liquid flow through a hollow fiber membrane. As the liquid flowed vertically upwards through the membrane, it absorbed carbon dioxide (CO_2) from the flue gas and simultaneously permeated out through the membrane. A combination of higher temperature and vacuum maintained on the exterior of the membrane resulted in release of the absorbed carbon dioxide (CO_2) through flashing. Since the process effectively employed vacuum stripping, absorbent regeneration was at a lower temperature and permitted the use of waste heat. As the process was developed further, scalability became a greater factor and the researchers decided to separate the absorber from the desorber. In the modified configuration, absorption still took place in a conventional column but to desorb the carbon dioxide (CO_2) a flash tank was used. Energy consumption for the membrane flash process was estimated at around 1.8 Gigajoules/ton-CO_2, significantly lower than that for monoethanolamine (MEA) [56, 57].

3.3 Scope for advancing carbon capture research

The discussion in §3.2 explains about current research initiatives to advance gas absorption technology to reduce the cost of carbon capture. However, few technologies have been commercialized. The main hindrance towards the commercialization of these novel processes has been cost - none of them has been successful in bringing a serious reduction in the cost of carbon capture. Major and minor problems can be identified with all the technologies discussed in previous sections; some of the more

prominent ones are discussed here.

Potassium carbonate promoted by piperazine was found to be a promising absorbent in lab studies. However, researchers at the University of Texas at Austin observed several incidents of foaming behavior with the absorbent in pilot plant studies [58]. Foaming problems in columns result in reduced mass transfer efficiency along with operational issues. Hence, absorbents susceptible to foaming problems are typically considered inferior to comparable non-foaming alternatives. Piperazine, which is currently promoted by University of Texas as a 2nd generation amine, capable of replacing monoethanolamine (MEA) suffers suffers from potential operational problems. Piperazine as well as the products of its reactions with carbon dioxide (CO_2) have limited solubility in water. This requires the operation of the absorption process within relatively strict tolerances to avoid the precipitation of salts which can result in equipment scaling and other problems. Additionally, piperazine does not biodegrade and is reported to form nitrosamines when in contact with nitrogen oxides (NO_x) [59]. Ionic liquids are currently at early stages of development and it will require significant amounts of optimization, lab and pilot scale testing before industrial operators adopt them for use.

We have previously discussed the potential for achieving energy savings by modifying the operating conditions for the amine absorption process. Further, operating the stripper unit under vacuum create opportunities to use waste heat; which can significantly reduce economic costs. However, when researchers at University of Texas

studied the performance of the amine absorption process utilizing a vacuum stripper operating at 30 kilopascals (kPa); they concluded that the process was infeasible due to enormous compression costs and decided not to pursue further research. This conclusion, however, has been drawn based on a few unrealistic assumptions. In their work, the researchers assumed that because the vacuum stripper was operating at 30 kilopascals (kPa); separated carbon dioxide (CO_2) would be delivered to the compression train at the same pressure. Thus, it seems to have been assumed that vacuum pumps will be used in an industrial-scale stripper column - an impractical proposition. Further, an operating pressure of 30 kilopascals (kPa) itself is low and it may be possible to operate under vacuum but much closer to atmospheric pressure. Thus, a more complete study is required to assess the potential of vacuum stripping and waste heat use. Similarly, it has been claimed by researchers at Alstom that the chilled ammonia process is superior to conventional amine absorption. However, the comparisons they present are based on reboiler duty alone. It has been shown through detailed studies by independent groups that additional refrigeration required to cool the absorber increases the energy penalty of the chilled ammonia process by a significant enough margin that it cannot be discounted [60]. The membrane flash process suffered from flow instability problems in addition to the inherent problem of scalability to industrial operation.

3.4 Direction of our research work

The direction of our research has been motivated by novel, original ideas and the desire to advance promising concepts previously studied. The research performed as a part of this dissertation can be divided into three distinct parts, as follows:

- **Exploring the viability of the use of waste heat for absorbent regeneration in carbon capture application**

In this part of our work, we have used the process modeling software - ProMax to study the performance of the amine absorption process under different stripper operating conditions. While keeping the energy source (60 psia steam) constant, we explore the effect of varying the stripper operating pressure between 150 kilopascals (kPa) and 300 kilopascals (kPa). Similarly, we study the effect of varying the vacuum in a stripper column between 30 kilopascals (kPa) and 75 kilopascals (kPa), while using waste heat (20 psia steam). Based on the sizes and rating for various equipment, we calculate the capital cost of each scenario using Aspen Process Economics Analyzer software.

- **Developing superior absorbents**

We have performed a detailed analysis of the distribution of energy to the various physiochemical processes taking place in the reboiler and stripper column. This analysis revealed that the two processes responsible for consuming a majority of the energy in the reboiler and stripper are the energy required for heating the amine solution entering the stripper and the energy consumed to vaporize water to generate stripping

vapor. This knowledge has helped us identify superior absorbent formulations that are estimated to reduce energy consumption by between 20 - 25%.

- **Developing the 'combined pressure and temperature contrast process for carbon dioxide (CO_2) separation'**

In the final part of the work performed as a part of this dissertation, we work on developing a process that combines the absorber and stripper column into a single integrated unit. The objective of combining them is driven by the desire to reduce equipment size, auxiliary equipment and to potentially achieve better heat integration. We use novel ceramic materials called ceramic foams which have significantly higher surface area than conventional tower packing as gas-liquid contactors. The tasks performed towards this project have aimed as taking an original concept and moving it through various stages of process development to eventually conducting a proof-of-concept demonstration of the novel process.

In the following chapters, we discuss our research efforts, present our analysis and draw conclusions about the viability of these ideas.

Chapter 4

Effects of variation in stripper operating pressure on the performance of the amine absorption process for carbon capture: a technical perspective

4.1 Motivation

Alkanolamine absorption is considered to be the most deploy-ready technology for carbon dioxide (CO_2) removal from power plant flue gas. Extensive operational experience is available about this process due to its widespread use in natural gas sweetening application. A notable difference between the two applications of the same technology, however, is the availability of energy resources at the plant location. Amine absorption units are an integral part of a gas sweetening plant and boilers to provide process steam are incorporated into original plant design. Existing coal and natural gas fired power plants, however, will be retrofitted with this technology and required steam must be sourced through reconfiguration or existing resources or added at the facility. While a coal fired power plant, likely will not have sufficient capacity to provide process steam to the stripper unit(s); there is a higher likelihood

of large, waste heat sources being available at these power generation utilities. The conventional amine absorption process, as adapted for carbon capture employs an absorber column operating at a pressure close to atmospheric and a stripper unit operated between 150 kilopascals (kPa) and 200 kilopascals (kPa). A majority of the energy consumed in the amine absorption process is utilized towards absorbent regeneration. Thus, it can be expected that system performance as gauged by reboiler energy duty and process economics is sensitive to a change in the stripper operating conditions. Further, by operating the stripper column under low vacuum conditions; it could be possible to use waste heat for absorbent regeneration instead of low pressure steam. The work discussed in this chapter describes our research into studying the effects of operating the stripper column at pressures ranging from 30 kilopascals (kPa) and 300 kilopascals (MPa) and exploring the feasibility of the use of waste heat for absorbent regeneration.

4.2 Research approach

4.2.1 ProMax and amine systems modeling

As described in 3.1.1, the absorption of carbon dioxide (CO_2) in alkanolamine solutions is accompanied by exothermic reactions. The reaction occurs in the liquid phase (amine) in a film close to the gas - liquid interface. This enhances the carbon dioxide (CO_2)mass transfer. It also results in a coupling of the reaction kinetics, mass and heat transfer phenomena. Traditionally, modeling of reactive absorption systems

has been based on the equilibrium stage model, which assumes that each gas stream leaving a tray or a packing segment (stage) is in thermodynamic equilibrium with the corresponding liquid stream. However, the assumption of thermodynamic equilibrium is seldom realized in actual operation. To account for these physical realities, correlation parameters such as tray efficiencies and height-equivalent-to-theoretical-plate (HETP) are used. However, these simplified concepts fail for multicomponent mixtures; which is the case for amine absorption. In the view of the failure of these simplified approaches to modeling, a more physically consistent approach which involves the direct evaluation of the rates of multicomponent mass and heat transfer and reaction kinetics must be adopted. Additionally, the presence of alkanolamines, carbon dioxide (CO_2) and their intermediates in aqueous solutions results in their ionization which leads to large non-idealities in their behavior. These must be accounted for with the use of suitable models for electrolytes [13, 61, 62]. Figure 4.1 shows the variations in the complexity of the different models used most commonly.

Due to the involvement of such complexity in predicting the performance of amine absorption units, we have selected a process simulation software, ProMax (developed by Bryan Research & Engineering), to model the operation of the amine absorption process under different conditions. ProMax has a built-in package, TSWEET which accounts for the amine - CO_2 reaction kinetics in the absorber. The actual mechanism which limits the rate of carbon dioxide (CO_2) absorption in amines is its ionization in water. This is handled in ProMax by the TSWEET kinetics model which is analogous

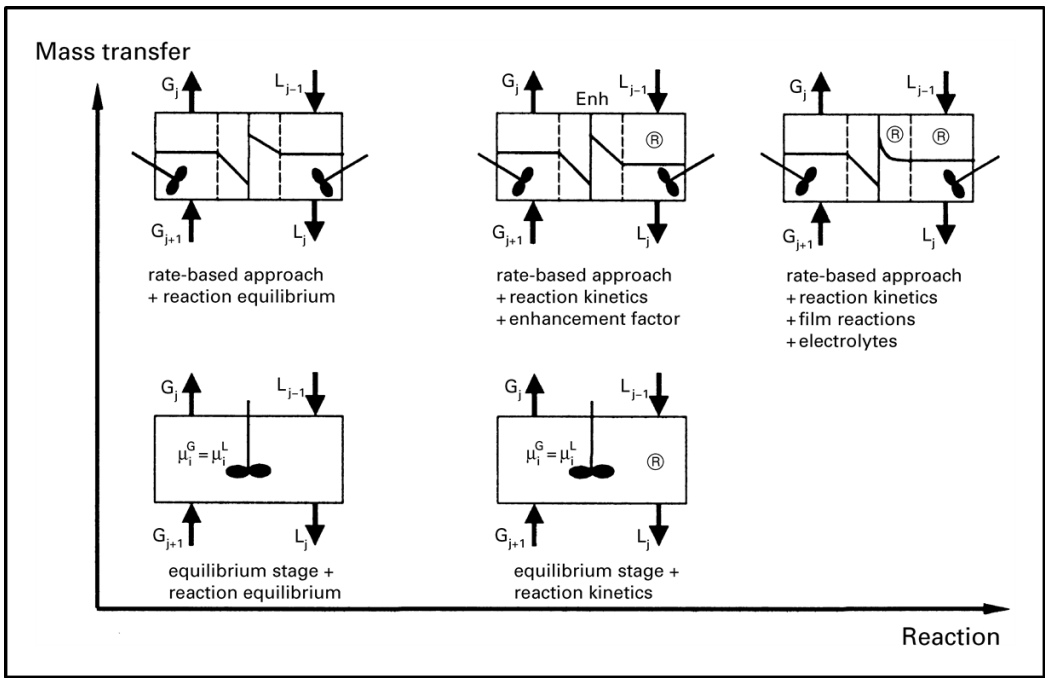

Figure 4.1 : Graphic explanation of model complexity [13]

to a liquid-side resistance in a mass transfer model. The TSWEET kinetics model calculates simultaneous distillation and chemical reaction to account for the relatively slow CO_2 - amine reaction rate. The total contacting time between the sour gas and the absorbent streams is a major factor in determining the amount of carbon dioxide (CO_2) picked up. In ProMax, columns are often simulated using ideal trays rather than real trays. The liquid residence time on an individual tray is evaluated based on the tray geometry and further used to evaluate the total residence time in the column by multiplying it with the ratio of ideal to real stages. ProMax has been demonstrated to be reliable in predicting the performance of amine gas sweetening units under a variety of system operating conditions [63, 64, 65]. In addition to accurately modeling amine absorption, ProMax has in-built functionalities to provide

several analyses useful for optimizing the amine absorption process. This includes an evaluation of the acid gas loading of the amine solution and a calculation of the lean and rich approach of the amine solution (which aids in fine-tuning the absorbent flow-rate).

4.2.2 Flowsheet development

For the purposes of our study, we have designed flowsheets for the amine absorption train, the carbon dioxide (CO_2) compression train and the glycol dehydration plant. Figure 4.2 and 4.3 show the flowsheets developed for studying the amine absorption process with high pressure strippers and vacuum strippers respectively. Flue gas enters the system at atmospheric pressure. A blower pressurizes the flue gas in order to overcome pressure drop encountered in the absorber column. Before entering the carbon capture unit, flue gas passes through the Flue Gas Desulfurization (FGD) unit which reduces the sulfur oxides (SO_x) concentration to around 100 ppmv [66]. Sulfur oxides (SO_x) compounds form Heat Stable Salts (HSS) with alkanolamines which result in absorbent losses. To minimize these losses, the flue gas is passed through a polishing scrubber where the Sulfur oxides (SO_x) concentration is reduced to 10 ppmv by contacting it with a dilute sodium hydroxide solution [67]. After passing through the polishing scrubber, flue gas enters a cooler where it's temperature is brought down to around 30^oC. At this temperature, flue gas enters the absorber column. Lean amine solution flows in at the top of the absorber at a temperature of

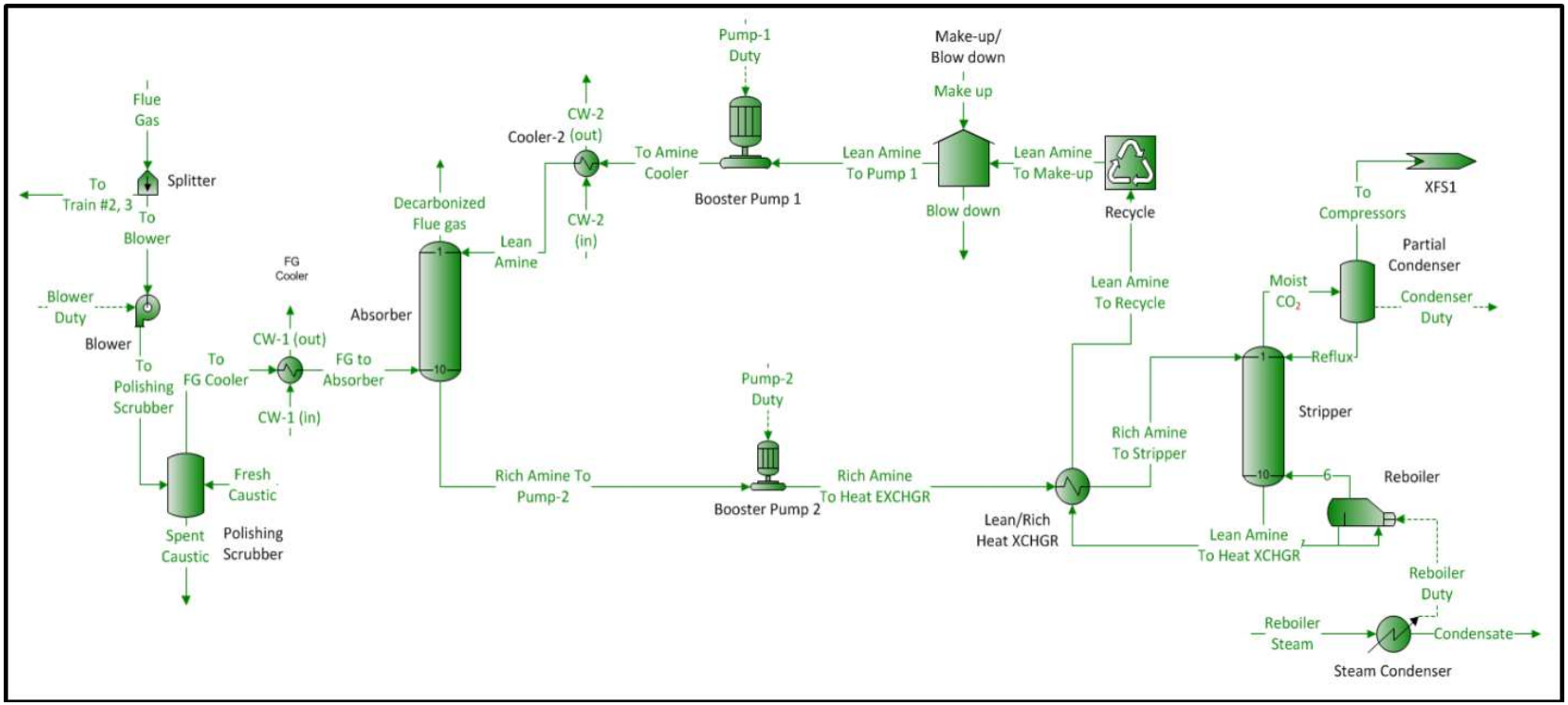

Figure 4.2 : Flowsheet for the amine absorption process for CO_2 separation with high pressure strippers

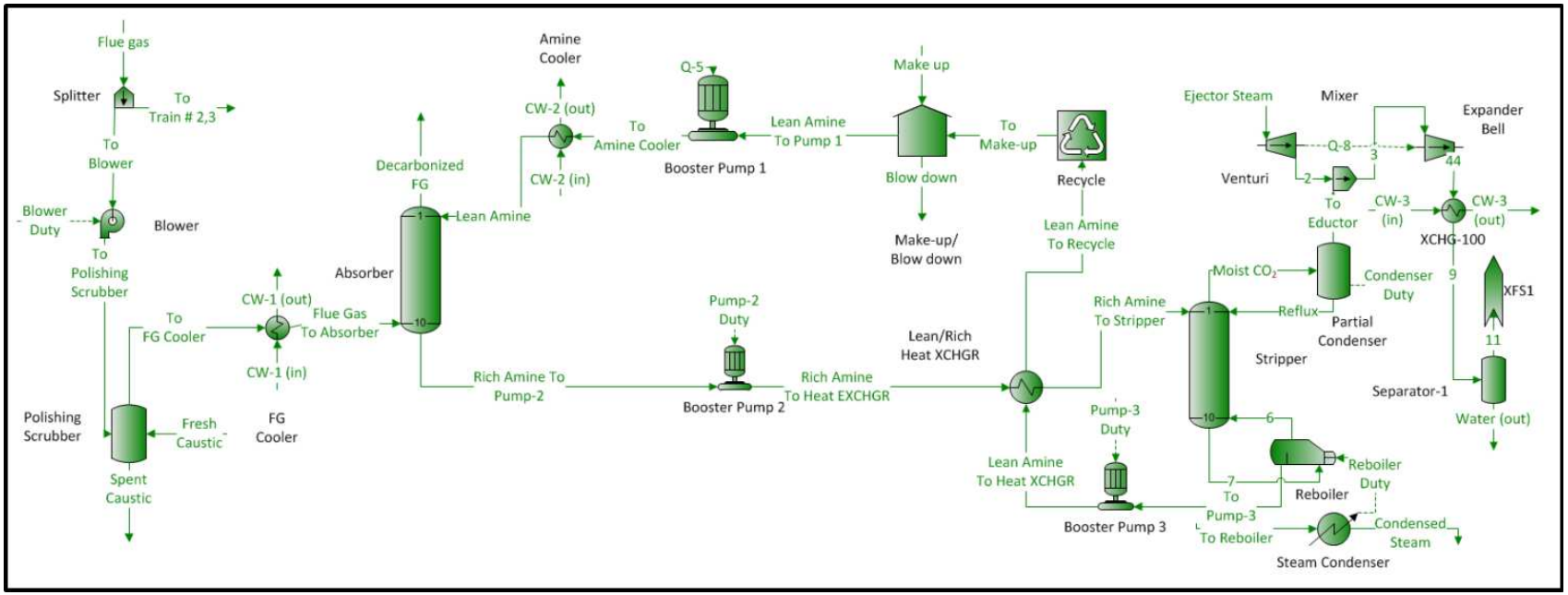

Figure 4.3 : Flowsheet for the amine absorption process for CO_2 separation with vacuum strippers

45^oC. As the amine solution flows down, carbon dioxide (CO_2) from flue gas dissolves in the absorbent and reacts reversibly with the amine to form a soluble intermediate. The amine - CO_2 reaction is exothermic and results in a moderate increase in the solution temperature. The decarbonized flue gas leaves the absorber column at the top along with some absorbent vapors. For volatile amines like monoethanolamine (MEA), these losses can be significant and a water wash section at the top of the absorber is required to recover lost absorbent. Rich amine solution exits the absorber at the bottom, where a booster pump provides the hydraulic head to overcome the flow resistances downstream. Rich amine solution from the absorber is contacted with hot lean amine exiting the reboiler in a heat exchanger to transfer sensible heat. After passing through the heat exchanger, lean amine enters a make-up/blow-down unit where water and/or amine is added or removed to maintain the set absorbent concentration and flow rate. A booster pump provides pressure head to the lean amine. At this point, lean amine temperature is around 65^oC which is brought down to 45^oC in the amine cooler. Rich amine solution enters the stripper, where the amine - CO_2 intermediate dissociates to release the carbon dioxide (CO_2) and amine molecules. Energy for the stripping process is provided by steam to a reboiler located at the base of the stripper column.

When operating the stripper under vacuum, a mechanical assembly called a 'steam jet ejector' is used to create and maintain vacuum in the column. Figure 4.4 is a schematic representation of a steam jet ejector. A steam jet ejector works on the

concept of a converting - diverging nozzle to transform the pressure energy of a motive fluid to kinetic energy which creates a low pressure zone which draws and entrains the suction fluid [68]. In industrial processes, steam jet ejectors are preferred to vacuum pumps due to their simplicity, absence of moving parts and the resulting reliability. Steam jet ejectors have a low isentropic efficiency of around 80% and require high pressure steam as a motive fluid. Carbon dioxide (CO_2) along with water vapor exits the stripper at the top. It passes through a partial condenser where most of the water vapor condenses and is refluxed back into the stripper. In case of vacuum strippers, an additional gas-liquid separator is used to separate out the condensed steam from the ejector.

Carbon dioxide (CO_2) leaving the condenser enters a compressor–intercooler train for compression to a pipeline pressure of 16 MPa. Before the compressed carbon dioxide (CO_2) can, however, be moved to the pipeline; it must be conditioned appropriately to lower its water content below 150 ppm. At high pressures and low temperatures, such as those prevalent in the pipeline transport, the presence of water can lead to formation of hydrate plugs; a major flow assurance problem. The compressed carbon dioxide (CO_2) is conditioned by contacting it with triethylene glycol (TEG) in glycol dehydration unit. Once conditioned, the compressed carbon dioxide (CO_2) is ready to be transported. Figures 4.5 and 4.6 show the compression trains used for high pressure strippers and vacuum strippers respectively. Separated carbon dioxide (CO_2) from amine trains with vacuum strippers is delivered to the

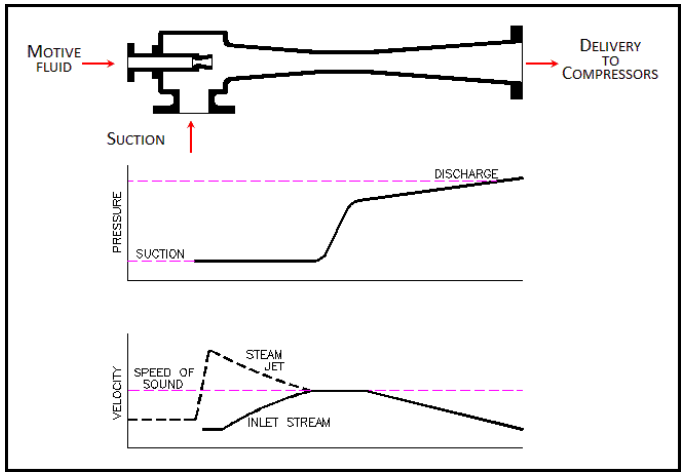

Figure 4.4 : Schematic representation of a steam jet ejector [14]

compression train at atmospheric pressure, lower than from the high pressure strippers. This results in the requirement of an additional compressor in the train. Figure 4.7 shows the glycol dehydration unit where the compressed carbon dioxide (CO_2) is conditioned to make it suitable for transportation.

4.2.3 Evaluating parasitic power loss

At a power plant retrofitted with amine absorption technology for carbon capture, there are several energy sinks that lead to a reduction in the net power output. In addition to the reboiler energy duty, which is the most significant of energy loads; plant auxiliaries such as flue gas blowers and pumps and compressors contribute to the reduction in output. The cumulative loss in plant output expected due to these energy sinks is termed as parasitic power loss. Energy consumed in the reboiler is typically reported as energy consumed per unit mass of carbon dioxide (CO_2) separated.

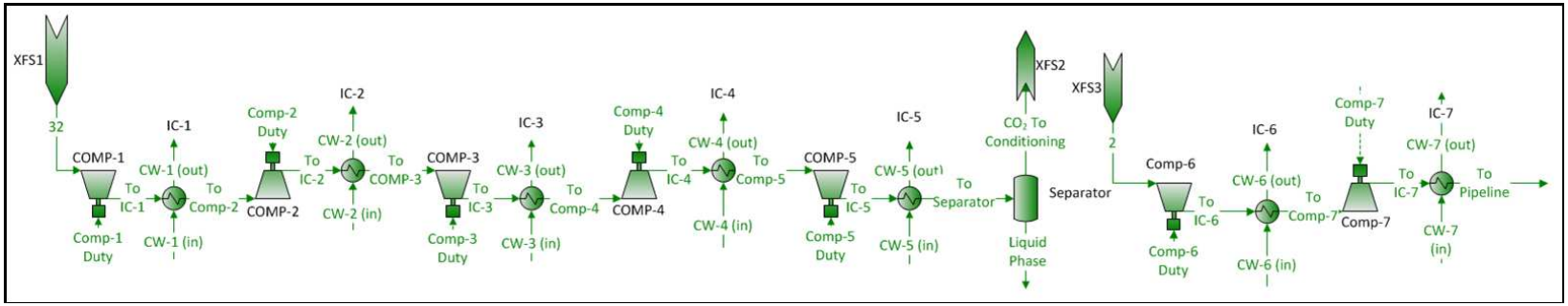

Figure 4.5 : Flowsheet for the compression of CO_2 separated with amine absorption trains using high pressure strippers

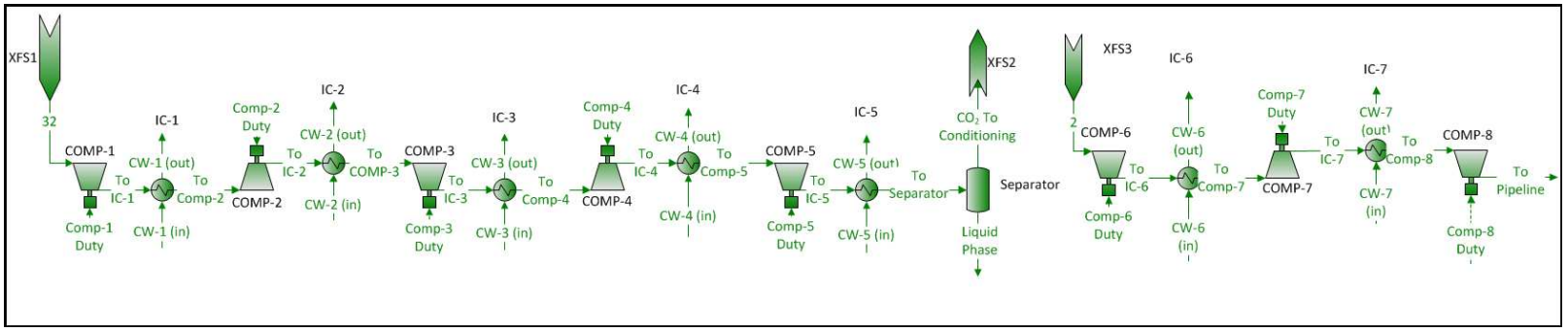

Figure 4.6 : Flowsheet for the compression of CO_2 separated with amine absorption trains using vacuum strippers

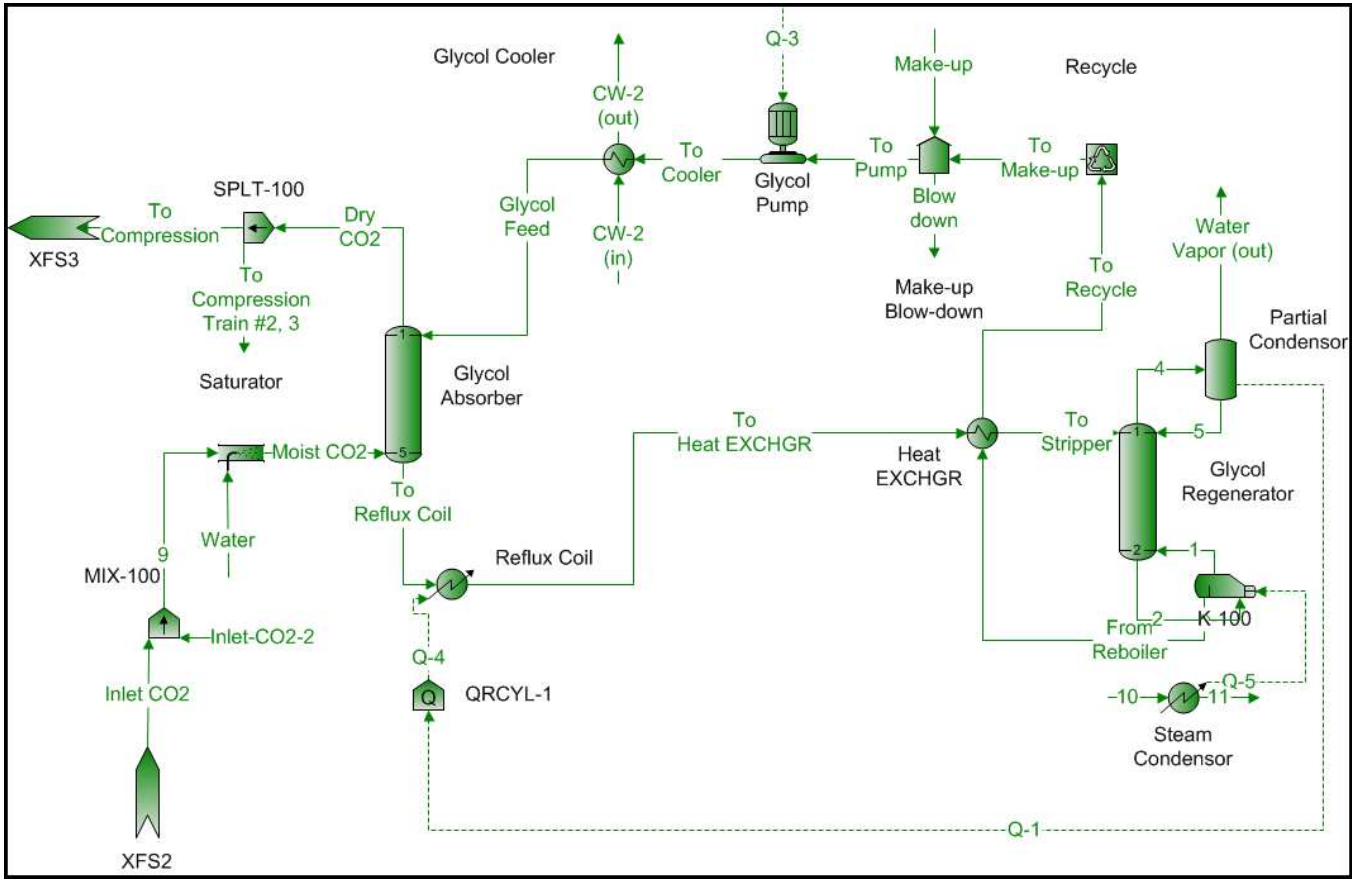

Figure 4.7 : Flowsheet for the glycol dehydration unit for conditioning CO_2 before transportation

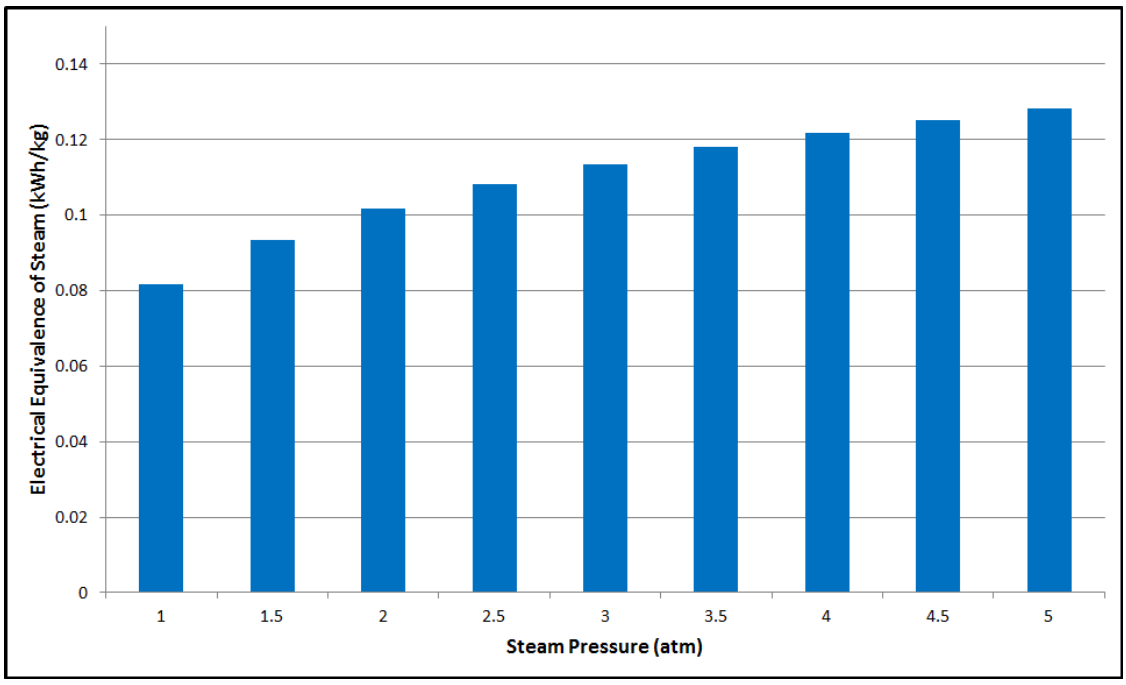

Figure 4.8 : Electric power equivalence of low pressure steam

However, such an evaluation is based on enthalpic considerations and is hence, independent of the equivalent work that can be extracted from the steam used in the reboiler. It is a well-understood fact that the equivalent work capacity of steam varies with pressure. Figure 4.8 shows a plot of the change in the electrical equivalence of steam with it's pressure.

Thus, the real impact of the carbon capture installation at a power plant can be gauged only by calculating the parasitic power loss, including the reduction in electrical output due to the reboiler. Some basic parameters are required to calculate the electrical equivalence of reboiler steam. These are compiled in Table 4.1. Assuming the expansion of steam through the turbine to isentropic, the amount of steam required to generate one unit of electricity depends only on the inlet and outlet

conditions of steam and the efficiency of the turbine. The relation between these is described in Equation 4.1 where the units of the steam flow rate are $\frac{kg}{kWh}$, η_t is the turbine efficiency, H_1 is the mass enthalpy of the steam at its inlet pressure and temperature into the low pressure (LP) turbine and H_{2s} is the mass enthalpy at exit pressure and the entropy corresponding to the inlet conditions [69]. It is known that the low pressure (LP) turbine contributes around 45% of the electric output of the power plant [18]. This allows for the calculation of the steam circulation rate to the low pressure (LP) turbine which is 324.4 kg/s. With the plant setup remaining unaltered, this is the maximum amount of steam available to the reboiler. For each simulation case, the reboiler steam consumption is known. This allows for evaluation of the power generated by the reboiler steam and thus, its contribution to the parasitic power loss.

4.2.4 Process and simulation parameters

A typical 400 MegaWatts (MW) coal–fired power plant emits approximately 3 million toness/year of carbon dioxide (CO_2) [70]. The corresponding flue gas flow rate is approximately 32 Million Sm^3/day, which is the flow rate used in this study. The molar composition of flue gas used in this study is provided in Table 4.2 [19].

$$Steam\,rate = \frac{1548.1}{\eta_t \cdot (H_1 - H_{2s})} \tag{4.1}$$

Table 4.1 : Parameters for Evaluation of Equivalent Power Losses [17, 18]

Parameters for Evaluation of Equivalent Power Loss				
Steam to: ↓ / Properties: →	**Pressure (kPa)**	**Temperature (^oC)**	**Enthalpy ($\frac{kJ}{kg}$)**	**Entropy ($\frac{kJ}{kg^oC}$)**
LP Turbine	630	284.6	3029.4	7.3
High Pressure Strippers	413.7	144	2928	7.3
Vacuum Strippers	122	140	2684	7.3
Downstream Condenser	5.52	34.5	2236.2	7.3
Steam Jet Ejector	630	284.6	3029.4	7.3

Table 4.2 : Composition of flue gas used in simulation studies [19]

Component	Value (mole %)
Water (H_2O)	11.69
Carbon dioxide (CO_2)	14.59
Oxygen (O_2)	2.85
Nitrogen (N_2)	69.95
Sulfur dioxide (SO_2)	0.01
Argon (Ar	0.91

As can be seen, the carbon dioxide (CO_2) concentration in flue gas is low which results in a low partial pressure. These are unfavorable conditions for the absorption of carbon dioxide (CO_2) into the absorbent. Coal combustion occurs in the presence of excess air, leading to the presence of unused oxygen in flue gas. Oxygen reacts with the alkanolamines and results in absorbent degradation problems. A single absorber – stripper train configuration results in an impractically large equipment design on account of the large flue gas, absorbent and stripping vapor flow rates to be handled. Hence, we use a 3 absorber - stripper train configuration for this study. We examine the performance of three alkanolamines; monoethanolamine (MEA) - a fast reacting primary amine with high heat of regeneration, diethanolamine(DEA) - a slow reacting secondary amine with a low heat of regeneration and diglycolamine(DGA) - another fast reacting primary amine with a high heat of reaction but lower vapor pressure

than monoethanolamine(MEA). In order to simulate the amine absorption process under conditions similar to those maintained in commercial practice, we introduce the following constraints and guides.

1. At least 90% of the entering carbon dioxide (CO_2) must be captured and compressed [71].

2. All amines are studied at the typical concentrations that they are used at in commercial practice. These are: monoethanolamine(MEA) - 20 wt%, diethanolamine(DEA) - 40 wt% and diglycolamine(DGA) - 60 wt% [9].

3. The maximum carbon dioxide (CO_2) loading of amine solutions is 0.4 moles-CO_2/ mole-amine [9, 16].

Corrosion problems in carbon steel equipment with alkanolamines, especially at high concentrations and high solution loadings are quite well known. It is possible to achieve significantly higher carbon dioxide (CO_2) loadings by switching to stainless steel equipment; however it comes at a significantly higher cost. Stainless steel is 2 – 3x more expensive than carbon steel. While it can be argued that the higher cost maybe justified by lowered parasitic power losses, carbon steel equipment represents current technology that has been found to be reliable and economically feasible. This forms the scientific rationale behind the constraints imposed above. Monoethanolamine (MEA) and diglycolamine (DGA) react with carbon dioxide (CO_2) much faster than diethanolamine (DEA); thus requiring fewer trays/stages in the ab-

sorber column. In this study, we used absorber columns with 2 ideal stages for all monoethanolamine (MEA) and diglycolamine (DGA) simulations and 10 ideal stages for all diethanolamine (DEA) cases. Various simulation parameters used in this study are compiled in Table 4.3.

Heat exchangers are important pieces of equipment at amine absorption facilities. Two of the most critical heat exchangers in the amine absorption flowsheet shown in Figures 4.2 and 4.3 are the lean/rich amine heat exchanger and the reboiler. Two key parameters which decide the sizing of the heat exchanger units are the end approach temperature and the energy duty (quantity of heat transferred). Both these parameters for the two heat exchangers for the different simulation cases are tabulated in Table 4.4. With an objective of avoiding excessive complexity, in this study, we have chosen to vary the reboiler steam properties only when transitioning from amine absorption units with vacuum strippers to those with high pressure strippers.

4.3 Results and analysis

4.3.1 Effect of stripper operating pressure on reboiler heat duty

Energy provided to the reboiler is consumed for heating the rich amine solution entering the stripper, to drive the amine–CO_2 desorption reaction and to vaporize water to generate stripping vapor (steam). A conventional stripper column is operated between 150 kilopascals (kPa) – 200 kilopascals (kPa) and at a temperature of around 105^{o} – 110^{o}; depending on the choice of absorbent. Stripper operating temperature

Table 4.3 : System parameters used in ProMax simulations

Parameter	Vacuum Strippers	High Pressure Strippers
Flooding Fraction	0.8	0.8
Tray Type	Sieve	Sieve
Tray Spacing	0.61 meters	0.61 meters
Weir Height	0.076 meters	0.076 meters
Condenser Temperature	30° C	30° C
Absorber # of Trays (MEA, DGA)	2	2
Absorber # of Trays (DEA)	10	10
Stripper # of Trays (MEA, DGA)	15	10
Stripper # of Trays (DEA)	10	10
Heat Exchanger End Approach Temperature	5° C	5° C
Steam Jet Ejector Delivery Pressure	101.3 (kPa)	101.3 (kPa)
Contribution of LP Turbine to Plant Output	45 %	45 %
Overall Efficiency of Turbine–Generator System	70 %	70 %
Isentropic Efficiency of Steam Jet Ejector	80 %	80 %
Steam flow to LP Turbine	324.4 (kg/s)	324.4 (kg/s)

Table 4.4 : Heat exchanger parameters in the amine absorption system simulations

Stripper Pressure (kPa) ↓	**Heat Exchanger Duty**			**Reboiler End Approach**			**Reboiler Duty**		
Absorbent →	MEA	DEA	DGA	MEA	DEA	DGA	MEA	DEA	DGA
30	111.4	30.50	37.50	33.80	34.80	32.00	499.5	139.8	219.1
50	175.6	63.00	47.40	21.70	23.00	20.00	341.7	122.7	163.0
75	207.4	92.50	53.80	11.30	14.70	09.80	280.4	112.2	136.7
150	218.2	137.1	89.10	32.40	34.30	34.00	215.1	104.7	99.90
175	187.2	149.2	96.20	27.60	30.30	31.70	181.3	102.2	91.90
200	190.3	168.9	101.9	23.5	28.1	28.9	161.1	99.5	89.8
250	189.2	187.8	111.6	16.2	22.3	24.3	141.0	97.0	87.1
300	197.6	203.5	119.1	10.1	17.5	20.8	131.3	94.8	84.7

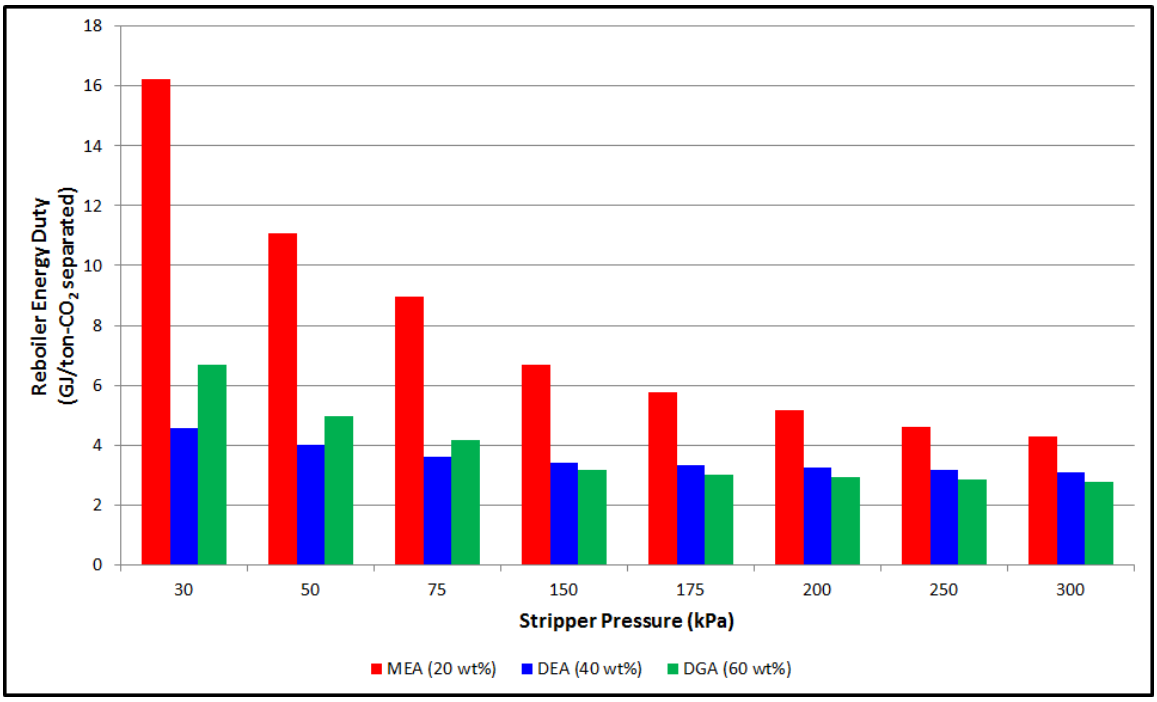

Figure 4.9 : Dependence of reboiler energy duty on stripper operating pressure

increases with pressure.As the stripper operating temperature increases, $\frac{p_{H_2O}}{p_{CO_2}}$; the ratio of the partial pressure of water to that of CO_2 in equilibrium with the amine solution decreases and results in a decreased stripping vapor (steam) requirement. Since, in this case the stripping vapor is steam; an increased stripper pressure results in a decrease in the total reboiler duty. Figure 4.9 shows the reboiler energy duty for separation of CO_2 for 20 wt% MEA, 40 wt% DEA and 60 wt% DGA.

The most noticeable feature of the plot is the significantly higher reboiler duty of monoethanolamine (MEA) for all the simulation cases. It is particularly large for the vacuum stripper cases, ranging from 16.2 GJ/ton-CO_2 for the 30 kilopascals (kPa) stripper to 9.0 GJ/ton-CO_2 for a stripper operating at 75 kilopascals to 4.3

GJ/ton-CO_2 for the 300 kilopascals (kPa) stripper. This trend of a gradual reduction in the reboiler energy duty with an increase in stripper pressure is also observed for diethanolamine (DEA) and diglycolamine (DGA). However, the reboiler duty for both diethanolamine (DEA) and diglycolamine (DGA) are significantly lower. It varies from 4.6 GJ/ton-CO_2 to 3.1 GJ/ton-CO_2 for diethanolamine (DEA) when the pressure is increased from 30 kilopascals (kPa) to 300 kilopascals (kPa). Under the same range of conditions, the reboiler duty for diglycolamine (DGA) decreases from 6.7 GJ/ton-CO_2 to 2.8 GJ/ton–CO_2. Where diglycolamine (DGA) has an advantage over diethanolamine (DEA) is in that diglycolamine (DGA) solutions can be used at a significantly higher concentration without serious corrosion or solvent loss problems. In spite of this, diethanolamine (DEA) has a lower reboiler duty than diglycolamine (DGA) in vacuum strippers; mainly because the diglycolamine–CO_2 complex is more stable than the corresponding diethanolamine (DEA) complex. This results in a lower equilibrium partial pressure for carbon dioxide (CO_2) in the stripper column, requiring larger quantities of stripping steam for dilution. However, the absorbent performance in high pressure strippers is significantly different, with 60 wt% diglycolamine (DGA) having a reboiler duty that is almost 10% lower than the 40 wt% diethanolamine (DEA). The decrease is energy consumption is primarily a result of reduced stripping vapor (steam) requirement. A detailed analysis of the contributions of the 3 constituent processes of absorbent stripping is given in §§6.2.

The reboiler duty values for monoethanolamine (MEA) in published literature

when the carbon dioxide (CO_2) concentration of flue gas is around 15% lie between 3.57 GJ/ton-CO_2 and 4.01 GJ/ton-CO_2. The reboiler duty value we report for monoethanolamine (MEA) with the 200 kilopascals (kPa) stripper is around 5.8 GJ/ton-CO_2 which is close to twice the previously reported value. To understand this, we must refer back to §§4.2.4 where we discussed that rich amine loading must be maintained below 0.4 moles-CO_2 mole-amine to avoid excessive corrosion. The carbamate formed by the reaction between monoethanolamine (MEA) and carbon dioxide (CO_2) is reasonably stable. In order to constrain the amine loadings, higher amine circulation and steam flow rate must be maintained. With other parameters unchanged, an increase in the amine circulation rate or the reboiler steam flow results in an increased carbon dioxide (CO_2) pickup in the absorber and consequently a higher rich amine loading. Consequently, significantly larger amounts of energy must be provided to the reboiler to maintain lower rich amine loadings. The reboiler duty for monoethanolamine (MEA) and diglycolamine (DGA) when the rich amine loading is constrained to 0.4 mole–CO_2/ mole-amine is similar to the value of 5.6 GJ/ton-CO_2, reported elsewhere in published literature [72].

4.3.2 Effect of stripper operating pressure on column sizing

In the design of an amine absorption unit, energy consumption is the most important contributor to the operating costs. One of the significant contributions to the capital investment is the absorber and stripper column size, which is also strongly

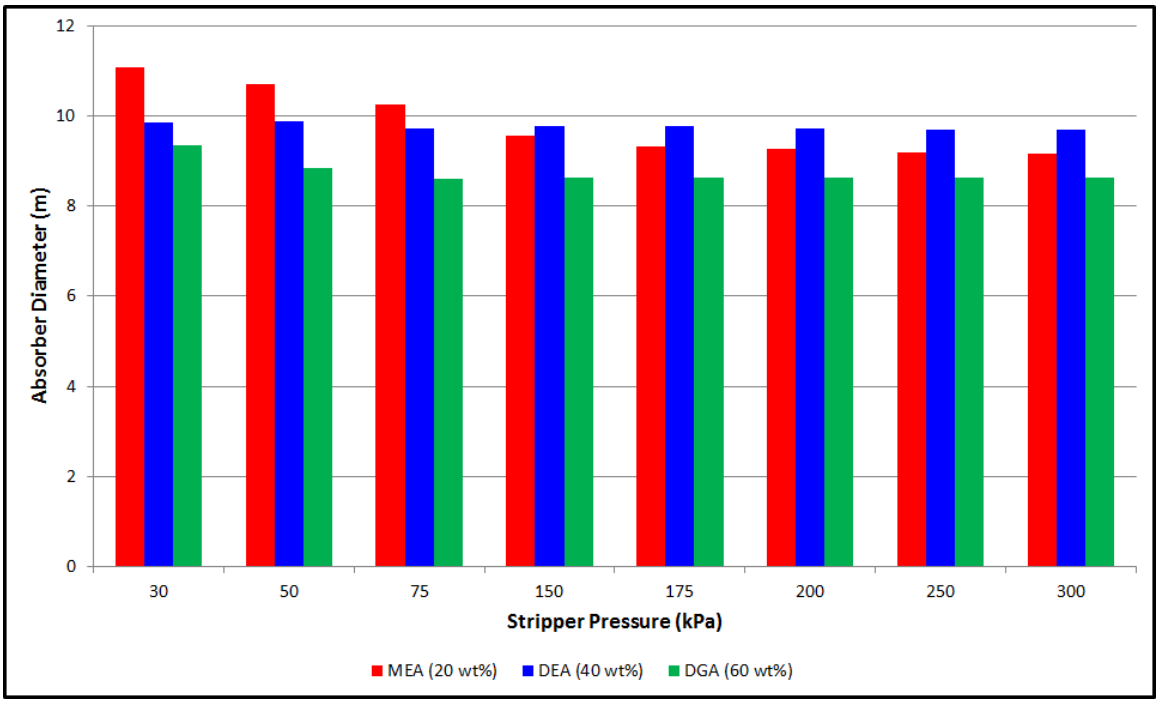

Figure 4.10 : Dependence of absorber diameter on stripper operating pressure

influenced by amine selection. ProMax uses the degree of fractional flooding as an input parameter to calculate column diameter. As disclosed in Table 4.3, all columns in this study are set to operate at 80% flooding. Figure 4.10 shows the effect of amine selection and stripper operating pressure on absorber diameter. It can be seen that the absorber diameter varies only marginally depending on the amine selected and the stripper pressure. This is because the most important factor influencing column diameters is the vapor flowrate. Since, in all cases flue gas inflow rate of flue gas remains constant, there's only a small change in the absorber diameter.

Figure 4.11 shows the effect of the stripper pressure and amine choice on the stripper diameter. Unlike absorbers; the stripper column shows a strong dependence

on both the choice of amines and the stripper pressure. As before, this can be explained by observing the vapor inflow rates to the stripper. As the stripper pressure increases, the stripping vapor (steam) requirement reduces. Due to an increase in the stripper pressure, there is also a reduction in the volume of the stripping vapor (steam) and the carbon dioxide (CO_2) flowing inside the column. These two factors combine to reduce the overall vapor flow rate in the stripper column which consequently reduces the stripper size. Since monoethanolamine (MEA) has the highest stripping vapor (steam) requirement it requires the largest stripper column for all amines compared, irrespective of stripper pressure. As with the reboiler heat duty however, diethanolamine (DEA) use requires smaller strippers than diglycolamine (DGA) with vacuum strippers. At higher pressures, strippers used for diglycolamine (DGA) are smaller than those used for diethanolamine (DEA).

4.3.3 Effect of stripper operating pressure on heat exchanger sizing

In addition to the absorber and stripper columns, the rich/lean heat exchanger is a critical and expensive piece of equipment at an amine absorption plant. Heat exchangers are typically rated on the basis of their surface area which is dependent on their heat duty and the temperature driving force. In all the simulations developed in this study, we have maintained a end approach temperature in the rich/lean heat exchanger at 5 ^{o}C. Thus, the energy duty is a reasonable measure for the heat exchanger sizing. Heat exchanger duties for all three absorbents at stripper operat-

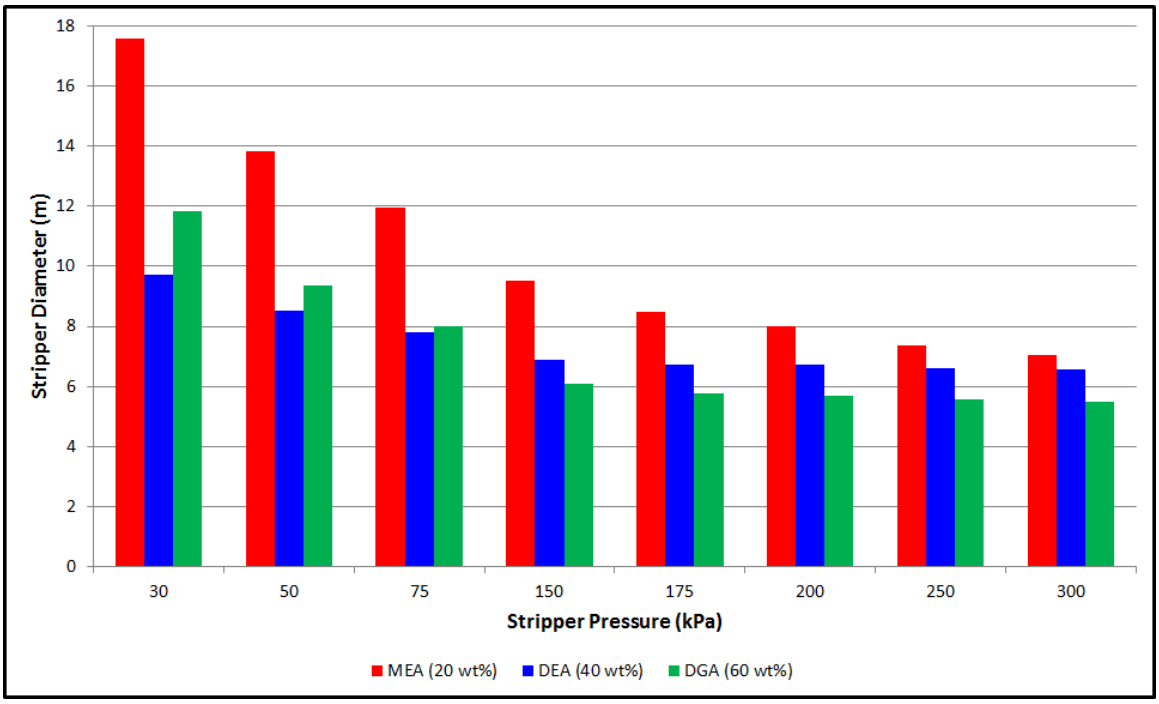

Figure 4.11 : Dependence of stripper diameter on stripper operating pressure

ing pressures between 30 kilopascals (kPa) and 300 kilopascals (kPa) are compiled in Table 4.4. A clear trend can be observed in case of diethanolamine (DEA) and diglycolamine (DGA) systems - the heat exchanger duty increases with an increase in the stripper pressure. This is consistent with an increased stripper/reboiler operating temperature, which results in a hotter lean amine stream entering the heat exchanger and thus, a larger quantity of energy transfer taking place in the heat exchanger. Monoethanolamine (MEA), has a similar trend while the stripper pressure increases from 30 kilopascals (kPa) to 150 kilopascals (kPa). However, there is no clear trend thereafter as the pressure is increased to 300 kilopascals (kPa). This can be explained by observing the absorbent flowrates for monoethanolamine (MEA) for

different stripper operating pressures. Table 4.5 is a compilation of the absorbent flowrates for all three absorbents under different stripper operating conditions. It can be observed from the data that the reduction in absorbent flowrate with an increase in stripper pressure for monoethanolamine(MEA) is much more significant than either of the other two amines. Whereas, there is negligible change in the absorbent flowrates for diethanolamine (DEA) and diglycolamine (DGA) when the stripper pressure is changed from 150 kilopascals (kPa) to 300 kilopascals (kPa); there is a 35% reduction for monoethanolamine (MEA). The rapid decrease in absorbent circulation can be attributed to the an increase in stripper temperatures at higher pressures, which results in a lower lean amine loading and hence, lower flowrates to achieve the twin goals of 90% carbon dioxide (CO_2) removal and a maximum rich amine loading of 0.4 moles-amine/mole–CO_2.

4.3.4 Effect of stripper operating pressure on compression duty

Carbon dioxide (CO_2) separated from the flue gas is compressed to a pipeline pressure of 16 Megapascals (MPa). Compression duty accounts for nearly 10% of the total energy consumption. As demonstrated in previous sections, an increase in the stripper pressure results in a reduction in the reboiler steam requirement. However, it also influences the compression duty since a change in the stripper pressure affects the pressure at which carbon dioxide (CO_2) is delivered to the compression train. Figure 4.12 shows the dependence of the compression duty on stripper pressure.

Table 4.5 : Absorbent flowrates under different stripper operating conditions

Amine	MEA 20 wt%	DEA 40 wt%	DGA 60 wt%
Stripper Pressure	**Flowrate (lpm)**	**Flowrate (lpm)**	**Flowrate (lpm)**
30 kPa	115,949	54,423	66,109
50 kPa	101,682	49,262	45,824
75 kPa	87,487	49,219	35,679
150 kPa	61,564	44,045	35,237
175 kPa	48,848	44,045	35,096
200 kPa	46,118	47,483	35,096
250 kPa	40,700	47,508	35,116
300 kPa	38,924	47,520	35,098

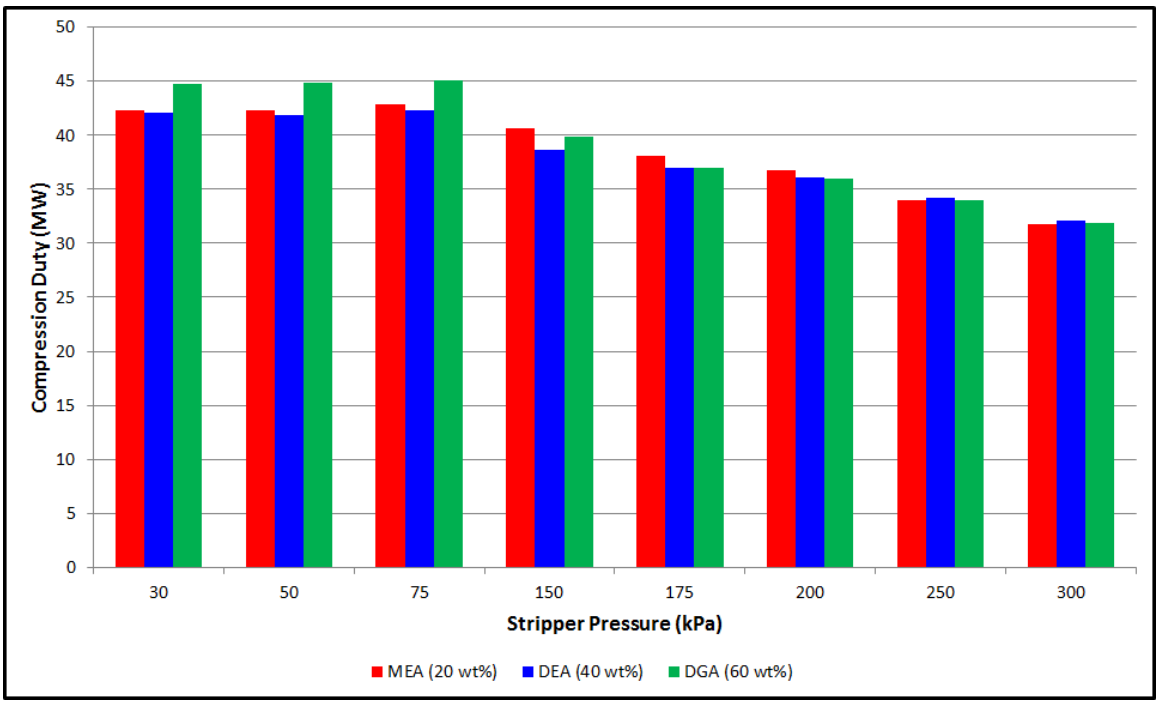

Figure 4.12 : Dependence of CO_2 compression duty on stripper operating pressure

As may be expected, the choice of absorbent has a negligble effect on the compression duty irrespective of the stripper pressure. It can be noticed that the compression duty is near constant for all vacuum strippers. This results from the use of steam jet ejectors which have been setup to deliver the separated carbon dioxide (CO_2) to the compressor train at 101.3 kilopascals (kPa). As the stripper operating pressure is increased, however, to 150 kilopascals (kPa) and beyond; there is a gradual reduction in the compression duty because carbon dioxide (CO_2) is delivered to the compressors at increasingly larger pressures and hence, lower specific volumes. The compression duty for amine absorption units with strippers operating at 300 kilopascals (kPa) is around 25% lower than those for vacuum strippers. This suggests that a higher stripper operating pressure has advantages in reducing the energy duty during the compression of carbon dioxide (CO_2).

4.3.5 Effect of stripper operating pressure on parasitic power losses

Figure 4.9 shows that the reboiler energy duty for vacuum strippers, expressed in terms of energy required per unit mass of carbon dioxide (CO_2) separated is greater than that for high pressure strippers. However, reboilers for vacuum strippers are supplied with steam at 122 kilopascals (kPa) which has significantly lower 'useful' energy content than the 415 kilopascals (kPa) steam required for high pressure strippers systems. Since the reboiler steam for vacuum and high pressure strippers is at different conditions, their resulting equivalent power loss is not the same - a larger

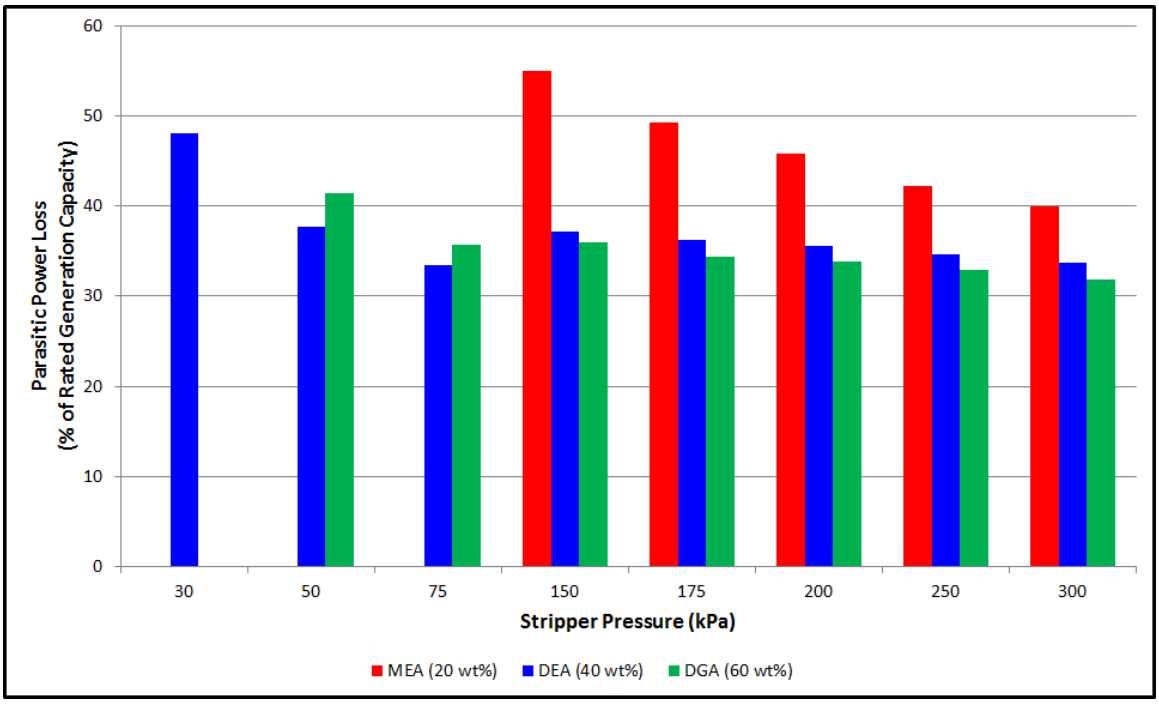

Figure 4.13 : Dependence of parasitic power losses on stripper operating pressure

quantity of the 122 kilopascals (kPa) steam must be drawn to result in the same power loss as the 415 kilopascals (kPa). Figure 4.13 is a plot of the parasitic power loss at the reference 400 Megawatt (MW) power plant, expressed as a % of the rated generation capacity.

The most remarkable feature of this plot is the absence of any data points for monoethanolamine (MEA) and diglycolamine (DGA) corresponding to a stripper pressure of 30 kilopascals (kPa) and for monoethanolamine (MEA) for 50 kilopascals (kPa) and 75 kilopascals (kPa). In all cases, this is a result of the reboiler steam requirement being greater than the flow-rate of steam circulated to the low pressure (LP) turbine, suggesting that it is practically impossible to implement the 30 kilopascals (kPa) configuration with any of the absorbents except diethanolamine (DEA). We

also note that with diethanolamine (DEA) and diglycolamine (DGA) as absorbents, the 75 kilopascals (kPa) stripper has a competitive performance with all the high pressure strippers. Diethanolamine (DEA) in particular has a lower parasitic power loss than all the high pressure stripper configurations.

In the case considered above, we have assumed that all the reboiler steam required for vacuum strippers is drawn downstream of the low pressure (LP) turbine. This, unavailability of waste heat represents the worst case scenario for vacuum strippers. In order to consider more realistic scenarios, we have considered five different scenarios of waste heat availability at the power plant. These are described in Table 4.6. At one end of the range is the case where no suitable sources of waste heat are available at the power plant (discussed above). At the other end of the spectrum is a case where enough waste heat is available at the power plant to provide all reboiler steam and no steam is required from the turbine system. Three other intermediate scenarios where 25%, 50% and 75% of the reboiler steam is provided by waste heat are considered in this study.

Figure 4.14 shows the variance in parasitic power loss for diethanolamine (DEA) and diglycolamine (DGA) systems with vacuum strippers under different scenarios of waste heat availability. There is a gradual reduction in the parasitic power loss as the source of the reboiler steam is switched from the turbine system to the waste heat source. The parasitic power losses reduce by 15–17 percentage points for the 50 kilopascals (kPa) strippers and by 12–15 percentage points for the 75 kilopascal (kPa)

Table 4.6 : Absorbent flowrates under different stripper operating conditions

Simulation Case	Assumption
0%	All reboiler steam is tapped from downstream of LP turbine at 122 kPa
25%	25% of the reboiler steam provided by waste heat sources
50%	50% of the reboiler steam provided by waste heat sources
75%	75% of the reboiler steam provided by waste heat sources
100%	100% of the reboiler steam provided by waste heat sources

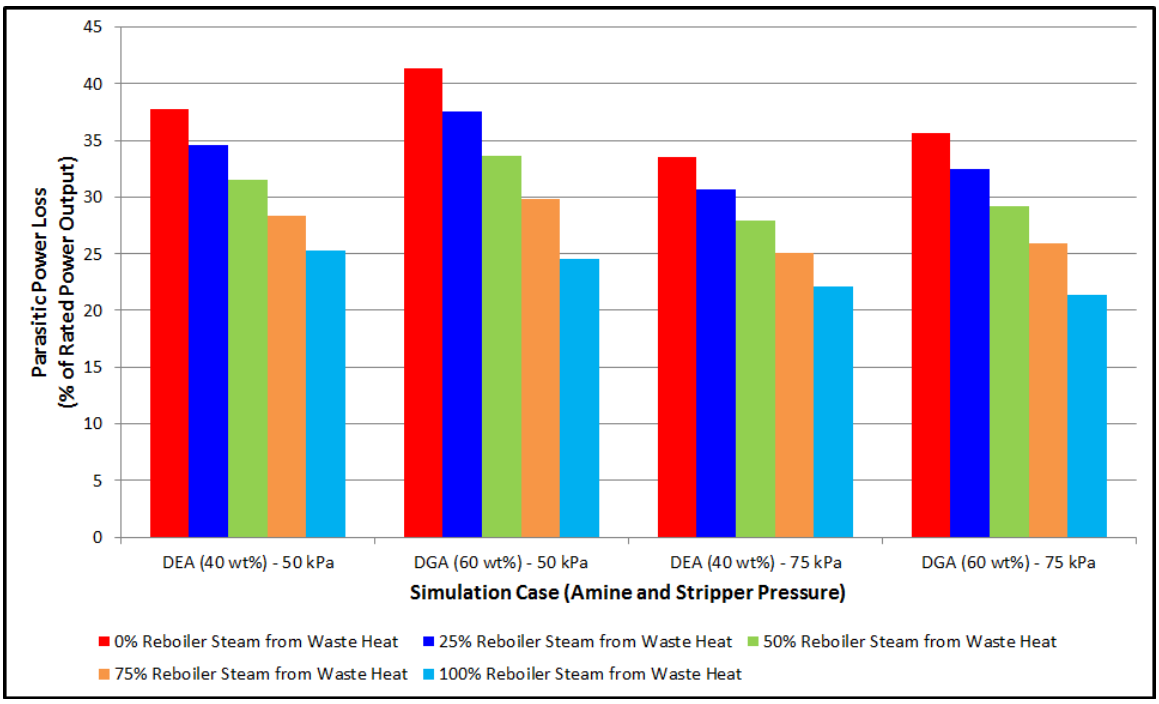

Figure 4.14 : Dependence of parasitic power loss for vacuum strippers on waste heat availability

strippers when the steam source is changed from the turbine system to waste heat. The main reason for the higher parasitic duty for the 50 kilopascal (kPa) strippers is the greater jet ejector steam requirement and increased duty for the pumps due to larger absorbent flowrates. As can be seen from Figure 4.14, when all the reboiler steam is provided by waste heat sources, the parasitic power loss for diethanolamine (DEA) and diglycolamine (DGA) at 75 kilopascals (kPa) is around 21% and the difference between them is less than 1%. This suggests that both these absorbents have a reasonably similar performance with the vacuum strippers.

4.4 Concluding Remarks

In this study, we have performed an in-depth exploration of the potential for using alternative stripper operating conditions than those used in current practice. In particular, evaluating the use of vacuum strippers utilizing waste heat for absorbent regeneration has been a major focus of this work. We have considered various relevant factors to analyze high pressure and vacuum strippers and remark that vacuum strippers, although previously discarded on the basis of excessive compression costs are competitive with conventional and high pressure stripper systems. In a scenario where a large supply of waste heat is available at the power plant site; however, utilization of a stripper column operated at 75 kilopascals (kPa) can result in parasitic power losses that are up to 15 percentage points lower than those for conventional and high pressure systems. There are operational advantages, disadvantages and

challenges towards the use vacuum strippers. These are summarized below:

1. When all reboiler steam is tapped from the turbine system and the stripper vacuum reduced from 50 kilopascals (kPa) to 75 kilopascals (kPa), the parasitic power loss for diethanolamine (DEA) decreases from 41.4% to 34.5% while that for diglycolamine (DGA) reduces from 41.3% to 32%. The parasitic power loss for both diethanolamine (DEA) and diglycolamine (DGA) is within 1% of that corresponding to a stripper pressure of 300 kilopascals (kPa).

2. Absorber diameters are not sensitive to a change the stripper pressure. We find that the absorber columns for vacuum stripper systems are almost the same size as the high pressure systems.

3. Stripper diameters are quite sensitive to the stripper operating pressures. When the stripper pressure is changed from 30 kilopascals (kPa) to 75 kilopascals (kPa), the size of the monoethanolamine (MEA) stripper decreases from 18 meters (m) to 11.8 meters (m), the diethanolamine (DEA) stripper from 9.7 meters (m) to 7.8 meters (m) and diglycolamine (DGA) stripper from 11.8 meters (m) to 8 meters (m). When compared to the high pressure strippers, we see that a 300 kilopascals (kPa) stripper with monoethanolamine (MEA) has a 6.5 meters (m) stripper column, diethanolamine (DEA) has 6.6 meters (m) and diglycolamine (DGA) has a 5.5 meters (m) column. Thus, vacuum strippers are significantly bigger in size than the conventional or high pressure strippers; which can be expected to increase the capital expenditure for the plant.

4. Since vacuum strippers operate a low temperature (less than 100ºC), they may be expected to have a major operational advantage over conventional systems - low equipment corrosion. In addition, the lower temperature will have no thermal degradation problems as opposed to the 300 kilopascals (kPa) configuration which may be expected to have solvent loss problems.

5. Under the conditions used in this study, it is practically infeasible to use MEA as an absorbent for amine absorption systems with vacuum stripping due to the extremely large requirement for reboiler steam and impossibly large stripper columns. Similarly, the 30 kilopascals (kPa) stripper configuration may be practically infeasible unless a very large source of waste heat is available at the power plant. Even then, this configuration will not be competitive with the 75 kilopascals (kPa) system.

6. We conclude that vacuum stripping at 75 kilopascals (kPa) and high pressure stripping at 300 kilopascals (kPa) are more competitive configurations than conventional amine absorption. While high pressure stripping may be challenged by problems like thermal degradation, corrosion and absorbent losses, finding sources of waste heat is critical to the cost effective deployment of vacuum strippers. The higher equipment cost of vacuum stripping maybe justified if a significant reduction in parasitic power loss can be achieved.

Since, the economics of a process - the capital and operating costs are critical to the success of any industrial process; an economic evaluation is a must to make

a reasonably accurate judgment of the superiority of a novel process configuration. In Chapter 5, we present the economic analysis conducted to compare the two best process configurations identified in this part of work.

Chapter 5

Effects of variation in stripper operating pressure on the performance of the amine absorption process for carbon capture: an economic perspective

5.1 Motivation

Economic feasibility of a chemical process is the ultimate factor considered in deciding its large-scale, commercial deployment. Several researchers have thoroughly analyzed the conventional alkanolamine process for its economic feasibility for carbon dioxide (CO_2) capture at coal-fired power plants [73, 74, 75, 42]. As described previously in Chapters 3 and 4, several new and clever rearrangements of the alkanolamine process have been suggested to reduce the energy consumption [57, 53, 52, 76]. Few of these research studies, however, have been concluded with an analysis to quantify the economic implications of these modifications. The work presented in this chapter was performed with the objective of conducting a reasonable economic assessment of the various modified configurations of the alkanolamine absorption process. Although

based off a relatively simple assessment, these results provide an objective assessment of the viability of these different process configurations.

5.2 Research approach

The basic requirement for conducting an economic assessment of any chemical process is a knowledge of the equipment sizing/rating. As described in Chapter 4, we have used ProMax to model the amine absorption process. In addition to simulating the amine absorption process, ProMax can also be used for sizing/rating most equipment used in it. We have chosen to rate the heat exchangers independently by evaluating their heat transfer areas using the heat transfer rate and logarithmic mean temperature difference (LMTD) values simulated in ProMax and overall heat transfer coefficients (U) and logarithmic mean temperature difference (LMTD) correction factors from published literature. This size/rating information, thus generated, is used as input in the Aspen Process Economic Analyzer software (formerly Aspen Icarus Process Evaluator). Aspen Process Economic Analyzer is a powerful project scoping tool that is commonly used for evaluation of the economic impacts of process designs. For simple, preliminary cost estimations similar in scope to this work; Aspen Process Economic Analyzer can generate estimates with a minimal number of sizing/rating parameters. In a few cases, where actual equipment size/rating generated with ProMax cannot be evaluated with the Economic Analyzer; the economic costs can be scaled off the cost of the maximum sized/rated equipment using the 6–10$^{\text{th}}$ rule (see

Equation 5.1 below) [77]. These parameters corresponding to each equipment type, required for economic evaluation and the method used to size/rate the equipment are listed in Table 5.1.

$$C_B = C_A \left[\frac{S_B}{S_A}\right]^{0.6} \tag{5.1}$$

5.3 Sizing and rating methodology

Table 5.1 lists the different type of equipment used at the carbon capture plant. While most equipment can be sized and rated in ProMax, it is important to present the methodology used to do so. In the subsections below, we have discussed the methods used to size/rate complex equipment such as separation columns, pressure vessels and heat exchangers.

5.3.1 Sizing separation columns

ProMax has a built-in package, TSWEET which accounts for the aminecarbon dioxide (CO_2) reaction kinetics in the absorber. The actual mechanism which limits the rate of carbon dioxide (CO_2) absorption in amines is its ionization in water. This is handled in ProMax by the TSWEET kinetics model which is analogous to a liquid-side resistance in a mass transfer model. The TSWEET kinetics model calculates simultaneous mass transfer (physical process) and chemical reaction to account for the relatively slow amine-carbon dioxide (CO_2) reaction rate.

Table 5.1 : Parameters used for economic evaluation of equipment cost

Equipment ↓	**Sizing/Rating Parameter(s))**	**Sizing/Rating Method**
Separation columns	Column Diameter & Height	ProMax
Pumps	Liquid Flowrate & Fluid Head	ProMax
Compressors	Vapor Flowrate (volumetric) & Compression Ratio	ProMax
Process Vessels	Vessel Diameter & Height	ProMax
Gas Blower	Vapor Flowrate (volumetric)	ProMax (6–10^{th} rule invoked)
Steam Jet Ejector	Vapor Flowrate (mass)	ProMax (6–10^{th} rule invoked)
Heat Exchangers	Surface Area	Calculated Independently

The total contacting time between the sour gas and the absorbent streams is a major factor in determining the amount of carbon dioxide (CO_2) picked up. In ProMax, columns are often simulated using ideal trays rather than real trays. The liquid residence time on an individual tray is evaluated based on the tray geometry and further used to evaluate the total residence time in the column by multiplying it with the ratio of ideal to real stages. In commercial operation, however, packed columns are often preferred to tray columns due to their higher efficiency. In order to estimate the equivalent height of packing required, a parameter called 'height equivalent to theoretical stage (HETP)' is used. The tower height is the product of the height equivalent to theoretical stage (HETP) and the number of trays in the column. In order to evaluate the column diameter, ProMax utilizes the degree of column flooding as an input parameter. With the degree of flooding, the liquid and vapor flowrates known; it is possible to evaluate the column diameter. The towers in the glycol dehydration unit use a similar methodology for evaluation of column height and diameter, except the Soave-Redlich-Kwong (SRK) package is utilized. Table 5.2 summarizes the dimensions of the different separation columns used in this study [78].

5.3.2 Sizing separator vessels

Horizontal and vertical 2-phase separators vessels are sized in Promax using correlations in published literature [79, 80, 81]. The sizing correlations for vapor/liquid

Table 5.2 : Dimensions of various separation columns in the carbon capture plant

Stripper Pressure (kPa) →	50	**75**	**150**	**175**	**200**	**250**	**300**	50	**75**	**150**	**175**	**200**	**250**	**300**
Parameter (m) ↓	**DEA (40 wt%)**							**DGA (60 wt%)**						
Amine Absorber Diameter	9.9	9.7	9.8	9.8	9.7	9.7	9.7	8.9	8.6	8.6	8.6	8.6	8.6	8.6
Amine Absorber Height	82	82	82	82	82	82	82	16.5	16.5	16.5	16.5	16.5	16.5	16.5
Amine Stripper Diameter	8.5	7.8	6.9	6.7	6.7	6.6	6.6	9.4	8.0	6.1	5.8	5.7	5.6	5.5
Amine Stripper Height	60.0	60.0	54.9	54.9	54.9	54.9	54.9	90.0	90.0	54.9	54.9	54.9	54.9	54.9
Glycol Absorber Diameter	2.3	2.3	2.2	2.1	2.0	1.8	1.9	2.4	2.4	2.2	2.1	2.0	1.8	1.9
Glycol Absorber Height	54.9	54.9	54.9	54.9	54.9	54.9	54.9	54.9	54.9	54.9	54.9	54.9	54.9	54.9
Glycol Stripper Diameter	0.3	0.3	0.3	0.3	0.3	0.3	0.3	0.3	0.3	0.3	0.3	0.3	0.3	0.3
Glycol Stripper Height	16.5	16.5	16.5	16.5	16.5	16.5	16.5	16.5	16.5	16.5	16.5	16.5	16.5	16.5

separation are based on the K-factor method outlined in Section 7 of the Gas Processors Suppliers Association (GPSA) Databook and Svrcek [80, 79]. The K-factor method is an empirical correlation which is dependent upon operating pressure, presence of mist eliminator, presence of glycol or amine, separator orientation, and minimum particle size carried overhead. For both the horizontal and vertical separator orientations, the maximum terminal vapor velocity, V, is calculated by a Souders-Brown equation using the appropriate K value and the vapor and liquid densities [82]. The terminal vapor velocity is used to determine the diameter of vertical separators and length of horizontal separators where disengagement is controlling. In this study, we have specified the material of construction for the vessels and the required corrosion allowance. Other parameters necessary for calculating vessel dimensions are used at their default values. The dimensions of various separation vessels as evaluated using ProMax are listed in Table 5.3.

5.3.3 Rating heat exchangers

When rating heat exchangers, the parameter of most interest is the heat transfer area. In this study, we have evaluated the heat transfer area for different heat exchangers independent of ProMax. For every heat exchanger that is a part of the carbon capture plant, the heat transfer rate, the inlet and outlet temperatures of the fluids and the log mean temperature difference (LMTD) are known. These values can be used to determine the heat transfer area by employing Equation 5.2, where $\dot{Q}$ is the heat

Table 5.3 : Dimensions of various separation vessels in the carbon capture plant

Stripper Pressure (kPa) →	50	**75**	**150**	**175**	**200**	**250**	**300**	50	**75**	**150**	**175**	**200**	**250**	**300**
Parameter (m) ↓	**DEA (40 wt%)**							**DGA (60 wt%)**						
SO_2 Scrubber Diameter	9.8	9.8	9.8	9.8	9.8	9.8	9.8	9.8	9.8	9.8	9.8	9.8	9.8	9.8
SO_2 Scrubber Height	10.2	10.3	10.3	10.2	10.2	10.2	10.2	10.2	10.2	10.2	10.2	10.2	10.2	10.2
Amine Condenser Diameter	5.5	4.9	4.0	3.8	3.8	3.5	3.4	5.6	5.0	4.1	3.8	3.7	3.5	3.4
Amine Condenser Height	6.5	5.8	5.1	4.9	4.8	4.6	4.4	6.9	6.1	5.0	4.7	4.5	4.3	4.2
2-Phase Separator 1 Diameter	4.3	4.3	0.0	0.0	0.0	0.0	0.0	4.4	4.4	0.0	0.0	0.0	0.0	0.0
2-Phase Separator 1 Height	5.2	4.9	0.0	0.0	0.0	0.0	0.0	5.3	5.0	0.0	0.0	0.0	0.0	0.0
2-Phase Separator 2 Diameter	2.0	2.0	1.8	1.8	1.7	1.5	1.7	2.0	2.1	2.0	1.8	1.7	1.5	1.7
2-Phase Separator 2 Height	3.0	3.1	2.9	2.9	2.9	2.8	2.9	3.0	3.0	2.9	2.9	2.9	2.8	2.9
Glycol Condenser Diameter	0.5	0.5	0.5	0.5	0.5	0.5	0.5	0.5	0.5	0.5	0.5	0.5	0.5	0.5
Glycol Condenser Height	1.9	1.9	1.9	1.9	1.9	1.9	1.9	1.9	1.9	1.9	1.9	1.9	1.9	1.9

Table 5.4 : Overall heat transfer coefficients for various heat exchangers (U)

Heat Exchanger	**Overall HT Coefficient (W/m^2-K)**
Flue Gas Cooler Surface Area	200.00
Amine Cooler Surface Area	1200.00
Lean/Rich Amine Heat Exchanger	1250.00
Amine Reboiler	3000.00
All Intercoolers	200.00
Glycol Reboiler	750.00
Glycol Cooler	500.00
Glycol Heat Exchanger	300.00

Table 5.5 : Heat transfer surface areas for different heat exchangers in the carbon capture plant

Stripper Pressure (kPa) →	50	**75**	**150**	**175**	**200**	**250**	**300**	50	**75**	**150**	**175**	**200**	**250**	**300**
Surface area (m^2) ↓	**DEA (40 wt%)**							**DGA (60 wt%)**						
Amine Heat EXCHR (x 10^3)	10.7	16.5	15.2	15.5	17.8	20.8	22.5	7.8	9.0	9.4	9.6	10.0	11.3	11.6
Cooler 1 (x 10^3)	3.3	3.3	3.3	3.3	3.3	3.3	3.3	3.3	3.3	3.3	3.3	3.3	3.3	3.3
Cooler 2 (x 10^3)	1.4	1.4	1.2	1.2	1.3	1.3	1.3	1.4	1.1	1.0	1.0	1.0	1.0	1.0
Amine Reboiler (x 10^3)	1.1	1.3	1.0	1.0	1.0	1.3	1.4	1.6	2.0	0.9	0.8	0.9	1.0	1.1
Intercooler 1	258	259	284	277	273	268	265	277	277	293	277	272	266	263
Intercooler 2	322	324	322	311	305	297	293	345	346	333	311	304	295	290
Intercooler 3	361	364	361	347	340	333	331	387	388	373	347	339	331	329
Intercooler 4	388	390	397	356	373	352	388	416	417	410	357	372	349	385
Intercooler 5	364	367	369	386	412	516	317	391	392	382	386	411	512	314
Intercooler 6	390	395	647	800	812	762	804	418	420	669	800	808	757	798
Intercooler 7	844	855	485	231	123	0	0	906	909	498	231	122	0	0
Glycol Reboiler	2.9	3.0	2.5	2.4	2.3	2.6	2.4	3.2	3.2	2.6	2.4	2.3	2.6	2.3
Glycol Cooler	3.8	3.7	3.3	3.0	2.9	3.0	2.9	4.1	4.0	3.4	3.0	2.9	3.0	2.9
Glycol Heat EXCHR	27	27	20	18	17	18	17	28	29	21	18	17	18	17

transfer rate, U is the overall heat transfer coefficient, A is the heat transfer area, LMTD is the log mean temperature difference and f is the LMTD correction factor. The LMTD correction factor (f) is a configuration correction factor which depends on the exact arrangement of the streams within the heat exchangers, the number of exchangers in series and the temperatures of the incoming and outgoing streams. F factor values for various configurations of shell and tube heat exchangers, available in published literature were used in this study [83]. Overall heat transfer coefficients available in published literature and suitable for the fluids in each heat exchanger were used to evaluate the heat transfer surface areas. These are summarized in Table 5.4 The heat transfer areas for the different heat exchangers in the carbon capture plant are listed in Table 5.5.

$$\dot{Q} = U \cdot A \cdot LMTD \cdot f \tag{5.2}$$

5.3.4 Rating Fluid Drivers

Fluid drivers are simpler to rate than separation columns, vessels and heat exchangers. Booster pumps are rated on the basis of the liquid flowrate they process and their dynamic fluid head. Gas blowers and compressors are rated on the basis of the input vapor flowrates and their compression ratios. The dynamic fluid head for the pumps employed in the amine absorption and glycol dehydration trains and the compression ratios for the gas blower and compressors are listed in Table 5.6.

Table 5.6 : Parameters used for rate the various fluid drivers in the carbon capture plant

Stripper Pressure (kPa) →	50	**75**	**150**	**175**	**200**	**250**	**300**	50	**75**	**150**	**175**	**200**	**250**	**300**
Parameter ↓	**DEA (40 wt%)**							**DGA (60 wt%)**						
Blower Compression Ratio	1.9	1.9	1.9	1.9	1.9	1.9	1.9	1.9	1.9	1.9	1.9	1.9	1.9	1.9
Amine Pump 1 Head (m)	54.0	51.6	66.4	64.0	61.3	56.5	51.8	53.4	51.6	65.2	62.6	60.2	55.6	50.9
Amine Pump 2 Head (m)	3.8	3.8	3.8	4.8	7.0	12.7	19.0	3.8	3.8	3.8	4.7	6.9	11.3	15.7
Amine Pump 3 Head (m)	21.8	21.9	0.0	0.0	0.0	0.0	0.0	21.6	22.0	0.0	0.0	0.0	0.0	0.0
COMP 1 Compression Ratio	2.0	2.0	2.0	2.0	2.0	2.0	2.0	2.0	2.0	2.0	2.0	2.0	2.0	2.0
COMP 2 Compression Ratio	2.0	2.0	2.0	2.0	2.0	2.0	2.0	2.0	2.0	2.0	2.0	2.0	2.0	2.0
COMP 3 Compression Ratio	2.0	2.0	2.0	2.0	2.0	2.0	2.0	2.0	2.0	2.0	2.0	2.0	2.0	2.0
COMP 4 Compression Ratio	2.0	2.0	2.0	2.0	2.0	2.0	2.0	2.0	2.0	2.0	2.0	2.0	2.0	2.0
COMP 5 Compression Ratio	2.0	2.0	2.0	2.0	2.0	2.0	1.4	2.0	2.0	2.0	2.0	2.0	2.0	1.4
COMP 6 Compression Ratio	2.0	2.0	2.0	2.0	2.0	2.0	2.0	2.0	2.0	2.0	2.0	2.0	2.0	2.0
COMP 7 Compression Ratio	2.0	2.0	2.0	1.7	1.4	1.2	1.3	2.0	2.0	2.0	1.7	1.4	1.2	1.3
COMP 8 Compression Ratio	1.3	1.3	0.0	0.0	0.0	0.0	0.0	1.3	1.3	0.0	0.0	0.0	0.0	0.0
Glycol Pump Head (m)	655	655	657	657	657	656	657	656	655	657	657	657	656	657

5.3.5 Generic simulation parameters employed for economic evaluation

In addition to the size and rating parameters listed in Tables 5.2 - 5.6, others parameters are required for providing an accurate economic evaluation of equipment costs. This includes the material of construction, corrosion allowances, tower packing type, amongst others. These parameters are summarized in Table 5.7.

5.4 Effects of variation in stripper pressure on cost of carbon capture

In Chapter 4, we have discussed the effects of varying stripper pressure and reboiler steam source on the energy cost of carbon capture and the parasitic power loss at the reference power plant. As argued previously, however, such a technical analysis alone, fails to identify the optimal operational configuration. The economic assessment conducted in this chapter aids in analyzing the effect of stripper pressure and reboiler steam source on the cost of various plant equipment and thus, the overall cost of the carbon capture plant. In the following subsections, we discuss the effects of these variations on the cost of major equipment such as amine absorber and stripper, the lean/rich amine heat exchanger, the amine reboiler and the carbon dioxide (CO_2) compression train.

Table 5.7 : Generic parameters used in evaluation of equipment costs [20, 21, 22, 23]

Parameter	Value
All equipment - Material of Construction	Carbon Steel
Amine Absorber - Corrosion Allowance	3.2 mm
Amine Stripper - Corrosion Allowance	6.4 mm
Glycol Absorber - Corrosion Allowance	3.2 mm
Glycol Stripper - Corrosion Allowance	3.2 mm
Heat Exchanger Tubes - Corrosion Allowance	0.06 mm
Tower Packing Type	Ceramic Intalox Saddle
All Absorbers - HETP	1.83 m
High Pressure Strippers - HETP	1.83 m
Vacuum Strippers - HETP	2.0 m

In current practice, it is common to construct these with carbon steel. However, as discussed previously in Chapter 4; equipment corrosion problems are commonplace when alkanolamines are used as absorbents for carbon dioxide (CO_2). To limit the extent of corrosion; the carbon dioxide (CO_2) loading of absorbent solutions is maintained at or below 0.4 moles-CO_2/mole of amine. Stainless steel equipment is corrosion resistant, however, it can also cost 2x-3x higher than carbon steel equipment of the same size and its commercial viability is questionable. In this study, we have considered carbon steel as the standard material of construction.

5.4.1 Effect of variation in stripper pressure on the cost of amine absorber and stripper

The amine absorber and stripper columns are central to the carbon dioxide (CO_2) absorption process and are thus, critical pieces of equipment. Several design parameters such as equipment dimensions, pressure rating and material of construction play a role in determining the cost of an equipment. In this study, all amine absorber columns are operated at the same pressure - slightly above atmospheric pressure. They also handle the same vapor flowrates since the flue gas inflow is the same across all simulation cases. However, due to the lower reactivity and the resulting slower reaction kinetics; absorber columns with diethanolamine (DEA) as the solvent are 5 times taller than those with diglycolamine (DGA). In addition, due to a difference in the absorbent flowrate and the fluid properties, diethanolamine (DEA) columns have

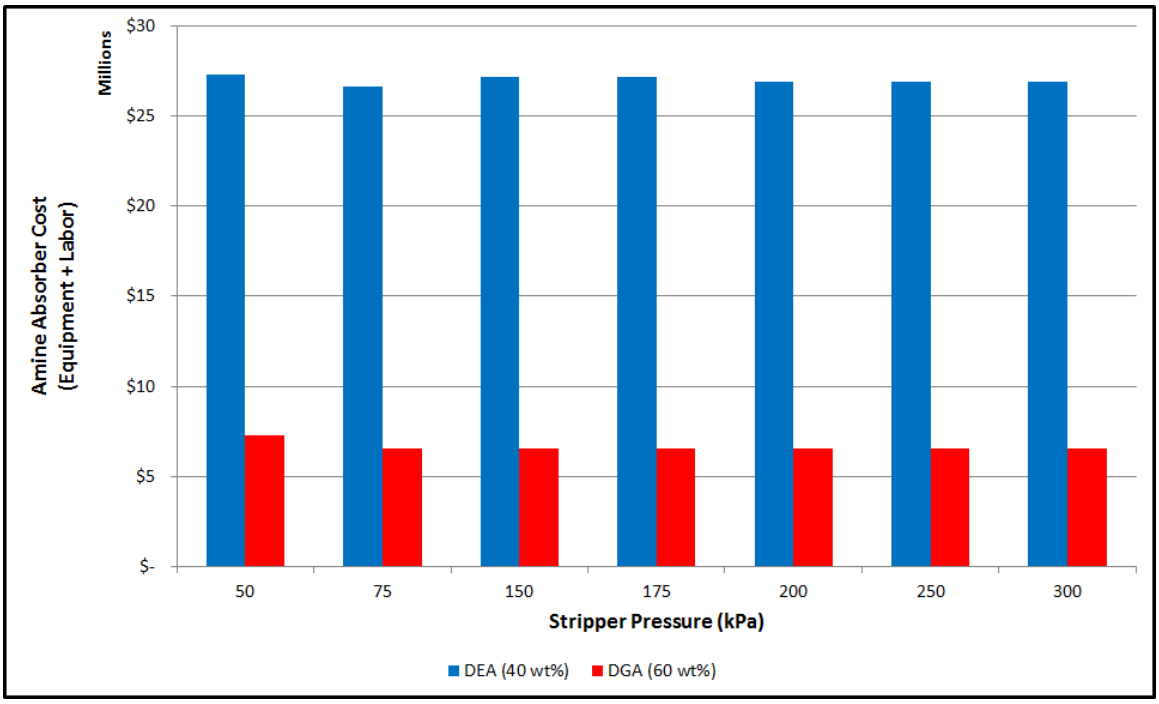

Figure 5.1 : Dependence of absorber costs on stripper operating pressure

a slightly larger diameter than those for diglycolamine (DGA). Figure 5.1 shows the variation in the cost (equipment + labor) of absorber columns for both diethanolamine (DEA) and diglycolamine (DGA) with stripper pressure. It can be observed that for a given absorbent choice, there is negligible variation in the cost of the amine absorber columns. This can be expected because the absorber diameters are only weakly sensitive to the stripper operating pressure. The cost of absorber columns for diethanolamine (DEA) as a solvent, however, are nearly 4 times those for diglycolamine (DGA). This can be attributed to a combination of the larger column diameters for diethanolamine (DEA) as well as the taller columns; both of which result in an increase in the expenditure.

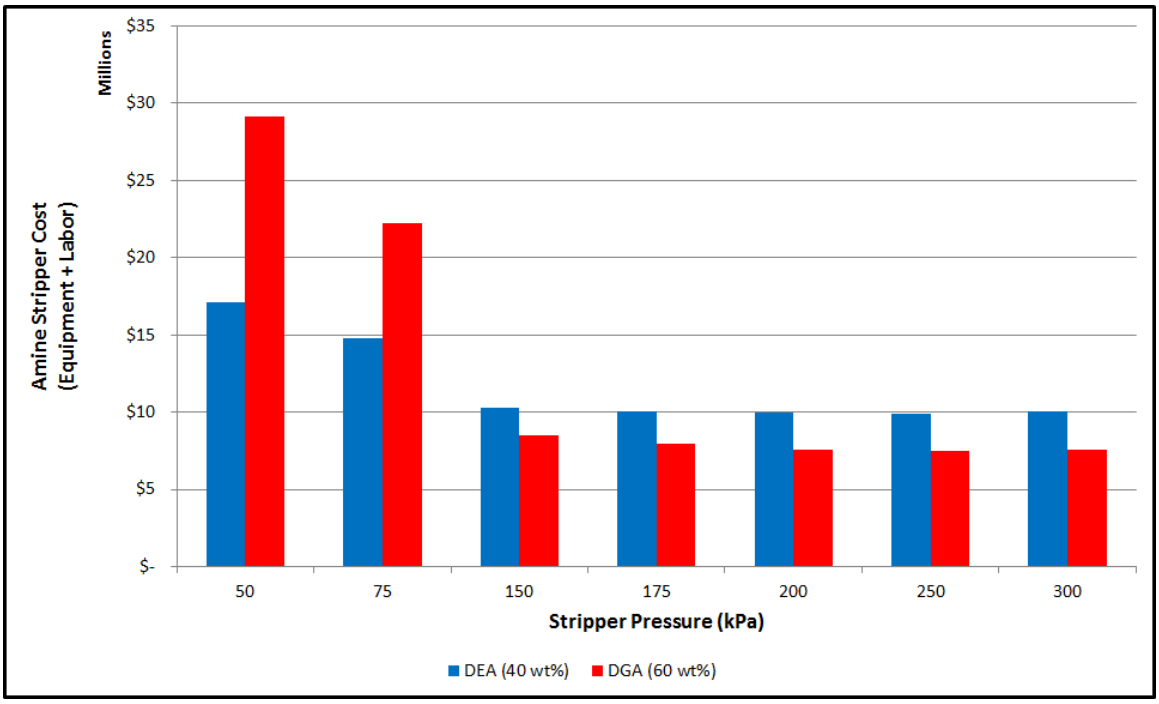

Figure 5.2 : Dependence of stripper costs on stripper operating pressure

The dependence of amine stripper column diameter and height was described in detail in §4.3.2. The diameter of amine strippers is largely dependent on the stripping vapor (steam) flowrates. As seen in Figure 4.11, across the entire operating pressure range considered in this study; diethanolamine (DGA) strippers have a larger diameter than those using diglycolamine (DGA) as a solvent. Stripper height has much lesser variance - with both diethanolamine (DEA) and diglycolamine (DGA) strippers operating at high pressure having the same height of 55 meters.

Vacuum strippers using diethanolamine (DEA) are shorter than those using diglycolamine (DGA) since diethanolamine (DEA) regeneration is less sensitive to stripper temperatures, which are lower in vacuum strippers than high pressure strippers.

Thus, diethanolamine (DEA) vacuum strippers have a height of 60 meters as compared to diglycolamine (DGA) strippers which are 90 meters tall. Figure 5.2 shows the dependence of stripper costs (equipment + labor) on stripper pressure. A clear trend can be seen from the plot - amine stripper costs decrease significantly when the pressure increases from 50 kilopascals (kPa) to 150 kilopascals (kPa); which signifies the transition from vacuum strippers to high pressure strippers. Between 150 kilopascals (kPa) and 300 kilopascals (kPa), however, there is insignificant change in the stripper cost. This is contrary to the trend observable in Figure 4.11 where the stripper diameter decreases consistently as the operating pressure increases. All other factors unchanged, a reduction in column diameter should result in decrease in costs - which is contrary to the observation of this study. This can be explained by a change in the pressure and temperature rating of the amine strippers. As the stripper pressure is increased from 150 kilopascals (kPa) to 300 kilopascals (kPa), the additional internal pressure and temperature must be accounted for in the construction of the column by increasing its thickness. This negates any potential savings that maybe achieved through a reduction in column diameter. As might be expected, however, the larger diethanolamine (DEA) columns are slightly more expensive than diglycolamine (DGA) columns at all stripper pressures except when operating under vacuum.

5.4.2 Effect of variation in stripper pressure on the cost of lean/rich amine heat exchanger

The lean/rich amine heat exchanger plays a critical role at an amine absorption facility by transferring a large quantity of sensible heat from the hot, lean amine solution exiting the reboiler to the cooler, rich amine solution entering the stripper column. The quantity of heat exchanged depends on factors such as the absorbent flowrate, lean and rich amine inlet temperatures. From Table 4.5, we can observe that for the stripper operating pressure range considered in this economic analysis (50 kilopascals (kPa) to 300 kilopascals (kPa); the absorbent flowrate for all of diethanolamine (DEA) cases is higher than those for diglycolamine (DGA). For vacuum strippers, the difference in flowrates ranges between 7% and 27 % whereas for high pressure strippers, the difference is almost constant at approximately 25%. Consequently, as listed in Table 4.4; the heat exchanger duty for diethanolamine (DEA) cases is higher than the diglycolamine (DGA) systems by between 25% - 40%. With the minimum end approach temperature for the lean/rich heat exchanger across all system configurations at a constant 5° C; the larger heat transfer rate translated into a larger heat transfer surface area in the exchanger. Figure 5.3 shows the variation in the cost of lean/rich amine heat exchanger with stripper pressure. The dependence of amine heat exchanger costs closely followed the trend in amine heat exchanger surface area seen in Table 5.5. As with the costs of the amine absorber and stripper columns in §§5.4.1, diglycolamine (DGA) heat exchangers significantly less than those for diethanolamine

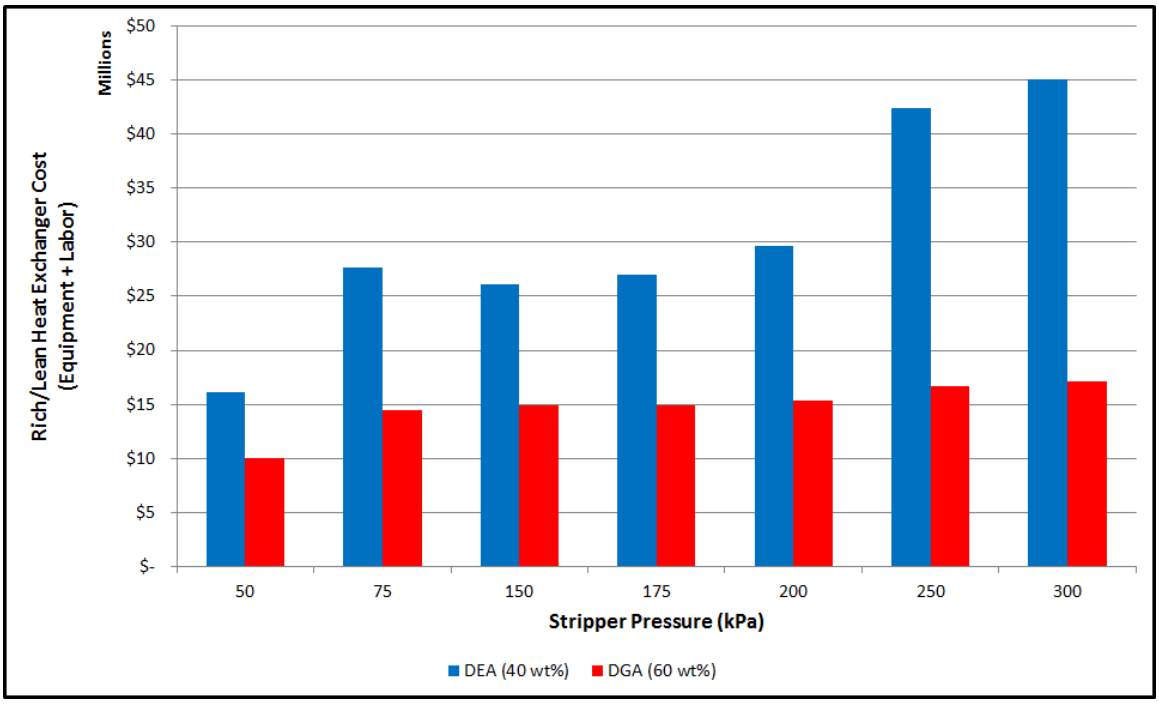

Figure 5.3 : Dependence of amine heat exchanger costs on stripper operating pressure

(DEA) systems; by as much as 60% in some configurations.

5.4.3 Effect of variation in stripper pressure on the cost of amine reboiler

The amine reboiler located at the base of the stripper is a heat exchanger where a part of the lean amine solution is vaporized to generate stripping vapor that flows through the column. The amine reboilers utilize steam as the heating fluids. Reboilers in vacuum strippers utilize steam at 122 kilopascals (kPa) whereas those in high pressure stripper columns use steam at 450 kilopascals (kPa). In this entire study, we have chosen to maintain a constant pressure for the reboiler steam across different stripper pressures. Consequently, the minimum end approach temperature and the

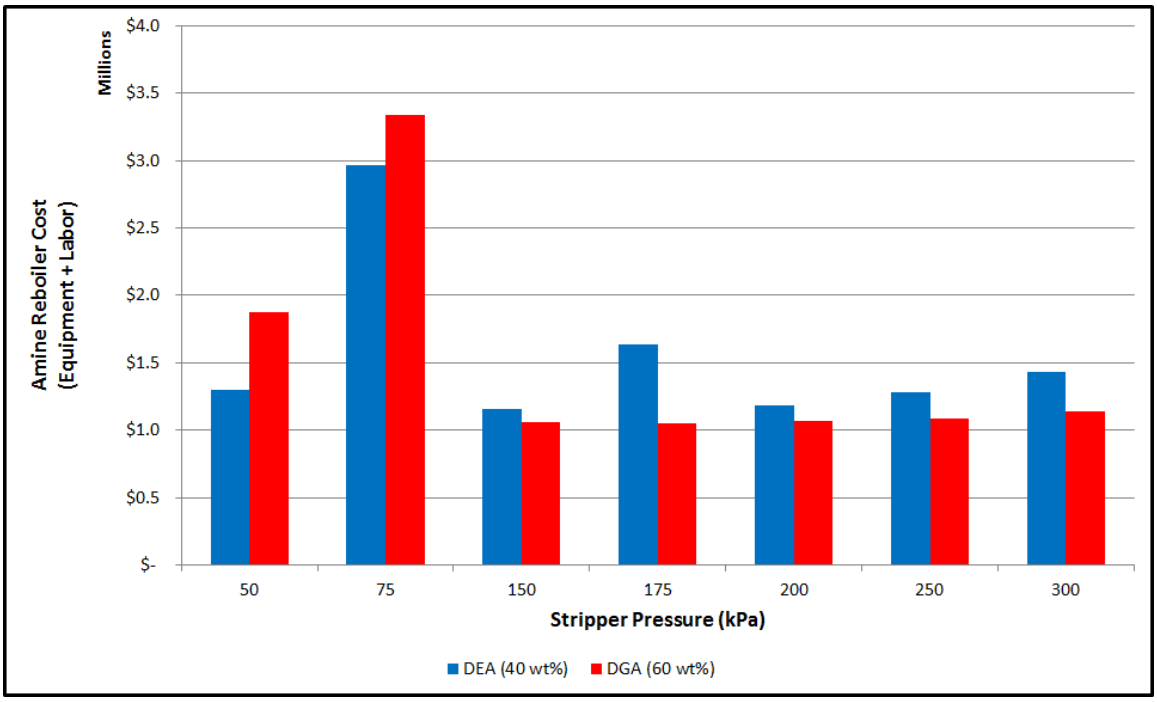

Figure 5.4 : Dependence of amine reboiler costs on stripper operating pressure

log mean temperature difference (LMTD) in the reboiler varies with a change in stripper operating pressure. Figure 5.4 shows the variation in the cost of the amine reboiler with stripper pressure. Similar to the lean/rich amine heat exchanger, reboiler costs rise as the stripper pressure is increased. This results from a decrease in the log mean temperature difference (LMTD) with an increase in stripper pressure; which results in a need for greater heating surface area. Diethanolamine (DEA) reboilers have lower costs than diglycolamine (DGA) in the vacuum stripping configuration due to the relatively lower reboiler duty. However, for high pressure strippers; diglycolamine (DGA) has a slightly lower reboiler duty than diethanolamine (DEA) which lowers the cost by 10%-20%.

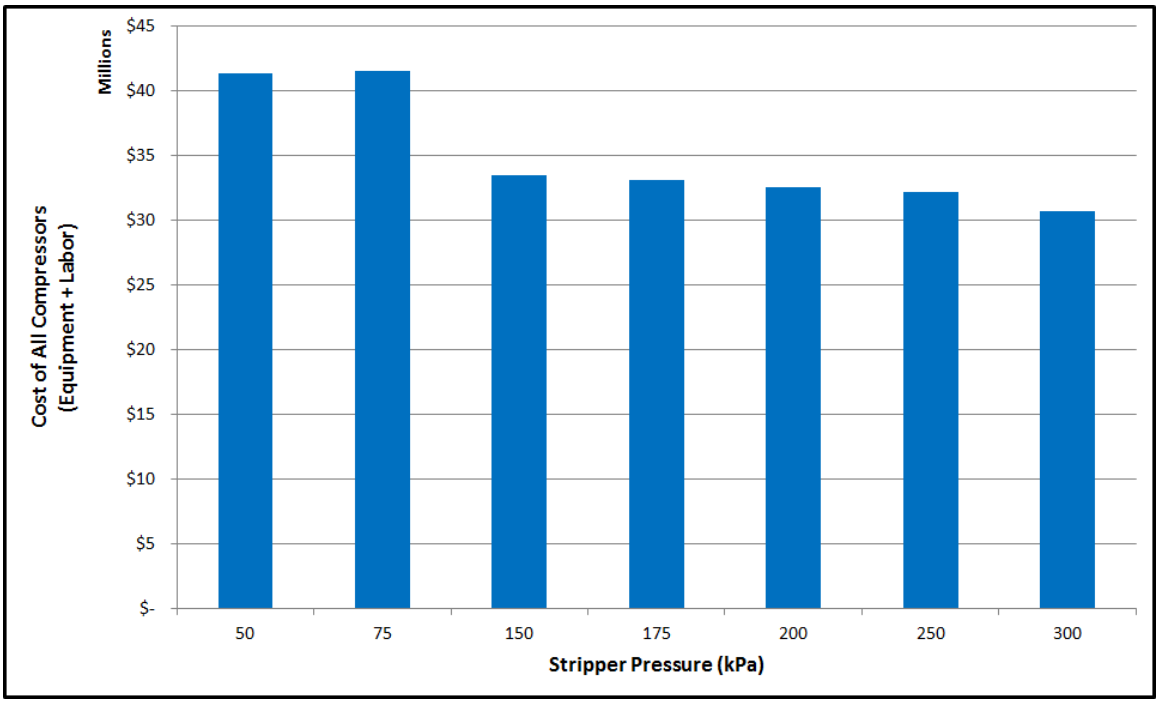

Figure 5.5 : Dependence of carbon dioxide (CO_2) compression train costs on stripper operating pressure

5.4.4 Effect of variation in stripper pressure on the cost of carbon dioxide (CO_2) compression train

Carbon dioxide (CO_2) compression is a significant contributor to the energy consumption and the parasitic power loss at coal-fired power plant. Carbon dioxide (CO_2) leaving the amine absorption plant must be compressed to a pressure of 16 Megapascals (MPa) for long distance transportation through pipelines. Compressor units are costed on the basis of the compression ratio of the outgoing and incoming vapor and the input vapor flowrate. In case of the compression train, no particular absorbent has an advantage over another since the cost is dependent only on the quantity of car-

bon dioxide (CO_2) separated - which is the same for both diethanolamine (DEA) and diglycolamine (DGA). Figure 5.5 shows the variation in the cost of the compression train with a change in stripper pressure. A clear trend can be observed in this plot - both vacuum stripping configurations have the same equipment cost whereas the compression costs decrease steadily with an increase in stripper pressure. All of this observed behavior can be attributed to the delivery pressure of the separated carbon dioxide (CO_2) to the compression train. In case of vacuum strippers, irrespective of the stripper pressure; the carbon dioxide (CO_2) is delivered at atmospheric pressure - due to the use of a steam jet ejector. In case of the high pressure strippers, the compressors must process a decreasing volume of carbon dioxide (CO_2) with increase stripper pressure which results in a lowering of compressor costs.

5.4.5 Effect of variation in stripper pressure on the overall cost of carbon capture plant

Figure 5.6 shows the dependence of the cost of a carbon capture plant on the stripper operating pressure. A more complete breakdown of plant costs is provided in Tables 5.8, 5.9 and 5.10. Clearly, Figure 5.6 is a culmination of the major trends observed in Figures 5.1 - 5.5. Carbon capture trains with vacuum strippers clearly cost more than high pressure strippers. Carbon capture plants with amine strippers operating at 75 kilopascals (kPa) cost approximately 25% more than those with strippers operating at 150 kilopascals (kPa). In case of diethanolamine (DEA) systems, plant cost has

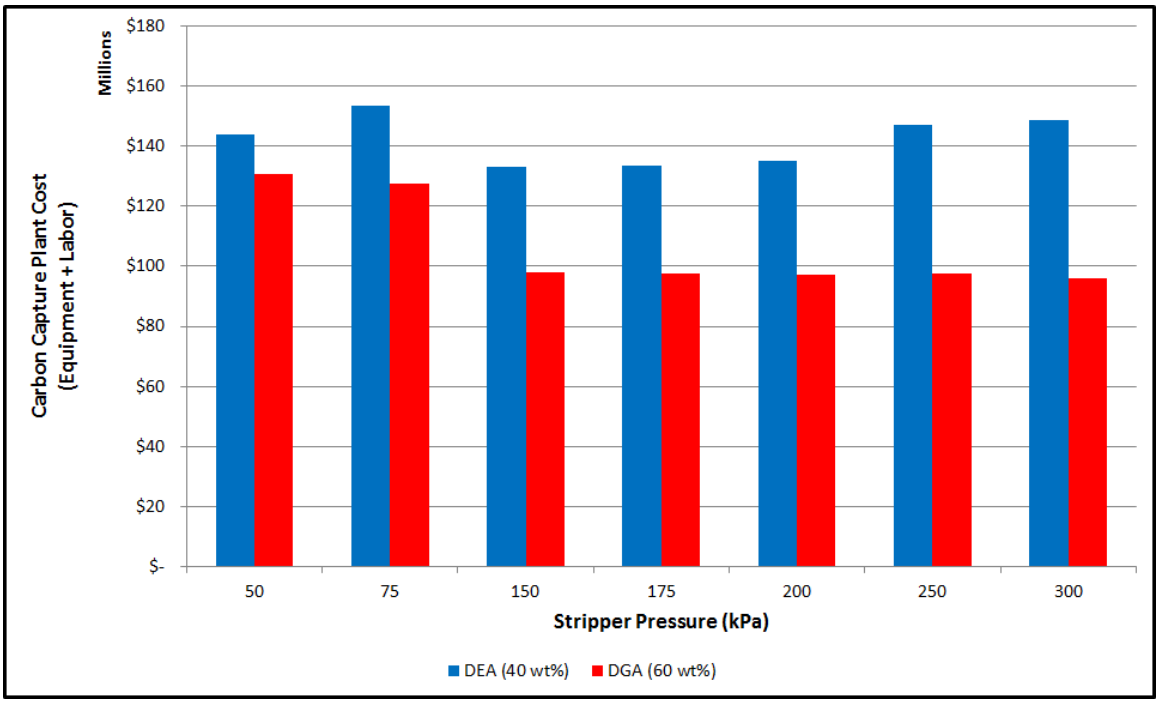

Figure 5.6 : Dependence of the overall cost of carbon capture plants on stripper operating pressure

a minimum when operating at 150 kilopascals (kPa) with the cost maximum at 75 kilopascals (kPa) and 300 kilopascals (kPa) stripper systems. In contrast, diglycolamine (DGA) high pressure strippers costs have negligble dependence on stripper operating pressure. These numbers about the cost of carbon capture plants under various system configurations, now provide an opportunity to review their pros and cons. Vacuum strippers are superior to high pressure strippers in that they operate at a lower temperature, have lower corrosion problems, and can be constructed with cheaper, less corrosion resistant materials.

Table 5.8 : Individual cost of carbon capture plant equipment

Stripper Pressure (kPa)	50	**75**	**150**	**175**	**200**	**250**	**300**	50	**75**	**150**	**175**	**200**	**250**	**300**
Parameter	**DEA Absorption Train Cost ($ MM)**							**DGA Absorption Train Cost ($ MM)**						
Blower	17.1	17.1	17.1	17.1	17.1	17.1	17.1	17.1	17.1	17.1	17.1	17.1	17.1	17.1
Cooler 1	2.6	2.6	2.9	2.9	2.9	2.9	2.9	2.6	2.6	2.9	2.9	2.9	2.9	2.9
Amine Absorber	27.3	26.6	27.2	27.2	26.9	26.9	26.9	7.3	6.6	6.6	6.6	6.6	6.6	6.6
Cooler 2	1.3	1.3	1.3	1.3	1.3	1.3	1.3	1.3	1.2	1.1	1.1	1.1	1.1	1.1
Amine Heat EXCHR	16.1	27.6	26.1	27.0	29.7	42.4	45.1	10.1	14.4	14.9	14.9	15.4	16.7	17.1
Amine Pump 1	1.4	1.4	1.3	1.3	1.3	1.3	1.3	1.3	1.0	1.1	1.0	1.0	1.0	1.0
Amine Pump 2	0.9	0.9	0.9	0.9	0.9	0.9	1.1	0.9	0.7	0.6	0.7	0.7	0.7	0.7
Amine Pump 3	1.2	1.2	0.0	0.0	0.0	0.0	0.0	1.1	0.8	0.0	0.0	0.0	0.0	0.0
Amine Reboiler	1.3	3.0	1.2	1.6	1.2	1.3	1.4	1.9	3.3	1.1	1.0	1.1	1.1	1.1
Amine Stripper	17.1	14.8	10.3	10.1	9.9	9.9	10.0	29.1	22.3	8.5	8.0	7.6	7.5	7.6
SO_2 Scrubber	2.9	2.9	2.9	2.9	2.9	2.9	2.9	2.9	2.9	2.9	2.9	2.9	2.9	2.9
Amine Condenser	1.3	1.1	0.8	0.7	0.7	0.7	0.7	1.3	1.1	0.8	0.7	0.7	0.7	0.7
2-Phase-separator 1	1.2	0.7	0.0	0.0	0.0	0.0	0.0	1.3	0.8	0.0	0.0	0.0	0.0	0.0
Steam Eductor	1.3	1.3	0.0	0.0	0.0	0.0	0.0	1.3	1.3	0.0	0.0	0.0	0.0	0.0

Table 5.9 : Individual cost of carbon capture plant equipment (contd..)

Stripper Pressure (kPa)	50	**75**	**150**	**175**	**200**	**250**	**300**	50	**75**	**150**	**175**	**200**	**250**	**300**
Parameter	**DEA Absorption Train Cost ($ MM)**							**DGA Absorption Train Cost ($ MM)**						
COMP 1	9.1	9.1	6.3	6.3	5.3	5.3	5.2	9.2	9.2	6.3	6.3	5.3	5.3	5.2
COMP 2	5.3	5.3	5.3	5.2	5.2	5.2	4.2	5.3	5.3	5.3	5.2	5.2	5.2	4.2
COMP 3	5.2	5.2	4.1	4.1	4.2	4.1	4.1	5.2	5.2	4.2	4.1	4.2	4.1	4.1
COMP 4	4.1	4.1	4.1	4.1	4.1	4.2	4.2	4.2	4.2	4.2	4.1	4.1	4.2	4.2
COMP 5	4.1	4.1	4.2	4.2	4.9	4.9	4.2	4.2	4.2	4.2	4.2	4.9	4.9	4.2
COMP 6	4.9	5.0	4.9	4.8	4.8	4.7	4.8	5.0	5.0	5.0	4.8	4.8	4.7	4.7
COMP 7	4.8	4.8	4.5	4.2	4.1	3.8	3.9	4.8	4.8	4.6	4.2	4.1	3.8	3.9
COMP 8	3.9	4.0	0.0	0.0	0.0	0.0	0.0	4.0	4.0	0.0	0.0	0.0	0.0	0.0
Intercooler 1	0.6	0.6	0.6	0.6	0.6	0.6	0.6	0.6	0.6	0.6	0.6	0.6	0.6	0.6
Intercooler 2	0.6	0.6	0.6	0.6	0.6	0.6	0.6	0.6	0.6	0.6	0.6	0.6	0.6	0.6
Intercooler 3	0.6	0.6	0.6	0.6	0.6	0.7	0.7	0.6	0.6	0.6	0.6	0.6	0.7	0.7
Intercooler 4	0.7	0.7	0.7	0.7	0.7	0.7	0.8	0.7	0.7	0.7	0.7	0.7	0.7	0.8
Intercooler 5	0.7	0.7	0.7	0.8	0.8	1.0	0.8	0.7	0.7	0.7	0.8	0.8	1.0	0.8

Table 5.10 : Individual cost of carbon capture plant equipment (contd..)

Stripper Pressure (kPa)	50	**75**	**150**	**175**	**200**	**250**	**300**	50	**75**	**150**	**175**	**200**	**250**	**300**
Parameter	**DEA Absorption Train Cost ($ MM)**							**DGA Absorption Train Cost ($ MM)**						
Intercooler 6	0.8	0.8	1.4	1.7	2.0	2.2	2.0	0.9	0.9	0.3	1.7	2.0	2.2	2.0
Intercooler 7	2.1	2.1	1.6	1.1	0.9	0.0	0.0	2.1	2.1	1.6	1.1	0.9	0.0	0.0
2-Phase-separator 2	0.4	0.4	0.5	0.5	0.4	0.4	0.5	0.4	0.4	0.5	0.5	0.4	0.4	0.0
Glycol Absorber	1.3	1.3	0.5	0.5	0.5	0.5	0.5	1.4	1.4	0.5	0.5	0.5	0.5	0.5
Glycol Stripper	0.3	0.3	0.1	0.1	0.1	0.1	0.1	0.3	0.3	0.1	0.1	0.1	0.1	0.1
Glycol Pump	0.3	0.3	0.1	0.1	0.1	0.1	0.1	0.3	0.3	0.1	0.1	0.1	0.1	0.1
Glycol Cooler	0.2	0.2	0.1	0.1	0.1	0.1	0.1	0.2	0.2	0.1	0.1	0.1	0.1	0.1
Glycol Heat Exchanger	0.3	0.3	0.1	0.1	0.1	0.1	0.1	0.3	0.3	0.1	0.1	0.1	0.1	0.1
Glycol Reboiler	0.2	0.2	0.1	0.1	0.1	0.1	0.1	0.2	0.2	0.1	0.1	0.1	0.1	0.1
Glycol Condenser	0.2	0.2	0.1	0.1	0.1	0.1	0.1	0.2	0.2	0.1	0.1	0.1	0.1	0.1

In the presence of a suitable source of waste heat, carbon capture facilities with vacuum strippers have significantly lower parasitic power losses than high pressure strippers. Systems with high pressure strippers, as seen in Figure 5.6 are less costly to construct and are not dependent on the availability of waste heat sources. However, corrosion can be a serious concerns especially at elevated pressures; which also result in higher temperatures.

5.5 Concluding Remarks

Based on the economic evaluation of the carbon capture facility at the reference coal-fired power plant, we have drawn the following conclusions:

1. Carbon capture facilities benefit from operating strippers at higher pressure due to a decrease in the parasitic power loss. However, we have found no significant reduction in the capital expenses. In case of diethanolamine (DEA), there is an increase in the capital expenditure with an increase in the stripper pressure. Thus, the choice of operating pressure narrows down to choosing a configuration with lower capital costs and minimal operational problems.

2. In general, carbon capture plants utilizing vacuum stripping technology are more capital intensive than those using high pressure strippers. The specific magnitude of this cost difference is sensitive to the absorbent used in the process. Based on our results, we conclude that diglycolamine (DGA) at high concentrations is a more suitable choice for absorbent than diethanolamine (DEA). It

maybe generalized that slower reacting absorbents will require longer absorber columns which increase the capital expenditure significantly.

3. Since the parasitic power loss at carbon capture plants with vacuum strippers at power plants lacking waste heat sources is almost comparable with that of high pressure strippers, the additional capital expenses incurred are not justified. At facilities with sufficient waste heat supply, however, carbon capture systems with vacuum stripping are more likely to be considered due to their significant energy savings and increased, but reasonable capital expenses.

Chapter 6

Development of superior absorbents for carbon dioxide (CO_2) removal: emphasizing the role of the solvent

6.1 Motivation

State-of-the-art amine absorption technology utilizes aqueous solutions of alkanolamines such as monoethanolamine (MEA), diethanolamine (DEA), diglycolamine (DGA) and several other similar compounds. The scientific rationale behind the use of these chemical absorbents along with water - a physical absorbent (albeit, a poor one) was to achieve good gas absorption even under conditions of low acid gas partial pressure. Since the days of the invention of triethanolamine (TEA) in 1930, scientific research has almost solely focused on the development of superior compounds for use as chemical absorbents [84]. This has led to the development of novel chemical absorbents such as hindered amines, alkanolamine blends and activated absorbents such as activated methyldiethanolamine (MDEA) and piperazine (PZ) promoted aqueous potassium carbonate (K_2CO_3). Few of these novel absorbents have been widely accepted

in commercial operation and even fewer have resulted in a quantum leap in acid gas removal technology. As was been discussed in previous chapters, monoethanolamine (MEA) is still widely considered the standard absorbent for gas treating and carbon dioxide (CO_2) capture. In spite of a high heat of reaction, it has the highest reactivity with carbon dioxide (CO_2) amongst all alkanolamines and a low molecular weight; both of which are very important characteristics in a good absorbent. When searching for a better absorbent, with the focus being on reducing energy consumption; one must develop compounds with a lower heat of reaction than monoethanolamine (MEA) without compromising much on the chemical reactivity. These two characteristics, however, have an direct relationship - lower the heat of reaction and you get a slower reacting amine and vice versa. As a result, few novel alternatives to monoethanolamine (MEA), diethanolamine (DEA) and diglycolamine (DGA) have been commercialized beyond pilot-scale plants. The research presented in this chapter has been motivated by a curiosity to develop a deeper understanding for the distribution of reboiler duty amongst the physiochemical processes occurring in the stripper unit. Further, we examine the role that a solvent (e.g. water) plays in determining the reboiler energy duty and present a few proof-of-concept studies to estimate energy savings when methanol is added to diethanolamine (DEA) as an absorbent.

6.2 Research Approach

Removal of carbon dioxide (CO_2) from flue gas for carbon capture application is very energy intensive. Energy is provided by low pressure steam to a reboiler installed at the base of the stripper column. Reboiler energy consumption is commonly reported in terms of the energy consumed per unit mass of separated carbon dioxide (CO_2). However, energy consumed in the stripper column is utilized for three different physiochemical processes. These are:

1. Sensible Heating: Increasing the temperature of the incoming fluids to the operating temperature of the stripper column

2. Heat of Reaction: Energy required to drive the endothermic carbon dioxide (CO_2) desorption reaction

3. Generation of stripping vapor: Energy consumed to vaporize a part of the solvent (mostly water) to generate stripping vapor responsible for diluting the desorbed carbon dioxide (CO_2)

Dissecting the reboiler energy consumption into the above constituent processes can be helpful in developing a deeper insight into stripper operation and the influence of absorbent selection. Energy required for absorbent regeneration in the stripper can be described as the sum of contributions of three processes, as shown below in Equation 1 [85].

$$\dot{Q}_{reboiler} = \dot{Q}_{reaction} + \dot{Q}_{sensible} + \dot{Q}_{stripping} \tag{6.1}$$

In Equation 6.1, $\dot{Q}_{\text{reboiler}}$ is the reboiler duty, $\dot{Q}_{\text{reaction}}$ is the heat of reaction for desorption of carbon dioxide (CO_2), $\dot{Q}_{\text{stripping}}$ is the energy consumed to generate stripping vapor (steam) and $\dot{Q}_{\text{sensible}}$ is the energy required for sensible heating of the incoming rich amine solution to the stripper operating temperature. To evaluate these three component terms, we have to make the following simplifying assumptions.

1. All stripping vapor (steam) is condensed in the partial condenser and returned to the reboiler. Thus, the condenser duty corresponds to the energy carried by the stripping vapor (steam)

2. Heat of reaction for the amine CO_2 desorption reaction is independent of temperature, pressure and amine concentration

$$\dot{Q}_{\text{reboiler}} = \dot{m}_{\text{vapor}} \cdot \dot{H}_{\text{vapor}} - \dot{m}_{\text{condensate}} \cdot \dot{H}_{\text{condensate}} \tag{6.2}$$

$$\dot{Q}_{\text{stripping}} = \dot{m}_{\text{moist CO2}} \cdot \dot{H}_{\text{moist CO2}} - \dot{m}_{\text{reflux}} \cdot \dot{H}_{\text{reflux}} - \dot{m}_{\text{dry CO2}} \cdot \dot{H}_{\text{dry CO2}} \tag{6.3}$$

$$\dot{Q}_{reaction} = \dot{m}_{CO2} \cdot \Delta H_{reaction} \tag{6.4}$$

$\dot{Q}_{\text{reboiler}}$ is the net energy provided to reboiler by condensing steam. As represented in Equation 6.2, it is the difference between the enthalpy of entering steam and exiting condensate. Based on assumption # 1 above, $\dot{Q}_{\text{stripping}}$ is the condenser duty, which can be evaluated by performing an energy balance on the partial condenser. Based on

assumption #2, $\dot{Q}_{\text{reaction}}$ is the energy required to drive the endothermic amine-CO_2 desorption reaction. Using equations 6.1, 6.2, 6.3 and 6.4, we can calculate $\dot{Q}_{\text{sensible}}$ which remains as the unknown from Equation 6.1. With the value of $\dot{Q}_{\text{stripping}}$, $\dot{Q}_{\text{sensible}}$ and $\dot{Q}_{\text{reaction}}$ known; the effect of various system parameters on their contribution to $\dot{Q}_{\text{reboiler}}$ can be studied.

6.3 Contribution of various constituent physiochemical processes to reboiler duty

Use of the equations developed in §6.2 allows for the evaluation of the energy consumption by the physiochemical processes occurring in the stripper and reboiler units. Figure 6.1 shows the energy required to generate the stripping vapors (mostly steam) flowing in the stripper column. It can be clearly observed that irrespective of the choice of absorbent, energy consumption decreases as the stripper pressure is increased from 30 kilopascals (kPa) to 300 kilopascals (kPa). A noticeable feature of the plot is the significantly higher energy consumption for generating stripping vapor under vacuum stripping conditions. While all three absorbents exhibit this behavior, the increase is particularly noticeable for monoethanolamine (MEA). The significantly higher energy required to generate stripping vapors with monoethanolamine (MEA) can be attributed to a lower partial pressure of carbon dioxide (CO_2) in equilibrium with the monoethanolamine (MEA), especially at low amine loadings. The dependence of the energy duty for generation of stripping vapor on stripper pressure is

remarkably stronger for monoethanolamine (MEA) than for the other two amines and this maybe attributed to the higher sensitivity of the equilibrium partial pressure of carbon dioxide (CO_2) on temperature. Thus, for the same reduction in stripper pressure and hence, temperature; energy requirement for the monoethanolamine (MEA) system increases more rapidly. In general, the drop in energy consumption with an increase in stripper pressure is a result of the change (increase) in the ratio of the partial pressures of carbon dioxide (CO_2) and water with an increase in stripper pressure. One of the most noticeable features of Figure 6.1 is its close similarity to trend in Figure 4.9, which presents the effect of stripper pressure on the reboiler duty. This suggests that the energy consumed for generating stripping vapor is a strong contributor to the overall pressure sensitivty of the reboiler duty. Figure 6.2 is a plot of the lumped contribution of sensible heating and heat of reaction to reboiler heat duty. As seen in the plot, the combined contribution of these two processes is near constant and is only weakly sensitive to changes in stripper pressure. This confirms the hypothesis made previously that the pressure sensitivty of reboiler duty is a direct result of changes to the stripping vapor generation duty.

The dependence of stripping vapor (steam) requirement on pressure can itself be explained by analyzing the ratio of partial pressure of carbon dioxide (CO_2) in equilibrium with the rich amine solution to that of water. Using a modified form of the Clausius-Clapyeron equation (6.5), the ratio of the partial pressure of carbon dioxide (CO_2) to water can be expressed as shown below [85].

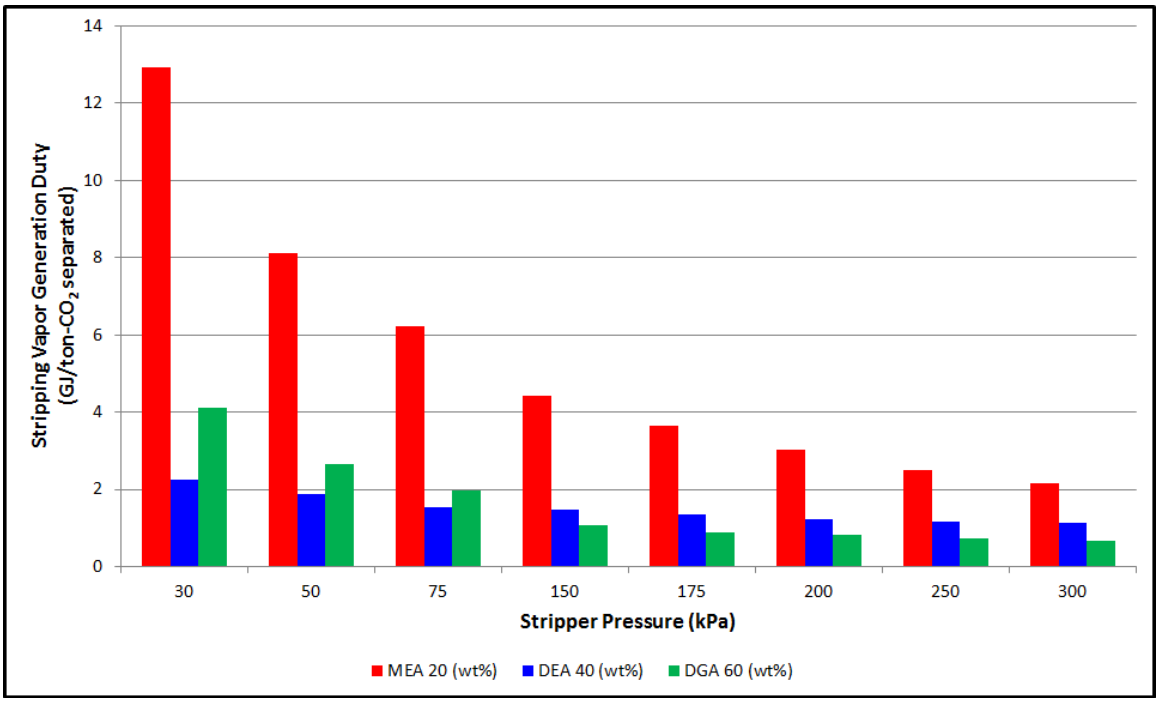

Figure 6.1 : Contribution of stripping vapor energy consumption to reboiler heat duty

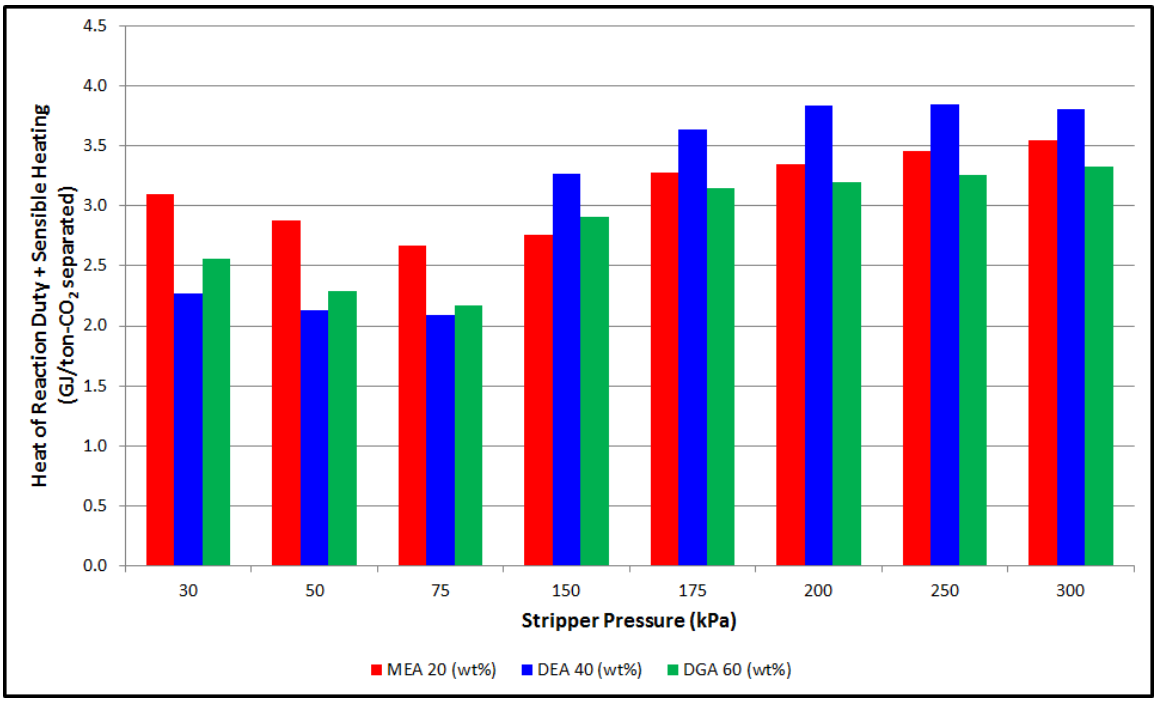

Figure 6.2 : Lumped contribution of heat of reaction and sensible heating duty to the reboiler heat duty

$$\left(\frac{p_{wat}^{sat}}{p_{co2}^{sat}}\right) = \left(\frac{p_{wat,Tref}^{sat}}{p_{co2,Tref}^{sat}}\right) \cdot \left(\left[\frac{T - T_{ref}}{RTT_{ref}}\right] [\Delta H_{vap,H2O} - \Delta H_{abs,CO2}]\right) \tag{6.5}$$

Figure 6.3 shows the changes in ratio of the partial pressures of carbon dioxide (CO_2) and water at different temperatures between carbon dioxide (CO_2) and carbon dioxide (CO_2) for monoethanolamine (MEA), diethanolamine (DEA) and diglycolamine (DGA). The partial pressure of carbon dioxide (CO_2) presented here is measured above an aqueous alkanolamine solution with a carbon dioxide (CO_2) loading of 0.5 moles-CO_2/mole-amine [86, 9, 87, 88, 89]. As seen here, this ratio increases rapidly with temperature which results in a sharp reduction in the stripping vapor requirement and thus, the reboiler duty. Figure 6.3 explains both the pressure dependence of stripping vapor requirement and the higher reboiler duty for monoethanolamine (MEA) as compared to diethanolamine (DEA) and diglycolamine (DGA).

Figures 6.4, 6.5 and 6.6 show the contribution of each of the three physiochemical processes to the total reboiler duty in percentage (%) terms. Clearly, at lower stripper pressures (and hence, temperatures); energy consumption to generate stripping vapor dominates the reboiler duty. From the data presented in these figures, it is also apparent that when primary amines - monoethanolamine (MEA) and diglycolamine (DGA) are selected; a larger fraction of the reboiler duty is consumed to generate stripping vapor. This can be explained on the basis of their relateively stronger binding with the absorbed carbon dioxide (CO_2) and hence, a lower equilibrium partial

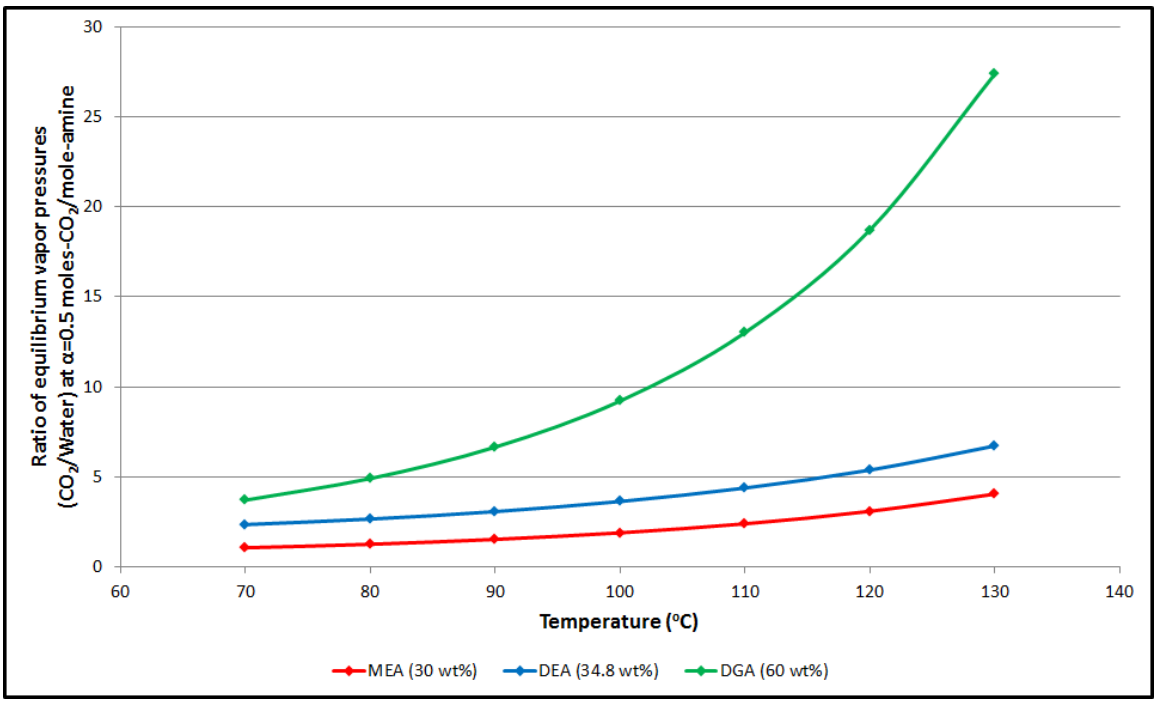

Figure 6.3 : Ratio of CO_2 to H_2O partial pressures in equilibrium with different alkanolamines ($\alpha = 0.5$ moles-CO_2/mole-amine)

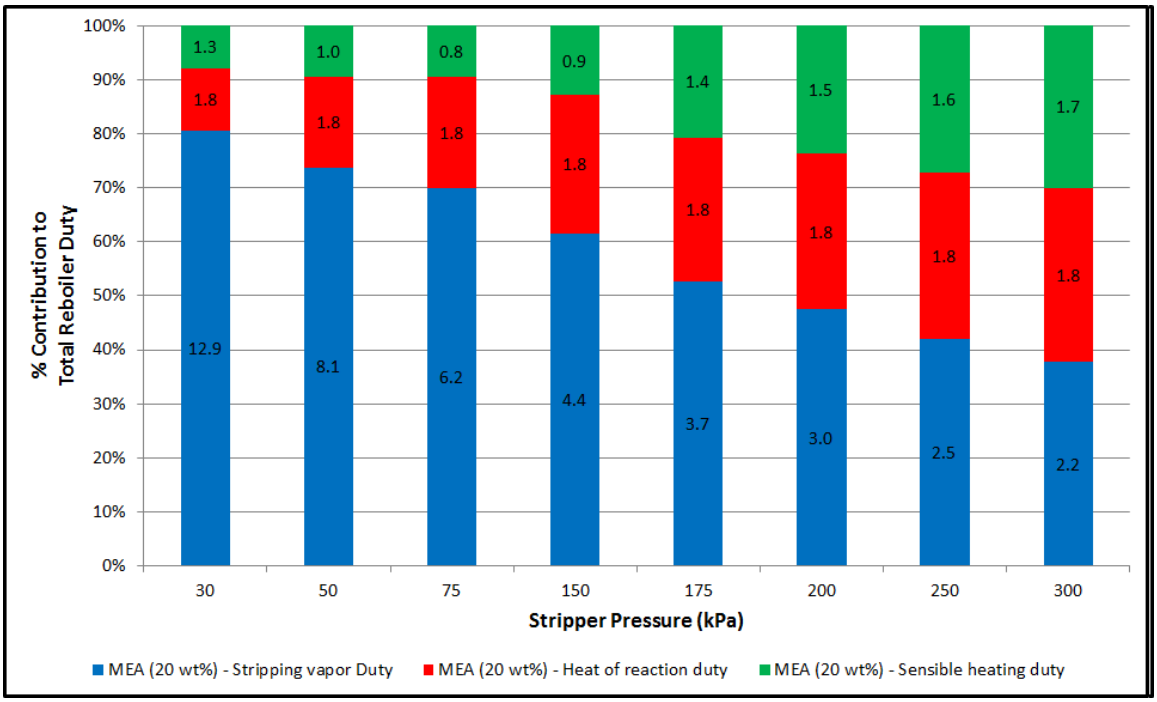

Figure 6.4 : Contribution of physiochemical processes to reboiler duty - (MEA 20 wt%)

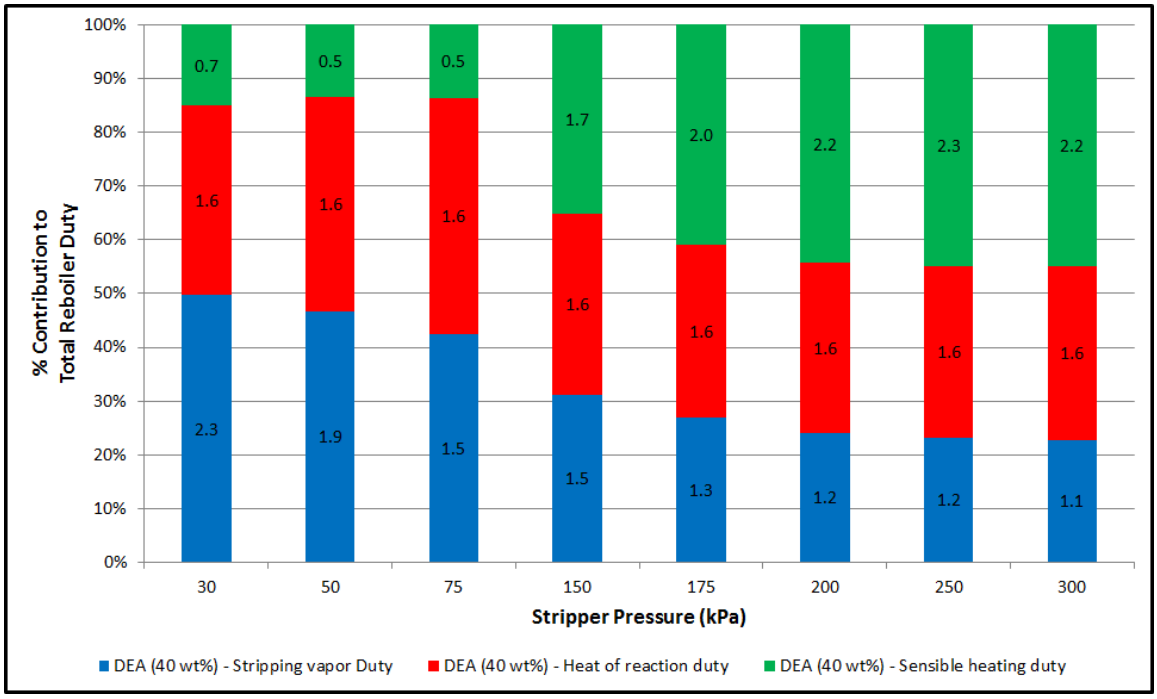

Figure 6.5 : Contribution of physiochemical processes to reboiler duty - (DEA 40 wt%)

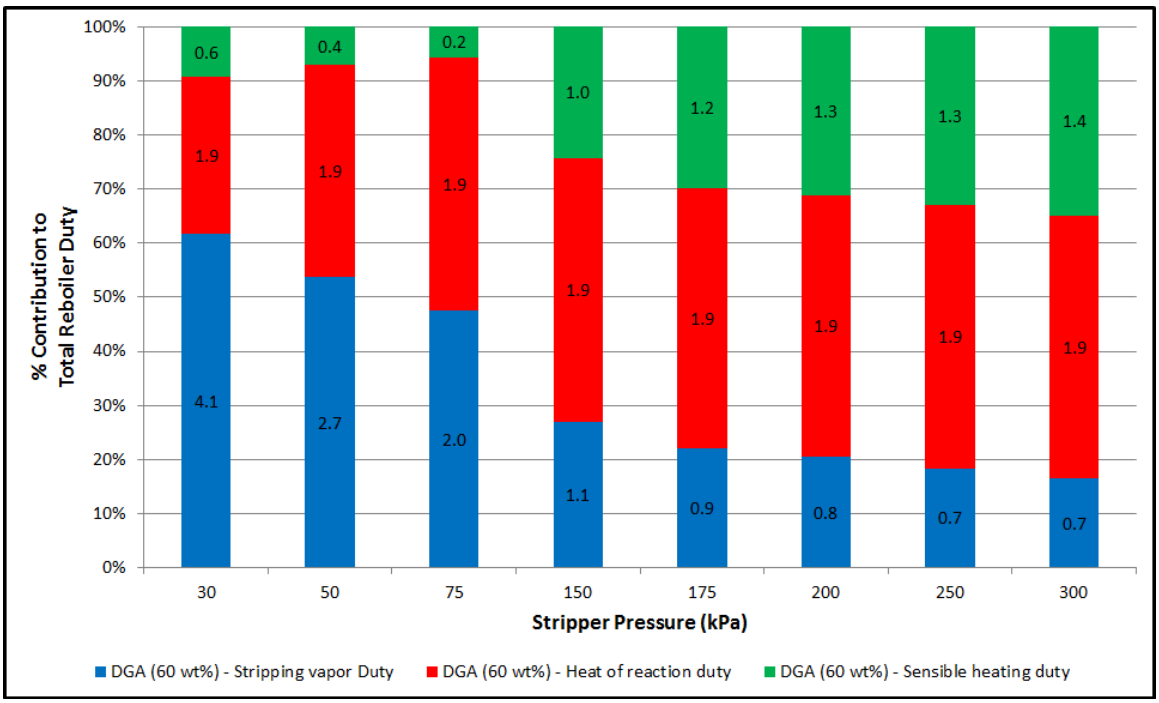

Figure 6.6 : Contribution of physiochemical processes to reboiler duty - (DGA 60 wt%)

pressure as compared the secondary amine - diethanolamine (DEA). The contribution of energy consumed for the carbon dioxide (CO_2)-amine desorption reaction is almost independent of stripper pressure (it is assumed that the heat of reaction has no temperature dependence, although in reality there is a weak temperature dependence). As with stripping vapor generation energy duty, it is also apparent from the data that the sensible heating requirement is slightly higher for diethanolamine (DEA) than for monoethanolamine (MEA) and diglycolamine (DGA). This can be attributed to two factors - a stripper temperature which is not significantly lower than that for the primary amines and a lower temperature for the rich amine exiting the absorber column (due to its lower heat of reaction).

6.4 Role of the alkanolamine solvent

As discussed previously, all scientific research in the area of chemical absorption for carbon dioxide (CO_2) capture is focused on the development of better absorbent chemicals. However, commercially used absorbents are composed of between 7% (mole) and 30% (mole) alkanolamine with the rest being water. Water has been the solvent of choice for alkanolamines because it is ubiquitous, cheap and is miscible with most amines in all proportions. This choice of solvent, however, plays a crucial role in several of the physiochemical processes occuring during the absorption and stripping processes. Since, water is the primary component of the circulating absorbent solution; it plays a determining role in physiochemical properties. These include carbon

dioxide (CO_2) solubility, the carbon dioxide (CO_2)-amine vapor liquid equilibrium, solution viscosity, specific heat capacity, heat of vaporization, surface tension amongst others. Carbon dioxide (CO_2) solubility plays a key role in determining the rate of mass transfer of carbon dioxide (CO_2) from the vapor phase into the liquid. Specific heat capacity of the solution is one of the factors that controls the degree of sensible heating that must take place in the stripper. Similarly, the heat of vaporization of the absorbent solution determines the energy input required to generate sufficient stripping vapor in the column. Finally, a solvent can affect the vapor liquid equilibrium that exists between the carbon dioxide (CO_2) and the amine solution. From purely an energy standpoint, the specific heat capacity and the heat of vaporization are the two most important physiochemical properties of the selected solvent. A solvent with a low specific heat capacity and low heat of vaporization might be preferable over one with higher values for these two properties. Figures 6.7 and 6.8 show a comparison between the specific heat capacity and the heat of vaporization for water and a select few alcohols [68]. It is apparent from both these charts that most alcohols are superior as compared to water on the basis of these two properties. The change in solvent could further affect the rate of the carbon dioxide (CO_2)-amine reaction and will result in a novel ternary system, the vapor liquid equilibria for which could be significantly different from that of the aqueous alkanolamine one. Based on this scientific rationale, we hypothesize that if water used in the circulating alkanolamine absorbent were to be replaced - partially or fully with an alcohol; then there are

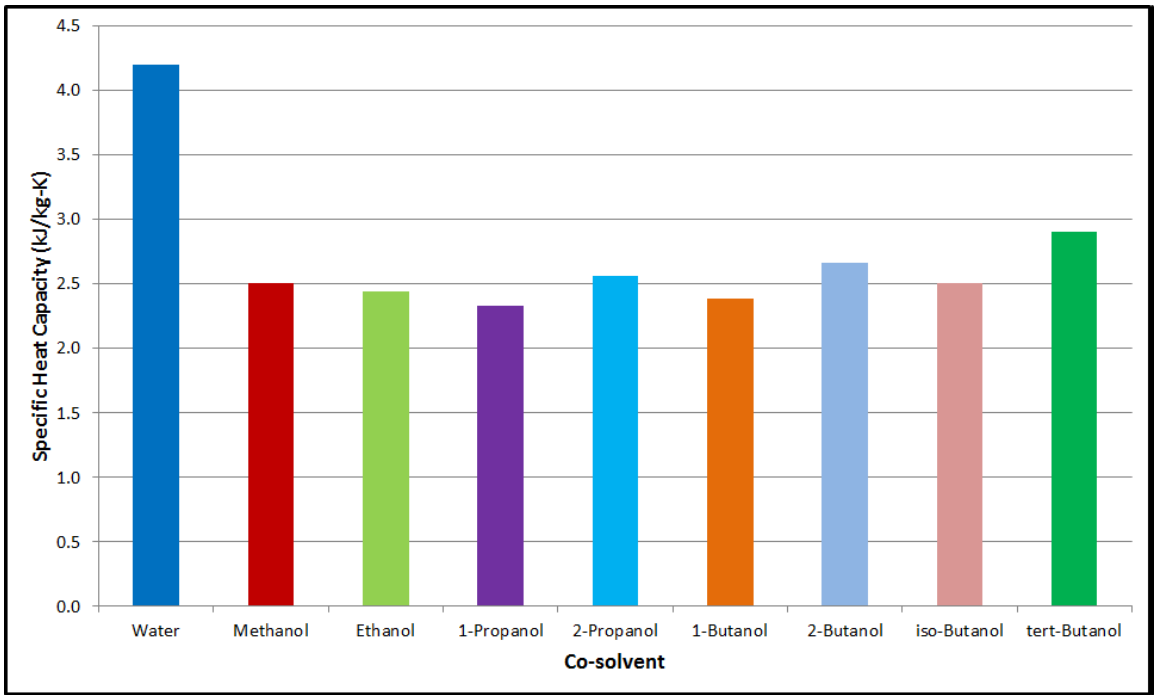

Figure 6.7 : A comparison of the specific heat capacity of water and various alcohols

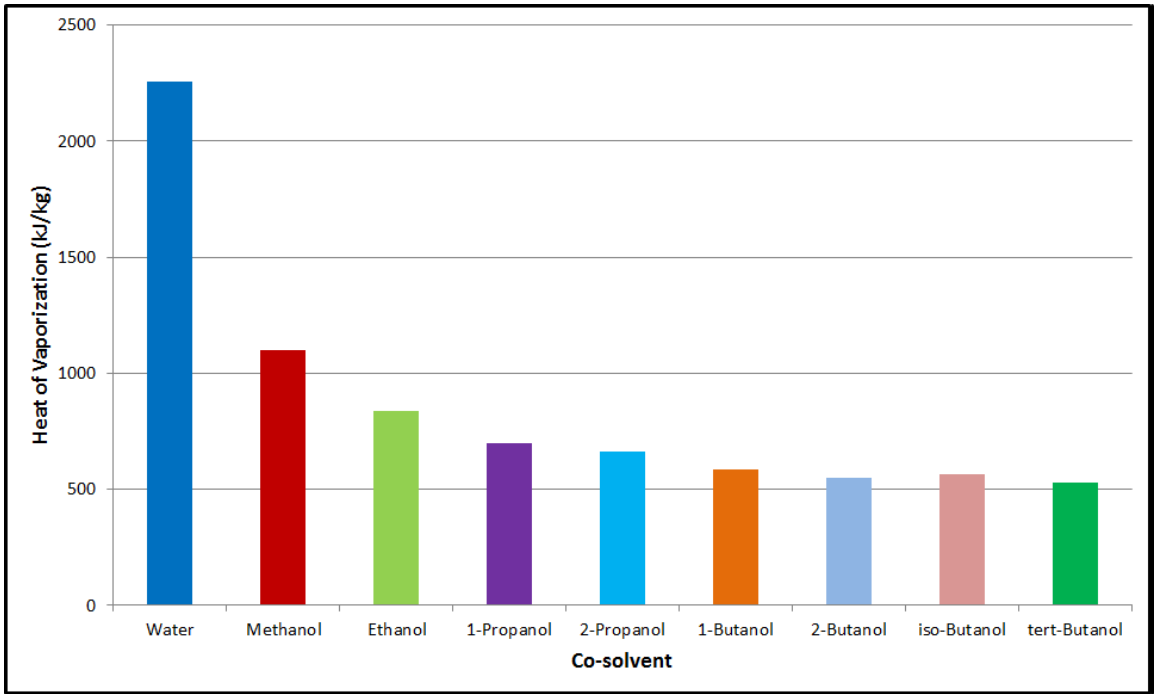

Figure 6.8 : A comparison of the heat of vaporization of water and various alcohols

potential energy savings to be achieved [35]. In the next section, we examine the available information from published literature where the effects of alcohol addition to aqueous alkanolamines have been studied to some extent. We have also assumed vapor-liquid equilibrium to estimate the reboiler energy duty for scenarios where these novel absorbent formulations are used in the amine absorption process.

6.5 Estimating the effect of addition of alcohol to alkanolamines on energy consumption

6.5.1 A brief review of published literature

We have hypothesized in §6.4 that the complete or partial replacement of water in industrial absorbents for carbon dioxide (CO_2) removal can result in energy savings in the absorption process. In order to estimate the energy consumption in the amine absorption process using these novel solvent formulations, information is required regarding the vapor-liquid equilibria (VLE) and heats of mixing for the quaternary system involving the alkanolamine, water, alcohol and carbon dioxide (CO_2). When such thermodynamic data is available, it can be used to model the non-ideal behavior exhibited by the solvent by fitting available experimental data to a suitable thermodynamic model (e.g. Non Random Two Liquids (NRTL), Electrolyte Non Random Two Liquids (E-NRTL)). However, there is little information in published literature documenting the effect of alcohols on the behavior of aqueous alkanolamine systems. The thermodynamic behavior (vapor liquid equilibria (VLE) and heats of

mixing) of the ternary system - water, methanol and diethanolamine (DEA) has been studied by Horstmann and coworkers. They have fitted the experimentally measured vapor liquid equilibria (VLE) and heats of mixing data to the Non Random Two Liquids (NRTL) model and obtained the temperature dependent coefficients for the expressions used to predict the binary interaction parameters [90]. Archane and coworkers have studied the effect of methanol addition on the vapor-liquid equilibrium to aqueous diethanolamine (DEA) at room temperature [91]. A similar, however, much more detailed study was performed by Tounsi and coworkers to characterize the vapor-liquid equilibrium for the quaternary system of water, methanol, diethanolamine (DEA) and carbon dioxide (CO_2) at 50°C, 60°C, 80°C, 100°C and 120°C. Additionally, they have attempted to correlate the measurements using the Kent and Eisenberg approach for describing the behavior of alkanolamine systems [92, 93]. Figure 6.9 shows the comparison between the equilibrium partial pressure of carbon dioxide (CO_2) for two different diethanolamine based absorbent blends at a temperature at 100°C. The red curve represents a conventional aqueous alkanolamine blend containing 34.8 % diethanolamine (DEA) by weight, balance water (Aq). The blue curve shows the carbon dioxide (CO_2) partial pressure for an absorbent blend containing 40 % diethanolamine (DEA), 40 % water (Aq) and 20 % methanol (MeOH) by weight. Clearly, under the temperature conditions at which conventional amine strippers are operated; carbon dioxide (CO_2) has a much higher partial pressure for the formulation containing alcohol than the conventional absorbent. A higher carbon

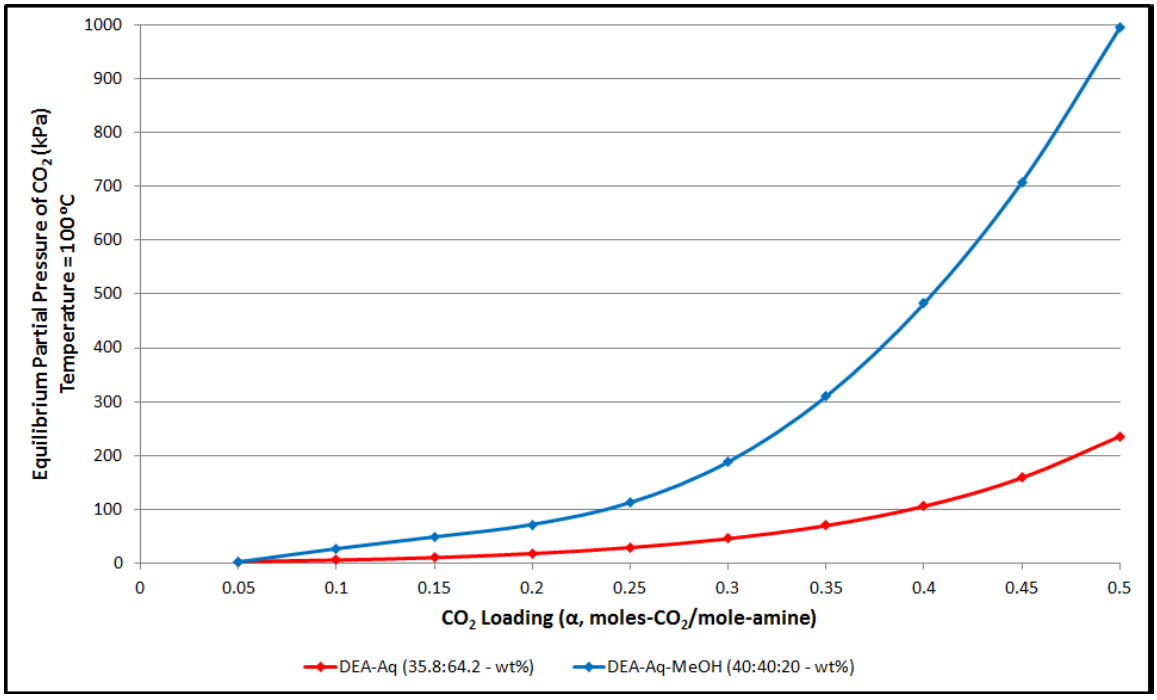

Figure 6.9 : A comparison of the equilibrium partial pressure of carbon dioxide (CO_2) above two diethanolamine (DEA) based absorbent formulations at 100°C

dioxide (CO_2) partial pressure for the absorbent is favorable in the stripper unit as it results in lower stripping vapor requirement and potentially, a lower reboiler energy consumption. It is however a disadvantage in the absorber unit because corresponding to the same partial pressure of carbon dioxide (CO_2) in the feed gas, a lower carbon dioxide (CO_2) loading can be achieved in the absorbent solution. This reduction in the carbon dioxide (CO_2) loading capacity of the absorbent must be compensated for either by increasing the flue gas pressure or by increasing the absorbent circulation rate.

6.5.2 Approach to estimating reboiler duty

Aqueous diethanolamine (DEA) blended with methanol is the most studied system of its type in published literature. However, as discussed in §§6.5.1; even for this system, there is no data on the heats of mixing for scenarios when carbon dioxide (CO_2) has been dissolved into the absorbent liquid. In the absence of sufficient thermodynamic data, two different approaches can be adopted to estimate the reboiler duty. One approach involves using available Non Random Two Liquid (NRTL) binary interaction parameters for the ternary system - methanol, water and diethanolamine; and fitting the Henry's Law constant (without accounting for temperature dependence) to match the vapor-liquid equilibrium (VLE) data. This approach involves the use of a process simulation software such as AspenPlus or AspenHYSYS and the tedious process of attempting to fit a suitable Henry's Law constant. One source for error in calculations conducted using this approach are the lack of temperature dependence of the fitted Henry's Law constant. Another source of error stems from the fact that the Non Random Two Liquid (NRTL) model doesn't account for the ionization of the diethanolamine (DEA), water, carbon dioxide (CO_2) and their reaction products present in the liquid phase. Additionally, closed loop simulations in AspenPlus and AspenHYSYS are difficult to converge in the absence of suitable guesses for system parameters which are typically based on existing plant data.

An alternate and simpler approach involves assuming the existence of equilibrium between the vapor and liquid phases. This approach was widely used before

sophisticated rate-based models could be used in process simulators. In this approach, various system parameters such as the absorbent circulation rate, rich amine loading and temperature, reboiler temperature and stripping vapor composition and flow-rate, amongst others are calculated using available physical properties and vapor-liquid equilibrium data and by performing simple, mass and enthalpy balances. The reboiler duty itself can be calculated by estimating the energy consumed for generating stripping vapor, the sensible heating requirement for the absorbent solution and energy consumed by the endothermic amine-CO_2 desorption reaction. The main source for error in the calculations performed using this approach is the assumption for an ideal liquid phase which can result in calculated vapor pressures for water and methanol that deviate from experimentally measured values. Additionally, since the column calculations have to be performed manually and don't involve the use of process simulators; it is infeasible to predict the pressure and temperature profiles at each stage/tray inside the column. The use of process simulators in this approach is limited to predicting the pressure, temperature and physical properties of various material streams.

Since our interest in performing these calculations is purely to produce a proof-of-concept of our hypothesis; we have selected to utilize the simpler and faster equilibrium method. In order to verify the validity of the results generated using this approach, however, we first use vapor-liquid equilibrium data (VLE) from published literature to estimate the reboiler duty for an aqueous diethanolamine (DEA) system

containing 34.8% amine by weight. We evaluate the reboiler duty for this system under two different stripper operating pressures - 150 kilopascals (kPa) and 200 kilopascals (kPa). The results are compared to those generated for the same system conditions in ProMax. After establishing the validity of this approach, we proceed to calculating the reboiler duties for a process using an absorbent formulation of 40 wt% diethanolamine (DEA), 40 wt% water and 20 wt% methanol under the same two stripper operating pressures. We make several simplifying, yet reasonable assumptions to ease our calculations. These are listed below:

1. Flue gas entering the absorber column is composed of water, nitrogen(N_2) and carbon dioxide (CO_2).

2. Exactly 90% of the incoming carbon dioxide (CO_2) is removed.

3. The only component of flue gas transferring to the absorbent is carbon dioxide (CO_2). There is no loss of water, methanol or diethanolamine (DEA) occurring in the absorber column. This is a reasonable assumption since nitrogen(N_2) has a very limited solubility in water and diethanolamine (DEA) has an extremely low pressure even at high temperatures. In reality, some water and methanol is transferred to the vapor phase; however, losses can be minimized by using a solvent wash stage for recovery.

4. Decarbonized flue gas leaving the absorber is in thermal equilibrium with the lean absorbent solution entering the column.

5. Rich absorbent solution leaving the absorber is compositionally in equilibrium with the incoming flue gas. Thus, the rich amine loading is determined by the temperature of amine solution and the partial pressure of carbon dioxide (CO_2) in the flue gas.

6. Vapors exiting the stripper column and entering the partial condenser are in equilibrium with the incoming rich absorbent solution.

7. Energy consumed for sensible heating in the stripper column is the difference between the enthalpies of the hot lean amine solution exiting the reboiler and the rich absorbent entering the stripper.

8. For the cases involving aqueous diethanolamine blended with methanol, the partial condenser is operated at a lower temperature than for the conventional, aqueous diethanolamine (DEA) case to minimize methanol carryover with the carbon dioxide (CO_2). Carryover losses, if any, are assumed to be small.

9. The heat of reaction for the diethanolamine-CO_2 reaction is unchanged by the addition of methanol to aqueous diethanolamine (DEA).

In the following section, we discuss the framework used to performing the equilibrium calculations. The results of these calculations are presented as well.

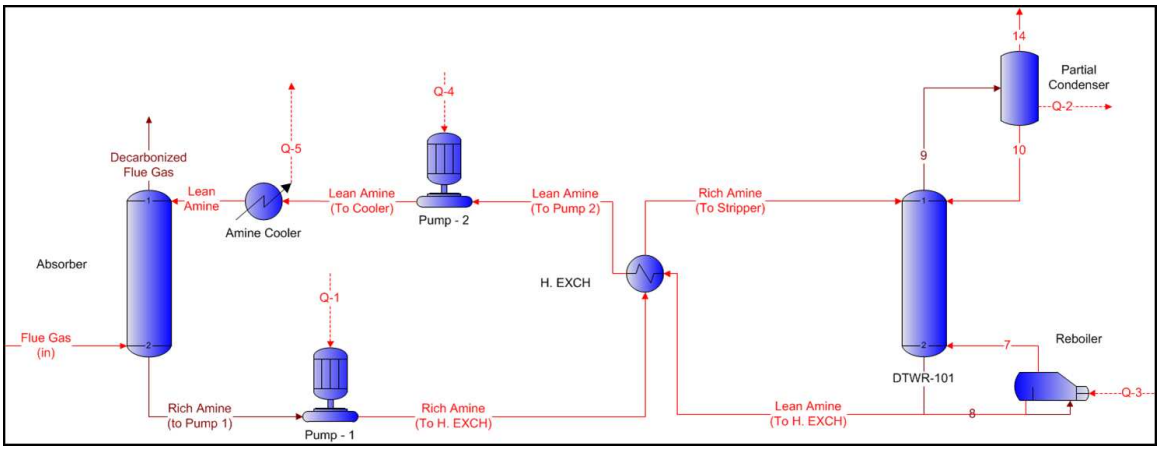

Figure 6.10 : Simplified schematic representation of a typical amine absorption unit

6.5.3 General framework for evaluating reboiler duty using equilibrium approach

Figure 6.10 shows a schematic of an amine absorption plant complete with various auxiliary units such as heat exchangers, coolers and pumps. When performing amine absorption process calculations using the equilibrium approach method, the first parameter to determine is the absorbent circulation rate. This is typically determined by evaluating the carbon dioxide (CO_2) loading of the lean and rich amine solutions - using vapor-liquid equilibrium (VLE) and previously, plant data. Once these values are fixed, the carbon dioxide (CO_2) loading capacity of the absorbent solution is known and the amine circulation rate can be determined on the basis of the carbon dioxide (CO_2) to be removed. Since, the absorbent composition is known a priori; the absorbent circulation rate can be determined. In Equations 6.6 and 6.7, $\dot{m}_{DEA}$ is the molar flow rate of diethanolamine (DEA), $\dot{m}_{CO2}$ is the molar removal rate of carbon

dioxide (CO_2), α_{rich} and α_{lean} are the carbon dioxide (CO_2 loadings of rich and lean absorbent, $\dot{M}_{absorbent}$ is the mass flow-rate of the absorbent, MW_{DEA} is the molecular weight of diethanolamine (DEA) and w_{DEA} is the weight fraction of diethanolamine (DEA) in the absorbent.

$$\dot{m}_{DEA} = \frac{(\dot{m}_{CO2})}{(\alpha_{rich} - \alpha_{lean})} \tag{6.6}$$

$$\dot{M}_{absorbent} = \frac{(\dot{m}_{DEA} \cdot MW_{DEA})}{w_{DEA}} \tag{6.7}$$

With the lean and rich absorbent flow-rates known, the outlet temperature of the rich absorbent exiting the absorber can be evaluated by performing an enthalpy balance on the absorber. There are a total of 4 material streams entering and exiting the absorber. Additionally, there is an exothermic reaction taking place between diethanolamine (DEA) and carbon dioxide (CO_2) in the liquid phase. Equation 6.8 describes the enthalpy balance performed on the absorber column. In Equation 6.8, $\dot{H}_{rxn}$ is the product of the mass flow-rate of carbon dioxide (CO_2) and the heat of reaction for the diethanolamine-CO_2 reaction. The enthalpy of material streams is the product of their mass flow-rates, specific heat capacities and temperatures. Since the specific heat capacity of the rich amine solution itself has some temperature dependence, an iterative procedure must be used to determine the temperature of the rich absorbent stream.

$$\dot{H}_{rich} = \left(\dot{H}_{lean} + \dot{H}_{gas,in} + \dot{H}_{rxn}\right) - \left(\dot{H}_{gas,out}\right) \tag{6.8}$$

The next parameter to be determined is the reboiler temperature, which is also the temperature of the lean absorbent stream exiting the reboiler. In industrial operation, it is common to set the stripper/reboiler bottoms pressure; which then makes the stripper temperature a dependent variable. The pressure at the bottom of the stripper/reboiler is the cumulative contribution of the vapor pressures of carbon dioxide (CO_2) and other components of the liquid absorbent in equilibrium with the lean absorbent solution at the reboiler temperature. This is represented mathematically in Equation 6.9.

$$P_{stripper/reboiler} = P_{CO2} + P_{DEA} + P_{water} + P_{MeOH} \tag{6.9}$$

The reboiler temperature is determined by iteratively finding the temperature at which P_{DEA}, P_{Water}, P_{MeOH} (if present) and P_{CO2} - the partial pressure of carbon dioxide (CO_2) in equilibrium with the lean absorbent solution add up to the required stripper pressure. Once the stripper pressure is determined, it is possible to determine the temperature of the rich absorbent solution entering the stripper column by fixing the minimum end approach temperature in the lean/rich heat exchanger unit. The pressure of the rich absorbent solution should be sufficiently high to avoid the formation of a vapor phase through flash evaporation of the solution.

When the rich absorbent solution exits the lean/rich heat exchanger, it is at

a high pressure and doesn't comprise of any vapor. However, its entry into the stripper column; which is operated at a lower pressure results in flash evaporation which results in a drop in its temperature, pressure and a change in its composition. These flash calculations have been performed using the process simulation software - ProMax. Once the compositions of the vapor and liquid phases in the entering rich absorbent solution are determined, the pressure at the top of the stripper column can be evaluated. In a process simulator like ProMax and AspenPlus, a rigorous mass and energy balance is conducted on the top stage in the column to determine the composition of the vapors leaving the stripper. In the equilibrium approach method, the vapor composition can be determined by assuming it to be in equilibrium with the 'flashed' rich absorbent solution. As before, the total pressure is the sum of the partial pressures of carbon dioxide (CO_2), diethanolamine (DEA), water and methanol. In order to determine the flow-rates of each of these components in the overhead vapors, we take advantage of the fact that the mass flow-rate of carbon dioxide (CO_2) is known (90% CO_2 removal). With the molar composition and flow-rate of carbon dioxide (CO_2) known, the flow-rates of other components of the vapor can be determined.

With all the necessary information available, we can begin reconstituting the reboiler duty on the basis of the knowledge that it is the cumulative contribution of the energy expended in generating the stripping vapors, for the endothermic diethanolamine-CO_2 desorption reaction and the sensible heat required to raise the

temperature of the incoming rich amine solution to that of the reboiler. The contribution of each of these terms is expressed in Equations 6.10, 6.11, 6.12 and 6.12. In these equations, $\dot{Q}_{rxn}$, $\dot{Q}_{sensible}$, $\dot{Q}_{stripping}$ and $\dot{Q}_{reboiler}$ are the energy duties for heat of reaction, sensible heating, stripping vapor generation and total reboiler duty respectively. $\dot{M}_{CO2}$, $\dot{M}_{DEA}$, $\dot{M}_{water}$, $\dot{M}_{MeOH}$, $\dot{M}_{rich}$ and $\dot{M}_{lean}$ are the mass flow-rates for carbon dioxide (CO_2), diethanolamine (DEA), water, methanol, rich and lean absorbent respectively. $\Delta H_{vap,DEA}$, $\Delta H_{vap,water}$ and $\Delta H_{vap,MeOH}$ are the heats of vaporization for diethanolamine, water and methanol respectively. $c_{p,lean}$, $c_{p,rich}$, T_{lean} and T_{lean} are the specific heat capacity and temperatures of the lean and rich absorbent streams respectively. In the next section, we apply this framework to calculating the reboiler duty for two strippers operated at 150 kilopascals (kPa) and 200 kilopascals (kPa) with 34.8 wt% diethanolamine (DEA) as the absorbent.

$$\dot{Q}_{rxn} = \dot{M}_{CO2} \cdot \Delta H_{rxn} \tag{6.10}$$

$$\dot{Q}_{stripping} = \dot{M}_{DEA} \cdot \Delta H_{vap,DEA} + \dot{M}_{water} \cdot \Delta H_{vap,water} + \dot{M}_{MeOH} \cdot \Delta H_{vap,MeOH} \tag{6.11}$$

$$\dot{Q}_{sensible} = \left(\dot{M}_{lean} \cdot c_{p,lean} \cdot T_{lean}\right) - \left(\dot{M}_{rich} \cdot c_{p,rich} \cdot T_{rich}\right) \tag{6.12}$$

$$\dot{Q}_{reboiler} = \dot{Q}_{sensible} + \dot{Q}_{stripping} + \dot{Q}_{reaction} \tag{6.13}$$

6.5.4 Evaluating reboiler duty for aqueous diethanolamine (DEA) systems

We have discussed in sufficient detail the assumptions that have been made in evaluating reboiler duty using the equilibrium approach method. Before applying the framework developed in §§6.5.3 to aqueous diethanolamine (DEA) systems blended with methanol, it is important to verify the validity of these assumptions and estimate the degree of error they result in by comparing a baseline system against process simulator output. For this purpose, we have selected an aqueous diethanolamine (DEA) system containing 34.8 wt% amine. Vapor-liquid equilibrium (VLE) data for this system at a wide range of temperatures is available in published literature. Figure 6.11 shows the dependence of equilibrium partial pressure of carbon dioxide (CO_2) on amine loading for this system for a range of temperatures [94]. This vapor-liquid equilibrium (VLE) data will be used throughout these baseline calculations.

Before applying the framework developed in §§6.5.3, certain parameters such as the flue gas flow-rate, carbon dioxide (CO_2) loading of lean amine solution must be fixed. These are tabulated below in Table 6.1. Using these and the framework, other relevant parameters including the compositions of various material streams can be evaluated. In evaluating these parameters, the temperature dependence of the vapor pressure of water is expressed using the Antoine equation shown in Equation 6.14 below.

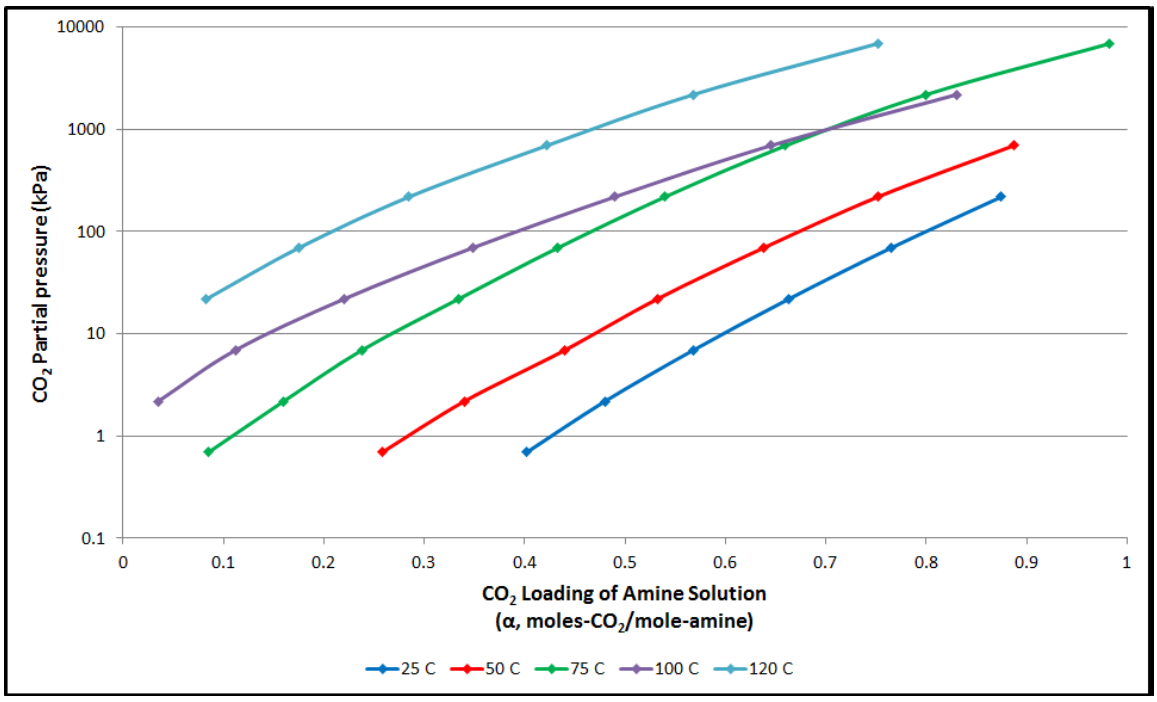

Figure 6.11 : Vapor liquid equilibrium data for aqueous diethanolamine (DEA) 34.8 wt%

$$P = 10^{A-\left(\frac{B}{C+T}\right)} \tag{6.14}$$

Table 6.1 lists the Antoine coefficients for water and methanol. Presented in Table 6.3 are the properties and composition of the decarbonized flue gas and the rich absorbent streams exiting the absorber column. We have previously stated our assumption that the only component transferred from vapor phase to the absorbent is carbon dioxide (CO_2). This allows evaluation of component mass flow-rates as well as the carbon dioxide (CO_2) loading of the absorbent. Temperature of the rich absorbent exiting the column is an unknown and this can be evaluated by performing an enthalpy balance on the absorber column. Enthalpy of reaction for the absorption of carbon

Table 6.1 : Antoine equation parameters for water and methanol

Component	A	B	C	Tmin (°C)	Tmax (°C)
Water	8.07131	1730.63	233.426	1	100
Water	8.14019	1810.94	244.485	99	374
Methanol	8.08097	1582.27	239.7	15	100
Methanol	7.9701	1521.23	234	65	214

dioxide (CO_2) is evaluated by linear interpolation between two values at different temperatures obtained from published literature.

Table 6.4 summarized the composition and properties of the rich amine before and after entering the stripper column. After exiting the absorber, the rich absorbent solution is sufficiently pressurized to avoid 2-phase flow in the pipelines. Rich absorbent flows through the lean/rich heat exchanger which operates at a minimum end approach temperature of 5°C. In order to simulate the flash evaporation of the rich absorbent stream that takes place after entering the stripper column, the rich absorbent is passed through a throttling valve in ProMax. As seen in Table 6.4, this results in approximately 8°C drop in the amine temperature along with a decrease in the amine loading due to the release of some carbon dioxide (CO_2) into the vapor phase.

Table 6.2 : Parameters used for reboiler duty calculations

Parameter ↓	**Stripper Pressure = 150 kPa**		**Stripper Pressure = 200 kPa**	
Material Stream →	**Flue gas (in)**	**Lean Amine**	**Flue gas (in)**	**Lean Amine**
Temperature (°C)	30.0	45.0	30.0	45.0
Pressure (kPa)	124.1	827.4	124.1	827.4
Mass flow-rate (kg/s)	144.4	800.0	144.4	900.0
Water mass fraction	4.4	63.1	4.4	62.9
CO_2 mass fraction	23.6	2.1	23.6	2.3
N_2 mass fraction	72.0	0.0	72.0	0.0
DEA mass fraction	0.0	34.9	0.0	34.8
CO_2 Loading	-	0.14	-	0.159

Table 6.3 : Properties and composition of material streams exiting the absorber

Parameter ↓	**Stripper Pressure = 150 kPa**		**Stripper Pressure = 200 kPa**	
Material Stream →	**Flue gas (out)**	**Rich Amine (out)**	**Flue gas (out)**	**Rich Amine (out)**
Temperature (°C)	45.0	60.0	45.0	58.3
Pressure (kPa)	110.3	124.1	110.3	124.1
Mass flow-rate (kg/s)	113.7	830.7	113.7	930.7
Water mass fraction	5.5	60.7	5.5	60.8
CO_2 mass fraction	3.0	5.7	3.0	5.5
N_2 mass fraction	91.5	0.0	91.5	0.0
DEA mass fraction	0.0	33.6	0.0	33.7
CO_2 Loading	-	0.40	-	0.39

Table 6.4 : Properties and composition of rich absorbent: aqueous diethanolamine (DEA), before and after entering stripper

Parameter ↓	**Stripper Pressure = 150 kPa**			**Stripper Pressure = 200 kPa**		
Material Stream →	**To Stripper**	**Flash (Liquid)**	**Flash (Vapor)**	**To Stripper**	**Flash (Liquid)**	**Flash (Vapor)**
Temperature (°C)	102.9	94.4	94.4	109.1	101.4	101.4
Pressure (kPa)	455.1	136.2	136.2	524.0	186.2	186.2
Mass flow-rate (kg/s)	830.7	815.0	15.6	930.7	914.1	16.6
Water mass fraction	60.7	61.2	33.8	60.8	61.3	31.1
CO_2 mass fraction	5.7	4.5	66.2	5.5	4.4	68.9
N_2 mass fraction	0.0	0.0	0.0	0.0	0.0	0.0
DEA mass fraction	33.6	34.3	0.0	33.7	34.3	0.0
CO_2 Loading	0.403	0.314	-	0.393	0.306	-

Table 6.5 : Comparison of stripper operational parameters evaluated using equilibrium approach and ProMax

Parameter ↓	**Stripper Pressure = 150 kPa**		**Stripper Pressure = 200 kPa**	
Evaluation Method →	**Equilibrium Approach**	**ProMax**	**Equilibrium Approach**	**ProMax**
Reboiler Temperature (°C)	108.5	111.4	114.9	117.7
P_{CO2} (Reboiler, kPa)	27.0	26.3	48.6	64.2
P_{H2O} (Reboiler, kPa)	123.1	123.7	151.4	135.8
P_{CO2} (Overhead, kPa)	44.5	54.8	63.2	82.8
P_{H2O} (Overhead, kPa)	73.0	81.3	95.2	103.4
y_{CO2} (Overhead)	0.38	0.40	0.40	0.44
P_{H2O} (Overhead)	0.62	0.60	0.60	0.56
CO_2 Flow-rate (kg/s)	30.7	30.7	30.7	30.7
H_2O Flow-rate (kg/s)	20.6	18.6	18.9	15.7
Reboiler Duty (GJ/ton-CO_2)	3.70	3.64	3.65	3.4
% Difference	1.57		6.05	

Since the objective of performing these calculations is to assess the validity of our assumptions and to gauge the adequacy of the equilibrium approach in estimating reboiler duty for alkanolamine systems, Table 6.5 provides a side-by-side comparison of various stripper operational parameters obtained using the equilibrium approach method and simulated using ProMax. The first and most important parameter to be noted is the reboiler duty. As seen, at a stripper operating pressure of 150 kilopascals (kPa), the difference between the two methods is less than 2%. At a higher pressure of 200 kilopascals (kPa), the reboiler duty estimated by the equilibrium approach calculations is 6% higher than that calculated with ProMax. Clearly, despite the significant number of simplifying assumptions made in using the equilibrium approach; reboiler duty estimated using this method is remarkably accurate. A more detailed analysis of the data compiled in Table 6.5 shows that there is little difference between the reboiler temperatures estimated by the two methods. Additionally, vapor phase compositions estimated using the two methods have only a small difference. One parameter that differs noticeably between the calculations made using these two methods is the stripper pressure at the top of column. Whereas the sum of the partial pressures of carbon dioxide (CO_2) and water as calculated by ProMax add up to the required value (136 kilopascals (kPa) and 186 kilopascals (kPa)) after accounting for a 14 kilopascals (kPa) pressure drop in the column, those estimated using the equilibrium approach deviate from this value by around 14%. This deviation is likely caused by the inability of the equilibrium approach to account for liquid phase non-idealities

resulting from the presence of electrolytes. In spite of this, the comparison clearly demonstrates the effectiveness of the equilibrium approach as a simple, fast and reasoanably reliable means of estimating reboiler duty. Having established the validity of our selected approach, we next proceed to evaluating the operational parameters and the reboiler duty for the aqueous diethanolamine (DEA) system blended with methanol.

6.5.5 Evaluating reboiler duty for aqueous diethanolamine (DEA) blended with methanol

In §§6.5.5 we have established the validity of applying the equilibrium approach method as a means of estimating reboiler duty with the use of vapor-liquid equilibrium (VLE) and physiochemical property data only. In this section, we apply the principles developed in §§6.5.3 to evaluate the reboiler duty for the amine absorption process utilizing an aqueous diethanolamine (DEA) absorbent blended with methanol. This absorbent is composed of 40 % diethanolamine (DEA) and water by weight and 20 % methanol. Figure 6.12 shows the dependence of the carbon dioxide (CO_2) vapor pressure on the carbon dioxide (CO_2) loading of the absorbent solution and on temperature.

A comparison of Figures 6.11 and 6.12 shows that the addition of methanol results in a significantly higher equilibrium vapor pressure of carbon dioxide (CO_2). This has two important implications, the first of which is a reduction

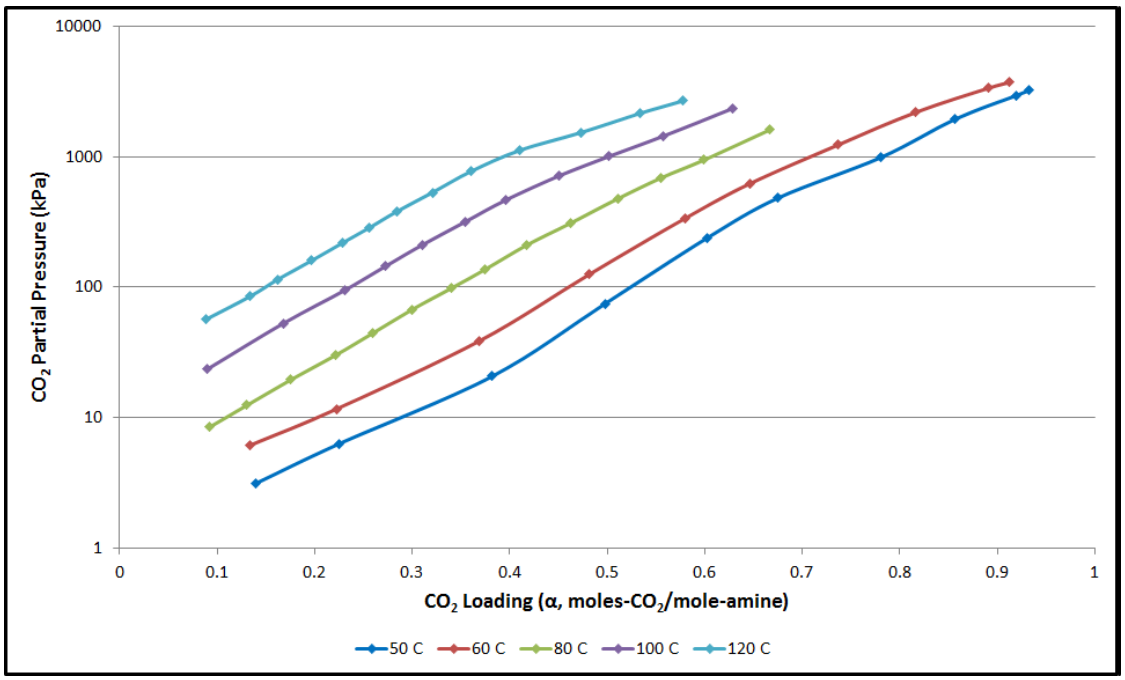

Figure 6.12 : Vapor liquid equilibrium data for aqueous diethanolamine (DEA) blended with methanol (40:40:20 - wt%)

in the stripping vapor requirement in the desorber column and second, a reduction in the maximum possible carbon dioxide (CO_2) loading in the rich absorbent, which in turn results in an increased absorbent circulation rate. This increase in absorbent circulation rate can be limited by reducing the temperature of the absorbent solution entering the absorber column. This results in a relatively cooler rich absorbent solution which can then absorb a greater quantity of carbon dioxide (CO_2).

As before, the properties and composition of the lean absorbent solution and the flue gas must be fixed before proceeding with the calculations. These are provided in Table 6.6. The temperature and composition of the decarbonized flue gas and the rich absorbent solution leaving the absorber is evaluated by performing a material

and enthalpy balance. These are summarized in Table 6.7. It can be noted that in comparison to the aqueous diethanolamine (DEA) case, the rich absorbent exits the column at a lower temperature. This is a result of a lower inlet temperature for the lean absorbent and and a higher circulation rate. Table 6.8 shows the properties and composition of the rich absorbent solution as it exits the lean/rich absorbent heat exchanger and enters the stripper column. Again, when compared to the aqueous diethanolamine (DEA) system analyzed previously; the righ absorbent exiting the heat exchanger has a lower temperature. In this case however, the lower temperature is a result of a reduced reboiler operational temperature. As shown in Table 6.9, the addition of methanol to aqueous diethanolamine (DEA) results in a significant reduction in the reboiler operational temperature. Thus a stripper column maintained at a pressure of 150 kilopascals (kPa) operates at 108.5 ^{o}C with aqueous diethanolamine (DEA) whereas with methanol blended aqueous diethanolamine (DEA), the operating temperature is dropped to 92.5 ^{o}C. For an operating pressure of 200 kilopascals (kPa), these temperatures are 114.9 ^{o}C and 100.8 ^{o}C respectively. To explain this behavior, we must refer back to Equation 6.9. When aqueous diethanolamine (DEA) is selected as the absorbent, the total pressure is the sum of the first three terms of the equation which represent the partial pressures of diethanolamine (DEA), carbon dioxide (CO_2) and water.

Table 6.6 : Parameters used for reboiler duty calculations

Parameter ↓	**Stripper Pressure = 150 kPa**		**Stripper Pressure = 200 kPa**	
Material Stream →	**Flue gas (in)**	**Lean Amine**	**Flue gas (in)**	**Lean Amine**
Temperature (°C)	30.0	37.5	30.0	37.5
Pressure (kPa)	124.1	827.4	124.1	827.4
Mass flow-rate (kg/s)	144.4	950.0	144.4	950.0
Water mass fraction	4.4	37.4	4.4	37.4
CO_2 mass fraction	23.6	2.6	23.6	2.6
N_2 mass fraction	72.0	0.0	72.0	0.0
DEA mass fraction	0.0	40.0	0.0	40.0
MeOH mass fraction	0.0	20	0.0	20
CO_2 Loading	-	0.155	-	0.155

Table 6.7 : Properties and composition of material streams exiting the absorber

Parameter ↓	**Stripper Pressure = 150 kPa**		**Stripper Pressure = 200 kPa**	
Material Stream →	**Flue gas (out)**	**Rich Amine (out)**	**Flue gas (out)**	**Rich Amine (out)**
Temperature (°C)	37.5	51.8	37.5	51.8
Pressure (kPa)	110.3	124.1	110.3	124.1
Mass flow-rate (kg/s)	113.7	980.7	113.7	980.7
Water mass fraction	5.5	36.2	5.5	36.2
CO_2 mass fraction	3.0	5.6	3.0	5.6
N_2 mass fraction	91.5	0.0	91.5	0.0
DEA mass fraction	0.0	38.7	0.0	38.7
MeOH mass fraction	0.0	19.4	0.0	19.4
CO_2 Loading	-	0.348	-	0.348

Table 6.8 : Properties and composition of rich absorbent: methanol blended aqueous diethanolamine (DEA), before and after entering stripper

Parameter ↓	**Stripper Pressure = 150 kPa**			**Stripper Pressure = 200 kPa**		
Material Stream →	**To Stripper**	**Flash (Liquid)**	**Flash (Vapor)**	**To Stripper**	**Flash (Liquid)**	**Flash (Vapor)**
Temperature (°C)	87.5	83.2	83.2	95.3	90.4	90.4
Pressure (kPa)	524.0	136.2	136.2	524.0	186.2	186.2
Mass flow-rate (kg/s)	980.7	970.5	10.2	980.7	968.7	12.0
Water mass fraction	36.2	36.5	15.1	36.2	36.5	14.5
CO_2 mass fraction	5.6	5.3	41.8	5.6	5.2	45.7
N_2 mass fraction	0.0	0.0	0.0	0.0	0.0	0.0
DEA mass fraction	38.7	39.2	0.0	38.7	39.2	0.0
MeOH mass fraction	19.4	19.1	43.1	19.4	19.1	39.9
CO_2 Loading	0.348	0.321	-	0.348	0.314	-

Table 6.9 : Stripper and reboiler operational parameters for methanol blended aqueous diethanolamine (DEA)

Parameter	**Stripper Pressure = 150 kPa**	**Stripper Pressure = 200 kPa**
Evaluation Method	**Equilibrium Approach**	**Equilibrium Approach**
Reboiler Temperature (°C)	92.8	100.8
P_{CO2} (Reboiler, kPa)	39.3	54.5
P_{H2O} (Reboiler, kPa)	51.4	69.2
P_{MeOH} (Reboiler, kPa)	59.3	76.3
P_{CO2} (Overhead, kPa)	103.3	148.2
P_{H2O} (Overhead, kPa)	34.9	53.0
P_{MeOH} (Overhead, kPa)	41.6	34.9
y_{CO2} (Overhead)	0.57	0.63
y_{H2O} (Overhead)	0.19	0.15
y_{MeOH} (Overhead)	0.23	0.22
CO_2 Flow-rate (kg/s)	30.7	30.7
H_2O Flow-rate (kg/s)	4.2	2.96
MeOH Flow-rate (kg/s)	9.0	7.98
Reboiler Duty (GJ/ton-CO_2)	2.82	2.71
% Savings (vs. DEA (34.8 wt%))	22.7	21.3

The reboiler temperature is calculated by determining the unique temperature at which the sum of these three vapor pressures is equal to the set stripper pressure. With the addition of methanol however; a fourth, significantly more volatile component is added to the liquid phase. In spite of a concentration of 20 mole % only, methanol is the largest contributor to the total pressure on account of its high volatility. As explained previously, the effect of flash evaporation is simulated by passing the hot, rich absorbent through a throttling valve in ProMax. A comparison between the conditions of the rich absorbent streams (before and after flash evaporation) for aqueous diethanolamine (DEA) and methanol blended diethanolamine (DEA) shows that the temperature drop for the latter of the two cases is much larger. This can be explained by noting that flash evaporation is mostly an adiabatic process. Energy required to convert the liquid into vapor is drawn from within the liquid itself. This results in the reduced temperature for the flash liquid and vapor as compared to the original liquid. Since the heat of vaporization of methanol is less than half that of water; less energy is consumed for the methanol blended diethanolamine (DEA) case.

Table 6.9 is a compilation of operational parameters for a stripper column operated with aqueous diethanolamine blended with methanol as the absorbent. There are several interesting distinctions between these and those for the aqueous diethanolamine (DEA) system compiled in Table 6.5. The most important of these, and the one of greatest interest to us is the reboiler duty. Addition of 20 wt% methanol (and removal of an equivalent amount of water) is estimated to reduce the reboiler duty by 22.7%

and 21.3% for the 150 and 200 kilopascals (kPa) cases respectively. These comparisons were made with reference to the results obtained for aqueous diethanolamine (34.8 wt%) using ProMax. The addition of methanol appears to affect the stripper operation in a significant way resulting in a lowered reboiler duty. This lowering of reboiler duty can be attributed to two important properties of the methanol blended diethanolamine (DEA) absorbent. First, as shown in Figure 6.12; the addition of methanol appears to significantly increase the equilibrium vapor pressure of carbon dioxide (CO_2). This has an important implication on the stripper system - when maintaining the same stripper pressure, carbon dioxide (CO_2) accounts for a larger fraction due to its higher partial pressure. Conversely, the quantity of stripping vapor required is decreased. Secondly, due to the addition of methanol; the stripping vapor is composed of almost equal parts of water and methanol. As shown in Figure 6.8, water and methanol have a heat of vaporization of 2260 kJ/kg and 1102.5 kJ/kg respectively. Thus, to generate the required stripping vapor; less energy must be expended on account of the addition of methanol. As noted previously, the stripper column and reboiler for the methanol blended diethanolamine (DEA) case operated at a lower temperature than for the aqueous system. This difference is quite significant - 15.8 ^{o}C and 10.7 ^{o}C for the 150 kilopascals (kPa) and 200 kilopascals (kPa) strippers respectively. Contrary to the case of the aqueous diethanolamine (DEA) systems, where the sum of the partial pressures of carbon dioxide (CO_2) and water evaluated using the equilibrium approach method was less than the expected set pressure; that

for the methanol blended diethanolamine (DEA) system is higher. The difference between the evaluated pressure and set pressures (assuming a 13.8 kilopascals (kPa) pressure drop) is around 30%, which is significantly higher than the 14% difference noted for the aqueous diethanolamine (DEA) systems. The increased deviation can be accounted as before by non-idealities in the liquid phase on account of the presence of electrolytes. Additionally, methanol and water form a strongly non-ideal system on account of their complex solvent behavior [95]. The relatively significant deviation of calculated pressure from the set point could result in reduced accuracy of the predicted reboiler duty. Nevertheless, these calculations provide a proof-of-concept for our original hypothesis that the addition of an alcohol would result in reduced reboiler duty for the amine absorption process.

6.6 Effect of addition of alcohol on carbon dioxide (CO_2) absorption kinetics

In Chapter 3, we have outlined the reaction scheme for absorption of carbon dioxide (CO_2) in aqueous alkanolamine solutions. As shown in Reaction scheme 3.3, the role of water is not just limited to a being a solvent for the amine but also to participate in the actual reactions. The first step in the absorption of carbon dioxide (CO_2) in aqueous alkanolamines is its mass transfer from vapor phase to liquid, followed by its ionization into a bicarbonate ion and a proton. Since, carbon dioxide (CO_2) forms the weakly acidic carbonic acid (H_2CO_3); the ionization process is slow and often rate-

limiting [9]. It may be expected then that solvent properties such as carbon dioxide (CO_2) solubility, polarity and viscosity can significantly affect the absorption kinetics. We have proposed the replacement of water in aqueous alkanolamine with an alcohol such as methanol or ethanol. Although water and alcohols are similar in many ways, there are significant differences in their physical properties; especially those mentioned above. In order to study the influence of addition of alcohols on carbon dioxide (CO_2) absorption, we have conducted simple, bench-scale experimental studies using the primary amine - diglycolamine (DGA). Diglycolamine (DGA) was selected as the absorbent due to its fast kinetics, low volatility at room temperature and easy availability through its manufacturer, Huntsman Chemicals.

6.6.1 Experimental setup for studying reaction kinetics

To study the effect of change in the solvent for diglycolamine (DGA) on the reaction kinetics, we have developed a simple experimental setup consisting of a counter-current flow absorption column. Figure 6.13 shows a schematic representation of the experimental setup. As seen here, the heart of the setup is a glass column 30 centimeters (cm) long with a diameter of 2.5 centimeters (cm). The glass column is filled with 6 millimeter (mm) ceramic Raschig rings. A peristaltic pump (FPU 500, FPUMT) supplied by Omega Engineering draws absorbent solution from the absorbent reservoir and delivers into the column at the top. Simulated flue gas, consisting of 13 (v/V) % carbon dioxide (CO_2), balance nitrogen (N_2) supplied by

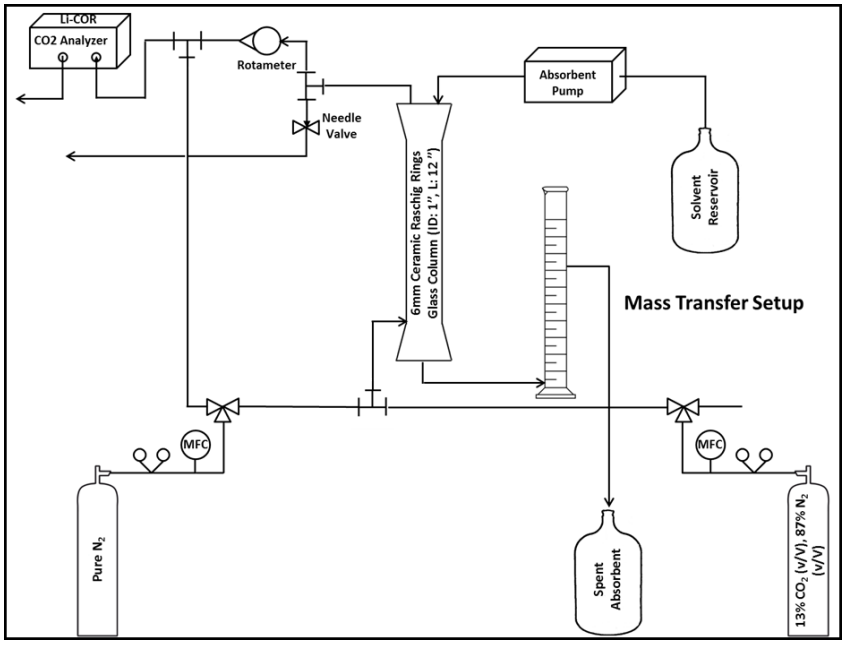

Figure 6.13 : Experimental setup used to studying the effect of diglycolamine (DGA) solvent on CO_2 absorption kinetics

Matheson TriGas is supplied to the column with the inflow rate being controlled using a mass flow controller (FMA6528ST) supplied by Omega Engineering.

The decarbonized gas leaves the top of the column where it is sampled, diluted with pure nitrogen (N_2) and fed to a non-dispersive infrared detector for analysis. The non-dispersive infrared detector (LI 820) is provided by LI-COR Biosciences. The need for sampling and dilution of the exit gas arises due to a flow limitation of 1 standard liter per minute (SLPM) and a upper carbon dioxide (CO_2) concentration detection limit of 20,000 parts per million (ppm). Volumetric flow rate of the sampled gas is measured using a rotameter whereas that of the dilution nitrogen (N_2) is controlled using another mass flow controller (FMA6528ST). Spent absorbent is collected in a

reservoir for suitable disposal whereas the decarbonized gas is let out in a fume hood.

6.6.2 Results and analysis of flow experiments to study carbon dioxide (CO_2) absorption kinetics

To study the effect of the diglycolamine (DGA) solvent on the carbon dioxide (CO_2) absorption kinetics, we have conducted counter-current 2-phase flow experiments using the experimental setup developed above. Absorbents prepared for these experimental studies contain 30 wt% diglycolamine (DGA) by weight, balance the solvent used. Experiments were conducted at a temperature of 30°C, a gas flow rate of 3 standard liter per minute (SLPM) and absorbent flow-rate of 20 cubic centimeters per minute (ccpm). Figure 6.14 is a plot of the degree of carbon dioxide (CO_2) removal taking place in the absorber column when water, methanol and ethanol are used as diglycolamine (DGA) solvents. Clearly, the diglycolamine (DGA) absorbents containing methanol and ethanol as solvents have a superior absorption performance than that containing water. Whereas under the experimental conditions described above, aqueous diglycolamine (DGA) achieves around 70% carbon dioxide (CO_2) removal; methanolic diglycolamine (DGA) achieves almost complete removal (98%) and ethanolic diglycolamine (DGA) - 90% removal of carbon dioxide (CO_2) from the inlet gas stream.

The dependence of absorption kinetics on solvent choice appears to be contrary to conventional reasoning. As shown in Figure 6.15, both methanol and ethanol are

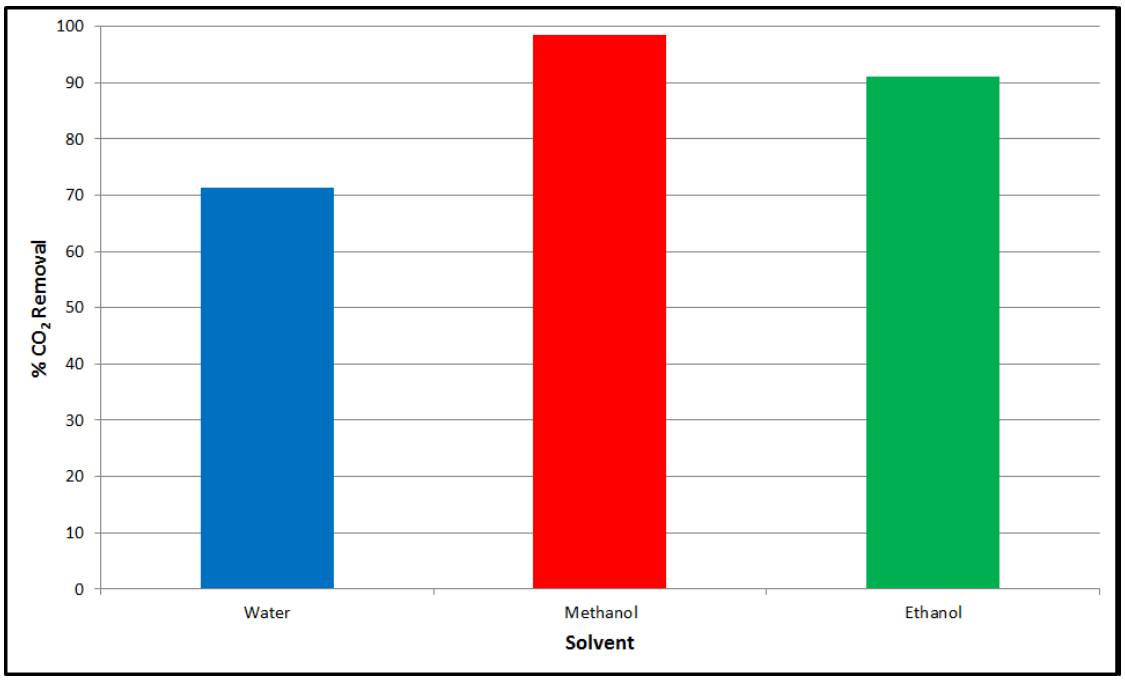

Figure 6.14 : Degree of CO_2 removal taking place in absorber column with various diglycolamine (DGA) solvents

solvents with much lower polarity than water and are as such unfavorable for the carbon dioxide (CO_2) ionization reaction. The unfavorable solvent environment may be expected to further slow the ionization reaction which is also the rate-limiting step in the carbon dioxide (CO_2) absorption process. The observed increase in the carbon dioxide (CO_2) removal kinetics in the absorber clearly suggest the presence of more than one solvent effect. To analyze this further, it is important to take a deeper look at the physical processes occurring during the absorption process. Physical absorption of carbon dioxide (CO_2 from vapor to liquid is dependent on its solubility in the selected absorbent. Once a carbon dioxide (CO_2) molecule is dissolved in the liquid, it must diffuse to the nearest water or amine molecule in order for a reaction to

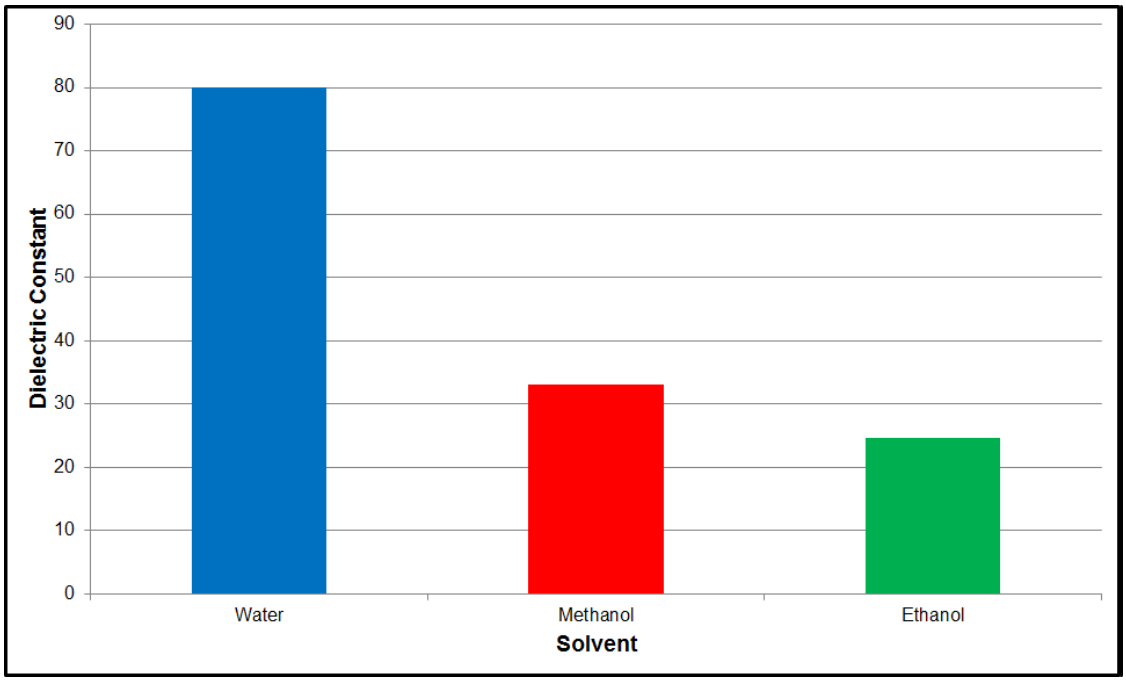

Figure 6.15 : Dielectric constant of different solvents - water, methanol and ethanol

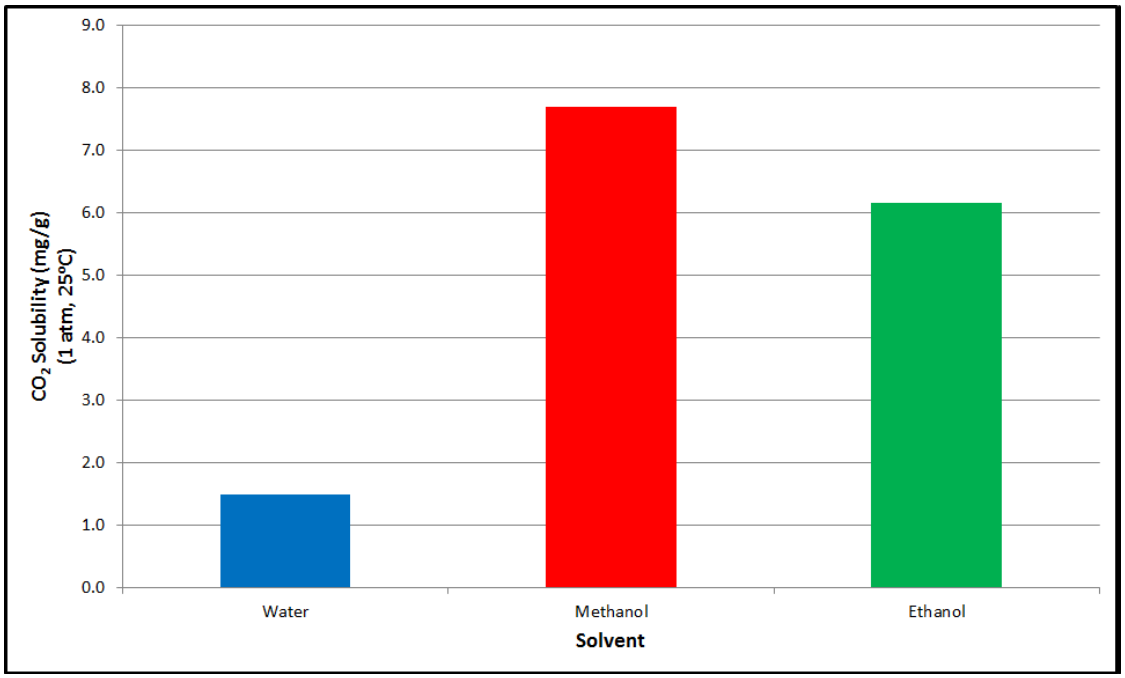

Figure 6.16 : CO_2 solubility in different solvents - water, methanol and ethanol

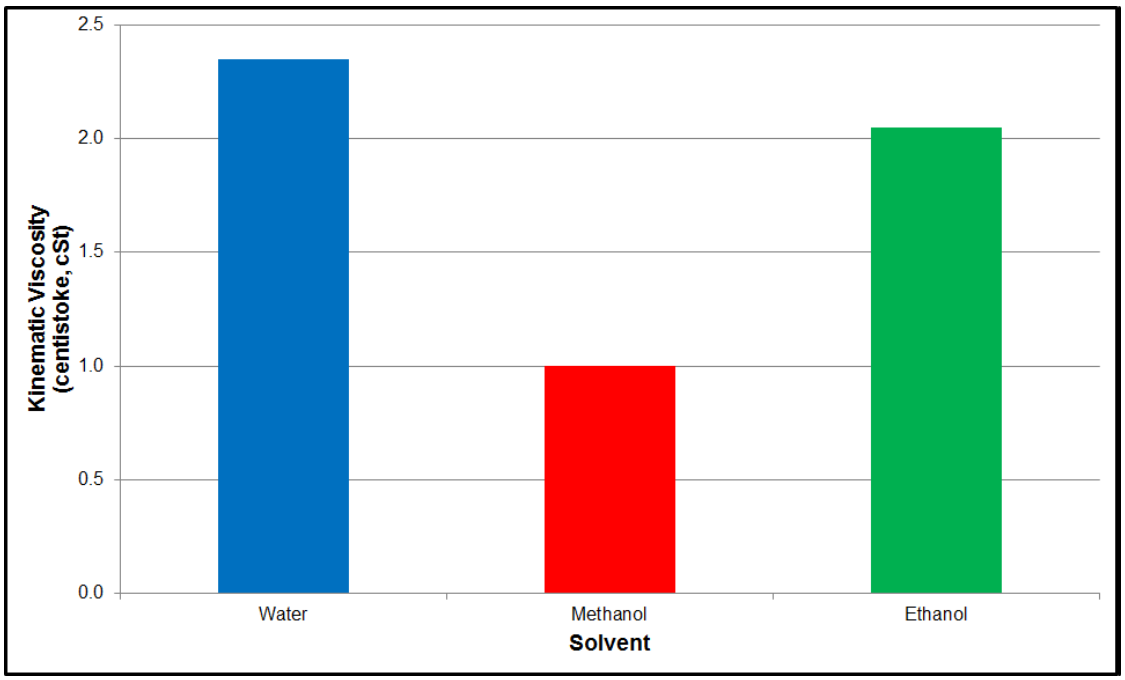

Figure 6.17 : Kinematic viscosity of various diglycolamine (DGA) absorbents with water, methanol and ethanol as solvents

take place. While the mass diffusivity of a gas molecule in a solvent is dependent on temperature and pressure, it is also a function of its kinematic viscosity (also called momentum diffusivity). Since, changing the diglycolamine (DGA) solvent from water to an alcohol changes both the carbon dioxide (CO_2) solubility and the kinematic viscosity; it is of interest to compare the trends of these parameters between water, methanol and ethanol. Figure 6.16 shows the solubility of carbon dioxide (CO_2) in water, methanol and ethanol at 25 °C and 101.3 kilopascals (kPa). Methanol has a solubility for carbon dioxide (CO_2) that is almost 6 times that of water. Ethanol has a lower solubility for carbon dioxide (CO_2) as compared to methanol, yet it is more than 4 times that of water under the same conditions. Figure 6.17 shows the

kinematic viscosities of the various 30 wt% diglycolamine (DGA) absorbents prepared using water, methanol and ethanol as absorbents. These kinematic viscosities were estimated at a temperature of 25 °C and a pressure of 101.3 kilopascals (kPa) using ProMax. Methanolic diglycolamine (DGA) clearly has the lowest kinematic viscosity amongst the three absorbents. It is less than half that of water. The kinematic viscosities of aqueous diglycolamine (DGA) and ethanolic diglycolamine (DGA) on the other hand are quite similar. On comparing the aqueous and ethanolic diglycolamine (DGA) properties side-by-side, it is clear that the biggest difference between the aqueous and alcohol based diglycolamine (DGA) is the carbon dioxide (CO_2) solubility. The results of our flow experiments and the comparisons made between the absorbent properties lead us to believe that although the low polarity of methanol and ethanol is unfavorable for the ionization of carbon dioxide (CO_2); the significantly higher solubility for carbon dioxide (CO_2) in these absorbents more than compensates for any slowing down of the absorption process. The absorption process is also aided by an increase in the mass diffusivity of the carbon dioxide (CO_2) in the methanolic and ethanolic diglycolamine (DGA) as compared to the aqueous diglycolamine (DGA).

6.7 Implications of replacing conventional absorbents with alcohol blended aqueous alkanolamines

We have demonstrated in §§6.5.5 that the addition of methanol to aqueous diethanolamine (DEA) reduces reboiler duty. Figure 6.18 shows a graphical comparison between the

reboiler duty for three conventional, aqueous absorbents - monoethanolamine (MEA) - 20 wt%, diethanolamine (DEA) - 40 wt% and diglycolamine (DGA) - 60 wt% and the aqueous diethanolamine (DEA) blended with methanol. Two cases of the monoethanolamine (MEA) system - 150 and 200 kilopascals (kPa) and three cases of diethanolamine (DEA) and diglycolamine (DGA) - 75, 150 and 200 kilopascals (kPa) are compared against the 150 and 200 kilopascals (kPa) configurations of the methanol blended aqueous diethanolamine (DEA). As seen, the two cases utilizing aqueous diethanolamine (DEA) blended with methanol have lower reboiler duties as compared to other systems.

The addition of methanol to aqueous diethanolamine (DEA) also results in a very interesting phenomenon. As stated in Table 6.9, when the stripper column is maintained at a pressure of 150 kilopascals (kPa); the reboiler operates at a temperature of 92.5 °C. This temperature is within 1 °C of the operating temperature of a vacuum stripper operating at 75 kilopascals (kPa) with 40 wt% aqueous diethanolamine (DEA) as the absorbent, which operates at 91.9 °C. As stated previously in Chapter 4, a vacuum stripper at 75 kilopascals (kPa) can be operated using waste heat - steam at approximately 125 kilopascals (kPa) and 140 °C. The ability to operate a stripper with waste heat without having to reduce stripper pressure below atmospheric pressure has significant practical implications. Some of these are:

1. Use of waste heat results in significantly reduced parasitic power loss. In a scenario that all the required waste heat is available at the power plant site, the

only parasitic power loss is that caused by the auxiliary equipment.

2. Unlike vacuum stripping, where a steam jet ejector is required to maintain vacuum and consumes low pressure steam as a motive fluid; no mechanism required to operate the 150 kilopascals (kPa) stripper.

3. Separated carbon dioxide (CO_2) exiting the stripper column will be delivered to the compression train at around 135 kilopascals (kPa) - significantly higher than the 101.3 kilopascals (kPa) for vacuum strippers.

4. Reduced compression requirements result in reduced parasitic power loss. Additionally, 1 fewer compressor and intercooler stage is required. This results in a reduction in the capital expenditure.

Figure 6.19 shows a comparison of the parasitic power loss for five different systems utilizing diethanolamine (DEA) absorbents. Three systems utilize aqueous 40 wt% diethanolamine (DEA) and are operated at 75, 150 and 200 kilopascals (kPa), with the 75 kilopascals (kPa) system using waste heat for reboiler steam. The remaining two systems considered utilize the methanol blended aqueous diethanolamine (DEA) and are operated at 150 and 200 kilopascals (kPa). As seen from the plot, the two systems utilizing waste heat have the lowest reboiler duties amongst all presented. Amongst these, the methanol blended system has a 2.25 percentage points advantage over the aqueous diethanolamine (DEA) system. While most of this advantage is a result of the reduction in the compression duty, a smaller fraction is also due to

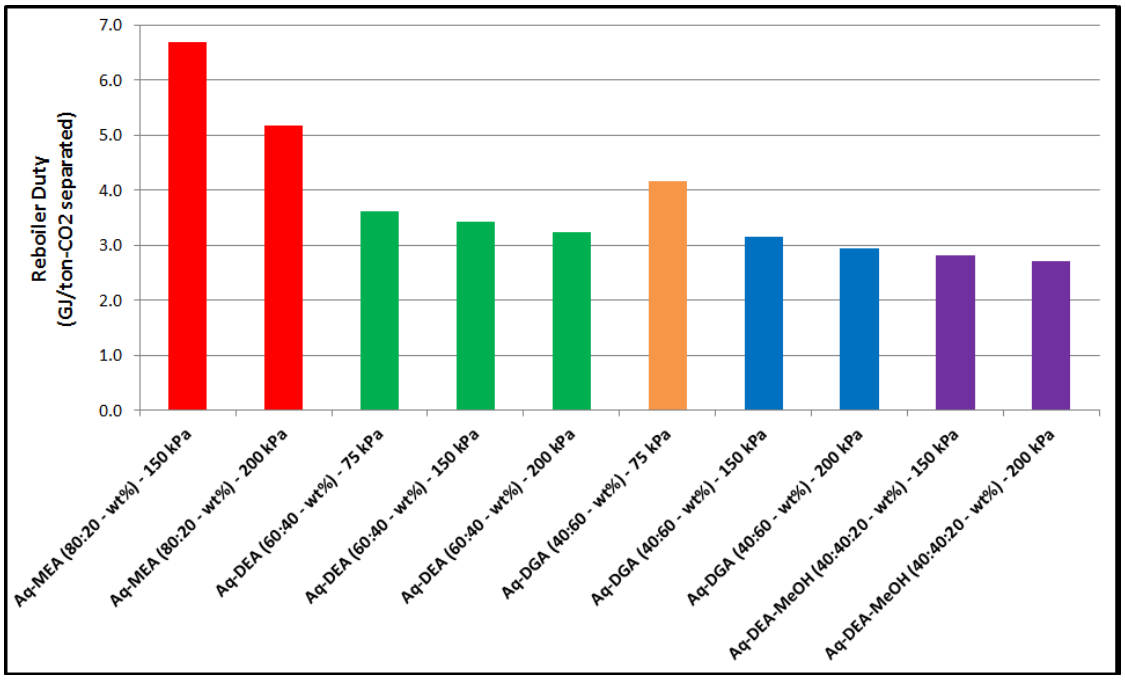

Figure 6.18 : A comparison of reboiler duty for common aqueous alkanolamines and methanol blended diethanolamine (DEA)

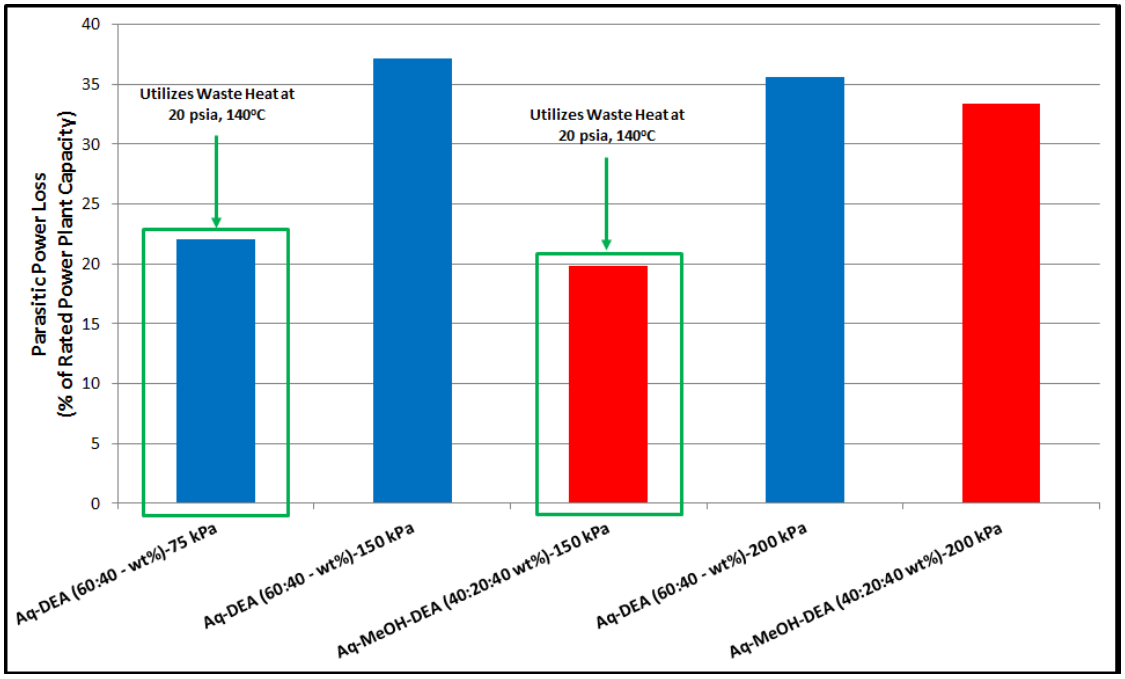

Figure 6.19 : A comparison of parasitic power loss for various amine absorption plant configurations using aqueous diethanolamine (DEA) - with and without methanol

the non-requirement of low pressure steam for the steam jet ejector. When the 150 and 200 kilopascals (kPa) systems utilizing different absorbents are compared side-by-side, it is again evident that the methanol containing absorbent performs better and reduces the parasitic power loss by around 2.25 percentage points.

As discussed in §6.6; the addition of alcohol to alkanolamines likely results in an improvement in the carbon dioxide (CO_2) absorption kinetics. This is a very favorable consequence of the addition of alcohols to aqueous alkanolamines, especially in the case of slower reacting amines such as diethanolamine (DEA). An increase in the reaction kinetics with a simultaneous reduction in the reboiler duty can be considered a significant step towards developing better absorbents for carbon dioxide (CO_2) capture than those that currently exist.

An important practical consideration to be accounted for in further developing the use of alcohol blended alkanolamines for carbon dioxide (CO_2) capture is the process hydrodynamics. As seen in Figure 6.9, in the specific case of adding methanol to aqueous diethanolamine (DEA); there is an increase in the equilibrium partial pressure of carbon dioxide (CO_2). In the stripper column, this results in a decrease in stripping vapor requirement which manifests itself in a reduced vapor flow-rate in the column. This has two important practical implications, the first of which is a reduction in the stripper column diameter. A reduction in the stripper column diameter might make it challenging to achieve stable hydrodynamic behavior for the high liquid flow-rates used in the amine process. Additionally, a reduction in the stripping vapor flow-rate

can result in a slowing down of carbon dioxide (CO_2) mass transfer due a lowering of the driving force. This could possibly result in the need for a longer stripper column when compared to the conventional alkanolamine process.

6.8 Concluding Remarks

We have developed and presented a simplified approach to resolve the energy contributions of various physiochemical processes taking place in the amine stripper to the reboiler duty. Based on our analysis, we hypothesized that the replacement of water in aqueous alkanolamine absorbents with an alternative solvent such as an alcohol is capable of bringing significant reduction in the reboiler energy consumption. We have developed a satisfactorily reliable framework to estimate reboiler duty for novel absorbent systems (in the absence of sufficient thermodynamic data) using physiochemical properties and vapor-liquid equilibrium (VLE) data alone. Our conclusions are summarized below:

1. Energy consumed in sensible heating of the absorbent and to generate stripping vapor is the largest contributor to the reboiler duty. This contribution varies between 40 and 65 % depending on the choice of solvent.

2. Application of the equilibrium approach method to evaluate reboiler duty for aqueous diethanolamine (DEA) was found to be sufficiently accurate. Results calculated by this method were compared with those obtained with the process simulation software, ProMax. The maximum error noted was 6%.

3. Application of the equilibrium approach method to evaluate reboiler duty for methanol blended aqueous diethanolamine (DEA) predicts an approximately 23% reduction in reboiler duty as compared to the aqueous diethanolamine (DEA) system under the same stripper operating pressure conditions.

4. Amine strippers utilizing methanol blended diethanolamine (DEA) operate at a significantly lower temperature than those using aqueous diethanolamine (DEA). A stripper column using the methanolic absorbent at 150 kilopascals (kPa) operates at the same temperature of 92 ^{o}C as a vacuum stripper operating at 75 kilopascals (kPa) and using aqueous diethanolamine (DEA).

5. The methanolic absorbent considered in this study produce an average of 2.25 percentage point reduction in the parasitic power loss as compared to aqueous absorbents. Since waste heat can, however, be used with a 150 kilopascals (kPa) methanolic stripper; its parasitic power loss can be reduced to approximately 19.5 % of the rated power generation capacity of a coal-fired power plant.

6. Addition of alcohols such as methanol and ethanol appears to improve the carbon dioxide (CO_2) reaction kinetics. We believe that this is primarily a result of the higher solubility for carbon dioxide (CO_2) in the alcohol as compared to water.

7. The analysis performed on methanol blended aqueous diethanolamine is unable to account for practical considerations such as column hydrodynamics. Careful

consideration needs to be given to understanding the effects of reduction in stripping vapor flow-rate on the stability of column operation as well as carbon dioxide (CO_2) mass transfer.

Chapter 7

Combined pressure and temperature contrast separation of carbon dioxide (CO_2): key concepts & process development

7.1 Motivation

In §3.3, we have discussed the state of current research and development in the area of carbon capture and storage. As described, different approaches have been adopted to improve existing technology in order to make it more suitable for the removal of carbon dioxide (CO_2) from power plant flue gas. As seen, however, most research is focused on reducing energy consumption - thereby attempting to achieve reductions in operational costs. From a practical standpoint, however, it is important to advance existing technology by developing and using superior materials and clever process configurations to reduce capital expenditure. Alkanolamine absorption is considered a favorable technology for use in post-combustion carbon capture. If implemented, existing coal and natural gas fired power stations will have to be retrofitted with this technology for the removal of carbon dioxide (CO_2). In such scenarios, space

availability may become a critical resource and the availability of novel, compact process configurations may become necessary. It is with these motives that we explore the idea of combining the absorber and stripper units of the amine absorption process into a single, integrated unit.

7.2 Combining the absorber and stripper columns: developing the concept of an integrated unit

Figure 7.1 shows a schematic illustration of the novel, proposed process for the separation of carbon dioxide (CO_2) from flue gas. The novelty of this process hinges on the idea of combining an amine absorber and stripper into a single integrated unit with the use of advanced materials and clever engineering. In the conventional alkanolamine absorption process, both the absorber and stripper columns operate separately in a counter-current flow pattern. In order to achieve carbon dioxide (CO_2) absorption and stripping in a single unit, a mechanism is required for facilitating the lateral flow of the liquid absorbent. Additionally, unlike in the conventional amine absorption process; the decarbonized flue gas exiting the absorption side must be prevented from mixing with the separated carbon dioxide (CO_2) leaving the stripper.

With the recognition of these basic requirements, a theoretical basis was developed for this novel process. At the heart of the process is a composite porous body (e.g. ceramic) that combines the absorption and stripping media. This composite porous body consists of three layers - a first layer (shown in blue in Figure 7.1) that acts as the

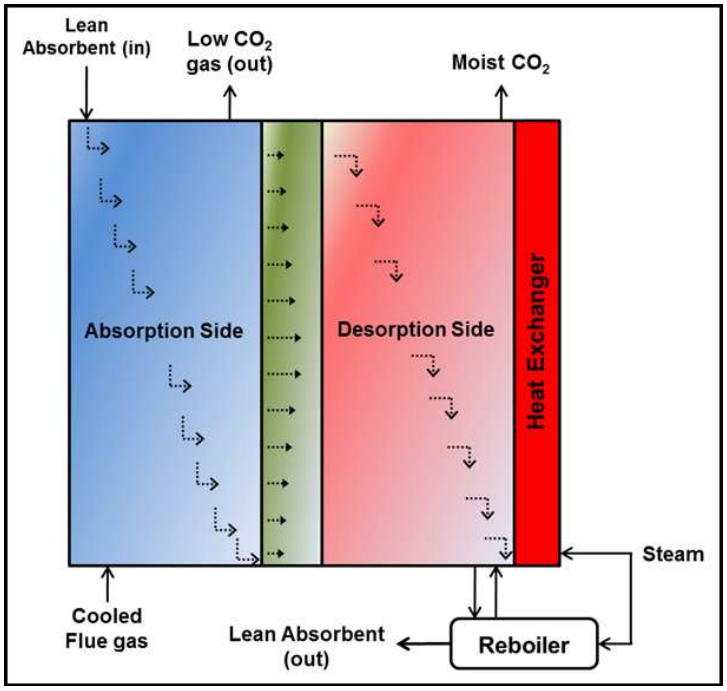

Figure 7.1 : Schematic representation of the novel process with an integrated absorber and stripper

gas absorber, a center layer (shown in green in Figure 7.1) that has a function similar to a semipermeable membrane for gas-liquid separation and a third layer (shown in red in Figure 7.1) that functions as the stripping section of the unit. Each layer should allow for the lateral flow of liquid from the absorption side to the stripping side - a characteristic that is critical to the success of the process. From a generic viewpoint, the properties of the absorption and stripping layers are selected such that good gas-liquid contacting can be achieved. This maybe achieved through the selection of a porous material with a bimodal pore-size distribution such that liquid transport occurs predominantly through the small pores in the material whereas gas flow takes place through the larger pores. The decarbonized flue gas can be prevented

from flowing into the stripper with the use of a porous membrane. The behavior of two fluids (e.g. gas and liquid) through porous materials can be explained on the basis of the Young-Laplace equation shown in Equation 7.1.

$$P_c = \frac{2\gamma cos\theta}{R} \tag{7.1}$$

In equation 7.1, P_c is the capillary entry pressure, γ is the surface tension, θ is the angle of contact and R is the radius of a capillary. When applied to the case of gas and liquid flowing through a porous membrane; equation 7.1 predicts that the non-wetting phase (i.e.gas) will displace the wetting phase (i.e.liquid) from a *saturated* capillary or pore of diameter R only after the pressure differential across the membrane is greater than the capillary entry pressure P_c. When the pressure differential between the absorption and stripping sides is maintained at or below capillary entry pressure; liquid absorbent will selectively flow between the two sides. Clearly, the choice of material for the gas-liquid separator membrane and its properties will be determined by the pressure differential to be maintained and the liquid throughput to be achieved. The regenerated absorbent will flow down in the stripping section and enter a reboiler installed at the bottom of the unit. Here, the absorbent solution will be heated using low pressure steam of waste heat to generate the required stripping vapor flow. After leaving the reboiler, the regenerated absorbent will flow to an amine cooler where its temperature will be reduced to the optimal choice for the process after which it will be pumped back into the integrated unit for another absorption

cycle. If implemented, this novel process configuration promises to incorporate several favorable characteristics discussed in §7.1 and could potentially bring significant cost savings.

7.3 Selecting the right material: ceramic foams

We have laid out the theoretical concepts for designing a novel process consisting of an integrated absorber and stripper for the removal of carbon dioxide (CO_2) from coal fired power plant flue gas. The key to advancing these theoretical concepts into a demonstrable bench-scale process is the choice of suitable advanced process materials. As discussed previously, the concept of a combined absorber and desorber unit rests in its entirety on achieving lateral flow of liquid absorbent through the gas-liquid contacting materials. In selecting the most suitable materials for gas-liquid contacting, a strong emphasis was laid on three indispensable characteristics, namely:

1. A bimodal pore-size distribution

2. Large geometric surface area for good gas-liquid contacting

3. Ease of reproducibility and commercial availability

The significance of the first two characteristics has been discussed previously whereas the third is critical to the advancement of the theoretical concepts of §7.2 to a bench-scale demonstration and further in a reasonable time-scale.

A rigorous search was conducted to determine suitable materials, the outcome of which was the discovery of a class of materials called ceramic foams. Ceramic foams are highly porous cellular ceramic structures. Figure 7.2 shows a sample of commercial alumina (Al_2O_3) foam. As shown in Figure 7.3, ceramic foams can be made by a variety of methods [96]. However, the most common approach to manufacturing ceramic foams on a commercial scale is to coat a sample of open cell polyurethane (PU) foam template of required shape and dimensions with a slurry of the required ceramic material followed by removal of the foam template by pyrolysis. Alumina (Al_2O_3) is the most frequently used ceramic, though others such as zirconia (ZrO_2), silicon carbide (SiC) can be used for specialized applications.

As can be seen in Figure 7.2, ceramic foams are highly porous with void fraction of the order of 0.9 or more, have high geometric surface areas and possess high tortuosity due to their interconnected cellular structure. At present, ceramic foams are mainly used for filtration of molten metals like aluminum and iron to remove inclusions [15]. They are also being explored as catalyst supports due to their excellent mass and heat transfer properties [97].

Figure 7.4 shows scanning electron micrographs (SEM) of a commercial alumina foam sample of 45 pores per inch (ppi) grade. These images are quite revealing and clearly show the presence of dual porosity. Figure 7.4a shows the alumina foam sample at a magnification of 50x. Millimeter (mm) sized pores present in the alumina foam are clearly seen in this image. Also seen in Figure 7.4c are the cracks and triangular

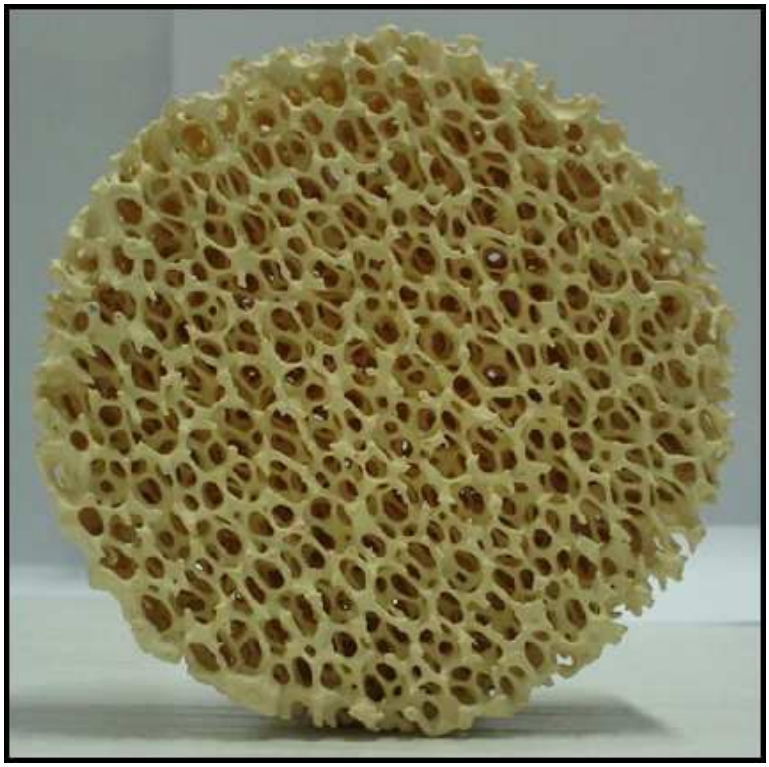

Figure 7.2 : A commercial sample of alumina foam

openings that exist in the struts of the alumina foam at a magnification of 290x. These openings form the high permeability conduits for the entry of liquid absorbent into the ceramic matrix. Figure 7.4b, d at magnifications of 280x and 11,000x clearly show the existence of a microporous ceramic matrix. The presence of a microporous matrix can facilitate the transport of liquid absorbent from the absorption section of the integrated unit to the stripping side.

In order to characterize the porosity in the alumina foam sample further, a 25 millimeter (mm) long and 25 millimeter (mm) diameter sample was cored in an alumina foam slab. This sample was then analyzed at Core Laboratories, Inc., Houston. Mercury

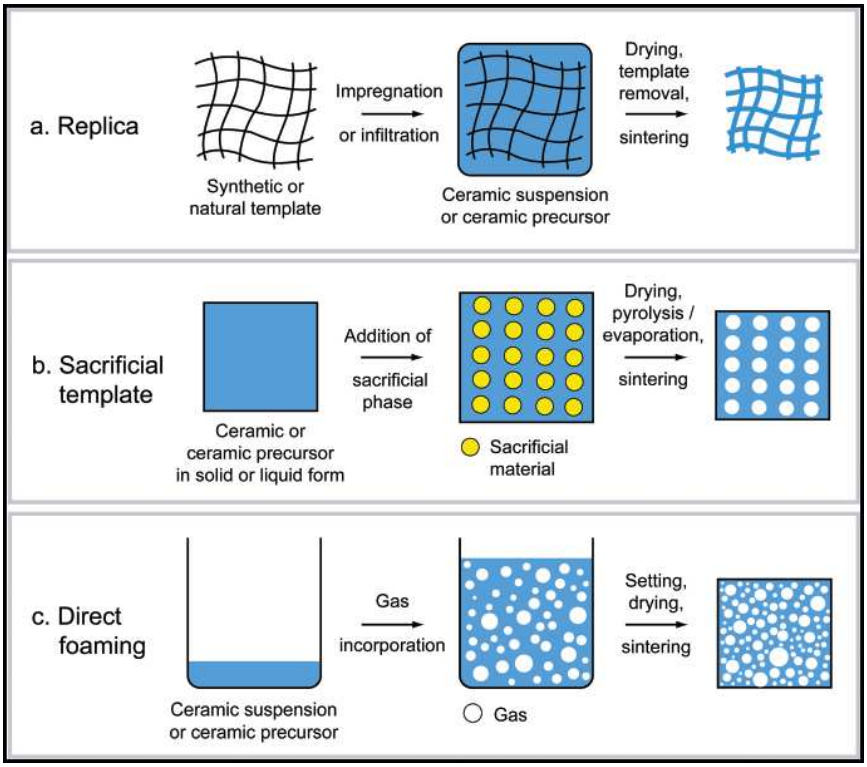

Figure 7.3 : Different routes to manufacturing ceramic foams [15]

porosimetry measurements were performed on the sample to determine the pore size distribution and the void fraction associated with the micro and macroporosity. Figures 7.5 and 7.6 show that almost 90% of the void volume is contained in pore spaces larger than 100 microns (μ) in radius. These large pores make up the macroporosity in the alumina foam. The remaining void volume is largely distributed, almost equally between two different types of porosities - microporosity in the alumina matrix which comprises of pores ranging from 0.25 to 0.5 microns (μ) and cracks and openings in the struts consisting of pores ranging from 25 to 50 microns (μ). It is apparent from these results that the material possesses the most critical characteristic necessary to

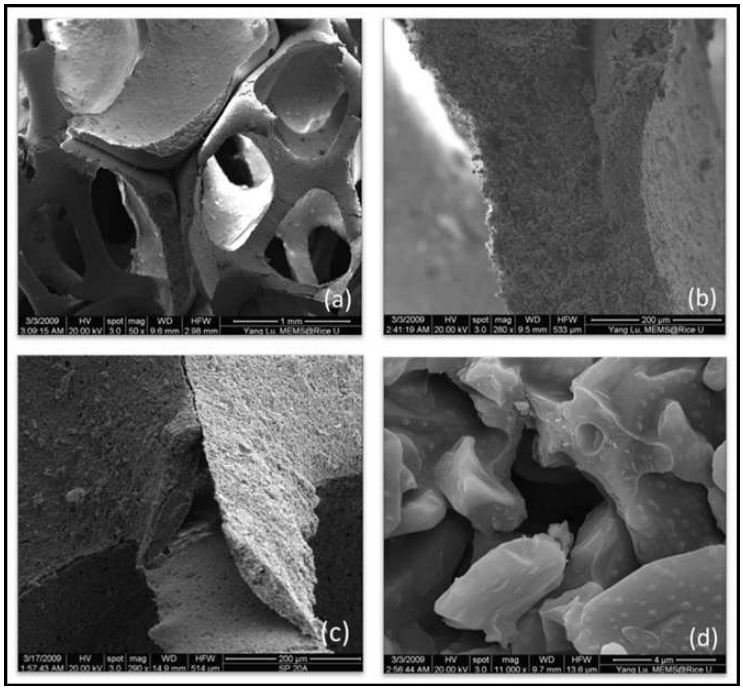

Figure 7.4 : Scanning electron micrographs of a 45 pores per inch (ppi) sample of alumina foam

be used for implementing the concept of a combined absorber and stripper. Additionally, ceramic foams possess a number of properties that makes them ideally suited for use in the novel carbon dioxide (CO_2) separation process being developed. Some of these are:

1. Low pressure drop due to the very high porosity and interconnected pores
2. Very high geometric surface area
3. High mass and heat transfer rates due to high geometric surface areas

Table 7.1 shows a comparison between the geometric surface area for ceramic foams and several commonly used tower packing materials [97, 98, 99]. Clearly,

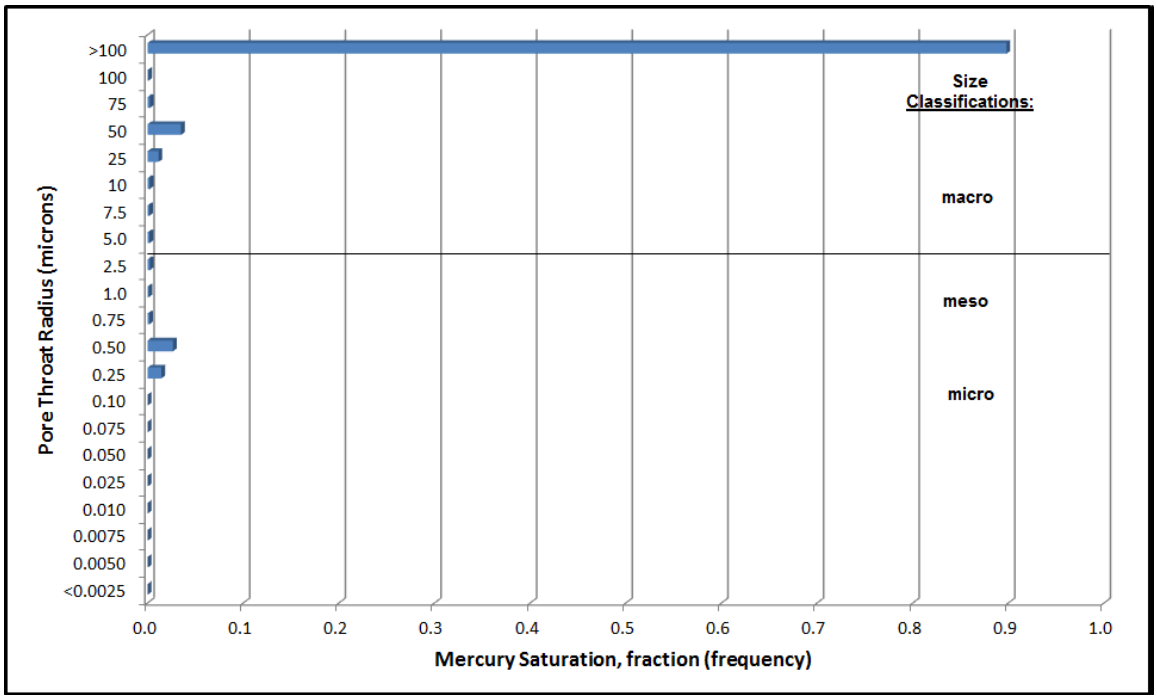

Figure 7.5 : Pore size distribution in a 45 pore per inch (ppi) sample of alumina foam

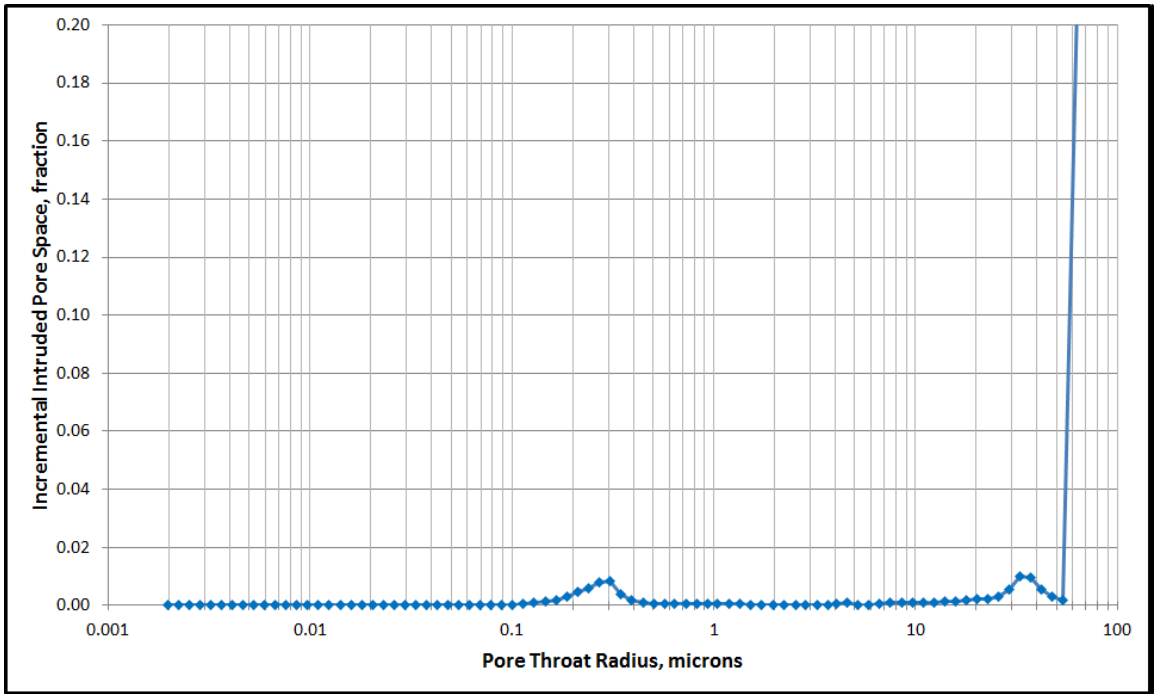

Figure 7.6 : Pore size distribution in a 45 pore per inch (ppi) sample of alumina foam

the 30 pores per inch (ppi) grade ceramic foam has a significantly higher geometric surface area as compared to conventional packing.

Table 7.1 : Comparison of geometric surface area of ceramic foam and various tower packings

Structure	**S (m^3/m^3)**	**Porosity (ϵ)**
5 mm packing spheres	600	0.392
Raschig ceramic rings, 6 mm	789	0.73
Raschig ceramic rings, 25 mm	200	0.646
Corrugated metal structured packing	500	0.93
30-PPI -Al_2O_3 foam	3360	0.83

Since, the rate of mass transfer is proportional to the gas-liquid interfacial surface area; a greater geometric surface area in the tower packing promotes better mass transfer. Thus, ceramic foams possess all the features required of the gas-liquid contacting material as described in this section and §7.2. Having selected ceramic foam as the material of choice for gas-liquid contacting, the next logical step in process development is to characterize the ceramic foam for its hydrodynamic and mass transfer behavior.

7.4 Characterizing the hydrodynamic behavior of ceramic foams

Selection of a tower packing material for gas absorption operation is an optimization problem with several variables to consider. Some of the factors considered are the geometric surface area of the packing material, pressure drop, hydrodynamic behavior under different gas-liquid flow conditions and corrosion resistance. The geometric surface of packing materials increase by reducing the void fraction or pore sizes. Thus, as seen in Table 7.1; 6 mm Raschig rings have a greater geometric surface area than 25 mm Raschig rings. However, as the void fraction and pore-sizes decrease; the resistance offered by the packing material to fluid flow which results in greater pressure drops. In commercial operation, it is often economical to operate a column at gas and liquid flow-rates close to their maximum limits. One of the main constraints on determining these limits is the hydrodynamic behavior of the packing material; more specifically, the flooding point. Flooding in case of an absorption or distillation column is the condition at which the vapor flow-rate and the pressure drop in the column is large enough to disrupt the unhindered downward flow of liquid. When flooded, liquid entrainment begins to take place in the column which results in a sharp increase in the differential pressure in the column and a reduced separation efficiency. It is clear from this description of flooding that increasing the surface area of tower packing by reducing the void fraction and pore size will result in lowering of the flooding point - an unfavorable characteristic. It is clear from this discussion

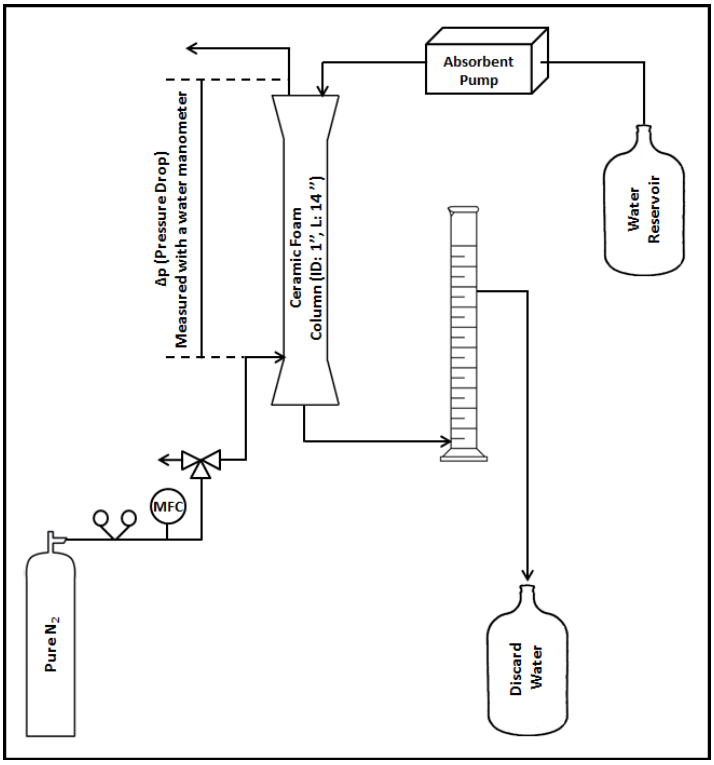

Figure 7.7 : Schematic representation of experimental setup developed for studying hydrodynamic behavior of ceramic foams

that while ceramic foams possess several favorable characteristics; developing an understanding of their hydrodynamic behavior is critical to further development of the novel process.

7.4.1 Experimental setup

In order to study the hydrodynamic behavior of the ceramic foams, a simple experimental setup was developed in-house. Figure 7.7 shows a schematic representation of this setup. The experimental setup involves a glass tube with an inner diameter (ID) of 2.8 centimeters (cm). The glass tube is designed to encase 7 foam plugs, each of

which is 5.1 centimeters (cm) in length with 5.1 centimeters (cm) headspace at the top and 2.54 centimeters (cm) space at the bottom. Ceramic foam plugs composed of 99.5% α alumina (Al_2O_3) with 2.54 centimeter (cm) diameter and 5.1 centimeter (cm) length were ordered from Ask-Chemicals, Alfred, NY. Three different grades of ceramic foams 20, 30 and 45 pores-per-inch (ppi) were procured. 6 foam plugs of the same grade were wrapped tightly, end-to-end in heat-shrink Teflon tubing to prevent the bypass of gas or liquid on the side of ceramic foam plugs. The 7^{th} foam is used as a sacrificial plug it serves to hold the water build up due to capillary end effects in the foam plugs [100]. The 7^{th} foam plug is inserted into the glass tube below the 30.5 centimeters (cm) long rod. Both the 30.5 centimeters (cm) rod and the 7^{th} foam plug are held in place using Viton fluoroelastomer O-rings (Dash #21). The O-rings prevent the bypass of gas or liquid through any empty spaces between the glass walls and the ceramic foam rod.

Pure nitrogen gas (N_2) supplied by Matheson Trigas was introduced above the last plug from the bottom. In order to prevent any escape of the entering gas with the exiting liquid, a plastic graduated cylinder was added to the experimental setup as shown to provide a liquid seal. The liquid seal works by providing a static head of water which acts as a back pressure regulator and prevents the escape of inlet gas through the liquid outlet port. Pressure drop across the column was measured using a water manometer built in-house. Since water is used as the manometer fluid, pressure differences as low as 20 Pascals (Pa) can be detected. This degree of sensitivity

is particularly important with our experimental setup due to the relatively short column of packing and the low pressure drops encountered in such porous materials. Water was delivered to the column using a peristaltic pump (FPU500, FPUMT) supplied by Omega Engineering. Liquid was distributed on the ceramic foam with a piece of stainless steel wool at the top of the ceramic foam column. Nitrogen (N_2) flow was controlled accurately using a mass flow controller (MFC) (FMA6528ST) manufactured by Omega Engineering. To minimize pressure drops caused by flow fittings used in the experimental setup, nylon fittings supplied by Swagelok were used along with plastic tubing where feasible.

7.4.2 Experimental procedure

When studying the hydrodynamic behavior of ceramic foam, the key parameters of interest are the dependence of pressure drop on gas and liquid flux and the flooding behavior of the material. Flooding in case of tower packing is defined as the condition in operation of a tray or packed column when the vapor flow-rate is large enough to severely hinder the downward flow of liquid. Operating a tray or packed column under flooding conditions results in an unstable environment due to a build-up of liquid in the column, resulting in poor conditions for gas-liquid mass transfer. Flooding in a tray or packed tower can be determined by a abrupt change in the slope of the pressure drop vs. gas flux curve. As a part of this study, we explored ceramic foam hydrodynamics between a wide range of gas and liquid flow-rates. The gas flow-rate

was varied between 0 and 9 standard liters per minute (SLPM) and the liquid flow-rate was varied between 0 and 0.1 liters per minute (LPM). The range of values was selected on the basis of the potential gas and liquid flux that are of interest for a later proof-of-concept demonstration. When performing the experiments, the gas flux was held constant at a specific value and the liquid flux was varied. For each flux, it was ensured that the system was operationally stable for at least 20 minutes. Pressure drops in the column corresponding to these operating conditions were recorded after the water levels in the manometer reached steady state. Since pressure drops in the ceramic foams are small, it is important to account for all external sources of pressure drop that contribute to the experimentally measured values. The most important of these factors are the tubing and fittings that are a part of the experimental setup. To quantify the value of these pressure drops, we conducted measurements on the empty glass tube with fittings and tubing unchanged from the hydrodynamic measurements. As before, the gas flux is varied to measure the corresponding pressure drop values. The pressure drop measurements conducted on the ceramic foam are then corrected for these external pressure drop resistances to derive the contribution of the ceramic foams to the pressure drop.

7.4.3 Experimental results

Figure 7.9 is a plot of the pressure drop versus flow-rate for 45 ppi alumina foam for the range of gas and liquid flow-rates measured as a part of this study. As can be

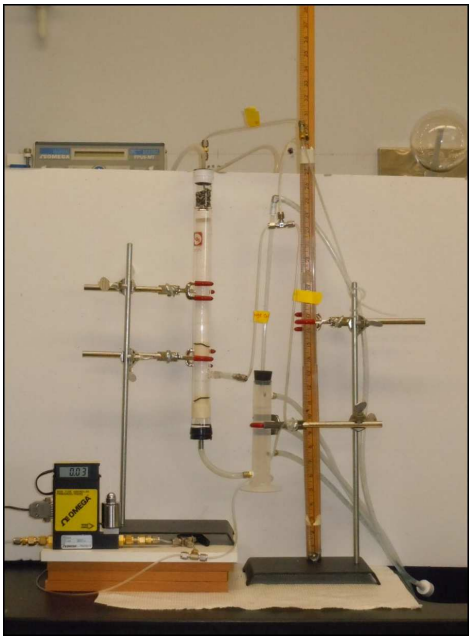

Figure 7.8 : Experimental setup for studying the hydrodynamic behavior of ceramic foams

seen in the plot, the pressure drop per meter of packing varies linearly with the gas flow-rate. Under the conditions explored in this study, we found that liquid flow-rate has little effect on the pressure drop in the ceramic foam column.

Under all the operating conditions explored, no flooding behavior was observed in this ceramic foam column; suggesting that flooding point had not been reached and the system was within the limits of operating conditions. Assuming a linear relationship between pressure gradient and gas flow-rate till the flooding point is reached allows for the estimation of the flooding point gas flow-rate by balancing the pressure gradient with the product of fluid density and gravitational acceleration. This is expressed in Equation 7.2.

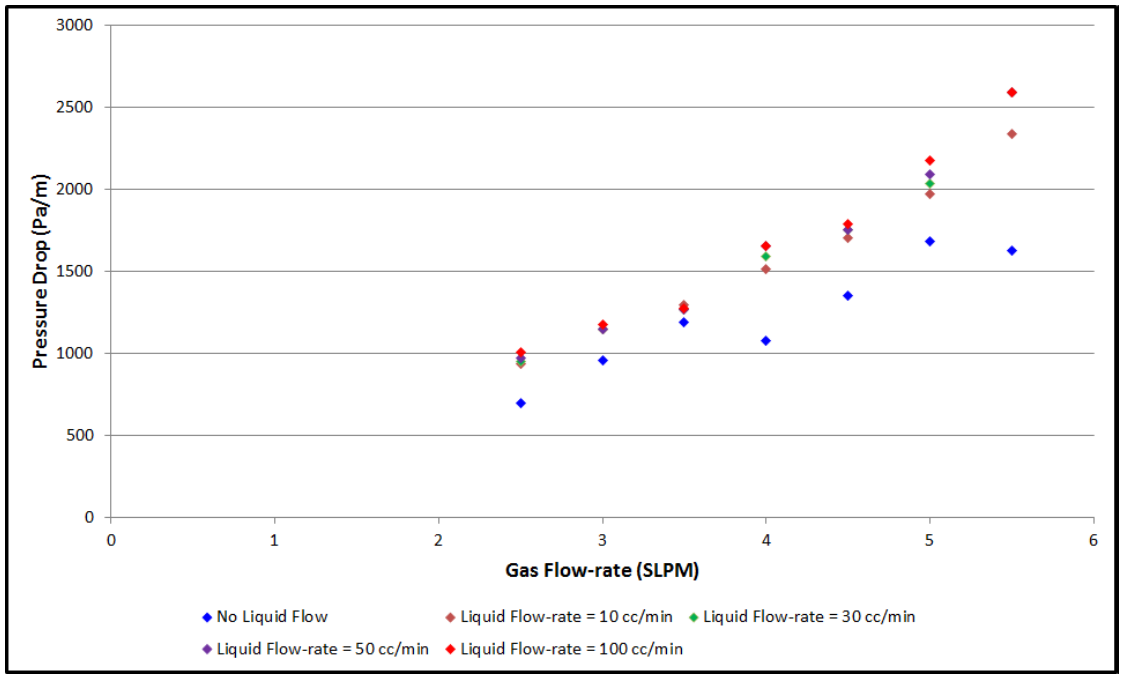

Figure 7.9 : Pressure drop in 45 pores per inch (ppi) ceramic foam at varying gas and liquid flow-rates

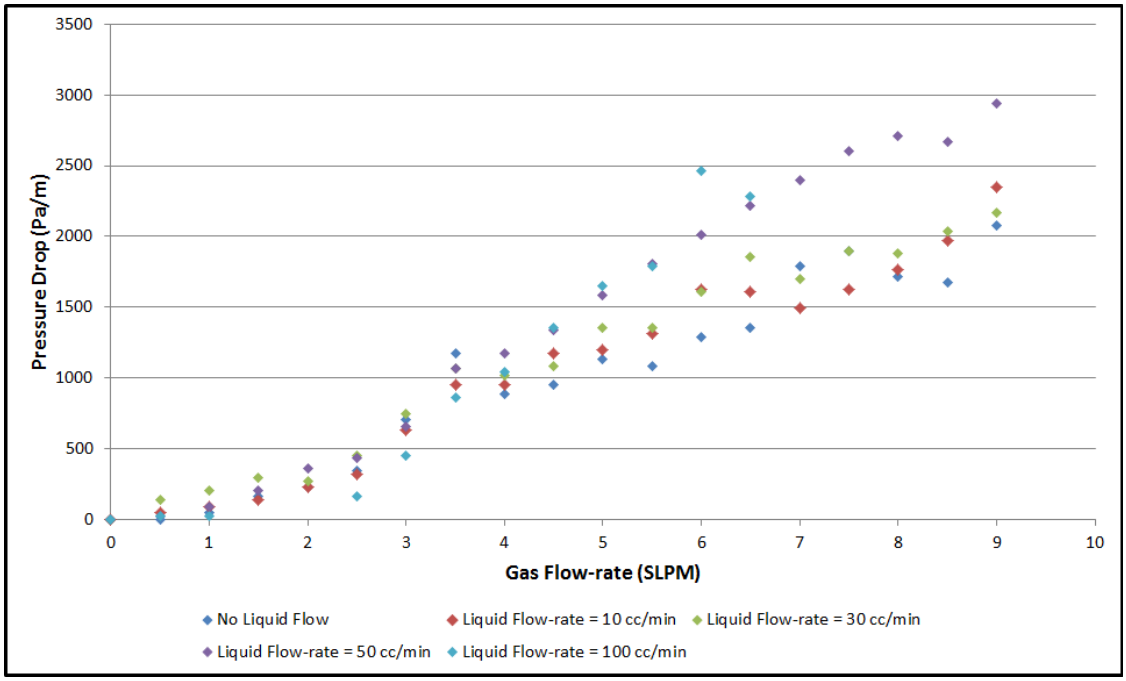

Figure 7.10 : Pressure drop in 30 pores per inch (ppi) ceramic foam at varying gas and liquid flow-rates

$$\frac{dp}{dx} = \rho \cdot g \tag{7.2}$$

For diglycolamine, ρ 1040 (kg/m^3) at 100 ^{o}F. This results in an approximate flooding point pressure gradient ($\frac{dp}{dx}$) of 10202.5 (Pa/m). Linear extrapolation of the experimental data in Figure 7.9 for the liquid flow-rate of 0.1 liter per minute (LPM) results in a mass flux of 0.93 kg-m^{-2}s^{-1} at the approximate flooding point for the 45 pores per inch (ppi) ceramic foam. For the 2.8 centimeter (cm) diameter glass column, this corresponds to a gas flow-rate of 22.5 standard liters per minute (SLPM). Figure 7.10 is a plot of the pressure drop versus flux for 30 ppi alumina foam for the range of gas and liquid flux studied as a part of this work. Comparing Figures 7.9 and 7.10 clearly shows that the 45 pores per inch (ppi) grade ceramic foam has a greater pressure drop as compared to the 30 pores per inch (ppi) grade material. This is clearly a result of an increase in the size of the macropores in the latter material. Performing the same calculation for pressure gradient and corresponding vapor flow-rates results in a flooding point gas flow-rate of 28.1 standard liters per minute (SLPM) or a mass flux of 1.16 kg-m^{-2}s^{-1}.

Figure 7.11 shows the dependence of pressure gradient on the gas and liquid flow-rates for 20 pores per inch (ppi) grade alumina foam. Clearly, there is a noticeable decrease in the pressure drop as compared to the 30 and 45 pores per inch (ppi) samples due to an increase in the size of the macropores in the foam. Using the same methodology for estimating flooding point yields a flooding point at a gas flow-rate of 33.5 standard

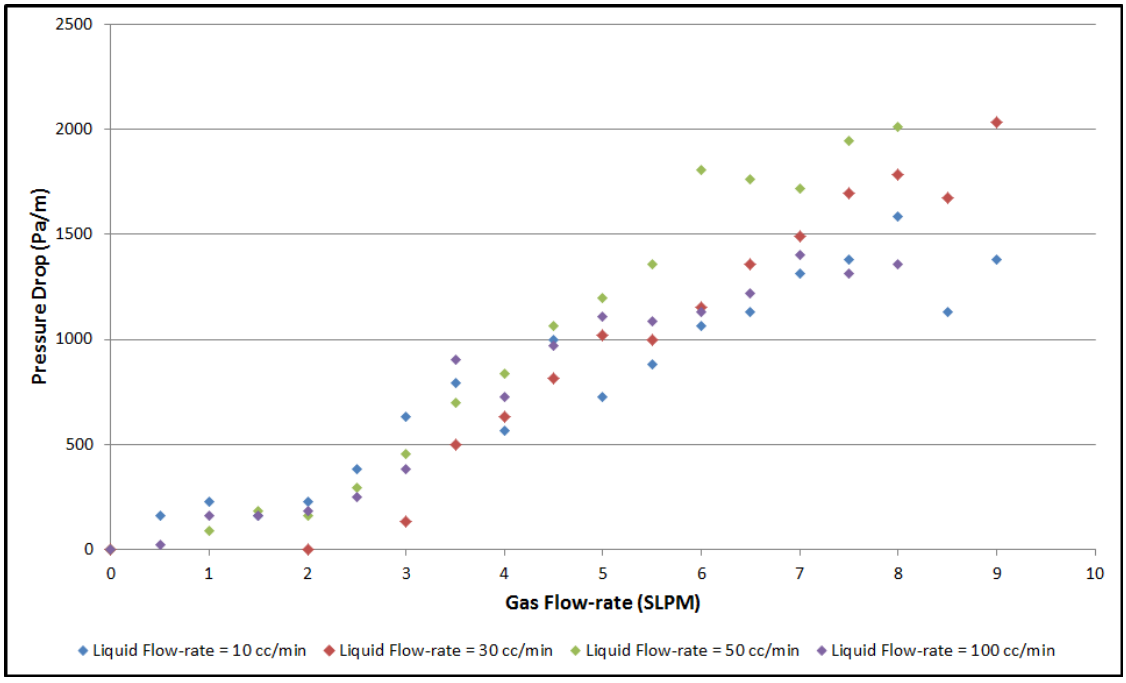

Figure 7.11 : Pressure drop in 20 pores per inch (ppi) ceramic foam at varying gas and liquid flow-rates

liters per minute (SLPM) or a gas mass flux of 1.385 kg-m^{-2}s^{-1}.

We have compared the values measured as a part of our study with those reported for 40 pores per inch (ppi) metal foams in published literature. The pressure drops for metal foams are roughly 1/10 th as compared to our measurements [101]. This can be attributed to the higher thickness of struts in alumina foam as compared to those in metal foams. Thicker struts result in smaller pores and lower porosity which eventually results in greater pressure drops in the column. Strut thickness is a variable that can be controlled during the manufacture of ceramic foam and thus a factor that can be worked upon with the ceramic foam manufacturer. Optimized ceramic foam materials will result in significantly lower pressure drops than what we are cur-

rently using for our studies. This would also mean significantly higher gas-flux at the flooding point. In conclusion, we remark that commercially available ceramic foams performed satisfactorily in the hydrodynamic studies. Next, we conduct experimental studies to determine the mass transfer performance of ceramic foams using simulated flue gas and aqueous diglycolamine (DGA).

7.5 Characterizing the mass transfer behavior of ceramic foams

When selecting tower packing for gas absorption operation, in addition to the hydrodynamic properties; mass transfer performance plays a critical role. Irrespective of physical or chemical gas absorption, the first step in the process is the transfer of the component of interest from the gas phase to the liquid. The rate of mass transfer from gas to liquid depends on the gas-liquid interfacial surface area and the driving force for mass transfer (difference in concentrations). Increasing the geometric surface of a packing generally increases the rate of mass transfer. The exact magnitude of this change, however, is dependent on several factors such as the actual increase in the interfacial surface area, effect of tower packing fluid flow properties and flow dynamics itself. Since most advanced packing materials such as ceramic foams possess extremely complex 3-dimensional structures; it is impossible to analytically predict their mass transfer performance. In this section, we describe the experiments performed to study the mass transfer behavior of various ceramic foam samples. In

addition, we use these results to start determining the dimensions of a stainless steel prototype that will be developed further for a proof-of-concept demonstration.

7.5.1 Experimental setup

Figure 7.12 is a schematic representation of the experimental setup that we have developed for conducting mass transfer studies on various grades of ceramic foam. In order to obtain a perspective, we compare the mass transfer performance of these ceramic foam samples with a reference tower packing material 6 mm ceramic Raschig rings. Conceptually, this setup is very similar to the one used for the hydrodynamic studies except no water manometer is required in these experiments. As can be seen, the core elements of the setup such as the glass column, gas delivery to the column on the side, below the 6th ceramic foam plug from the top are similar to the hydrodynamic studies setup of Figure 7.7. For mass transfer measurements, we are using a CO_2/N_2 mixture with 13% carbon dioxide (CO_2); balance nitrogen (N_2) supplied by Matheson TriGas as the 'simulated' flue gas (mass flow controller calibration ratio: 1.06). 30 wt% and 60 wt% diglycolamine (DGA) solutions prepared from 99.5% pure diglycolamine (DGA) agent supplied by Huntsman Chemicals were used as the absorbent. This absorbent solution is delivered from the solvent reservoir on to the ceramic foam plug by a peristaltic pump. Spent absorbent is collected in a carboy for discarding.

As shown in Figure 7.12, gas supply to the glass column can be switched between

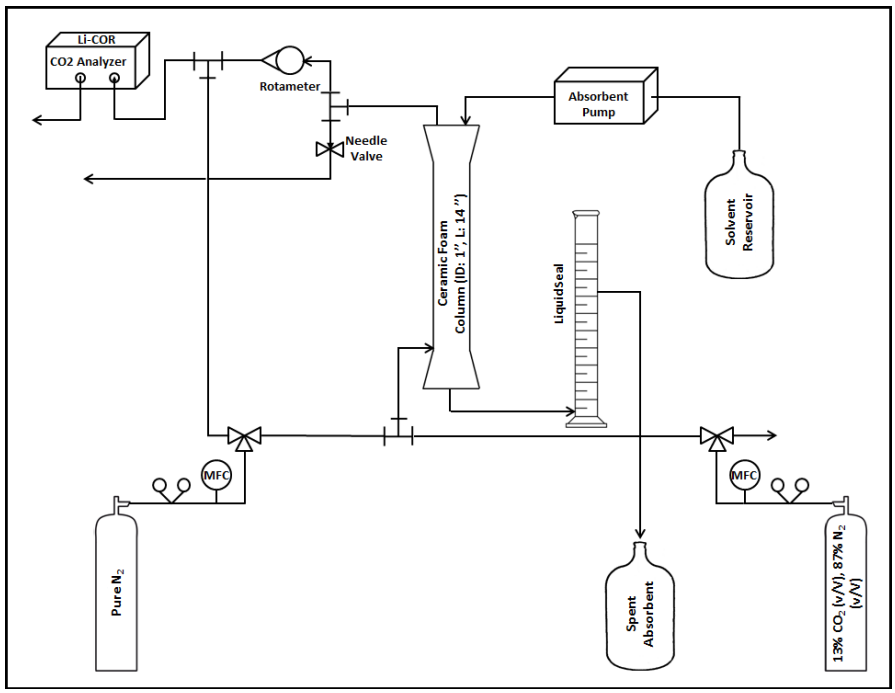

Figure 7.12 : Schematic representation of experimental setup developed for studying mass transfer performance of ceramic foams

pure nitrogen (N_2) and simulated flue gas using a 3-way valve. This arrangement has been implemented in order to facilitate purging the air in the glass column before commencing a trial. Outlet gas is analyzed for its carbon dioxide (CO_2) concentration with a non-dispersive infrared detector (LI 820) manufactured by LI-COR Biosciences. The detector can measure carbon dioxide (CO_2) concentrations between 0 and 20,000 ppm with 3% accuracy (measured value) and can handle inlet gas flux up to 1 standard liter per minute (SLPM). Since, the simulated flue gas has a carbon dioxide (CO_2) concentration of 130,000 ppm; we have implemented a dilution system as shown in Figure 7.12, wherein we sample a small part of the outlet gas stream from the glass column and dilute it with a known flux of nitrogen (N_2), controlled using a mass flow

controller (MFC). The quantity of exit stream being sampled is controlled using a needle valve and measured with a rotameter. The dilution ratio can be calculated using the following equation. In the Equation 7.3, D is the dilution ratio, $\dot{Q}_{N2}$ is the nitrogen (N2) flow-rate and $\dot{Q}_{sample}$ is the flow-rate of sampled exit gas.

$$D = \frac{\left(\dot{Q}_{N2} + \dot{Q}_{sample}\right)}{\left(\dot{Q}_{sample}\right)} \tag{7.3}$$

7.5.2 Experimental method

When comparing the mass transfer performance of ceramic foams against that of Raschig rings, the key parameter of interest is the degree of carbon dioxide (CO_2) removal under the same operating conditions (i.e. gas and liquid flow-rates). As described in §7.5, even if the geometric surface areas of the two packing materials are known to be the same; their geometric structure, surface properties and arrangement in the column are critical factors that affect the extent of gas absorption. As a part of this study, we have conducted the comparison between ceramic foams and Raschig rings under 2 different conditions of gas and liquid flow-rate conditions. These are:

- Gas flow-rate = 3 standard liter per minute (SLPM), Liquid flow-rate = 0.02 liter per minute (LPM)
- Gas flow-rate = 5 standard liter per minute (SLPM), Liquid flow-rate = 0.04 liter per minute (LPM)

The gas to liquid ratio in both these cases is similar to that maintained in industrial scale absorbers. In addition, we conduct trials at the above gas and liquid flow-rates with 30 wt% and 60 wt% diglycolamine (DGA) solutions respectively to study the effect of absorbent concentration on the degree of carbon dioxide (CO_2) pickup.

Before commencing a trial, we purge the ceramic foam column with pure nitrogen (N_2) to remove most of the air and residual carbon dioxide (CO_2) from previous experiments. Once the carbon dioxide (CO_2) concentration in the column is down to around 10 ppm, nitrogen (N_2) flow is stopped and simulated flue gas is introduced into the column. Simultaneously, the dilution nitrogen (N_2) stream to the detector is turned on. In all the trials conducted, a flow-rate of 0.8 SLPM was maintained for the dilution nitrogen (N_2) stream using a mass flow controller (MFC). The outlet carbon dioxide (CO_2) level measured by the analyzer is recorded using a desktop computer and data acquisition software provided by LI-COR Biosciences. The float level in the rotameter is recorded as a function of time since it is sensitive to fluctuations in the inlet gas flux as well as the composition of the outlet gas. After the experiment is complete, the analyzer is purged with the dilution nitrogen (N_2) stream till carbon dioxide (CO_2) levels are down to almost zero.

7.5.3 Experimental results

Figure 7.13 shows a plot of the comparison of the degree of carbon dioxide (CO_2) pickup taking place in a 30.5 centimeters (cm) long glass column filled with 45 pores-

per-inch (ppi) and 20 pores per inch (ppi) ceramic foams and 6 millimeter (mm) Raschig rings corresponding to a gas flow-rate of 3 standard liters per minute (SLPM), a liquid flow-rate of 0.02 liters per minute (LPM) and an absorbent concentration of 30 wt%. As can be seen from the above plot, the use of 6 millimeter(mm) Raschig rings results in around 60% carbon dioxide (CO_2) pickup, 20 pores per inch (ppi) ceramic foam achieves around 40% removal and 45 pores per inch (ppi) ceramic foam results in only 25% carbon dioxide (CO_2) pickup. The performance of the 20 and 45 pores per inch (ppi) ceramic foams, however, seems contrary to expectations. The 45 pores per inch (ppi) foam sample has almost 2x the geometric surface area that of the 20 pores per inch (ppi) foam. Since a larger geometric surface area is largely a favorable characteristic for good mass transfer, the 45 pores per inch (ppi) foam maybe expected to have a better carbon dioxide (CO_2) removal performance than the 20 pores per inch (ppi) sample. A closer examination of the 45 and 20 pores per inch (ppi) foams reveals that the macropores in the 45 pores per inch (ppi) foam are significantly smaller than the ones in the 20 pores per inch (ppi) sample. Whereas a large geometric surface area can aid in increasing the rate of mass transfer, it is of far greater importance that a high gas-liquid interfacial area be available. We hypothesize that during gas absorption operation, macropores in the 45 pores per inch (ppi) foam - now filled with liquid absorbent offer a smaller interfacial surface area as compared to the 20 pores per inch (ppi) sample. This could result from the presence of insufficient gas in the macropores of the foam or could result from a segregation

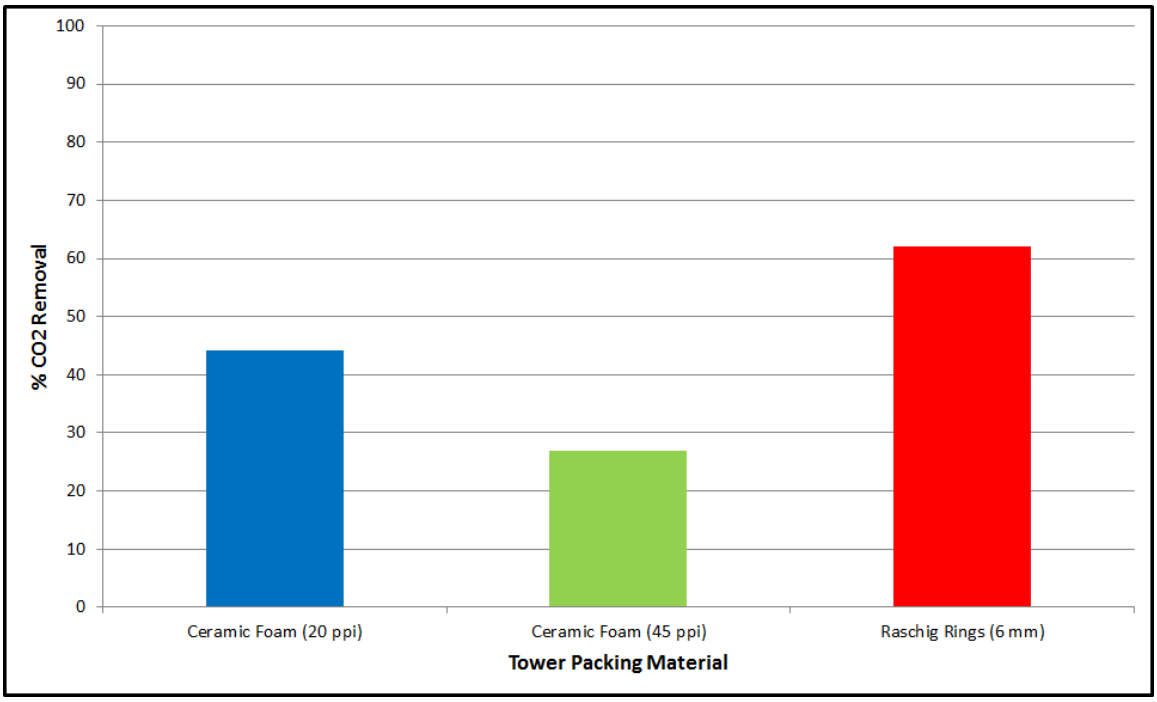

Figure 7.13 : Degree of CO_2 pickup with different tower packing (30 wt% DGA, gas at 3 SLPM, liquid at 0.02 LPM)

of flow, wherein there is almost a separate flow of gas and liquid through the pores of the foam resulting in poor mass transfer. The 20 pores per inch (ppi) foam has a relatively poorer performance as compared to the 6 millimeter (mm) Raschig rings even though their geometric surface areas are comparable. We believe this is also a result of the smaller pore spaces for gas-liquid flow in the ceramic foam as compared to the 6 millimeter (mm) Raschig rings. The smaller size of the macro-pores is a result of the ceramic struts of the foam being too thick, which can be optimized as was described previously in §§7.4.3.

Figure 7.14 shows a comparison of the degree of carbon dioxide (CO_2) removal with

the use of 20 pores per inch (ppi) ceramic foam and 6 millimeter (mm) Raschig rings. These experiments are conducted at a gas flow-rate of 5 standard liter per minute (SLPM), a liquid flow of 0.04 liter per minute (LPM) and absorbent concentration of 30 wt% diglycolamine (DGA). As can be seen from the plot, there is a slight change in the degree of carbon dioxide (CO_2) removal by both the ceramic foam and the Raschig rings. Whereas the ceramic foam shows a reduction in the carbon dioxide (CO_2) pickup (by around 7%), the Raschig rings exhibit an increase of around 5% in the carbon dioxide (CO_2) uptake. We believe that the explanation for this lies in the experimental conditions in the bench-scale column in which the experiments are being conducted.

When the gas flow rate is changed from 3 standard liter per minute (SLPM) to 5 standard liter per minute (SLPM), the residence time of the gas in the column reduces by 40%. A smaller time for gas-liquid contacting will result in lesser uptake of carbon dioxide (CO_2). However, the flow-rate of the absorbent solution is doubled as well which results in an increased carbon dioxide (CO_2) uptake. With two competing factors are play, the effectiveness of mass transfer depends on good gas-liquid contacting and the presence of sufficient interfacial surface area. We suggest that the smaller pore spaces in ceramic foam as compared to Raschig rings result in the observed changes in the carbon dioxide (CO_2) uptake.

Figure 7.15 shows a comparison of the degree of carbon dioxide (CO_2) uptake with 60 wt% diglycolamine (DGA) as the absorbent with gas flow-rates at 3 and 5

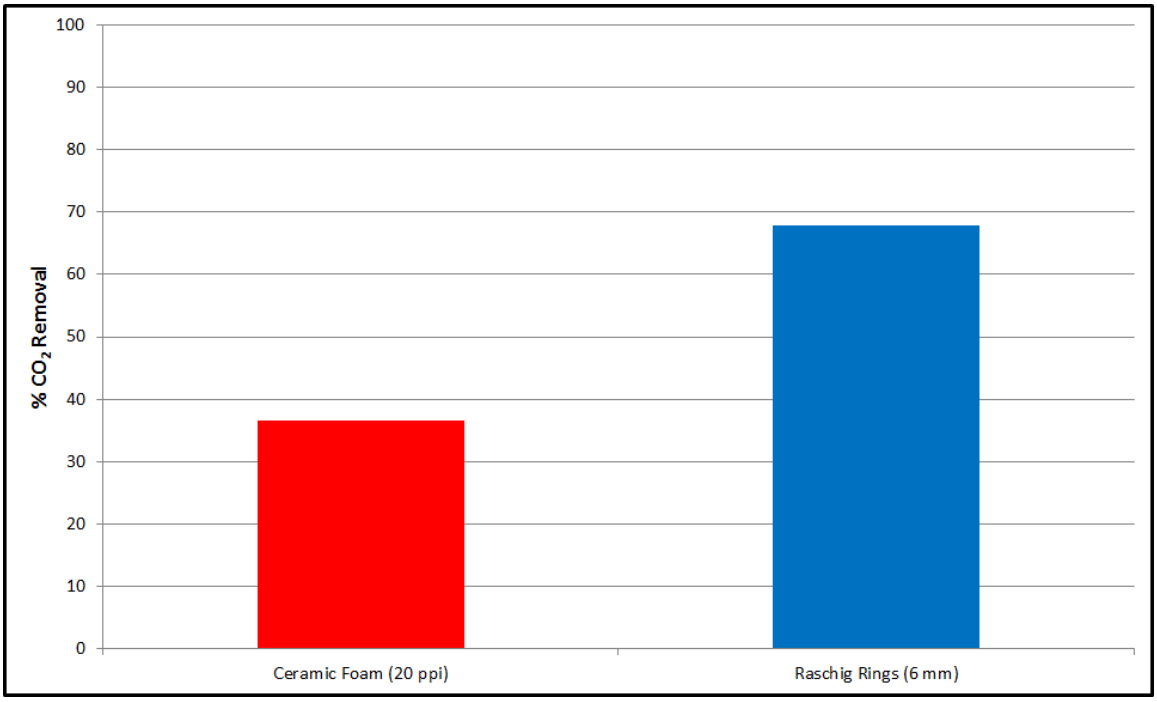

Figure 7.14 : Degree of CO_2 pickup with different tower packing (30 wt% DGA, gas at 5 SLPM, liquid at 0.04 LPM)

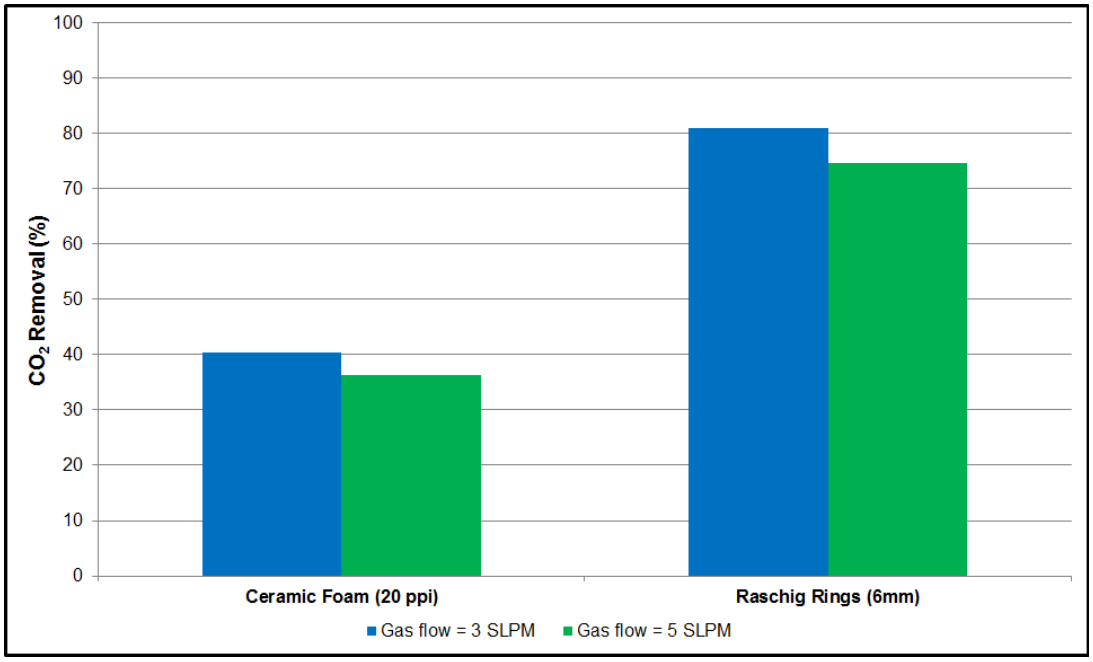

Figure 7.15 : Degree of CO_2 pickup with different tower packing (60 wt% DGA, gas at 3 & 5 SLPM, liquid at 0.02 & 0.04 LPM)

standard liter per minute (SLPM) and liquid flow-rate of 0.02 and 0.04 liter per minute (LPM). In the first case of lower gas and liquid flow-rates, carbon dioxide (CO_2) pickup with the ceramic foam sample is almost the same as that with 30% diglycolamine (DGA) whereas that with Raschig rings increases by around 30%. In the later case involving higher gas and liquid flow-rates, we observe that the 20 pores per inch (ppi) ceramic foam picks up around 36% of the entering carbon dioxide (CO_2) whereas the Raschig rings result in around 74% pickup. An increase in the amine concentration can normally be expected to increase the extent of carbon dioxide (CO_2) uptake except under a scenario where the degree of carbon dioxide (CO_2) removal isn't limited by the availability of unreacted amine molecules. This effect can clearly be observed in the case of Raschig rings, however in case of ceramic foam the carbon dioxide (CO_2) uptake surprisingly exhibits no change. Industrial absorbers are suitably optimized to maintain operating conditions to minimize mass transfer resistances in both gas and liquid phases. In case of carbon dioxide (CO_2) absorption, liquid phase resistances are crucial in particular since the carbon dioxide (CO_2) must first dissolve in the liquid absorbent and then undergo hydration to be able to react with the amine. The experimental conditions in the bench-scale apparatus we have setup in our lab are not optimized. Results from the carbon dioxide (CO_2) absorption experiments conducted thus far suggest the presence of liquid phase mass transfer resistances in the ceramic foam system and to a lesser extent in the Raschig ring setup. Thus, an increase in the amine concentration fails to have any significant

effect on the extent of carbon dioxide (CO_2) removal in ceramic foam system. This clearly suggests that carbon dioxide (CO_2) absorption is limited by its mass transfer from gas to liquid as opposed to the unavailability of unreacted amine molecules. In case of Raschig rings, mass transfer does not appear to be a significant limiting factor likely due to the larger macro-pores. Consequently, an increase in the diglycolamine (DGA) concentration results in an increase in the carbon dioxide (CO_2) uptake rate.

7.6 Experiments to determine design parameters for proof-of-concept demonstration

Experiments presented in §§7.5.2 and 7.5.3 were conducted with an objective of characterizing the mass transfer performance of ceramic foams. The end objective of this research is to develop a working prototype of the novel carbon dioxide (CO_2) separation process for conducting a proof-of-concept demonstration. In order to provide a direction for our design efforts, two important success criteria were designated for the proof-of-concept demonstration. These are:

- 90% or more carbon dioxide (CO_2) removal from inlet simulated flue gas stream
- Absorption and desorption of carbon dioxide (CO_2) in a single integrated unit using aqueous amine absorbent (e.g. diglycolamine)

The results presented in §§7.5.3 describe the mass transfer characteristics of the 20 pores per inch (ppi) ceramic foam. However, in all the cases considered; the degree

of carbon dioxide (CO_2) removal is less than 90%. Thus, further experiments needed to be performed to determine the gas-liquid flow-rates and the height of ceramic foam sufficient for removal of 90% of the inlet carbon dioxide (CO_2). It is important to clarify at this point that a proof-of-concept prototype is far from optimized. Thus, the gas-liquid flow-rates used in this design study for achieving 90% carbon dioxide (CO_2) removal are not representative of the performance of an optimized system.

7.6.1 Experimental procedure

The experimental setup used for conducting these studies has been described previously in §§7.5.1. The experimental procedure has been described in §§7.5.2. For all experiments, 30 wt% diglycolamine (DGA) was used as the absorbent. The key parameter of interest in these studies is the dependence of the degree of carbon dioxide (CO_2) removal on (i) gas flow rate, (ii) liquid flow rate and (iii) height of ceramic foam packing. As a part of this study, we have compared the performance of 20 pores per inch (ppi) ceramic foams of 4 different lengths under different conditions of gas and liquid flow. These are:

- Ceramic foam lengths = 10.2, 15.2, 20.3 and 25.4 centimeters (cm)
- Gas flow-rate = 0.25 standard liter per minute (SLPM), Liquid flow-rate = 0.01, 0.02, 0.03 liter per minute (LPM)
- Gas flow-rate = 0.50 standard liter per minute (SLPM), Liquid flow-rate = 0.01, 0.02, 0.03 liter per minute (LPM)

- Gas flow-rate = 0.75 standard liter per minute (SLPM), Liquid flow-rate = 0.01, 0.02, 0.03 liter per minute (LPM)
- Gas flow-rate = 1.0 standard liter per minute (SLPM), Liquid flow-rate = 0.01, 0.02, 0.03 liter per minute (LPM)

7.6.2 Experimental results

Figure 7.16 is a plot of the comparison of the degree of carbon dioxide (CO_2) pickup in a 20 pores per inch (ppi) ceramic foam column of 10.2 centimeters (cm) length under the different gas and liquid flow conditions listed above. As can be seen, there is a gradual increase in the carbon dioxide (CO_2) removal both as the liquid flow-rate is increased and the gas flow rate is decreased. The closest configuration to the required 90% carbon dioxide (CO_2) pickup is at a liquid flow-rate of 0.03 liter per minute (LPM) and a gas flow rate of 0.25 standard liter per minute (SLPM), under which condition, around 80% of the incoming carbon dioxide (CO_2) is removed.

Figure 7.17 is a plot of the performance of a 15.2 centimeters (cm) long ceramic foam column for carbon dioxide (CO_2) removal under different gas and liquid flow rates. It can be seen from the plot that the optimal configuration for 90% removal of inlet carbon dioxide (CO_2) is a gas flow-rate between 0.25 standard liter per minute (SLPM) and 0.5 standard liter per minute (SLPM) and liquid flow-rate between 0.02 and 0.03 liter per minute (LPM). Figure 7.18 is a plot of the degree of carbon dioxide (CO_2) removal in a ceramic foam column with a length of 20.3 centimeters (cm).

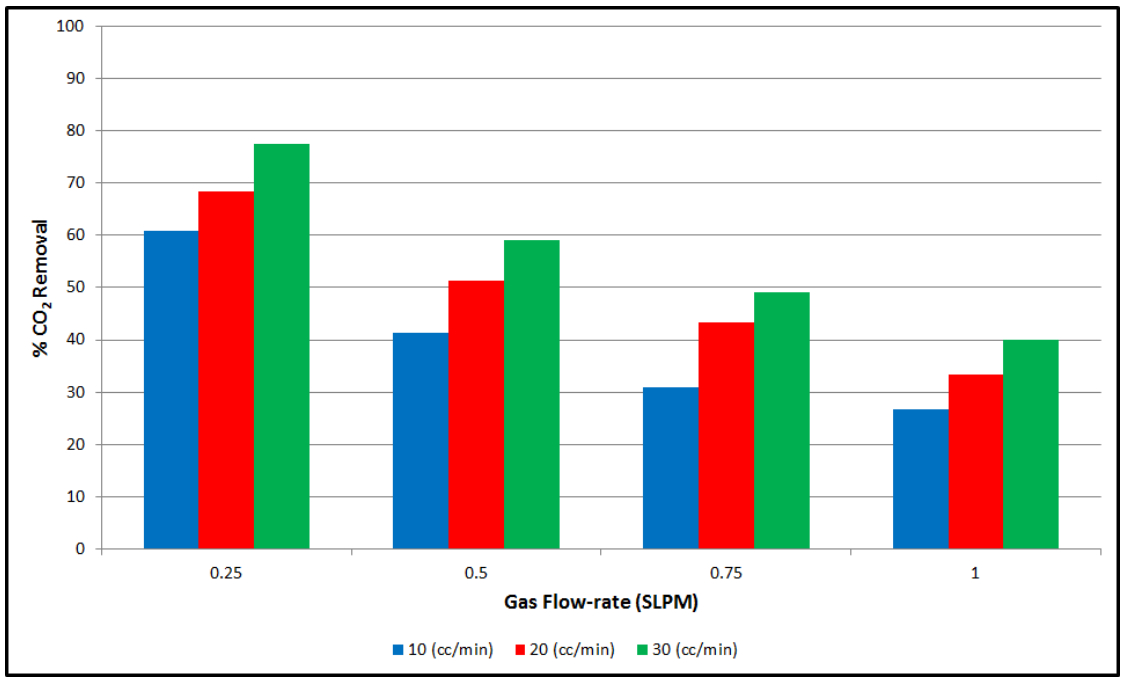

Figure 7.16 : Comparison of CO_2 removal performance under different gas and liquid flow conditions (10.2 cm long ceramic foam column)

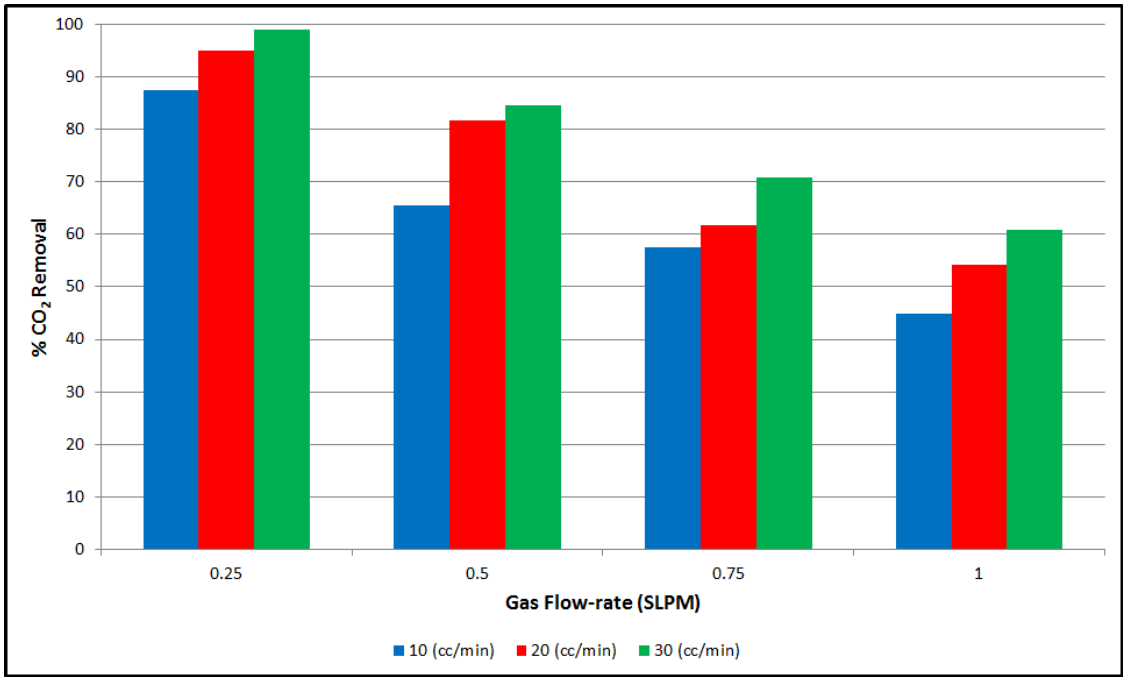

Figure 7.17 : Comparison of CO_2 removal performance under different gas and liquid flow conditions (15.2 cm long ceramic foam column)

The trend observed in the dependence of carbon dioxide (CO_2) removal on gas and liquid flow-rates is consistent with that noticed in Figures 7.16 and 7.17. However, while there is a significant change (increase) in the carbon dioxide (CO_2) removal with an almost identical change in system conditions between Figures 7.16 and 7.17, there is almost no change in the data represented in Figures 7.17 and 7.18. This suggests that the gains in carbon dioxide (CO_2) removal achieved by adding an extra 5.1 centimeters (cm) of ceramic foam is minimal. Figure 7.19 is a plot of the degree of carbon dioxide (CO_2) removal with a ceramic foam column of 25.4 centimeters (cm) length. As seen, there is only a marginal improvement in carbon dioxide (CO_2) pickup with the addition of the 5.1 centimeters (cm) ceramic foam plug to the 20.3 centimeter (cm) column used previously. Clearly, the addition of tower packing had little effect in increasing the removal of carbon dioxide (CO_2). This can be attributed to the macro-structure and the size of pore-spaces in the ceramic foam. The pore-spaces in ceramic foam are significantly smaller than those in the 6 millimeter (mm) raschig rings. The smaller pores in ceramic foam can result in liquid flow that is dominated by surface tension as compared to gravity. An outcome of this is be the channeling of liquid absorbent in the ceramic foam which could result in the observed, poor mass transfer performance in spite of large geometric surface area.

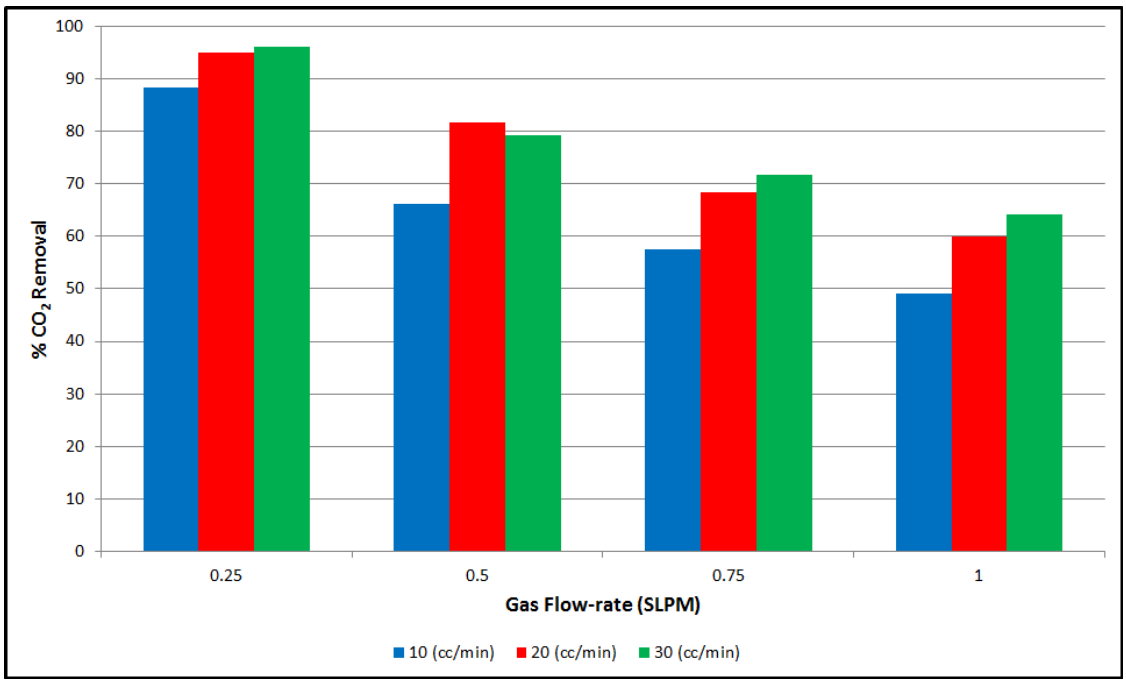

Figure 7.18 : Comparison of CO_2 removal performance under different gas and liquid flow conditions (20.3 cm long ceramic foam column)

7.7 Concluding Remarks

Based on the experimental studies performed to characterize the hydrodynamic and mass transfer properties of ceramic foams, we can reach the conclusions summarized in §§7.7.1 and 7.7.2.

7.7.1 Hydrodynamic studies

1. Hydrodynamic behavior of three different grades of ceramic foam 20 pores per inch (ppi), 30 pores per inch (ppi) and 45 pores per inch (ppi) were studied under a wide range of gas and liquid flux.

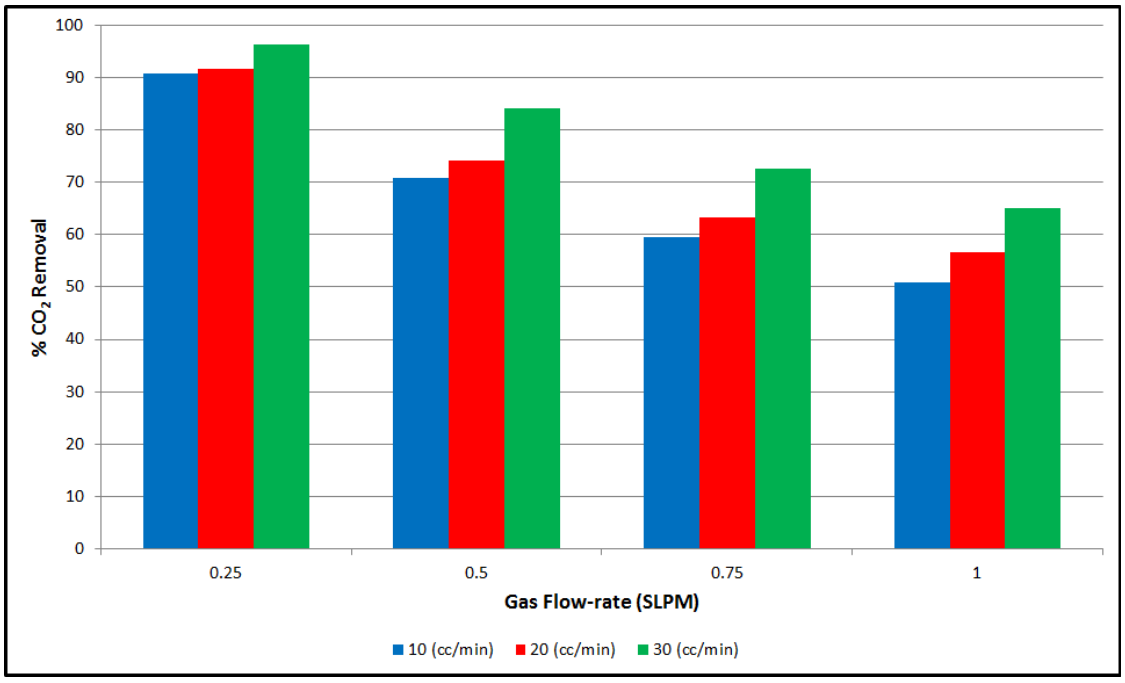

Figure 7.19 : Comparison of CO_2 removal performance under different gas and liquid flow conditions (25.4 cm long ceramic foam column)

2. Pressure drop in the ceramic foam columns was found to have a linear dependence on the gas flux and a low sensitivity to the liquid flux under the conditions studied.

3. Theoretically calculated flooding points for 20 pores per inch (ppi), 30 pores per inch (ppi) and 45 pores per inch (ppi) ceramic foams corresponding to a liquid flux of 3.33 kg-$m^{-2}s^{-1}$ is a gas flux of 1.385 kg-$m^{-2}s^{-1}$, 1.23 kg-$m^{-2}s^{-1}$ and 0.93 kg-$m^{-2}s^{-1}$.

4. The pressure drop in ceramic foams is relatively higher as compared to metal foams of similar grade. We believe that this is a result of thicker struts in

the ceramic foam and which is a feature that can be optimized to reduce the pressure drop in ceramic foam.

7.7.2 Mass transfer studies

1. 20 pores per inch (ppi) ceramic foam results in superior mass transfer performance as compared to 45 pores per inch (ppi) foam. This is due to smaller macropores in the finer grade foam sample which results in larger mass transfer resistances due to gas and liquid channeling.

2. 20 pores per inch (ppi) foam results in less carbon dioxide (CO_2) removal than 6 millimeter (mm) Raschig rings.

3. An increase in absorbent concentration results in a significant improvement in the carbon dioxide (CO_2) removal with Raschig rings. However, there is almost no improvement in the performance with the use of 20 pores per inch (ppi) ceramic foam.

4. 90% carbon dioxide (CO_2) removal can be achieved in a ceramic foam column 20.3 centimeters (cm) in length at a gas flow-rate of around 0.25 standard liter per minute (SLPM) and liquid flow-rate of 0.02 liter per minute (LPM).

Chapter 8

Integrating the absorber and stripper units for the separation of carbon dioxide (CO_2): proof of concept demonstration

In Chapter 7, we have discussed the concept of a novel carbon dioxide (CO_2) separation system that combines the absorber and stripper into a single, integrated unit. We have laid out the feasibility requirements for developing this novel process. Further, we have identified a class of suitable materials - ceramic foams and characterized their hydrodynamic and mass transfer performance using an experimental setup developed in-house. The next step in the process development cycle is to conduct a proof-of-concept demonstration by constructing a working experimental setup and operating it under different operating conditions. The proof-of-concept demonstration is a critical step in validating the technical feasibility of the proposed process. In this chapter, we discuss the design and construction of an experimental prototype for conducting the proof-of-concept demonstration. We also present the results of these demonstration type experiments.

8.1 Development of the experimental prototype

From the experiments conducted and described in Chapter 7, we have concluded that in order to achieve 90% carbon dioxide (CO_2) removal at a gas flow-rate of 0.25 standard liters per minute (SLPM) and an absorbent flow-rate of 0.02 liters per minute (LPM); the minimum height of ceramic foam required is 20.3 centimeters (cm). It is understood at this point that the more accurate measure of tower packing is its volume. However, in the present scenario; gas-liquid distribution on ceramic foams is not very well understood, thus requiring using the height of tower packing as a parameter. For the proof-of-concept demonstration, it was decided to construct a stainless steel prototype capable of withstanding high temperatures.

8.1.1 Choice of materials

20 pores per inch (ppi) alumina foam was selected as the material for gas-liquid mass transfer on the absorption and stripping sides. 99.5% α-alumina (Al_2O_3) foam blocks, 20.3 x 10.2 x 2.54 centimeters (cm) were procured from ASK-Chemicals, Alfred, NJ. The choice of a suitable material for the gas-liquid separator membrane was slightly challenging. Using a single microthin membrane is risky since it can easily get damaged (e.g. tear, punctures, etc.). Thus, it was decided to use a porous ceramic membrane of high permeability and lower entry pressure as a support for a microthin membrane. Such a 99.5% α-alumina (Al_2O_3) porous membrane was purchased from Refractron Technologies, Newark, NJ. The properties of this membrane

are summarized below in Table 8.1. Capillary connectivity between the ceramic foam and the microthin membrane was maintained using a hydrophilic fiber glass wool blanket purchased from the Ceramic Store Inc., Houston, TX as a wicking material.

Table 8.1 : Properties of porous alumina membrane

Property	**Value**
Material	Alumina (99.5 %)
Dimensions (mm)	203.2 x 101.6 x 25.4
Mean pore-size (μ)	19.3
Porosity (%)	43.4
Bubble point pressure (kPa)	5.8
Gas permeability (@ 30 psi) (m^2)	5.3 E-12 (5.38 Darcy)

For the gas-liquid separator membrane, several commercially available polymeric membranes were considered. One important characteristic required of this membrane material is for it to be hydrophilic or water-wetting. Additional requirements include good chemical resistance under alkaline conditions and thermal stability at temperatures up to 150 ^{o}C. Based on these properties, polyethersulfone (PES) was identified as the membrane material. Polyethersulfone (PES) has excellent chemical resistance against bases and has a glass transition temperature of 230 ^{o}C [102, 103]. Polyethersulfone (PES) membranes were provided by Pall Life Sciences Corporation,

Port Washington, NY (Part # S80720). The properties of these membranes are summarized in Table 8.2.

Table 8.2 : Properties of polyethersulfone membrane

Property	**Value**
Material	Polyethersulfone Membrane (Hydrophilic)
Glass transition temperature (°C)	220
Membrane thickness (μ)	114.3 - 165.1
Dimensions (mm)	203.2 x 101.6
Mean pore-size (μ)	0.8
Liquid Permeability ($L - s^{-1} - m^{-2}$)	13.3 - 63.3
Bubble point pressure (kPa)	103.4 - 213.7

8.1.2 Design considerations

Stainless steel was selected as the main material of construction with an aim of providing sufficient structural strength and avoiding corrosion problems. Several important design objectives that were critical towards the success of the proof-of-concept demonstration were identified. These are presented below.

- No gas or liquid bypass around the ceramic foam blocks

- No gas channeling along with liquid exiting the absorber or stripper at the bottom
- No gas leakage from absorption chamber to stripping chamber
- No leakage of ambient air into stainless steel prototype
- Staggered configuration for absorption and stripping side ceramic foams to maximize the gas-liquid contacting effect of ceramic foam
- Suitable distribution mechanisms for gases and liquids entering the prototype
- Capillary contact between ceramic foam and polyethersulfone (PES) membrane (using hydrophilic fiber glass wool)

After identifying the required features in the stainless steel prototype, LumaDyne LLC., a Houston based scientific design, analysis and manufacturing company was selected to design the prototype. Designers at LumaDyne, used SolidWorks - a 3D CAD design software to accomplish this task. Figures 8.1 - 8.3 show the 3-D renderings of the stainless steel prototype. It can be seen from these design images that the absorption and stripping chambers are sealed using mechanisms such as teflon spacers and o-rings. Additionally, lateral forces are exerted on the ceramic foam blocks on both sides with the use of incompressible teflon spacers to achieve good capillary contact which is crucial for lateral flow of the absorbent solution. In order to prevent gas bypass around the absorption or stripping side ceramic foam blocks, all the non-flowing faces of the ceramic foam blocks are sealed by painting them with waterproof

epoxy paint (McMaster Part # 7617T5). The epoxy paint prevents any escape of liquid through the non-flowing faces of the ceramic foam, thereby channeling all fluid flow through the main body of the ceramic foam. Finally, stainless steel 'tee' fittings purchased from Swagelok with appropriate sized bore holes were used for distributing all incoming gases and liquids. Since, a part of the proof-of-concept demonstration involves injecting steam into the stripping chamber; a steam generator is required. Commercially available steam generators were considered for this application, however, analysis showed that their capacity was too large for the present application. Hence, a miniature steam generator was designed by LumaDyne LLC. Figures 8.4 - 8.6 show the design details of this miniature steam generator. Five 80 Watt (W) cartridge heater elements purchased from Omega Engineering were installed in the miniature steam generator. A temperature controller purchased from Schneider Electric was used to control the heating elements. When operating with water at boiling temperature (i.e. 100 ^{o}C at 101.3 kilopascals (kPa), the miniature steam generator can generate steam at 0.64 kilograms per hour (kg/h).

8.1.3 Setup of experimental prototype

Having fabricated the stainless steel prototype and the miniature steam generator, the next step towards the proof-of-concept demonstration was to design the experimental setup for performing the experiments. Figure 8.7 shows a schematic representation of the experimental setup developed for performing the proof-of-concept demonstration.

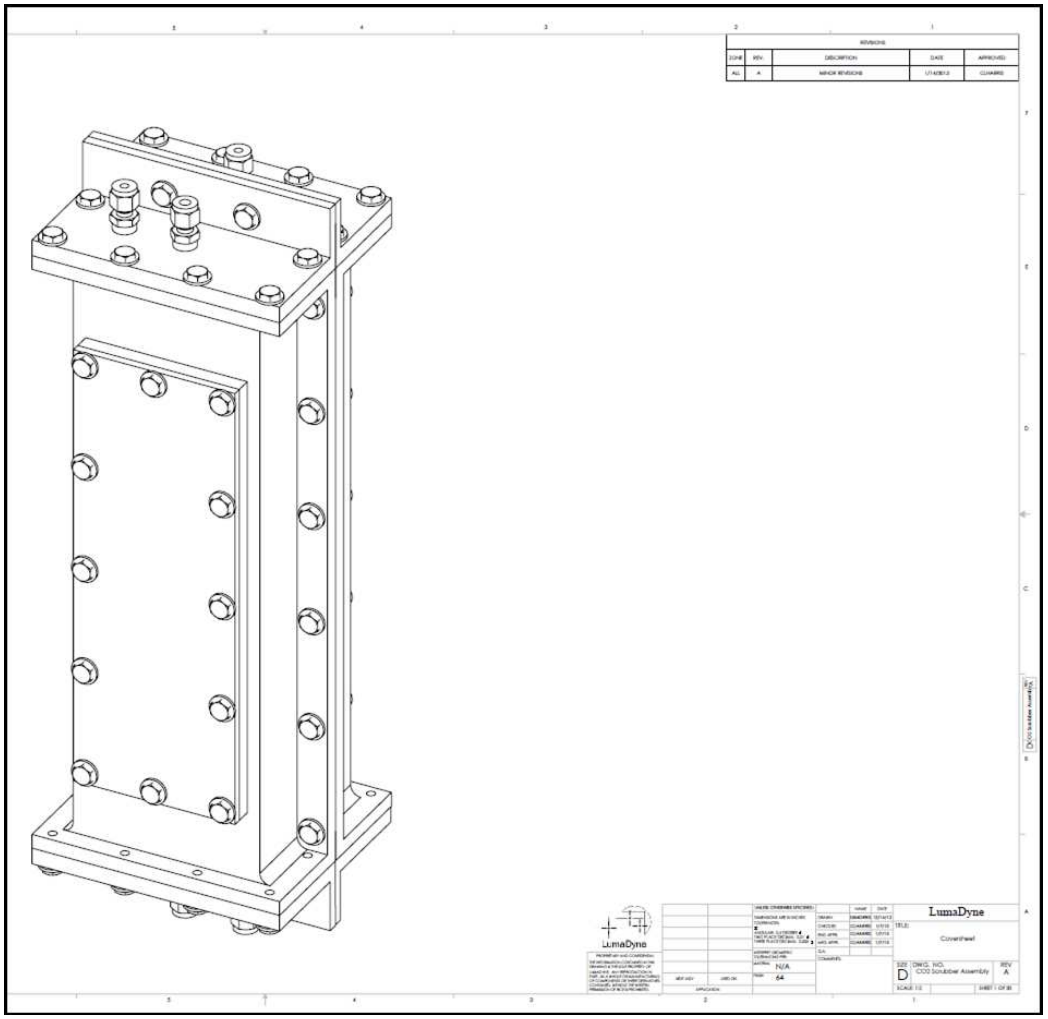

Figure 8.1 : Rendering of the stainless steel prototype

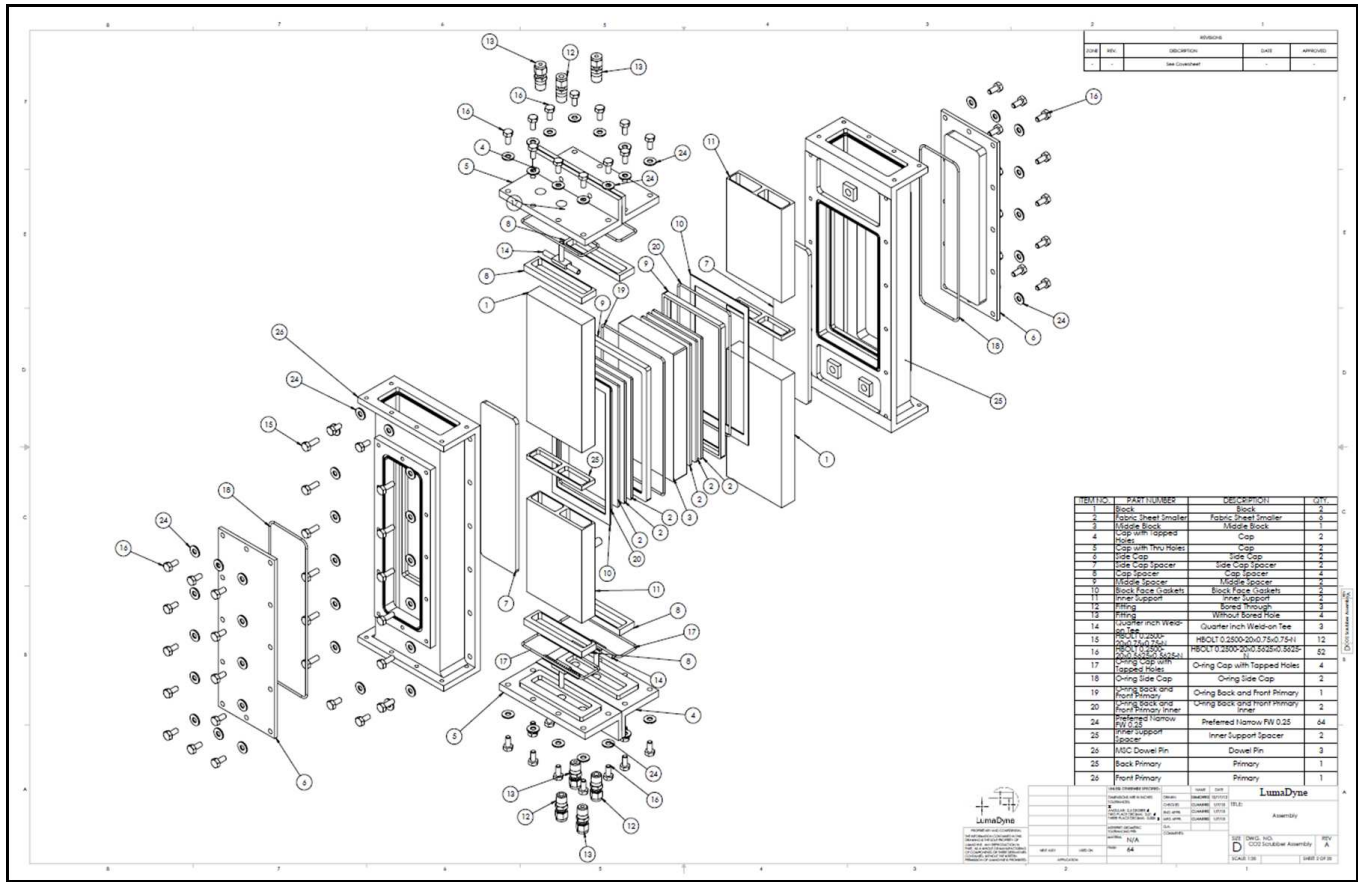

Figure 8.2 : An assembly view of the stainless steel prototype

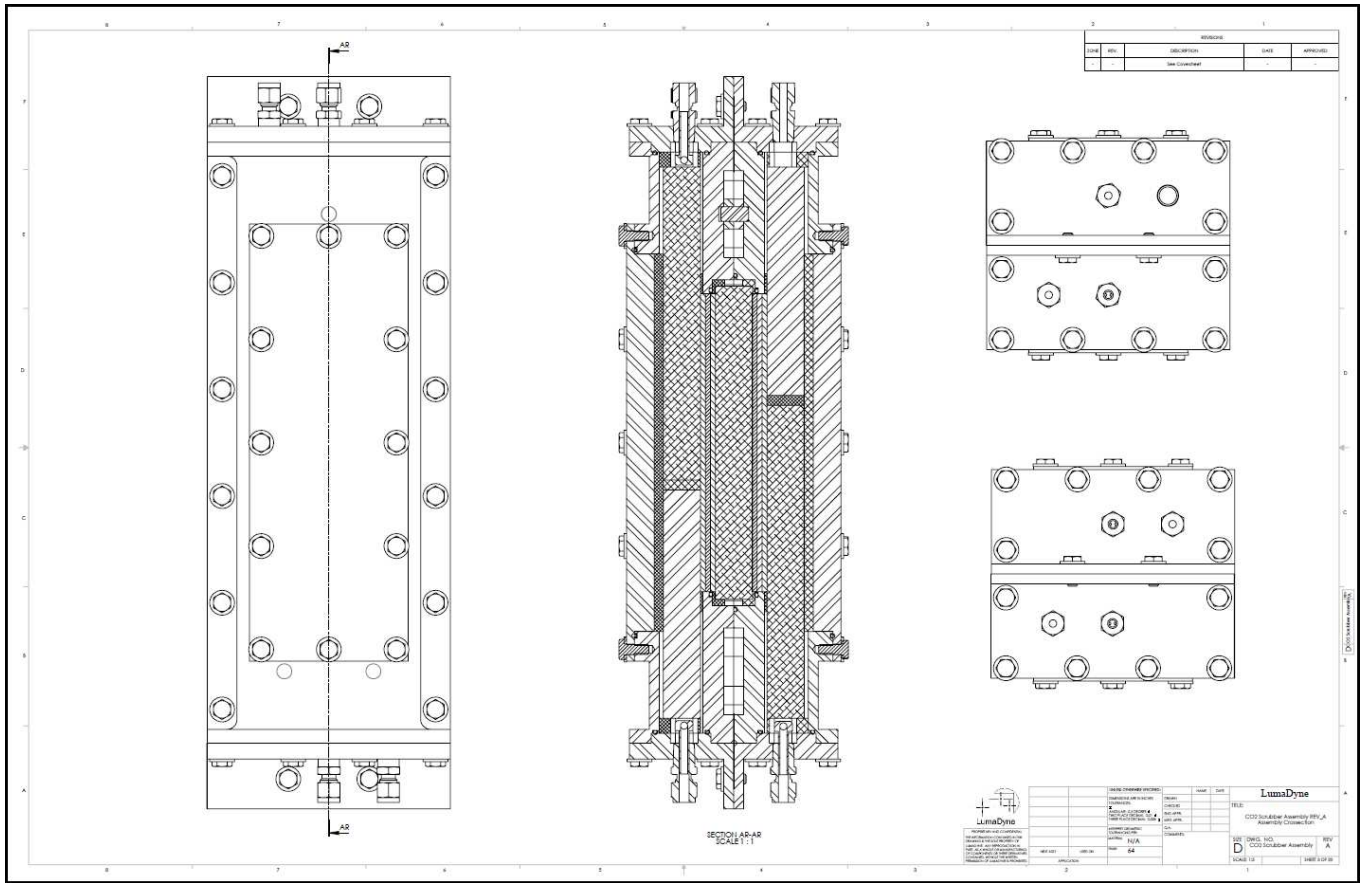

Figure 8.3 : An assembly cross-section view of the stainless steel prototype

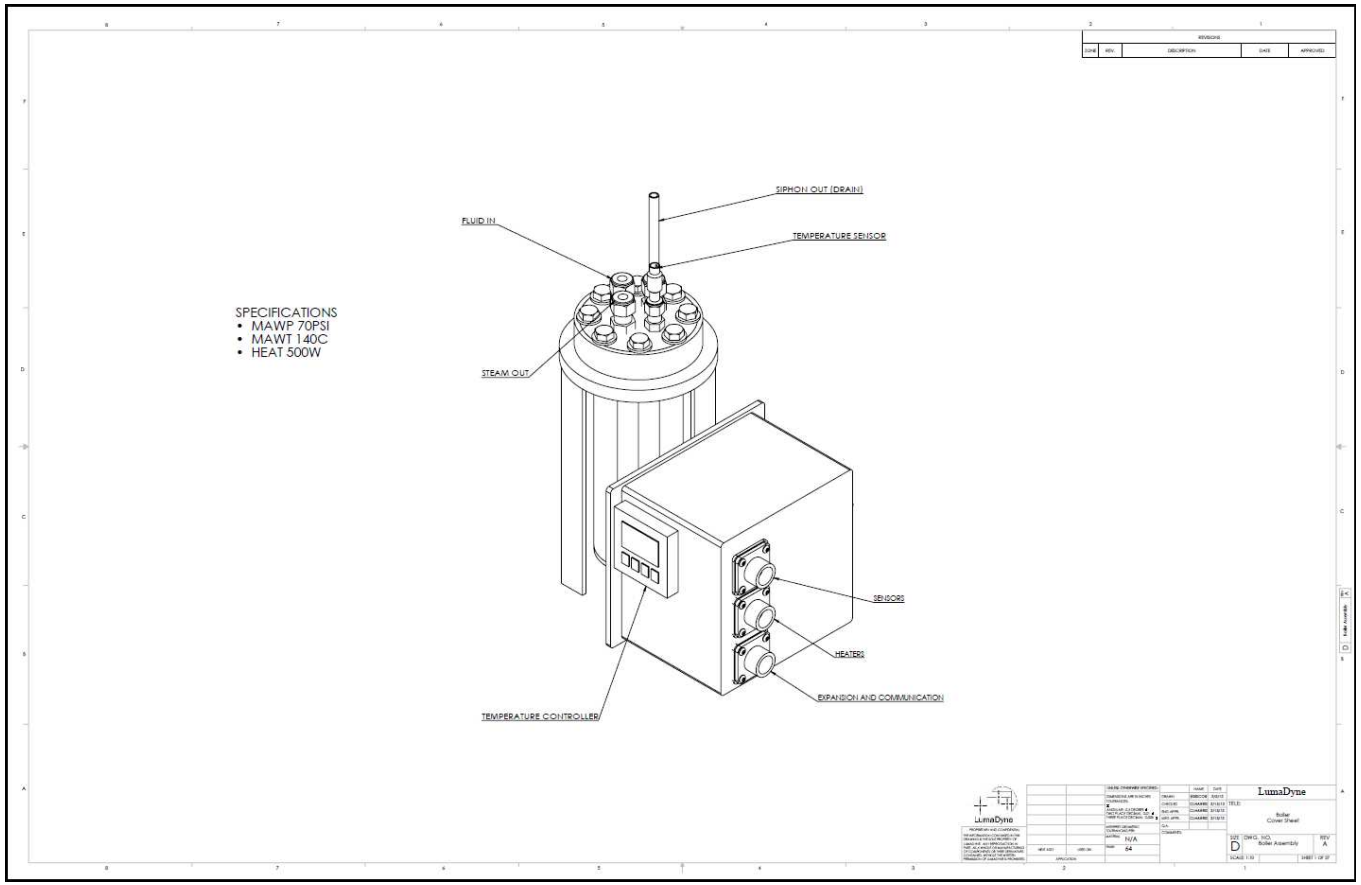

Figure 8.4 : Rendering of the miniature steam generator

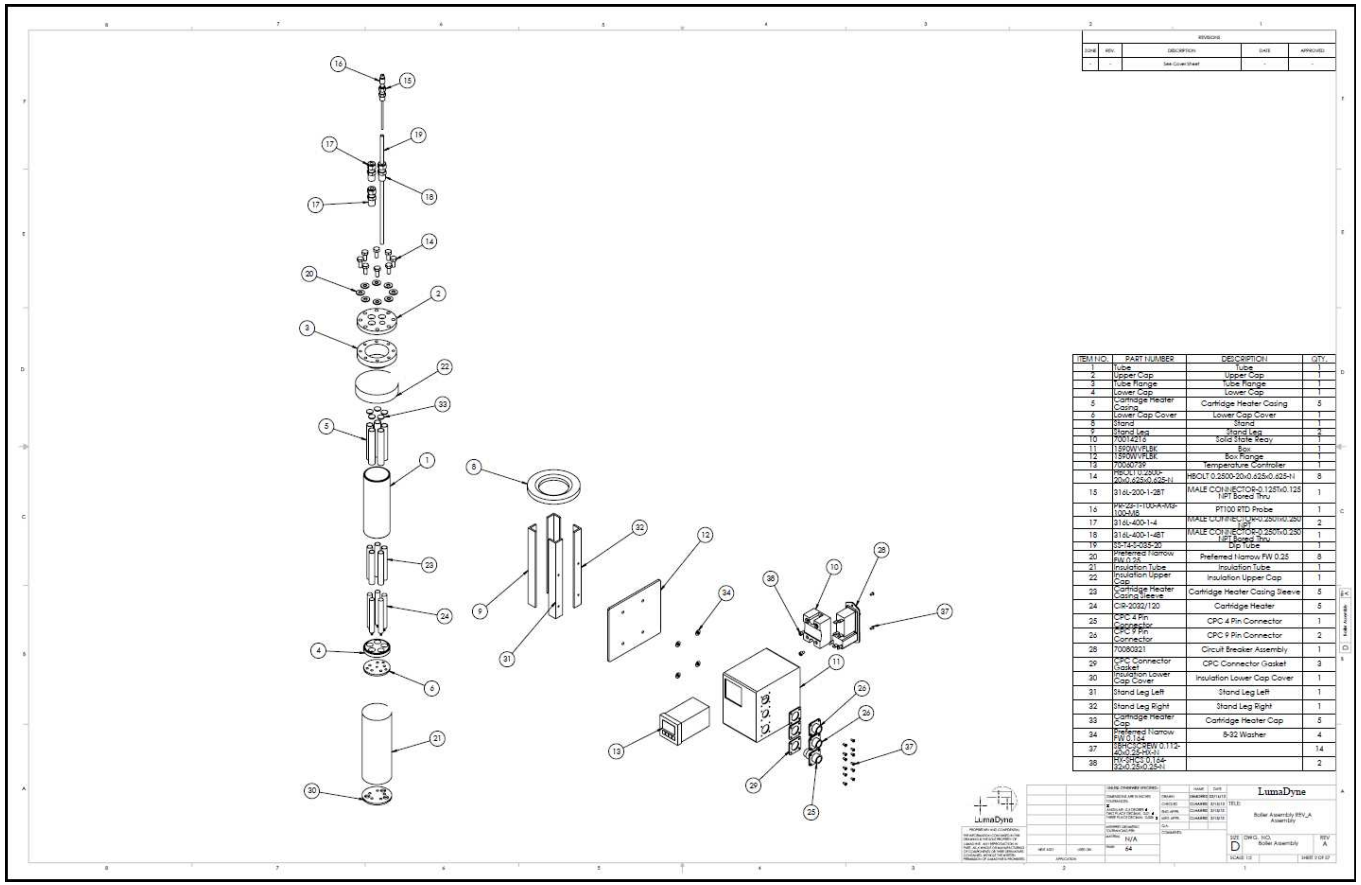

Figure 8.5 : An assembly view of the miniature steam generator

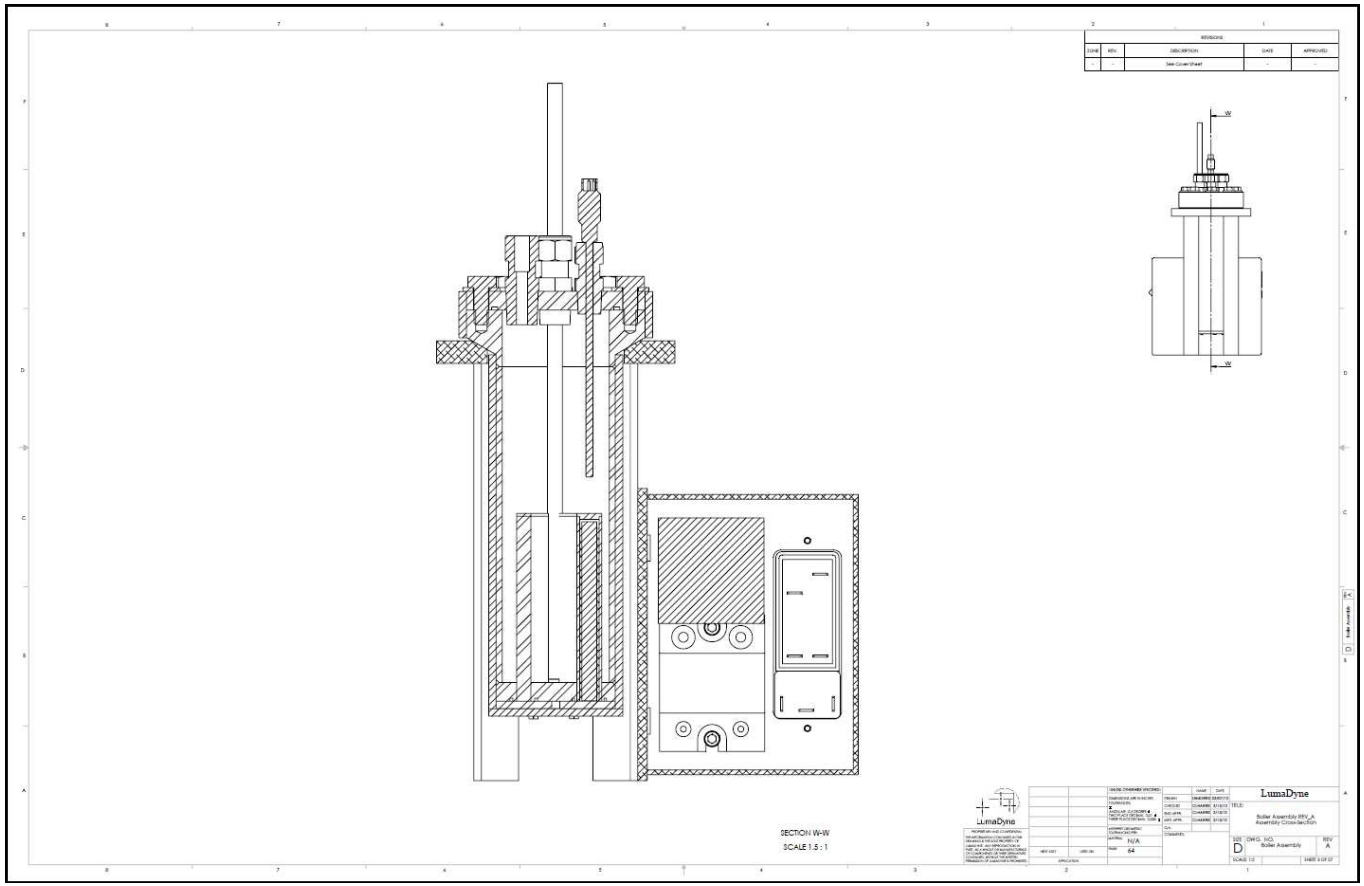

Figure 8.6 : An assembly cross-section view of the miniature steam generator

Conceptually, this setup is quite similar to that previously described in Chapter 7 and Figure 7.12. However, unlike the mass transfer setup which was operated at atmospheric pressure; the absorption chamber in the stainless steel prototype is pressurized between 0 and 20.7 kilopascals (kPa). This required making certain design changes to the setup, specifically to prevent the channeling of gas along with exiting absorbent. Whereas a liquid seal could be used in the experimental setup shown in Figure 7.12, application of a similar concept in the present case would result in the requirement of an improbably long liquid seal if water were used. To overcome this problem, a spent absorbent reservoir was added to the system as shown in Figure 8.7. The spent absorbent reservoir acts both as a reservoir for any spent absorbent leaving the absorption or stripping sides and prevents the escape of any gas. In order to maintain a set pressure in the absorption chamber, an adjustable back pressure regulator is installed downstream of the stainless steel prototype.

While in operation, a peristaltic pump draws the absorbent from a fresh absorbent reservoir and delivers it at the top of the stainless steel prototype where it is distributed on the ceramic foam surface. Simulated flue gas containing 13% carbon dioxide (CO_2) and 87 % nitrogen (N_2) is introduced at the required flow-rate by a mass flow controller. The decarbonized flue gas exiting the absorption chamber through the adjustable back pressure regulator is analyzed using a LI-COR carbon dioxide (CO_2) detector. Spent absorbent flowing across to the stripping chamber exits the prototype at the bottom of the stripping chamber.

When demonstrating simultaneous absorption and stripping operation, steam generated in the steam generator is introduced into the stripping chamber of the stainless steel prototype at the bottom. Hot water at a temperature in excess of 95°C produced in a metallic hot water reservoir is constantly delivered to the miniature steam generator using a second peristaltic pump. Absorbent along with steam condensate exits the chamber at the bottom where it accumulates in the solvent reservoir. Figure 8.8 shows the experimental setup developed for the proof-of-concept demonstration of the novel process with a combined absorber and stripper unit. As seen in this image, the external surface of the stripping side chamber is covered with a thermal insulation material made of alumina fiber material. The thermal insulation was purchased from McMaster-Carr and has a K-factor of 0.48 at 800 °F (Part # 87575K84). Metal fittings used for steam inlet and stripping side effluent were also wrapped in thermal insulation to prevent excessive heat loss. The hot water reservoir and peristaltic pump assembly used to operate the miniature steam generator on a continuous basis is also seen in this image.

8.2 Proof-of-concept demonstration

8.2.1 Choice of operating parameters

The objective of the proof-of-concept demonstration is threefold. The first of these is to demonstrate the feasibility of the proposed concept of achieving a lateral flow of the absorbent solution, from the absorption chamber to the stripping side. This

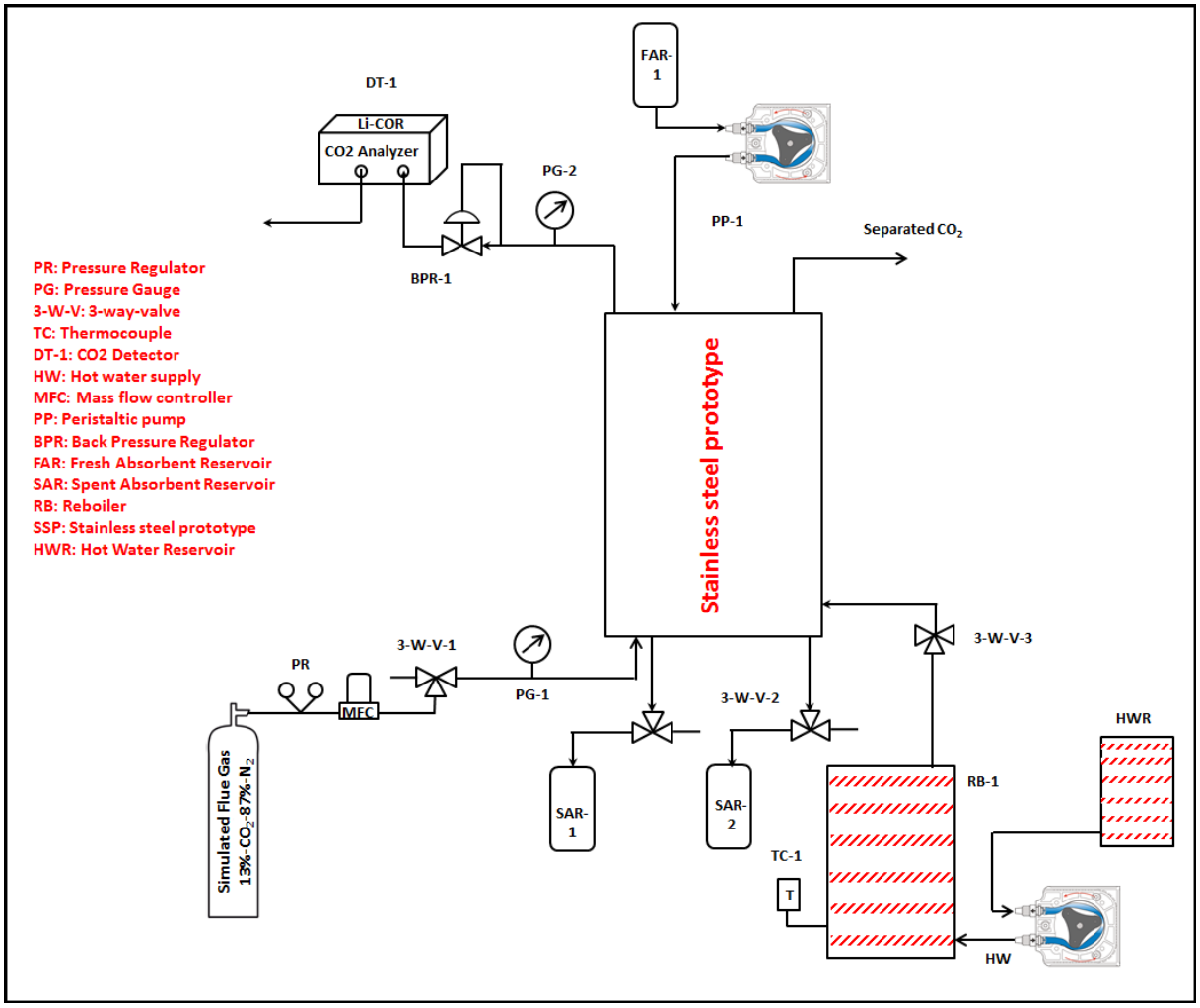

Figure 8.7 : Schematic representation of the experimental setup developed for the proof-of-concept demonstration

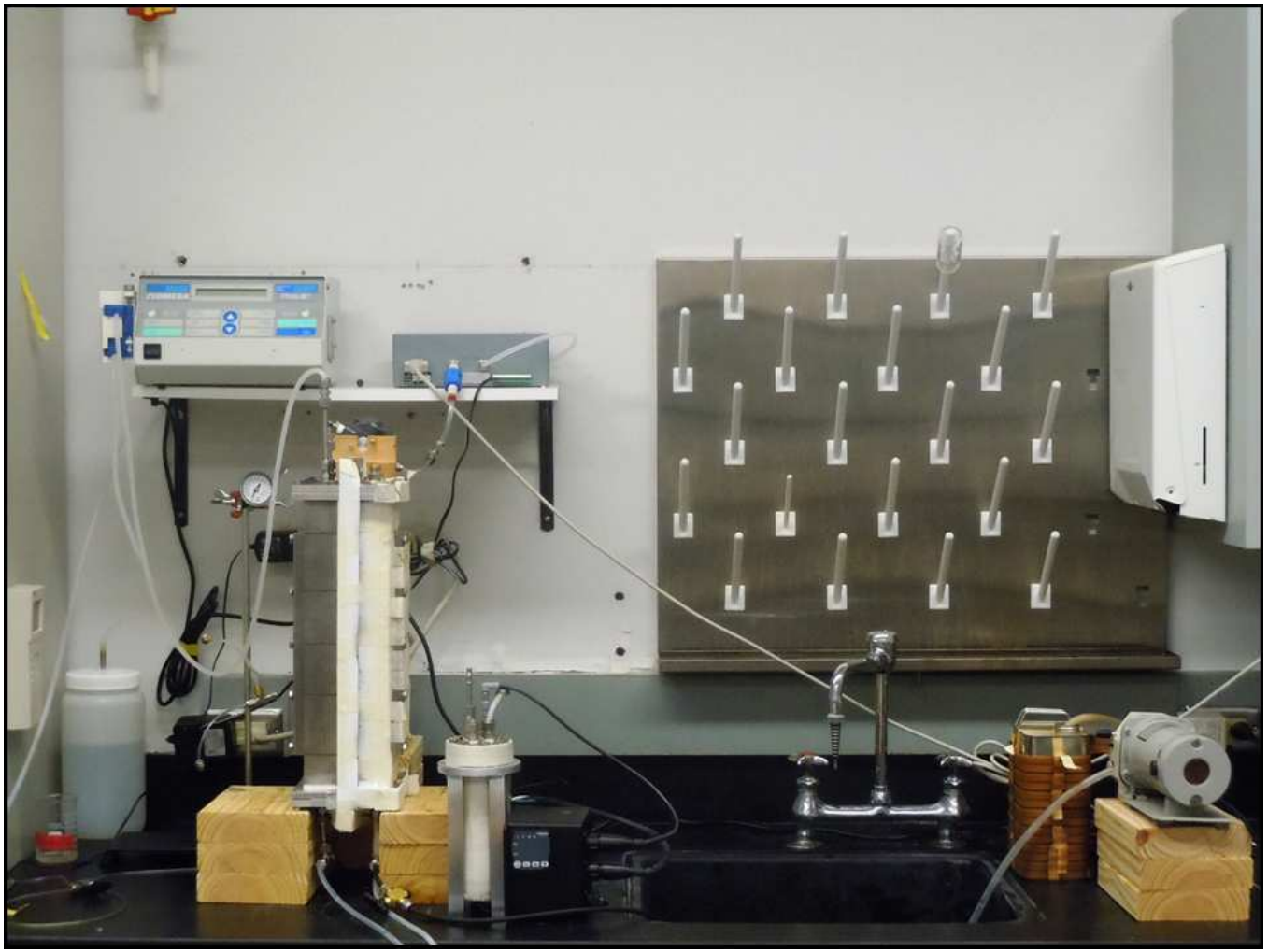

Figure 8.8 : Photograph of the experimental setup developed for the proof-of-concept demonstration

involves a complex operation of the prototype in which the simulated flue gas and lean absorbent enter the absorption chamber and steam enters the stripping side. A second goal is to operate the system at lower temperatures (without steam supply to the stripping chamber) but wider range of operating pressures and flow-rates to collect experimental data which can be used later to validate the results generated using a computer model developed for this process. Finally, this proof-of-concept demonstration provides the first opportunity to test the proposed concept for the novel carbon dioxide (CO_2) separation process and thus, is an opportunity to observe it for design and operational issues. As a part of the complete proof-of-concept demonstration, thus, we have operated the process with a pressure differential of 20.7 kilopascals (kPa) while injecting simulated flue gas at flow-rates of 0.25, 0.5 and 1.0 standard liters per minute (SLPM) and 30 wt% diglycolamine (DGA) at 0.01 liters per minute (LPM). Steam was introduced into the stripping chamber at a temperature of 102 °C and 109 kilopascals (kPa-absolute). When operating without steam, the differential pressures between the absorption and stripping chambers were varied between 6.9 and 20.7 kilopascals (kPa), simulated flue gas flow-rate was maintained at 0.25, 0.35, 0.5 and 1.0 standard liters per minute (SLPM) and the absorbent flow-rates studied were 0.01, 0.02 and 0.03 liters per minute (LPM).

8.2.2 Experimental procedure

The objectives of the proof-of-concept demonstration experiments have been clearly described in §§8.2.1. Since this stainless steel prototype was the first opportunity to test the concept of an integrated absorber and stripper, establishing experimental protocol was considered critical to collecting reliable experimental data. When operating the stainless steel prototype without steam, the absorption chamber was first purged with nitrogen. When the measured carbon dioxide (CO_2) concentration of the exiting gas reduced to very low levels (e.g. 50 ppm); simulated flue gas was introduced into the chamber. Simultaneously, the back pressure regulator installed downstream of the stainless steel prototype was adjusted to achieve the required pressure in the absorption chamber. This pressure was monitored with a pressure gauge connected to the back pressure regulator. The gauge pressure is also the pressure differential across the absorption and stripping chambers since the stripping side is maintained at atmospheric pressure. Once, the absorption chamber was pressurized, 30 wt% diglycolamine (DGA) was flowed into the absorption chamber.

It was observed that when the system operation was started from a dry condition (meaning the ceramic foam, fiber glass wool packing and alumina membrane were completely dry), all the absorbent flowed across laterally into the stripping chamber even at the lowest pressure difference tested (6.9 kilopascals (kPa)). However, when the effluent flow-rate from the stripping chamber was measured; it was found to be lower than the input rate. The lateral flow can be attributed to the existence of a large

pressure gradient between the absorption and stripping chambers which promotes the flow of liquid. The difference between the input and outlet flow-rates, suggested the accumulation of the absorbent liquid in the prototype. This can be attributed to an increase in the liquid saturation of the ceramic foam, the alumina membrane and the fiber glass wool. Collection of experimental data during this transient phase would lead to faulty interpretation of system behavior and was carefully avoided. After allowing the absorbent flow to continue in excess of 60 minutes, collection of experimental data was commenced. The parameters measured were the degree of carbon dioxide (CO_2) removed in the absorption column and the lateral throughput of liquid absorbent. Since the measurement of absorption side liquid effluent would result in a disruption of the system operation, stripping side liquid effluent was measured and a mass balance performed to determine the lateral flow-rate. Corresponding to each operating condition (i.e. gas and liquid flow-rate and pressure difference), at least three readings were made for the absorbent mass balance. Once these were found to be repeatable, the experimental data was noted. In Figures 8.11 and 8.12, the points corresponding to no data represent the cases under which no measurements were made because the lateral transport of the absorbent solution was significantly smaller than the inflow-rate. Specific precautions were taken to avoid absorbent accumulation in the absorption chamber by draining the any accumulated solution periodically.

Operating the stainless steel prototype with steam was conceptually similar but practically significantly more complicated due to the introduction of steam into the

stripping chamber. When operating with steam, the electrical heating tape on the metallic hot water reservoir was switched on before commencing the flow experiments. The heat rate was set to raise the water temperature to around 100 °C. Once this set temperature was reached, the miniature steam generator was switched on. The boiler vessel in the steam generator has a volume of 0.2 liters. This was loaded with approximately 0.2 liters of hot water to expedite steam generation. Once a steady flow of steam was observed coming out of the steam generator, the peristaltic pump supplying hot water to the steam generator was turned on and set to flow at 0.01 liters per minute (LPM).

Simultaneously, simulated gas flow was turned on and the absorption side chamber was pressurized. Once the chamber was pressurized, absorbent flow was initiated. After allowing the flow to reach steady state, steam was introduced into the stripping chamber. Simultaneously, temperature readings were made at the 10 equispaced nodes located on the side-faces of the stainless steel prototype. Measuring these temperatures using a conventional thermometer (e.g. thermocouple thermometer) is impractical due to the significant time lag involved in attaining a steady reading. Hence, a hand-held infrared thermometer purchased from McMaster-Carr was used for making the temperature measurements. The thermometer has a response time of around 1 second, a resolution of 0.1 °F and an accuracy of ± 1.8 °F. Temperature measurements were made every 10 minutes till the temperatures reached a steady state. It was observed that the heat losses, especially through the stripping side

of the stainless steel prototype were quite significant despite the use of thermal insulation. This resulted in steam condensation occurring in the stripping chamber. During constant operation, this steam condensate was periodically drained from the stripping chamber by opening a 3-way valve installed on the liquid outlet port. Since both the steam condensate and the laterally transported absorbent solution exit the stainless steel prototype through the same outlet port, a direct measurement of the lateral flow-rate is not possible. An indirect approach was developed to detect the presence of diglycolamine (DGA) in the stripping chamber effluent. Several samples of the stripping chamber effluent were collected in glass vials. A known quantity of the effluent was then titrated with 0.1 Normal (N) hydrochloric acid (HCl) using phenolphthalein as an indicator. Diglycolamine (DGA) is a base and reacts with hydrochloric acid (HCl) to form its chloride salt. Thus, the lateral flow of absorbent liquid can be confirmed by using the indirect acid-base titration technique. In the subsequent section, we present the results of the proof-of-concept demonstration experiments. Also presented are the results of the acid-base titration conducted to detect the presence of diglycolamine (DGA) in the stripping side effluent.

8.2.3 Experimental results and analysis

Figure 8.9 shows a plot of the degree of carbon dioxide (CO_2) removal taking place in the absorption chamber of the stainless steel prototype when operating without steam at a temperature of 23 ^{o}C and a liquid flow-rate 0.01 liters per minute (LPM). As

expected, the extent of carbon dioxide (CO_2) removal taking place decreases gradually as the gas flow-rate is increased. However, it appears that the degree of carbon dioxide (CO_2) removal has some dependence on the pressure differential maintained across the absorption and stripping sides. It can be observed that the degree of carbon dioxide (CO_2) removed decreases as the pressure differential is increased. This can likely be attributed to the dependence of the lateral flow of absorbent on the pressure differential. As shown in Figure 8.10, the maximum lateral flow of absorbent solution at a pressure difference of 6.9 kilopascals (kPa) is around 0.006 liters per minute (LPM). This would result in the excess absorbent flowing down on the entirety of the absorption side ceramic foam and exiting the chamber at the bottom. For the 13.8 and 20.7 kilopascals (kPa) cases, the maximum lateral flow-rates are both greater than 0.01 liters per minute (LPM) resulting in all of the absorbent flowing across to the stripping side. The dependence of lateral throughput on pressure drop is observed to be linear except when the pressure differential was maintained at 20.7 kilopascals (kPa). The linear behavior is consistent with Darcy's law (Equation 8.1) which states that for a fluid of constant permeability (k) and viscosity (μ); fluid flux ($\frac{Q}{A}$) is dependent only on the pressure gradient ($\frac{P}{L}$). At 20.7 kilopascals (kPa), however, it is possible that the absorbent solution flowing laterally to the stripping side did not wet the entire length of the absorption side resulting in the observed trend. As seen in Figure 8.10, however, the experimentally measured flow-rates are at least one order of magnitude lower than the calculated maximum flow-rate across

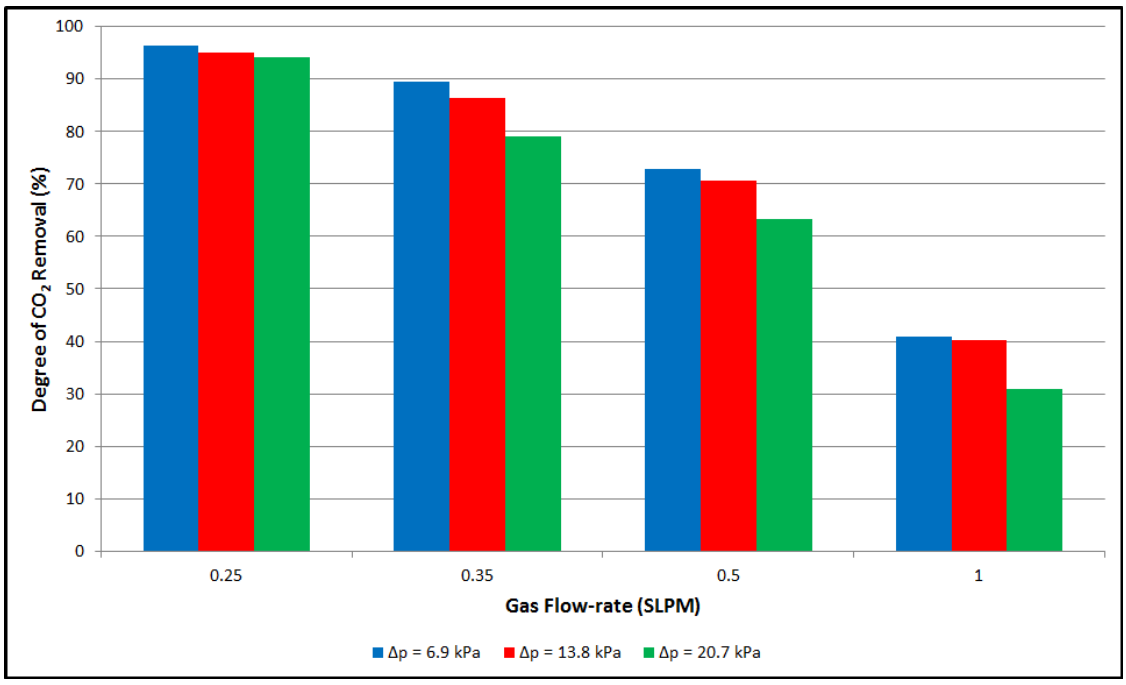

Figure 8.9 : Degree of CO_2 removal at variable gas flow-rates and absorbent flow-rate of 0.01 liters per minute (LPM)

the polyethersulfone (PES) and porous alumina membrane. This can be explained on the basis of the flow resistance offered by the microporous matrix of the ceramic foam. While the polyethersulfone (PES) and the porous alumina membranes have very high liquid permeability, the microporous ceramic matrix offers a much higher flow resistance and acts as the rate-limiting process.

$$\left(\frac{Q}{A}\right) = -\frac{k}{\mu} \cdot \left(\frac{P_a - P_b}{L}\right) \tag{8.1}$$

The difference between the extents of carbon dioxide (CO_2) removal corresponding to pressure differentials of 6.9, 13.8 and 20.7 kilopascals (kPa) at an absorbent flow-rate of 0.01 liters per minute (LPM) can be attributed to variations in the lateral

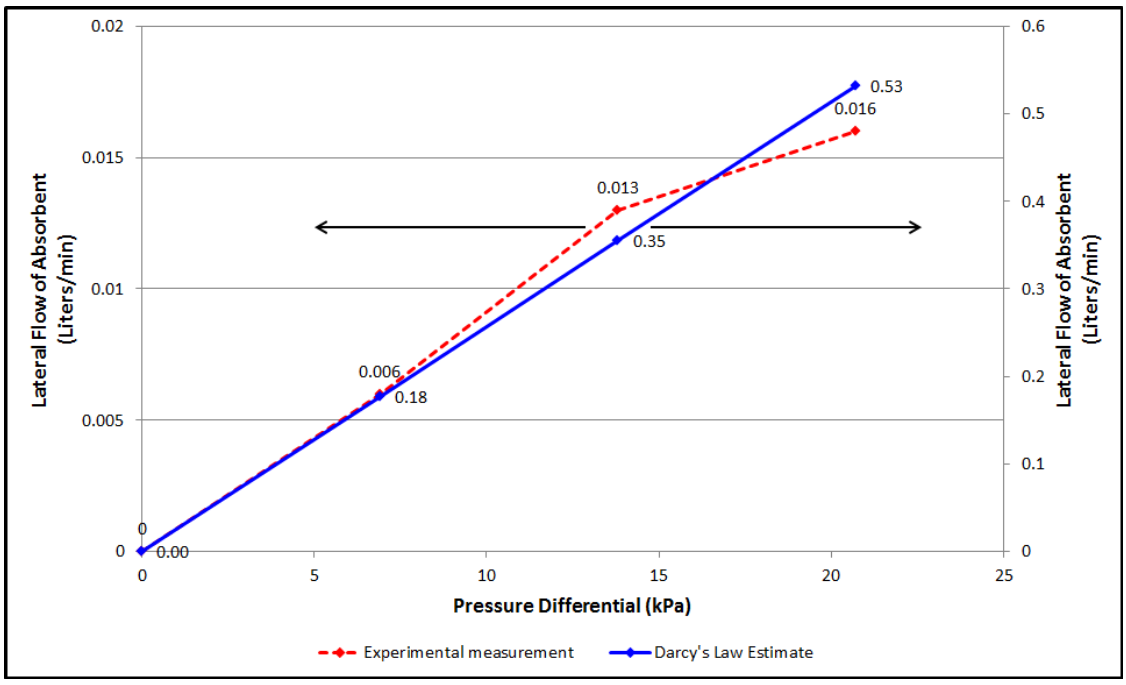

Figure 8.10 : Dependence of maximum lateral flow-rate of absorbent on pressure difference across absorption and stripping chambers

transport of the absorbent. At lower pressure differentials, the absorbent flows down a greater length of the ceramic foam before either draining at the bottom or completely flowing across to the stripping side. At higher pressure differentials, the liquid flows across laterally without wetting the entire ceramic foam surface which results in decreased carbon dioxide (CO_2) pickup. Figure 8.11 shows the extent of carbon dioxide (CO_2) removal for the two cases of 13.8 and 20.7 kilopascals (kPa) when operating at an absorbent flow-rate of 0.02 liters per minute (LPM). No experiment was conducted corresponding to a pressure differential of 6.9 kilopascals (kPa) case since the absorbent flow-rate significantly exceeded the maximum lateral flow achieved at that pressure. The trend observed for the dependence of carbon dioxide (CO_2)

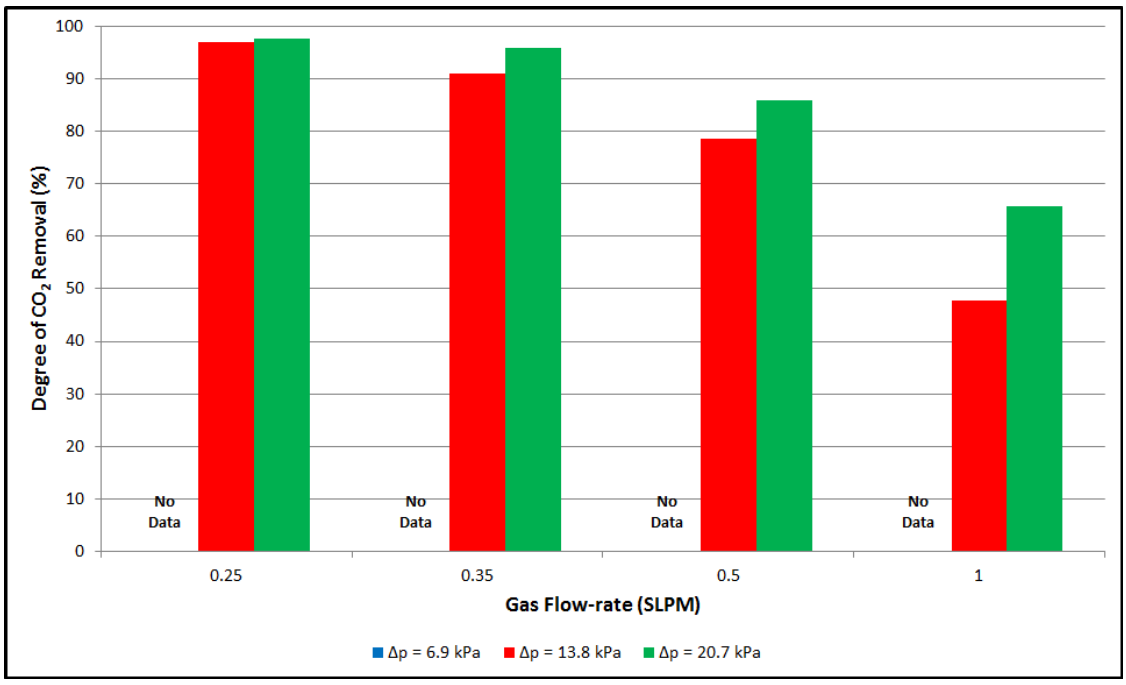

Figure 8.11 : Degree of CO_2 removal at variable gas flow-rates and absorbent flow-rate of 0.02 liters per minute (LPM)

removal on pressure difference in this plot is different from that in Figure 8.9. At an absorbent flow-rate of 0.02 liters per minute (LPM), excess absorbent flows down the entire length of the ceramic foam in both cases.

Figure 8.12 shows the degree of carbon dioxide (CO_2) removal at an absorbent flow-rate of 0.03 liters per minute (LPM) and a pressure differential of 20.7 kilopascals (kPa). Better carbon dioxide (CO_2) removal is observed in this case as compared to the previous two cases involving lower flow-rates. Based on these results, it can be concluded that it is possible to achieve more than 90% removal of inlet carbon dioxide (CO_2) in the combined absorption/desorption process while achieving lateral flow absorbent.

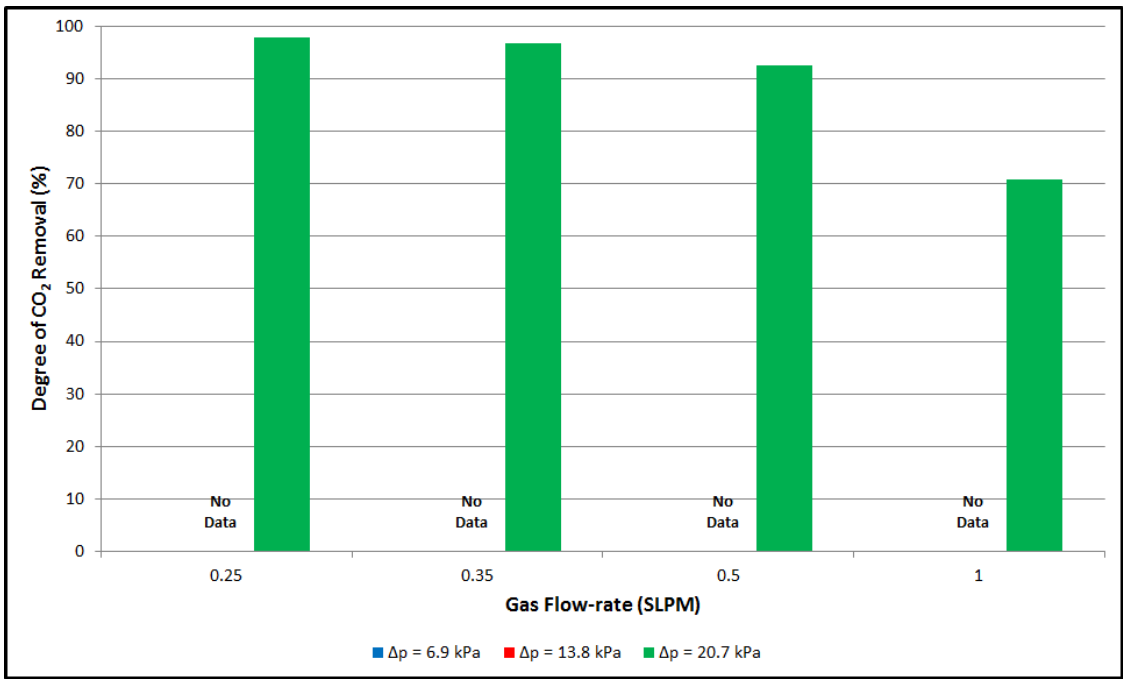

Figure 8.12 : Degree of CO_2 removal at variable gas flow-rates and absorbent flow-rate of 0.03 liters per minute (LPM)

Figure 8.13 shows a comparison of the degree of carbon dioxide (CO_2 removal taking place in the absorption chamber of the stainless steel prototype when operating without and with steam flowing into the stripping chamber. The simulated gas flow-rates maintained were 0.25, 0.5 and 1.0 standard liters per minute (SLPM), the absorbent flow-rate was 0.01 liters per minute (LPM) and the pressure differential between the absorption and stripping chambers was 20.7 kilopascals (kPa). During the experiment, it was observed that there was a constant flow of liquid exiting the absorption chamber. This observation is in contrast to the results of our previous experimental studies conducted without steam (see Figure 8.10). This significant reduction in lateral transport of absorbent solution can be attributed to the changes

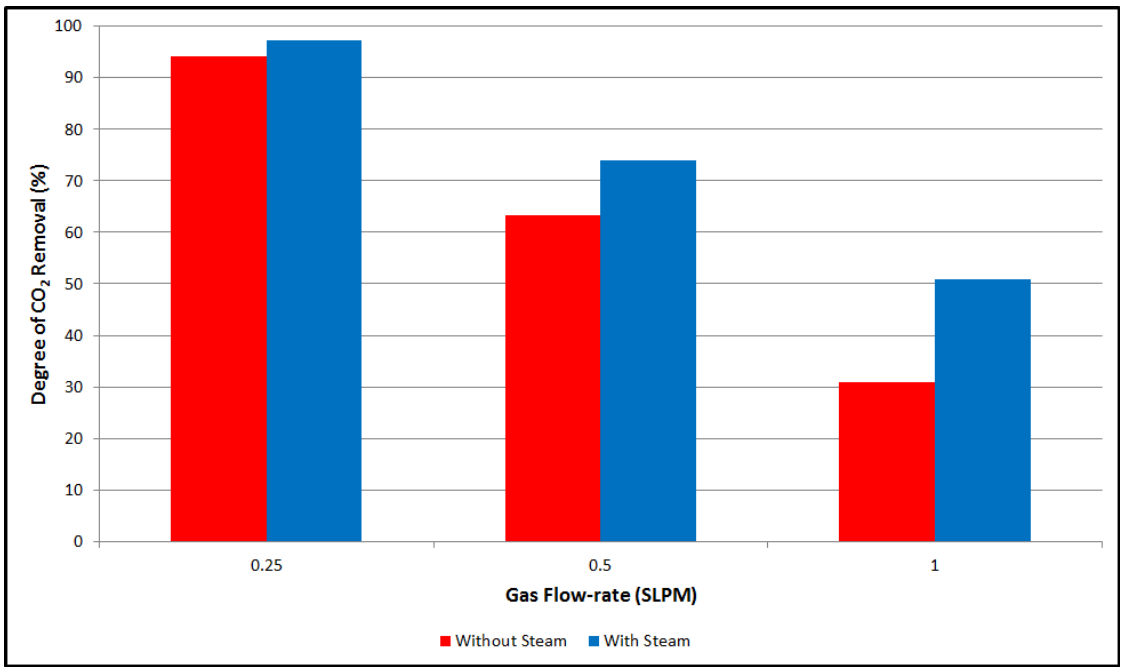

Figure 8.13 : Degree of CO_2 removal at variable gas flow-rates, absorbent flow-rate of 0.01 liters per minute (LPM) and pressure differential (Δ P) of 20.7 kPa - with and without steam

in its physical properties such as viscosity. Steam entering the stripping chamber increases the temperature in the absorption chamber which results in a reduction of the solution viscosity. This promotes the downwards flow of the absorbent solution by gravity drainage. The trend observed in the dependence of carbon dioxide (CO_2 removal is similar to those observed previously in Figures 8.9 - 8.12.

To verify the lateral flow of liquid from the absorption to stripping side, acid-base titrations were performed. The results of these are summarized in Table 8.3. The significant variance in the titration volumes can be attributed to the ejection of the stripping chamber effluent in spurts as the entering steam escapes along with the

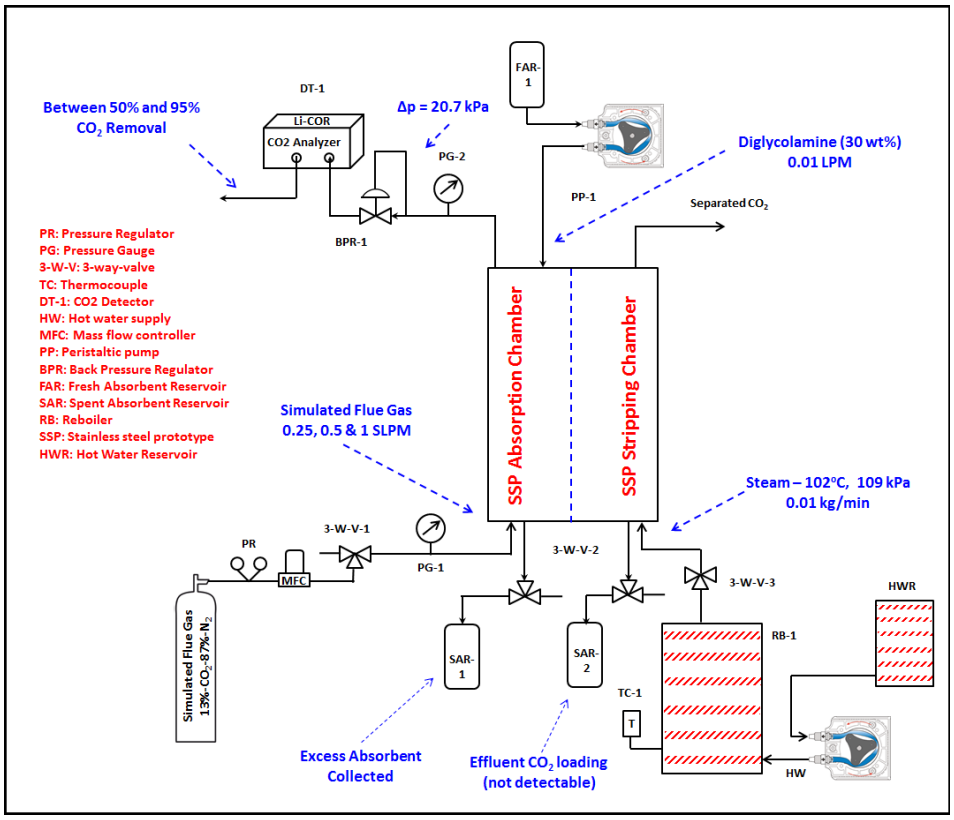

Figure 8.14 : A schematic representation of the experimental setup used for the proof-of-concept demonstration - with experimental measurements and observations

liquid. These results clearly show the presence of a base in the stripping chamber effluent. Since the steam condensate itself is 'distilled water' and because no other basic compound is injected into the stainless steel system, the source of this basicity was concluded to be diglycolamine (DGA) flowing across from the absorption chamber. Figure 8.14 shows a schematic representation of the experimental setup with the various measurements and observations made during the proof-of-concept demonstration with steam.

Figure 8.15 and Figure 8.16 show the temperatures measured on the external

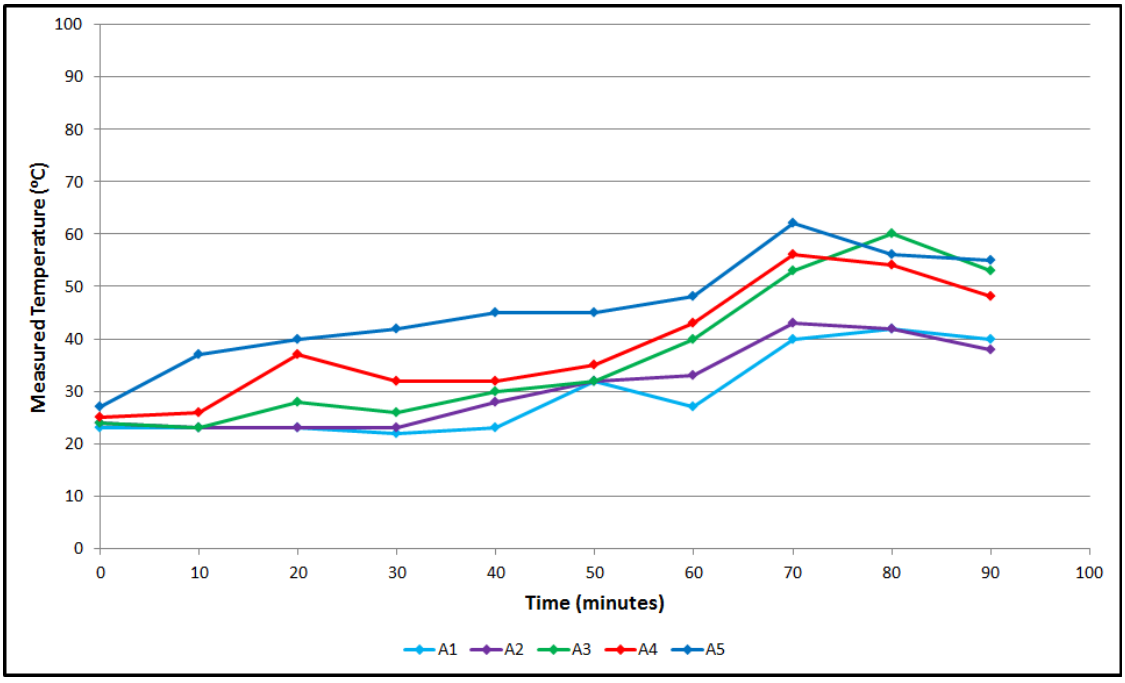

Figure 8.15 : Temporal dependence of absorption side external surface temperatures

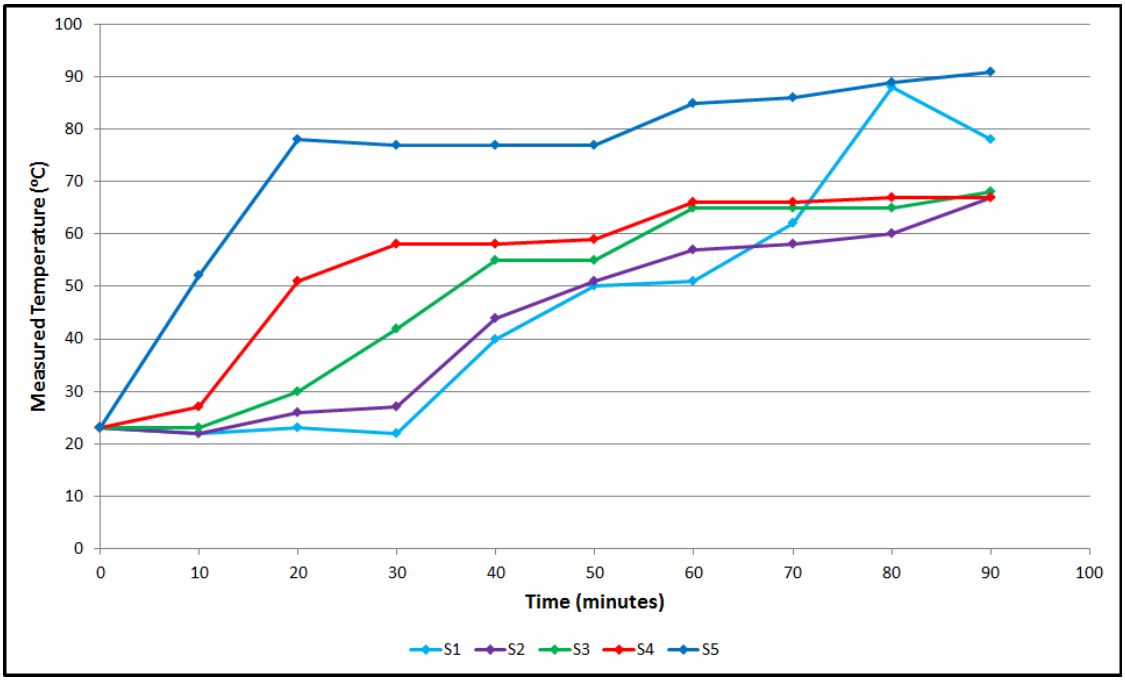

Figure 8.16 : Temporal dependence of stripping side external surface temperatures

Table 8.3 : Diglycolamine (DGA) concentration in stripping chamber effluent

Effluent Case #	Effluent Volume	Acid Concentration	Acid Volume	Base concentration in Effluent (N)
0.5 SLPM #1	10	0.1	11.4	0.114
0.5 SLPM #2	10	0.1	17.2	0.172
1.0 SLPM #1	10	0.1	10.1	0.101
1.0 SLPM #2	10	0.1	9.7	0.097

surfaces on the absorption and stripping sides of the stainless steel prototype. In these figures, the lower number represents nodes at the top of the stainless steel prototype whereas the higher number represents a node at the bottom. Addition of the steam clearly resulted in a heating of the stripping chamber. However, it also resulted in a significant increase in the absorption side temperature; a factor that could influence both the lateral flow of absorbent solution as well as the degree of carbon dioxide (CO_2) removal.

8.3 Concluding Remarks

Based on the experimental results and observations presented in §§8.2.2, we can conclude the following:

1. The concept of a performing carbon dioxide (CO_2) absorption and stripping in a single integrated unit is feasible. The experimental results shown in §§8.2.2 demonstrate that in excess of 90% carbon dioxide (CO_2) removal can be achieved using the combined absorber/stripper configuration.

2. As a material itself, ceramic foam can be used as a gas-liquid contactor in the combined absorption and stripping unit. Significant property optimization is however be required to improve hydrodynamic and mass transfer properties of ceramic foam. Specifically, the use of coarser grade ceramic foam with larger macro-pores may help in both, improving its hydrodynamic as well as mass transfer properties.

3. The present configuration of the combined absorption and stripping process is sufficient for a proof-of-concept demonstration. Optimization efforts are required next, to improve process design and operation.

Chapter 9

Recommendations for future work

The research results presented as a part of this thesis have provided answers to several previously unanswered questions. With the use of process simulation and economic evaluation softwares, we have demonstrated the feasibility of using vacuum stripping accompanied with the use of 'waste heat' for absorbent regeneration. Our simulation work has resulted in the invention of novel absorbent blends for the removal of carbon dioxide (CO_2). Using the limited thermodynamic data available, we have demonstrated the potential for these absorbent blends to reduce energy consumption by almost 25%. Similarly, we have advanced the innovative concept of a carbon dioxide (CO_2) separation process with a combined absorber and stripper to a proof-of-concept stage. The interesting nature of these results has raised further questions that must be answered in order to generate sufficient commercial interest. In this chapter, we summarize these as the recommendations for future work.

9.1 Calibrating the economic feasibility of using waste heat with coal-fired power plant operational data

In Chapters 4 and 5, we have focused on determining the technical and economic feasibility of using waste heat for absorbent regeneration. We have identified that using waste heat is a technically feasible proposition. In the absence of actual power plant data and waste heat availability details, different hypothetical scenarios were assumed to evaluate the parasitic power losses. While this has certainly helped in establishing the benefits of using vacuum strippers in conjunction with waste heat, these results are a step away from being of direct commercial use due to the lack of calibration with actual plant data. Thus, the logical next step in the research process is to collaborate with a power generation utility such as the Lower Colorado River Authority (LCRA) which operates the coal-fired Fayette Power Project located near La Grange, TX. A coal-fired power plant is a complex utility facility typically operated with tight resource optimization. Information about the plant's operation and resource availability will make it feasible to conduct a more accurate evaluation of the operational costs for the amine absorption process.

9.2 Development of novel absorbents

In Chapter 6, we have discussed our research on dissecting the reboiler energy duty into the contributions of the three constituent physiochemical processes taking place in the stripper/reboiler. This research has led to the invention of what we believe is

a new class of absorbents for the removal of carbon dioxide (CO_2). We hypothesized in Chapter 6 that the partial or complete replacement of water with an alternate solvent such as an alcohol could potentially result in a large reduction in the reboiler duty. Using the limited publicly available thermodynamic data describing the behavior of alkanolamine systems after the addition of alcohols, we have been able to demonstrate almost 23% reduction in the reboiler duty for for a system consisting of diethanolamine, methanol and water. While these certainly constitute as breakthrough results, much remains to be studied about this invention.

9.3 Generating thermodynamic data and modeling

As discussed in Chapter 6, there is a very limited thermodynamic data available in published literature to describe the behavior of carbon dioxide (CO_2) loaded alkanolamine solutions blended with alcohols. The only system explored in some detail is aqueous diethanolamine (DEA) mixed with methanol. However, as described in Chapter 6; the physiochemical properties of other alcohols - especially the specific heat capacity and heat of vaporization is as favorable towards reducing the reboiler energy duty as that of methanol. Additionally, based on our results; it maybe expected that increasing the methanol content of the diethanolamine (DEA) blend from 20 wt% will result in further lowering of reboiler duty. Clearly, the bottleneck factor toward advancing this research is the availability of sufficient, high quality thermodynamic data describing the vapor-liquid equilibrium and mixing behavior. Thus,

it is strongly recommended that the necessary thermodynamic data be obtained by conducting suitable experiments. At a minimum, the behavior of commonly used alkanolamine such as monoethanolamine (MEA), diethanolamine (DEA) and diglycolamine (DGA) mixed with alcohols such as methanol, ethanol and propanol(s) in various proportions be explored.

The thermodynamic data measured thus can be fitted to a suitable thermodynamic model such as the Electrolyte NRTL. The temperature dependent parameters can be used with a commercial process simulator such as ProMax or AspenPlus to simulate a closed loop amine absorption plant. Using process simulators to screen the performance of novel absorbent blends has a significant benefit - it allows for a complete estimation of the influence of alcohol addition to aqueous alkanolamines. Both methanol and ethanol are significantly more volatile than water. This suggests a significant escape of these alcohols along with the overhead vapors in both the absorber and stripper columns. The use of auxiliary equipment such as water wash stages in absorbers is a commonly used strategy to avoid excessive solvent loss. However, it maybe expected that a more significant operation will be required with the use of alcohol blended aqueous alkanolamines. On the stripper side, presence of significant quantities of alcohol in the overhead vapors may require the operation of the overhead partial condenser at a lower temperature than in case of conventional absorbents. Additional separation maybe required downstream to reduce the alcohol content of compressed carbon dioxide (CO_2) to acceptable levels. Since the addition

of alcohols to aqueous alkanolamines appears to result in significant change in process operation, it is important from a commercialization viewpoint to carefully analyze not just the beneficial elements but also potential increases in the capital and operational expenditure.

9.4 Exploring the potential for side reactions between alcohols and amines

A problem that the natural gas industry has worked on for a long time is equipment corrosion with the use of aqueous alkanolamines [104, 9]. Another problem commonly observed with the use of aqueous alkanolamines is the oxidative degradation of amines. Amines are known to react with oxygen (O_2) dissolved in the absorbent solution and undergo several side reactions. Diethanolamine (DEA), for example, is known to form tris(hydroxyethyl)ethylenediamine (THEED) in the presence of carbon dioxide (CO_2), oxygen (O_2) and sulfur dioxide (SO_2) in the liquid absorbent. Other commonly used amines are known to form complex ethylenediamine derivatives as well. However, amine degradation chemistry is not as straightforward as just the formation of these salts. Studies have shown that ethylenediamines are generated by the reactions taking place between a series of intermediate compounds formed because of amine degradation. Table 9.1 lists some of the more common degradation products formed during amine degradation [105, 106].

Table 9.1 : Amine degradation products

Absorbent	**Reactant**	**Reaction Products**
All amines	O_2	Carboxylic acids
		Imidazolidone
		Oxazolidone (OZD)
Monoethanolamine (MEA)	CO_2	Hydroxyethyl Imidazolidone (HEI)
		Hydroxyethyl Ethylenediamine (HEED)
Diglycolamine (DGA)	CO_2	bis-Hydroxyethyl-ethoxy Urea (BHEEU)
		Hydroxyethyl Oxazolidone (HEOD)
Diethanolamine (DEA)	CO_2	bis-Hydroxyethyl Piperazine (BHEP)
		tris-Hydroxyethyl Ethylenediamine (THEED)

Most of these compounds are formed only in small quantities after extended process operation. Alcohols, however, are chemically active solvents and can react with most of these degradation products to further form compounds such as amides, esters amongst others. For this reason, it is of great importance to study the effects of alcohol addition on the stability of aqueous alkanolamines and the rate of equipment corrosion.

9.5 Modeling of combined absorber stripper system

In Chapters 7 and 8, we have discussed our idea of a novel process for the separation of carbon dioxide (CO_2) which involves combining of the absorber and stripper columns into a single integrated unit. We have discussed our research efforts to identify suitable materials for use in this process, their characterization and finally - developed a bench-scale stainless steel prototype to demonstrate the proof-of-concept. As shown in Chapter 8, the bench-scale prototype was developed using off-the-shelf materials. This resulted in a system that was suitable for a proof-of-concept demonstration, however, will have to be significantly optimized to compete with existing technology. In order to optimize the process, it is important to first model it. Modeling the system will aid in determining the relationship between different material properties, process variables and design parameters. As an example, it was concluded in Chapter 7 that the commercial ceramic foam would have to be optimized to allow larger macropore sizes which would permit better gas-liquid mass transfer and lower pressure

drops. Similarly, the lateral flow of liquid through the ceramic foam matrix is strongly dependent on its material properties - specifically, the permeability. Modeling tools such as COMSOL Multiphysics or ANSYS Fluent can be used to model the fluid flow in this complex porous media. The results generated thus can be used to predict the optimal parameters for a scaled-up system.

To summarize, we believe that the research performed as a part of this dissertation holds significant promise in reducing the economic penalties associated with the removal of carbon dioxide (CO_2) from power generation utilities. Much work, of course, remains to be performed to move these developments forward out of a laboratory environment to commercialization. However, with dedicated research efforts; further refinement of these technologies is possible.

Appendix A

Design sheets for stainless steel prototype and miniature boiler

This appendix contains the design drawings for the stainless steel prototype and the miniature steam generator as provided by LumaDyne, LLC.

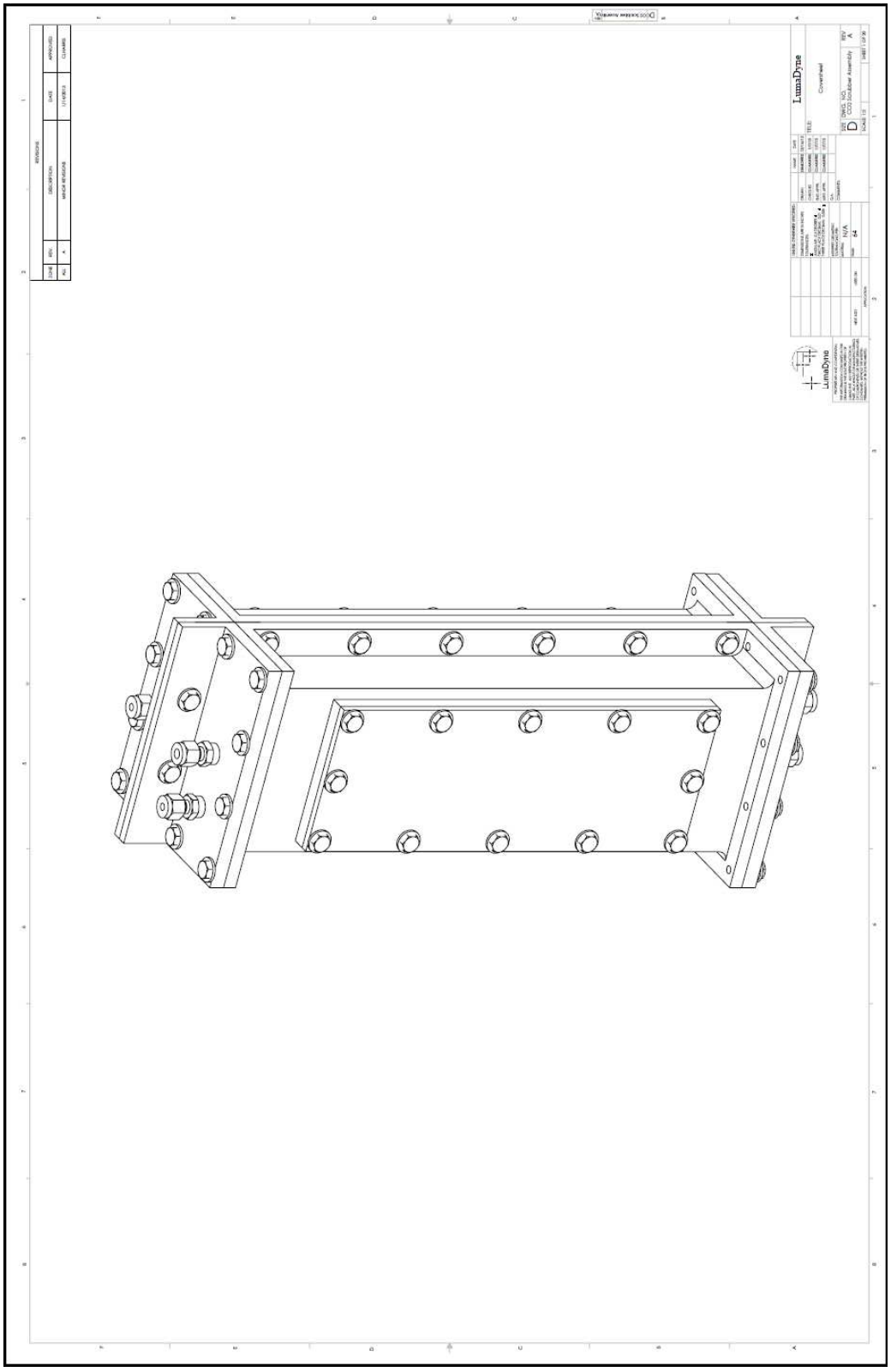
LumaDyne
Coverwheel
CCD Scribbler Assembly
D
CCD Scribbler Assembly
LumaDyne

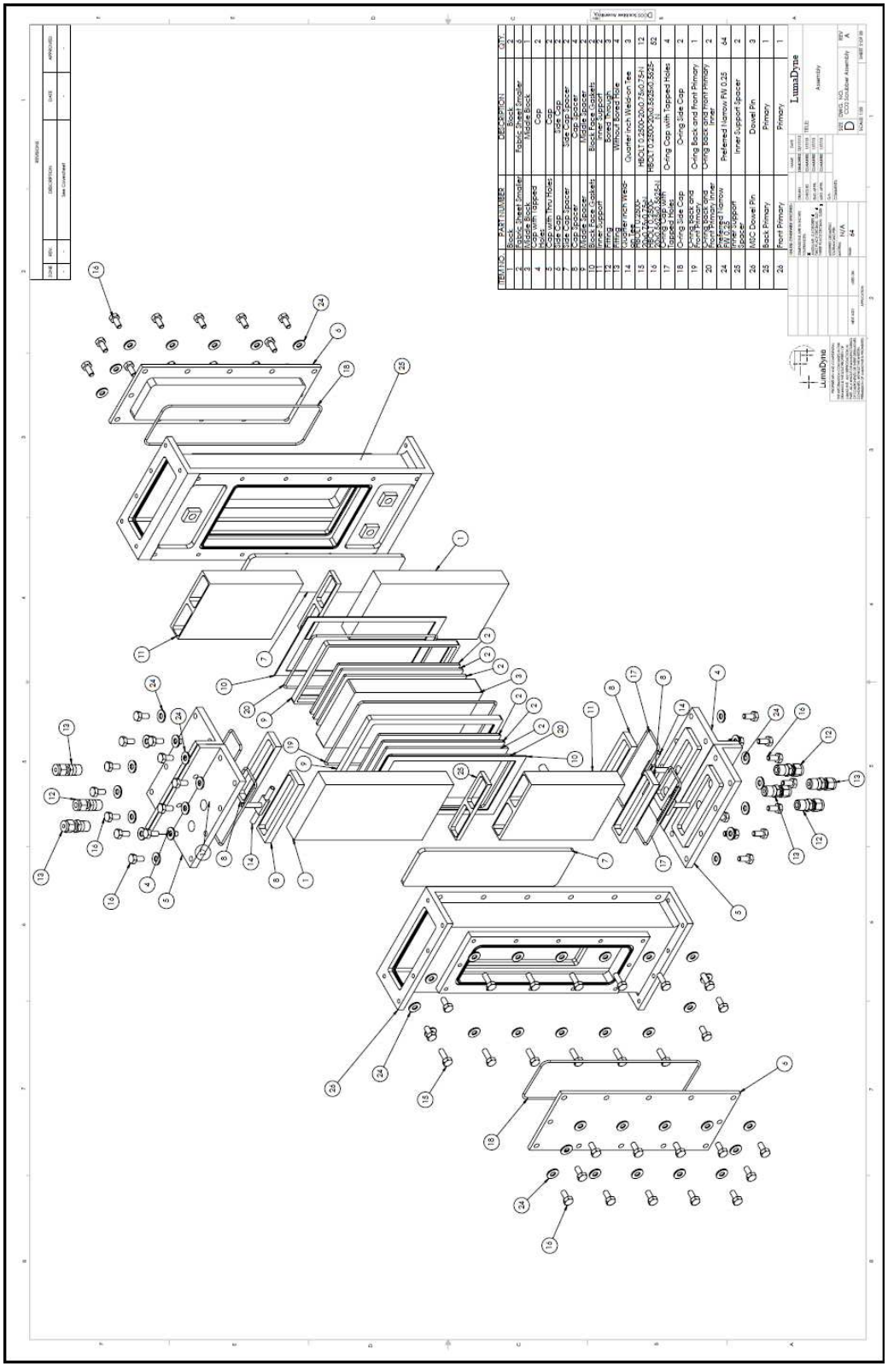
ITEM NO.
PART NUMBER
DESCRIPTION
QTY
LumaDyne
Assembly
CCD Scrubber Assembly
SIZE
DWG. NO.
REV
A
D
SHEET 1 OF 1

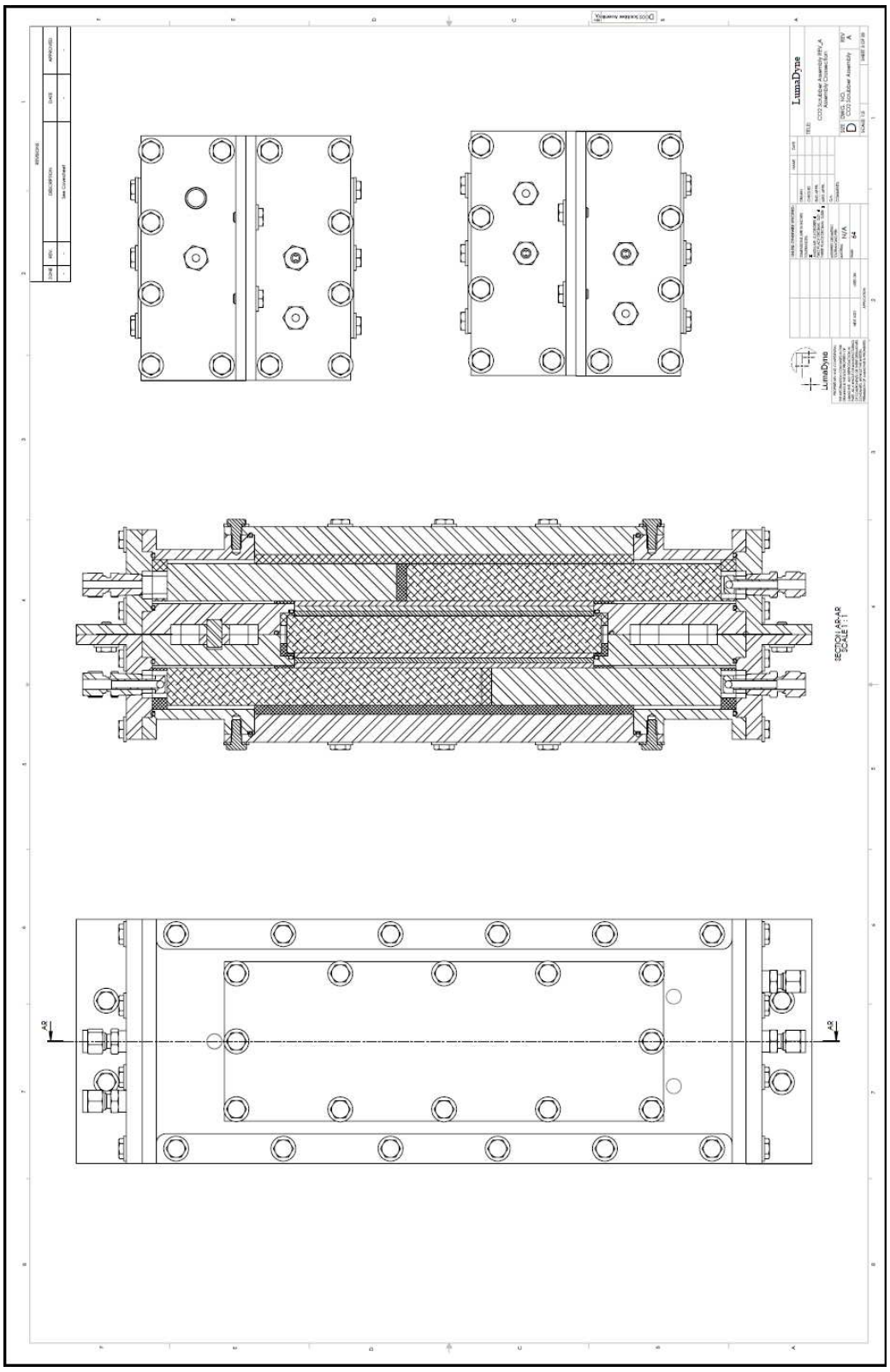
LumaDyne
SECTION A-A
SCALE 1:1
A2
A2

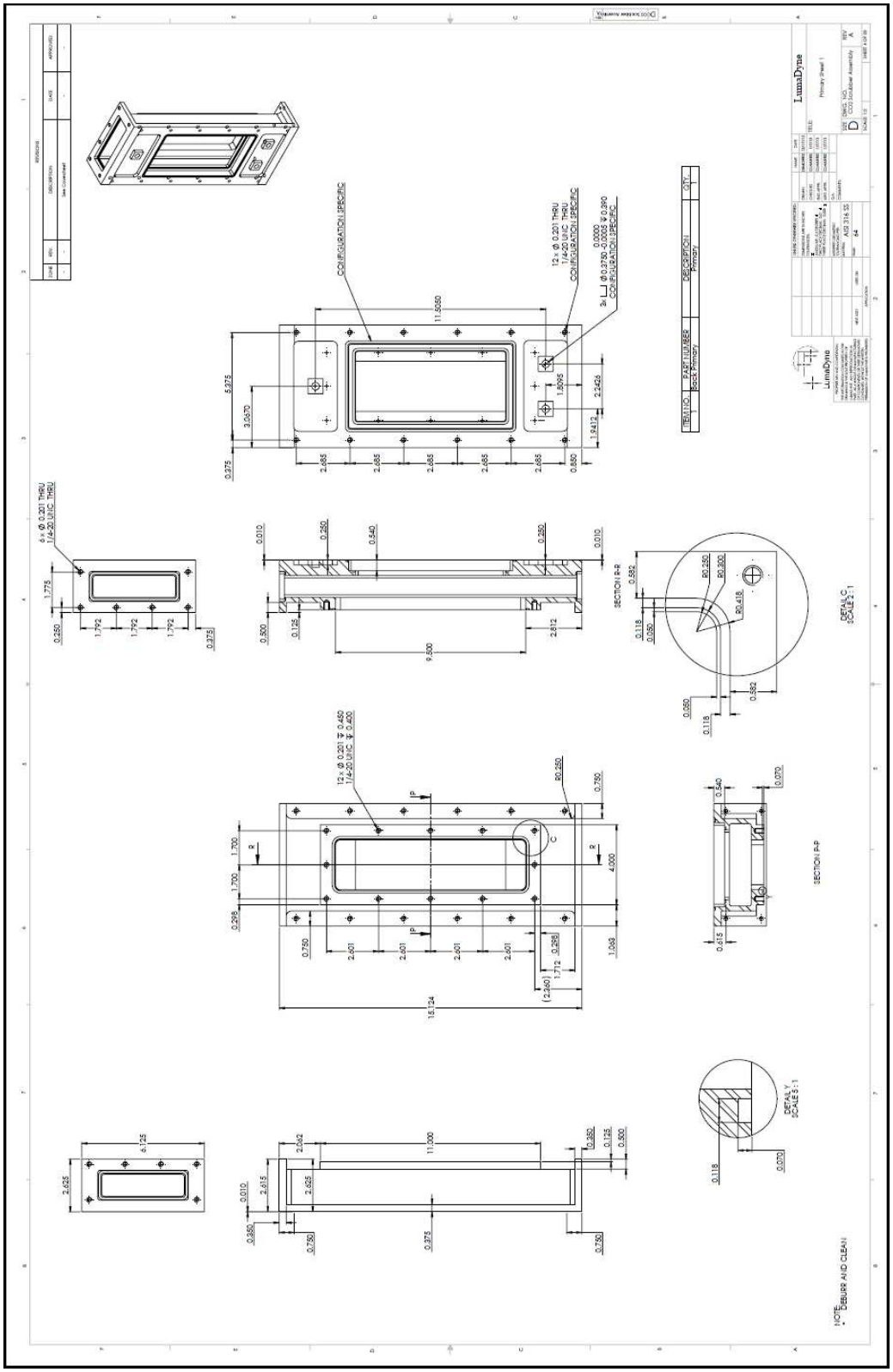
LumaDyne
CONFIGURATION SPECIFIC
11.5000
5.375
3.0370
0.375
2.465
0.850
1.9412
2.2425
1.8095
12 x Ø 0.201 THRU
1/4-20 UNC THRU
Ø0.3750 -0.0005 -0.0010
Ø0.390
ITEM NO.
PART NUMBER
DESCRIPTION
QTY.
Back Primary
Primary
6 x Ø 0.201 THRU
1/4-20 UNC THRU
1.775
1.792
0.250
0.375
0.010
0.540
0.500
0.125
2.812
9.300
SECTION R-R
Ø0.250
Ø0.300
Ø0.418
0.562
0.050
0.118
DETAIL C
SCALE 2 : 1
12 x Ø 0.201 ₮ 0.450
1/4-20 UNC ₮ 0.400
Ø0.250
0.790
1.700
4.000
0.298
0.750
2.601
1.712
0.295
1.069
18.124
(2.601)
0.540
0.070
0.615
SECTION A-A
DETAIL Y
SCALE 5 : 1
6.125
2.625
2.042
11.000
2.615
0.750
0.375
NOTE:
1. DEBURR AND CLEAN!

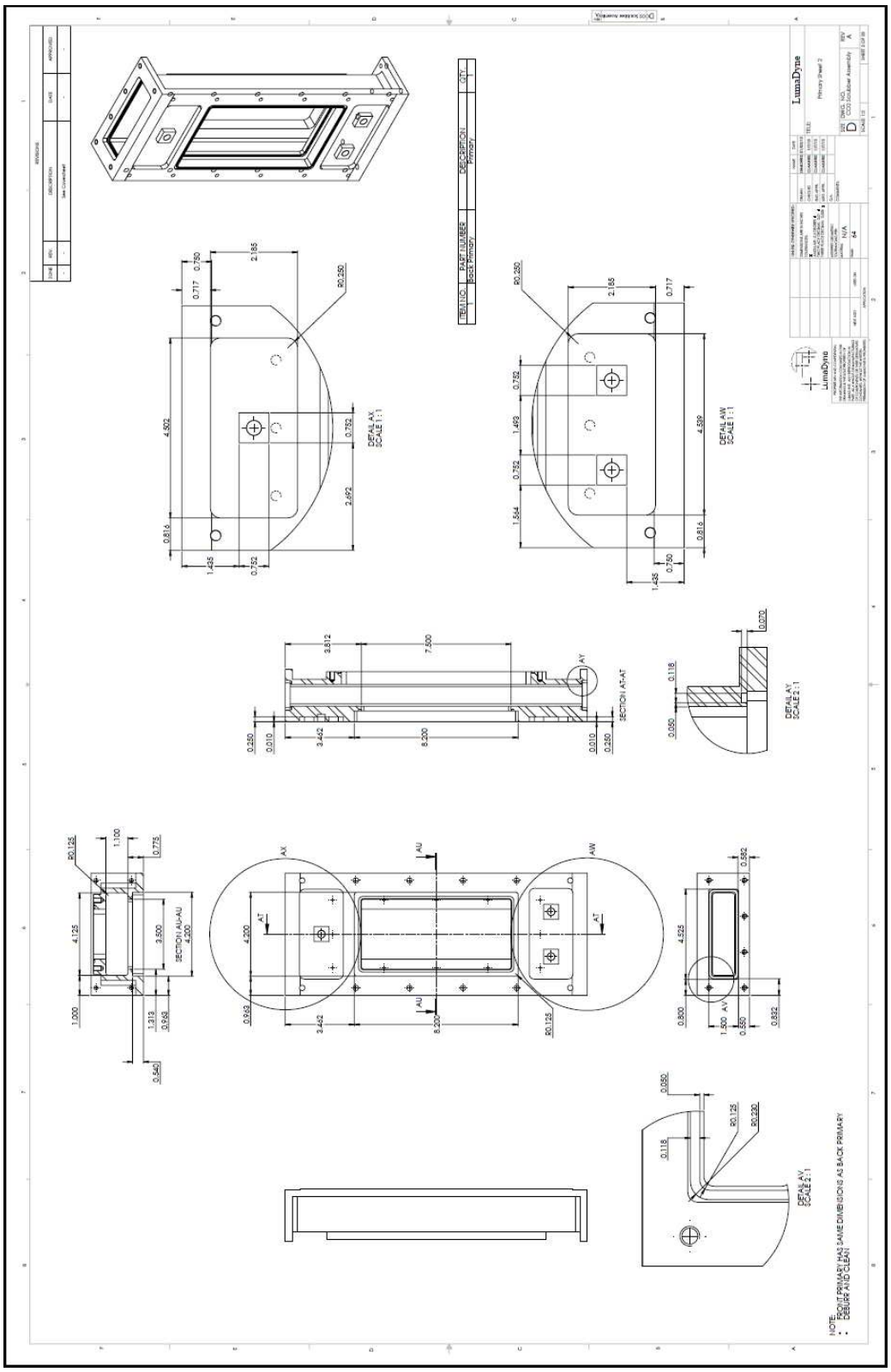
LumaDyne
DETAIL AX
SCALE 1 : 1
DETAIL AW
SCALE 1 : 1
SECTION AT-AT
SECTION AU-AU
DETAIL AY
SCALE 2 : 1
NOTE:
1. ROUT PRIMARY HAS SAME DIMENSIONS AS BACK PRIMARY
DEBURR AND CLEAN

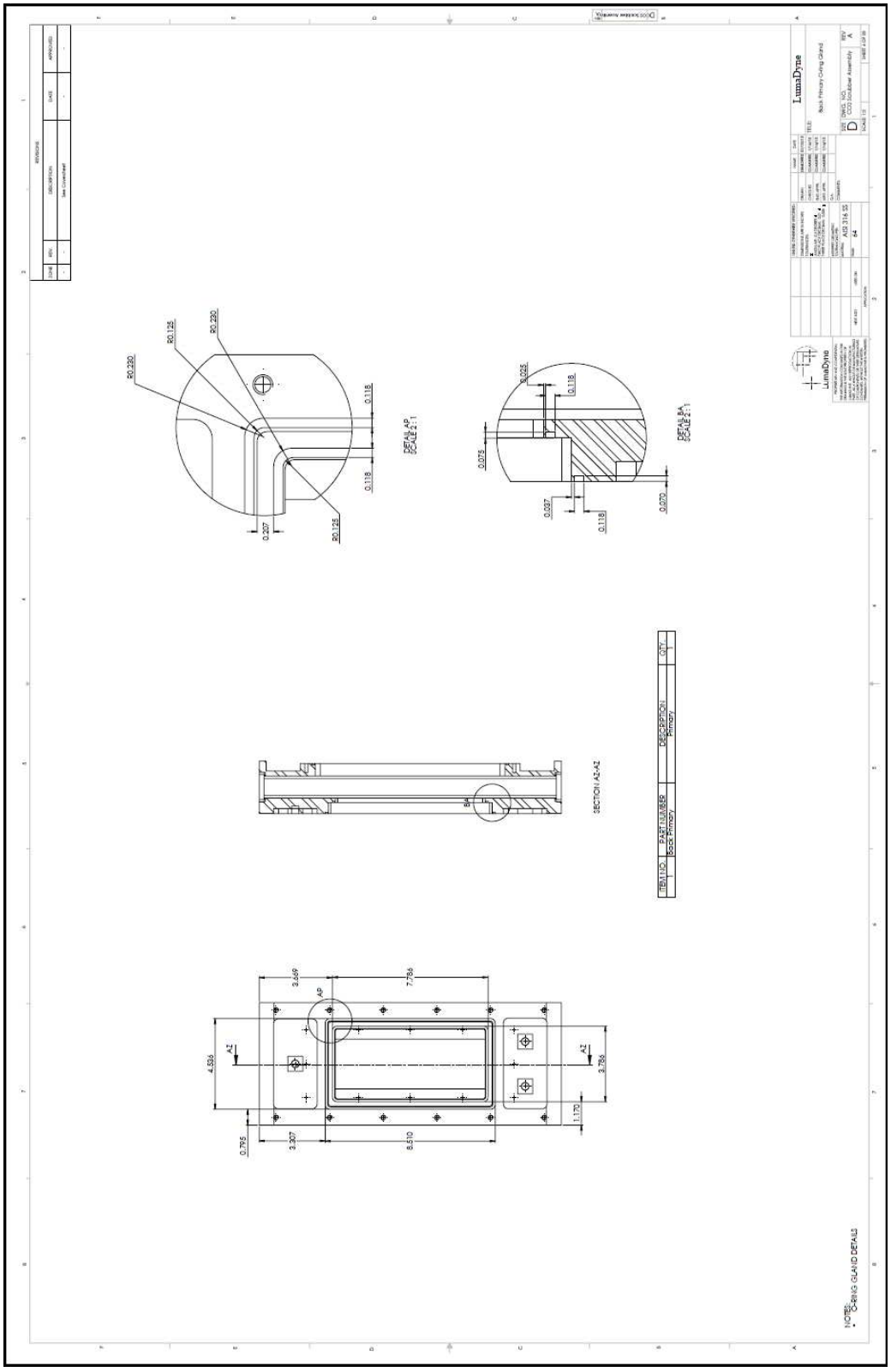
LumaDyne
Back Primary O-ring Gland
DETAIL AP
SCALE 2:1
DETAIL BA
SCALE 2:1
SECTION A2-A2
ITEM NO.
PART NUMBER
DESCRIPTION
QTY.
Back Primary
Primary
NOTES:
1. O-RING GLAND DETAILS

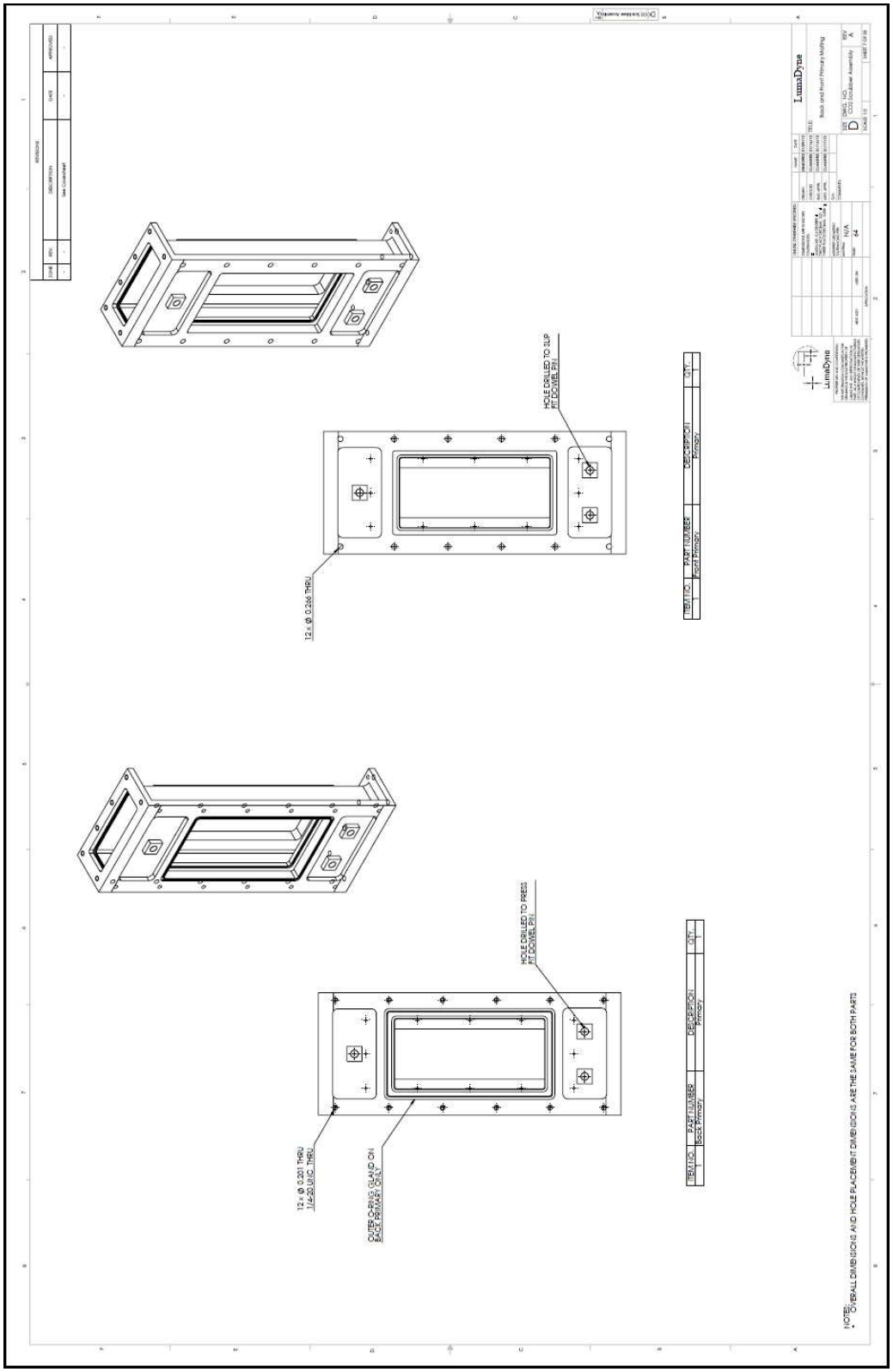
LumaDyne
Back and Front Primary Mating
D
CCD Scribber Assembly
A
HOLE DRILLED TO SLIP FIT DOWEL PIN
12 x Ø 0.266 THRU
ITEM NO.
PART NUMBER
DESCRIPTION
QTY.
Front Primary
Primary
HOLE DRILLED TO PRESS FIT DOWEL PIN
12 x Ø 0.201 THRU
1/4-20 UNC THRU
OUTER O-RING GLAND ON BACK PRIMARY ONLY
Back Primary
NOTE:
1. OVERALL DIMENSIONS AND HOLE PLACEMENT DIMENSIONS ARE THE SAME FOR BOTH PARTS

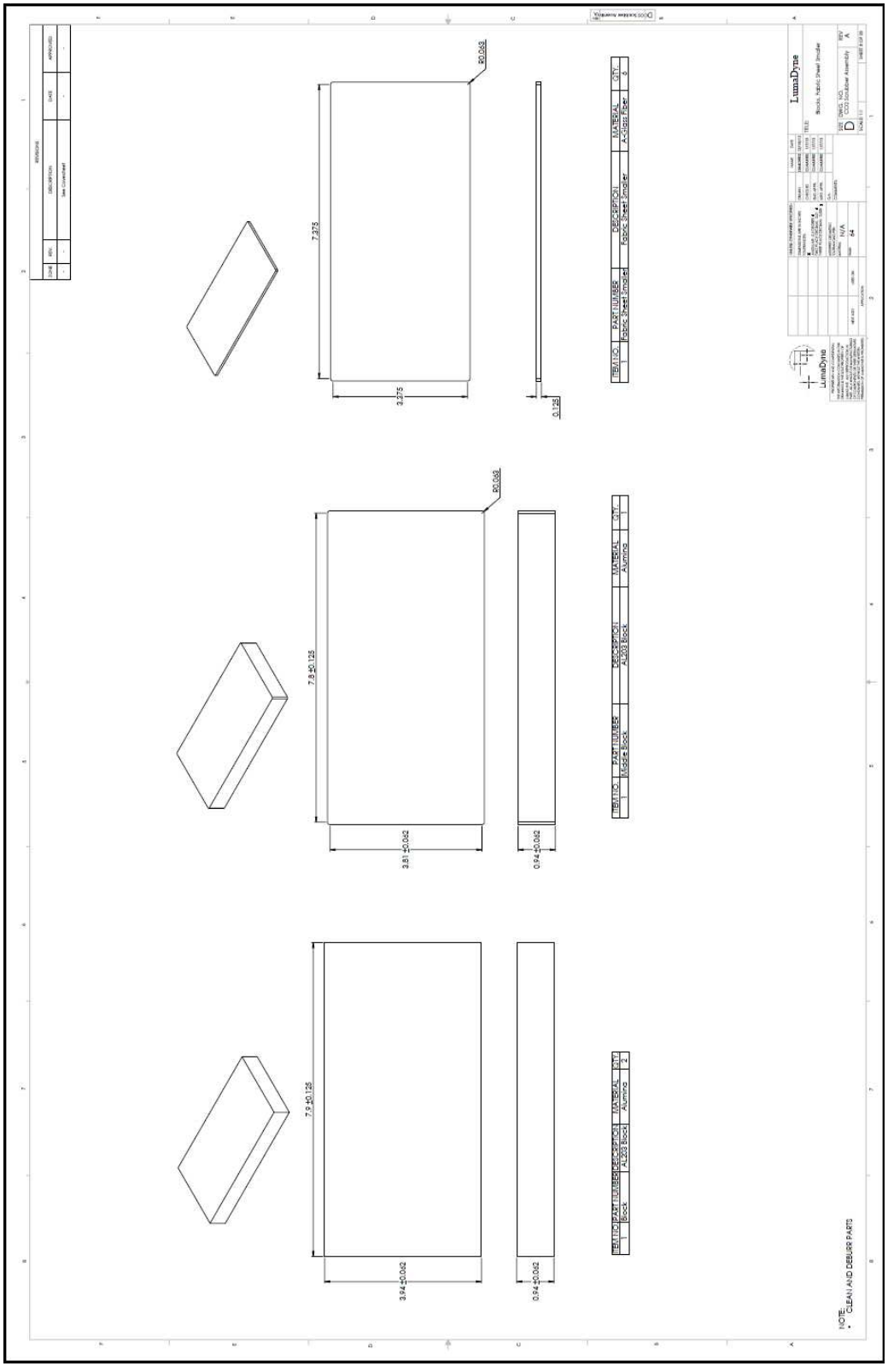
LumaDyne
Blocks, Fabric Sheet Smaller
CCD Scrubber Assembly
NOTE:
1. CLEAN AND DEBURR PARTS

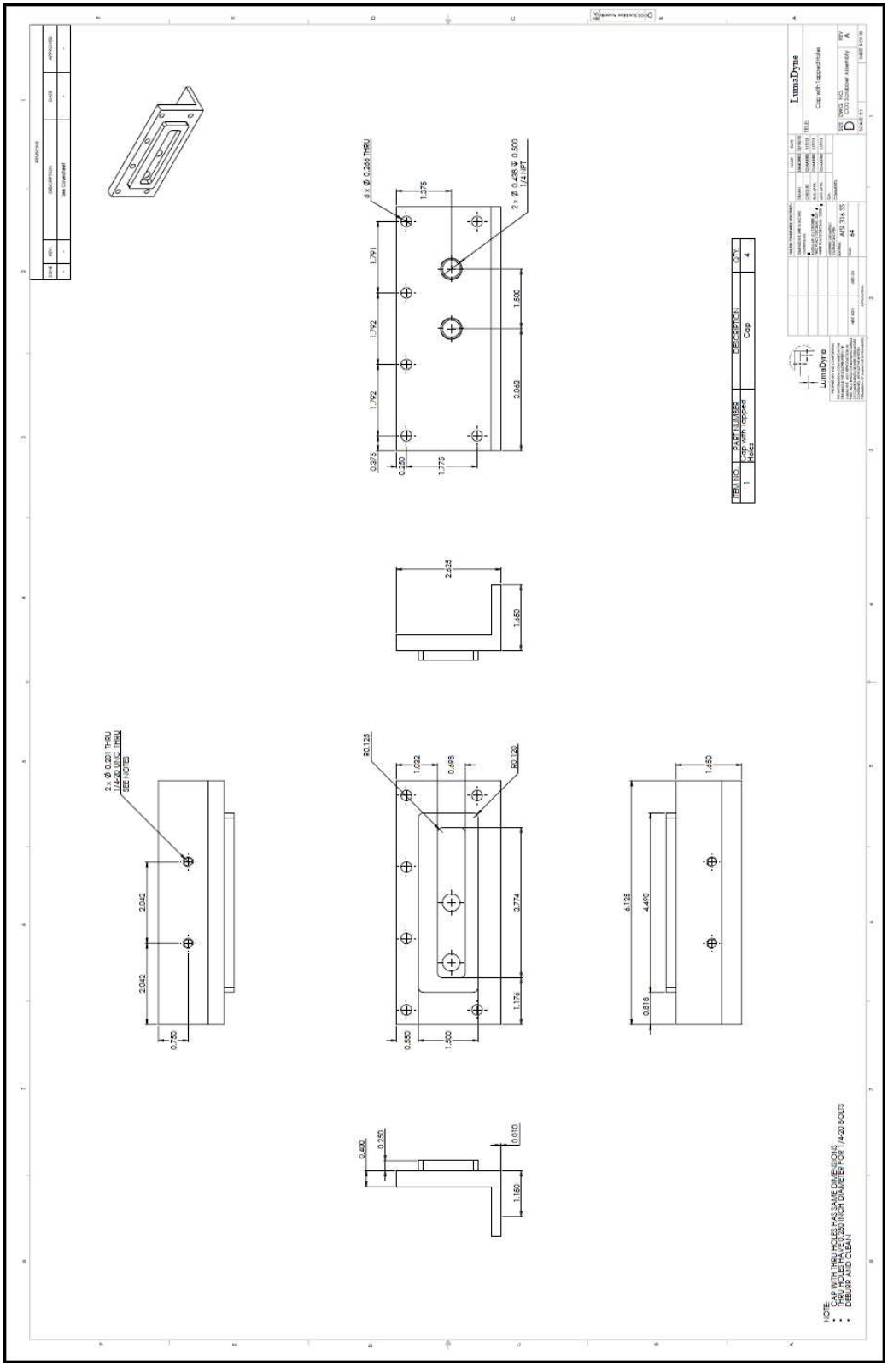
LumaDyne
Cap with tapped holes
CCD Scrubber Assembly
PART NUMBER
Cap with tapped Holes
DESCRIPTION
Cap
QTY
4
NOTE
DEBURR AND CLEAN

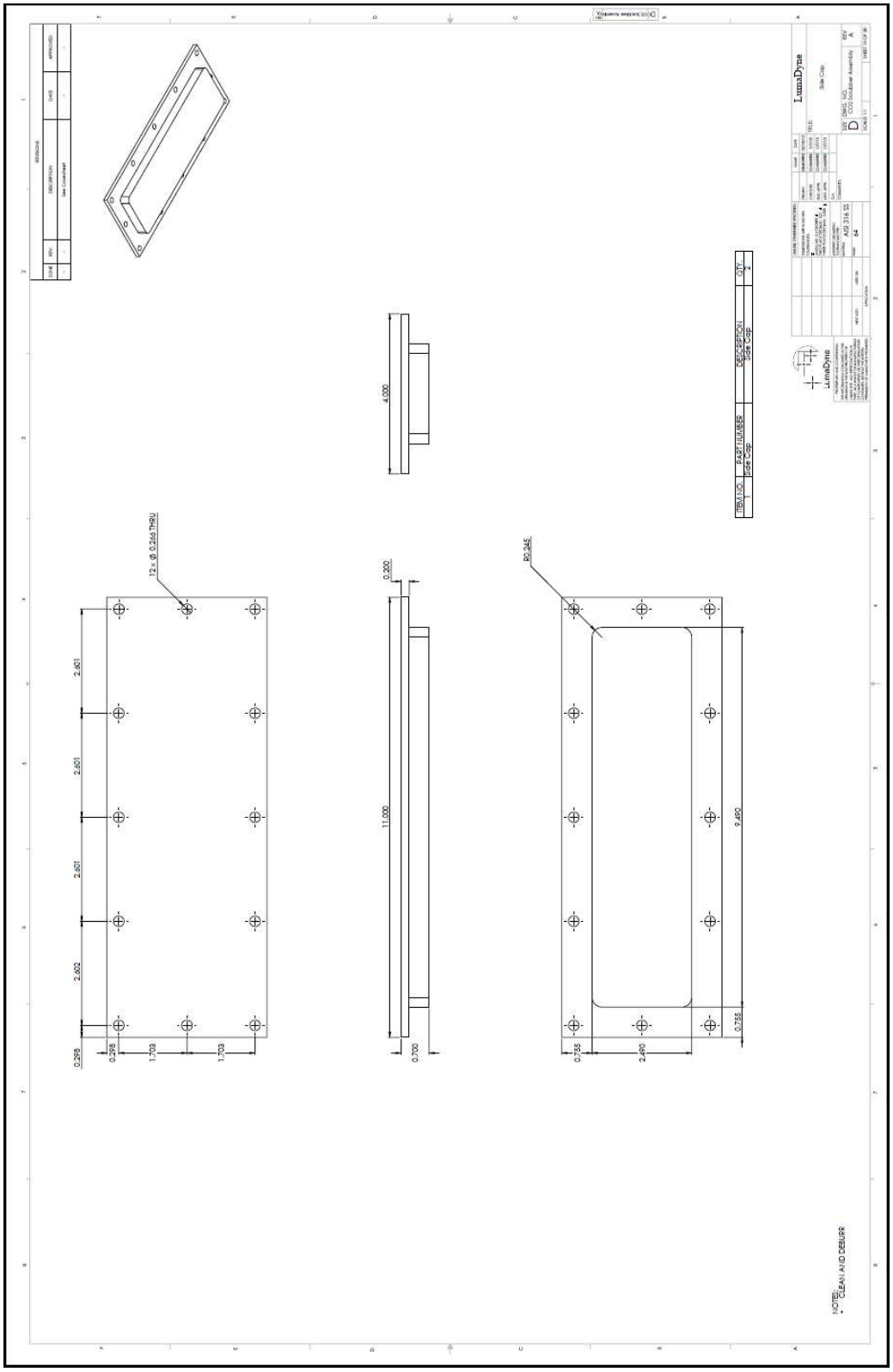
LumaDyne
Side Cap
NOTES:
1. CLEAN AND DEBUR

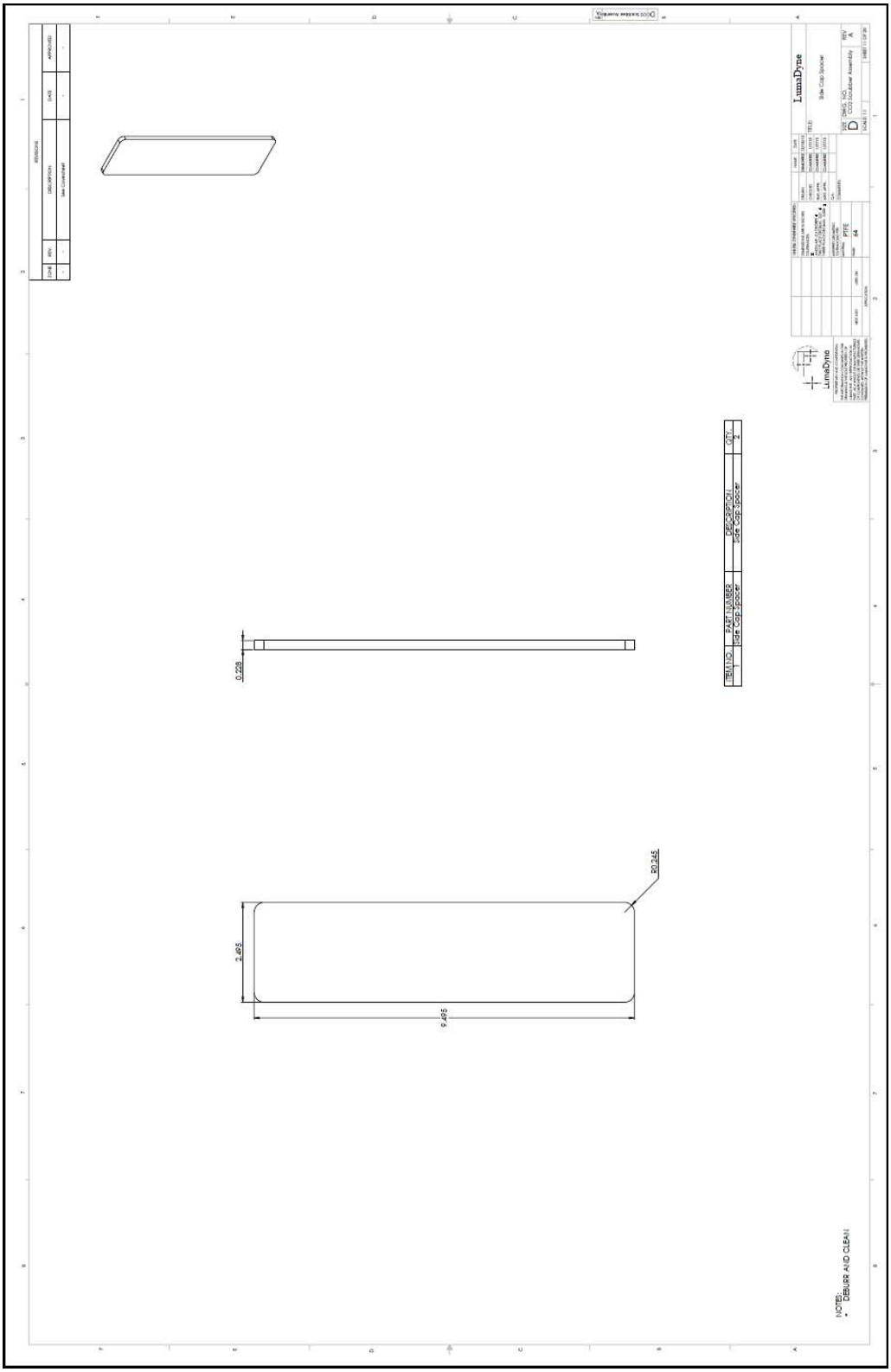
LumaDyne
Side Cap Spacer
PART NUMBER
Side Cap Spacer
DESCRIPTION
Side Cap Spacer
QTY
4
PTFE
0.228
2.495
6.495
R0.245
NOTE:
1. DEBURR AND CLEAN

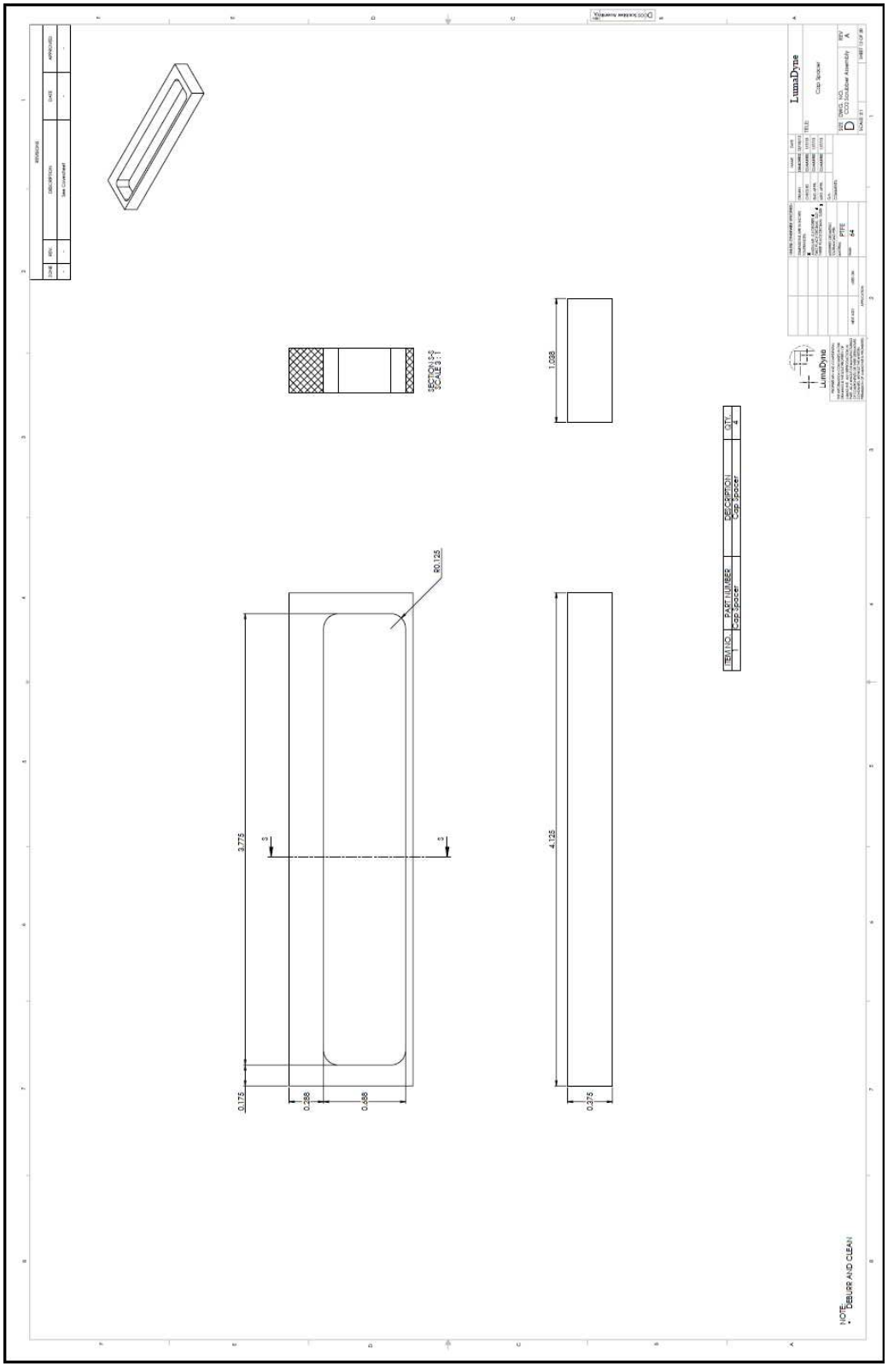
LumaDyne
Chip Spacer
CCD Socketed Assembly
D
NOTE:
DEBUR AND CLEAN
ITEM NO
PART NUMBER
DESCRIPTION
QTY
Chip Spacer
4
SECTION B-B
SCALE 3 : 1
R0.125
3.775
0.175
0.288
0.488
1.038
4.125
0.275

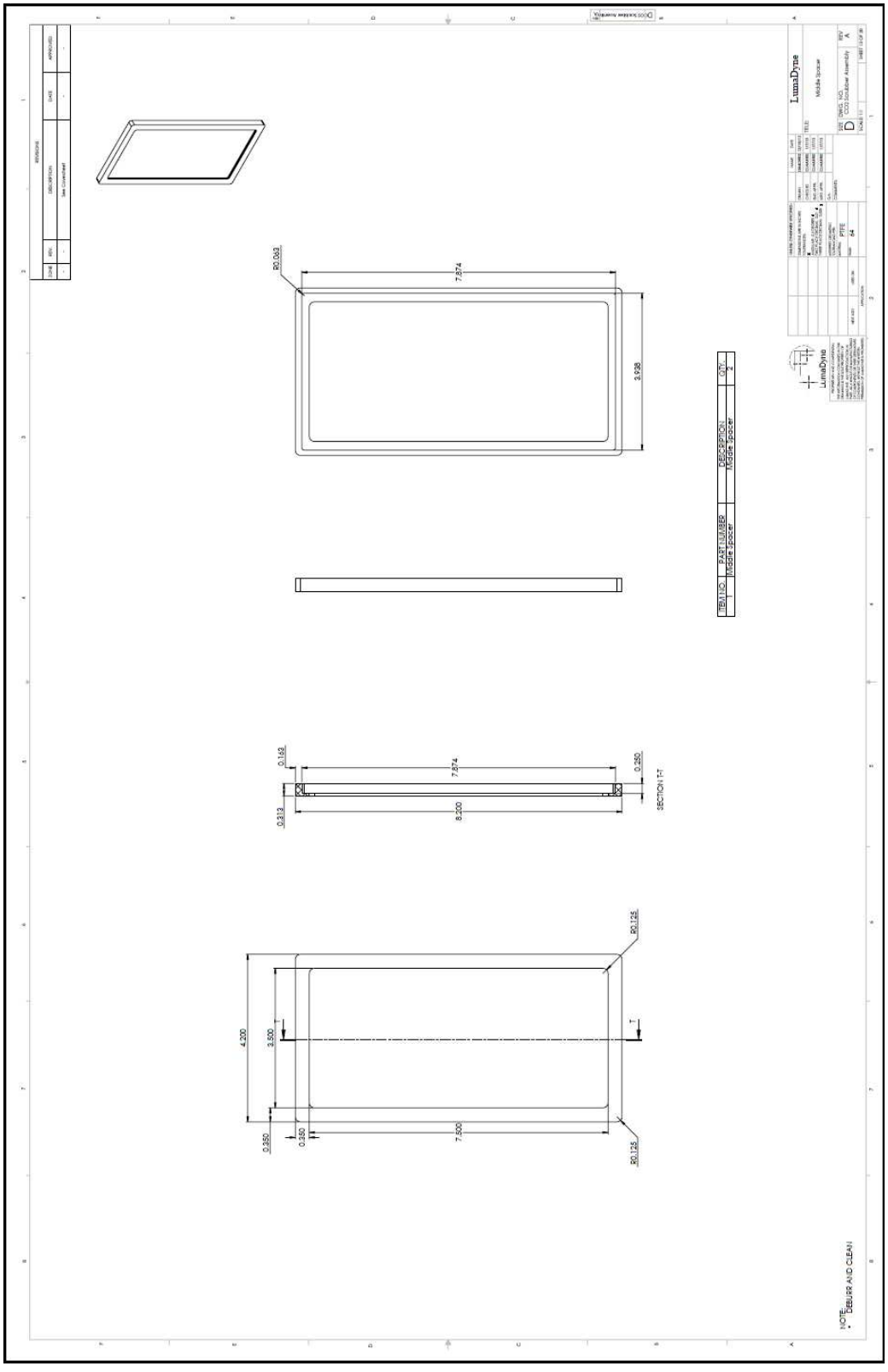
LumaDyne
Middle Spacer
CCO Solidbar Assembly
D
REV
A
ITEM NO.
PART NUMBER
DESCRIPTION
QTY.
Middle Spacer
Middle Spacer
2
7.874
3.938
R0.093
0.163
0.313
8.200
0.250
SECTION 1-1
4.200
3.500
7.500
0.350
R0.125
NOTE:
1. DEBURR AND CLEAN

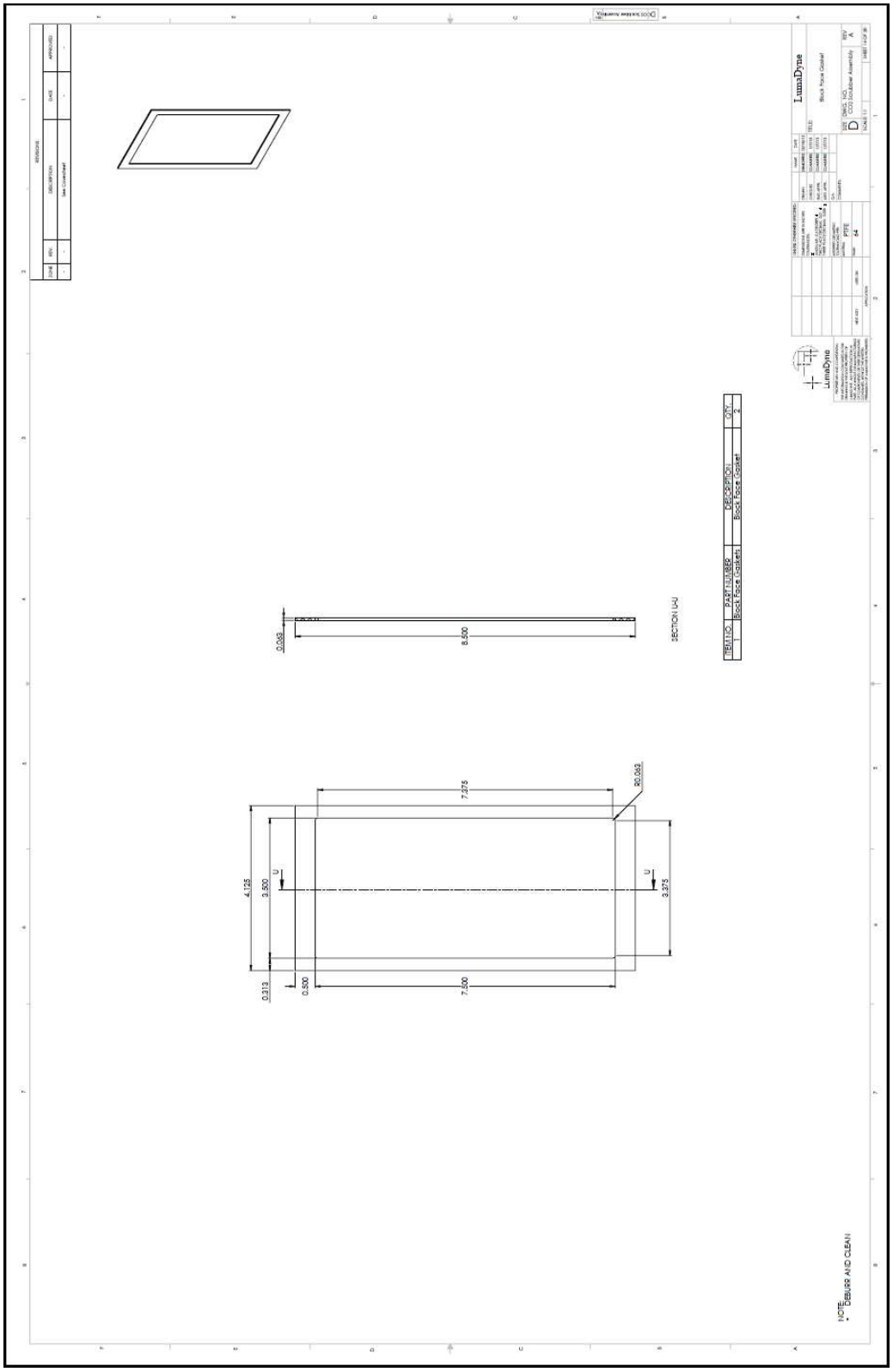
LumaDyne
Block Face Gasket
NOTE
* DEBURR AND CLEAN
SECTION U-U
0.063
8.500
7.375
R0.063
4.125
3.500
3.375
0.313
0.500
7.500

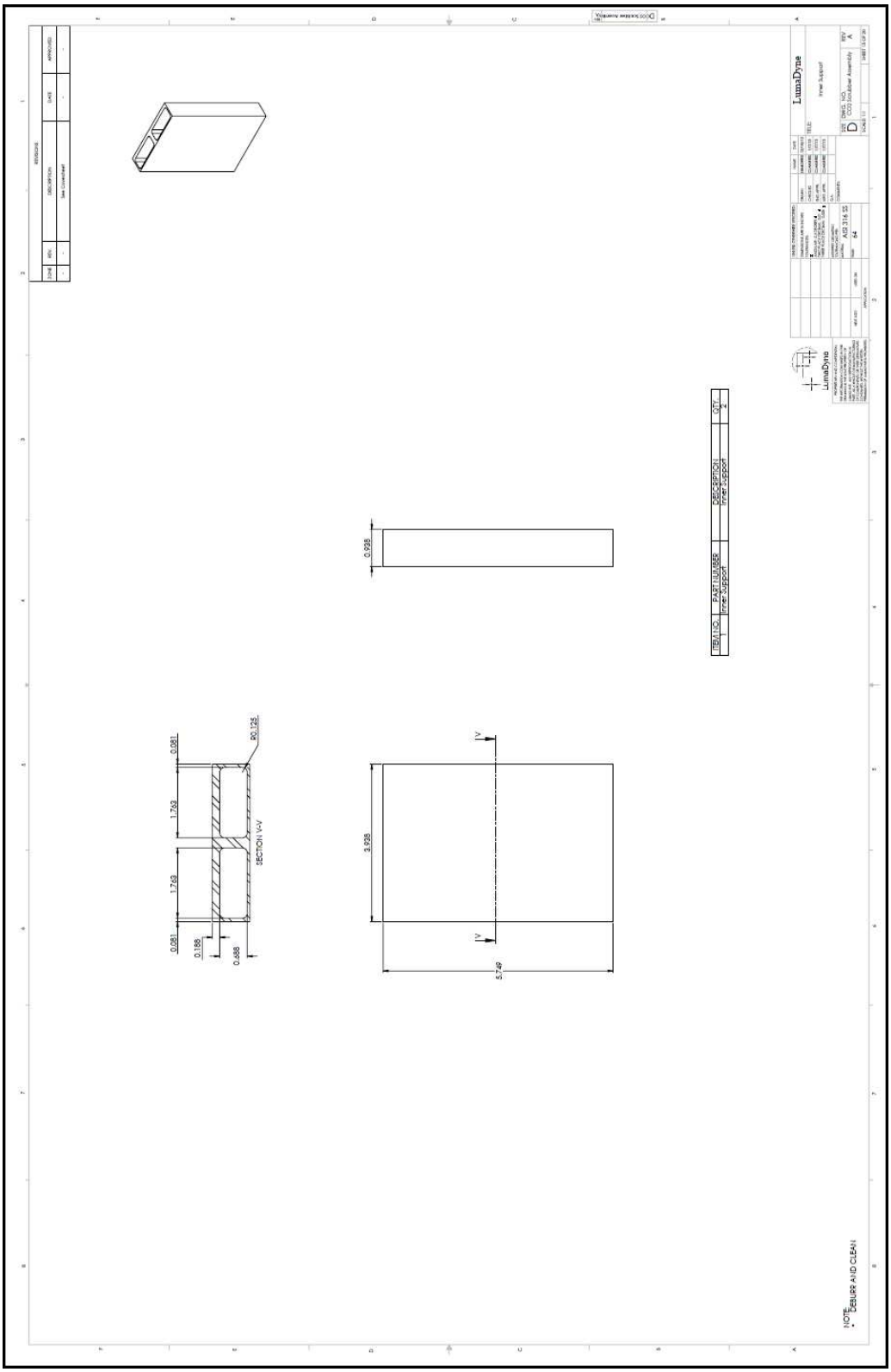
LunaDyne
Inner Support
CCD Isolation Assembly
PART NUMBER
Inner Support
DESCRIPTION
Inner Support
SECTION V-V
NOTE
DEBURR AND CLEAN

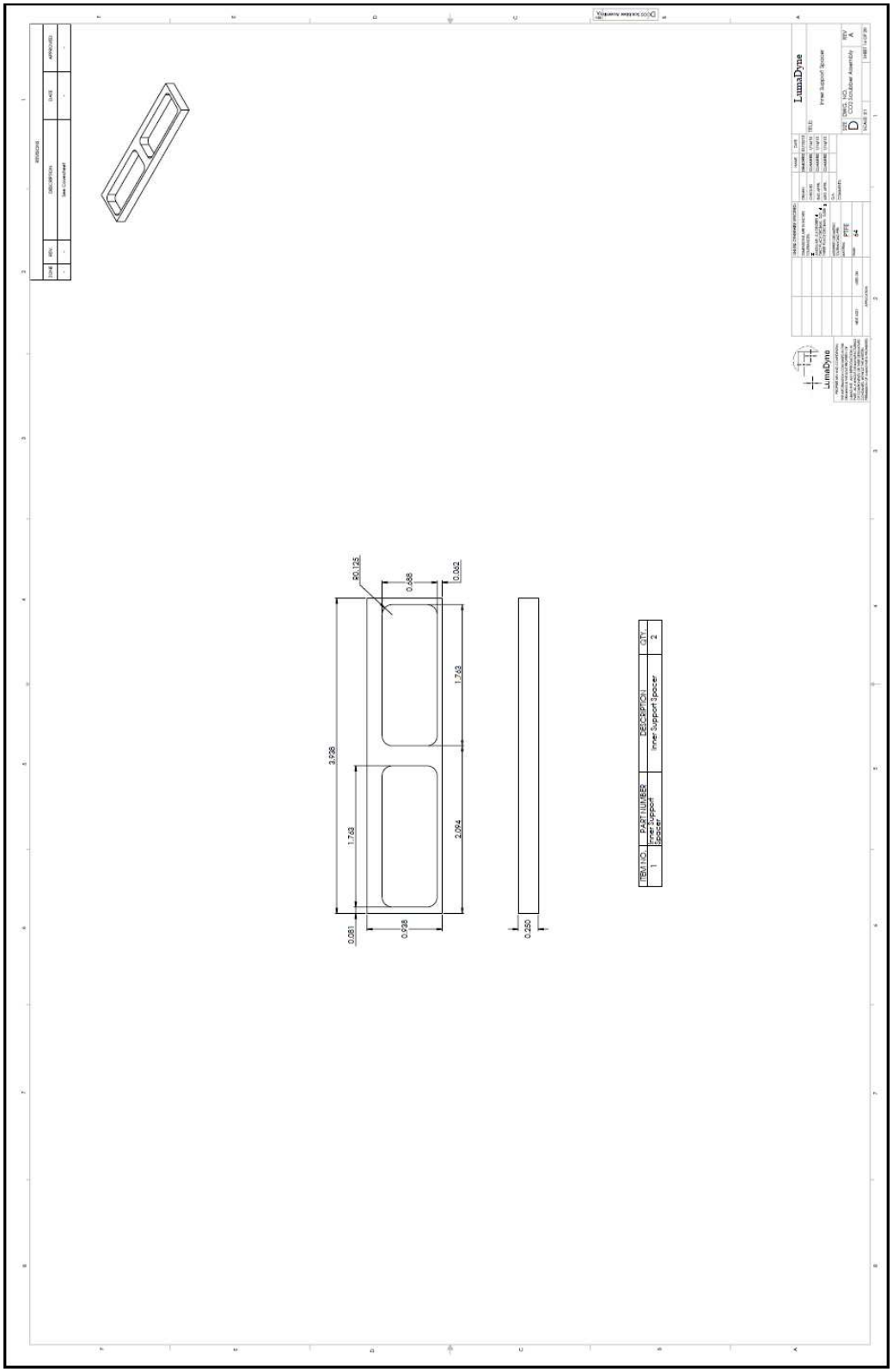
R0.125
0.688
0.062
3.936
1.748
1.748
2.054
0.081
0.938
0.250
ITEM NO.
PART NUMBER
DESCRIPTION
QTY.
1
Inner Support Spacer
Inner Support Spacer
2
LumaDyne
Inner Support Spacer
D
CCD Scrubber Assembly
A

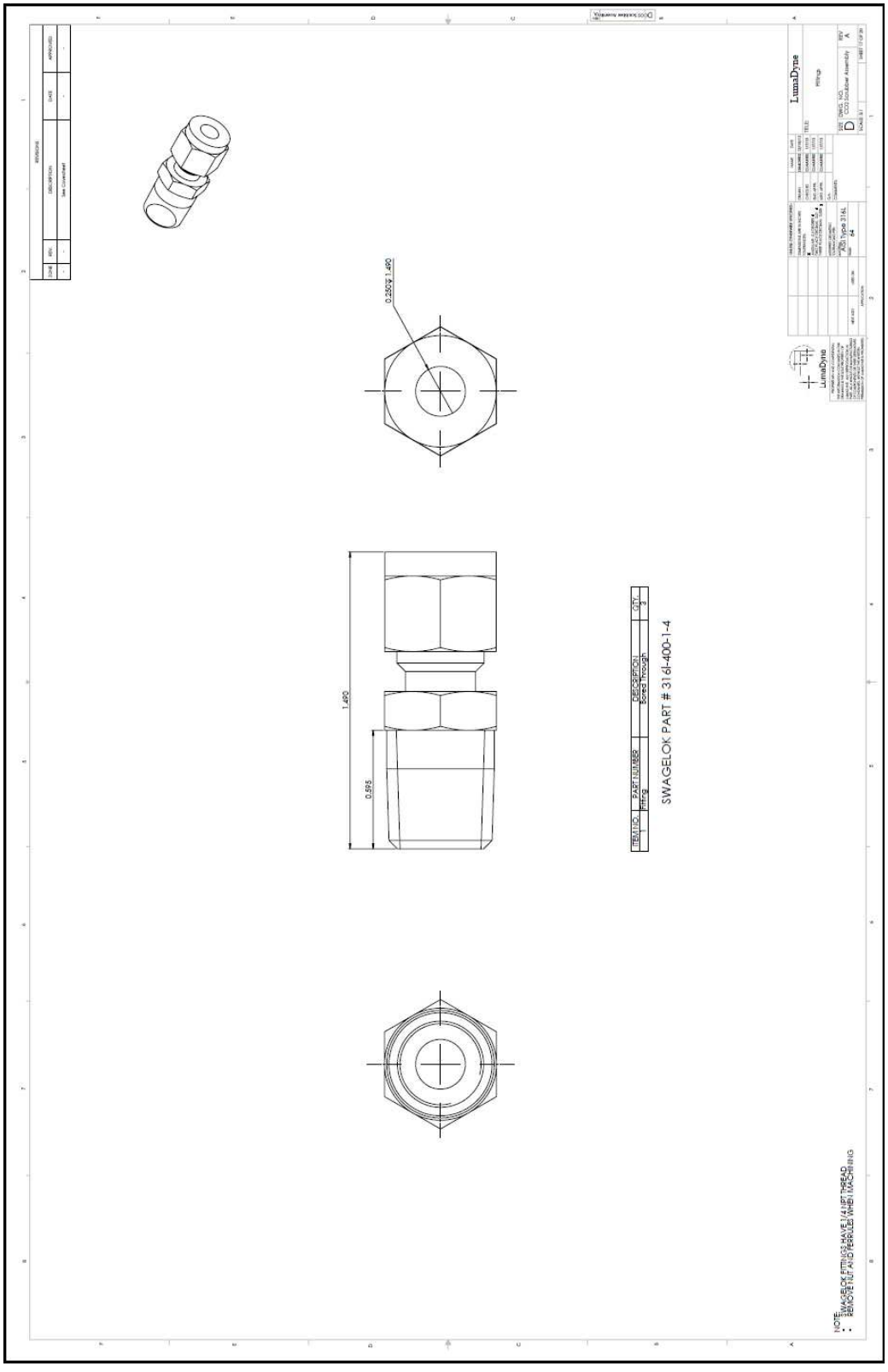
0.3503 1.490
1.490
0.595
SWAGELOK PART # 316l-400-1-4
NOTE:
1. SWAGELOK FITTINGS HAVE 1/4 NPT THREAD
2. REMOVE NUT AND FERRULES WHEN MACHINING
LumaDyne

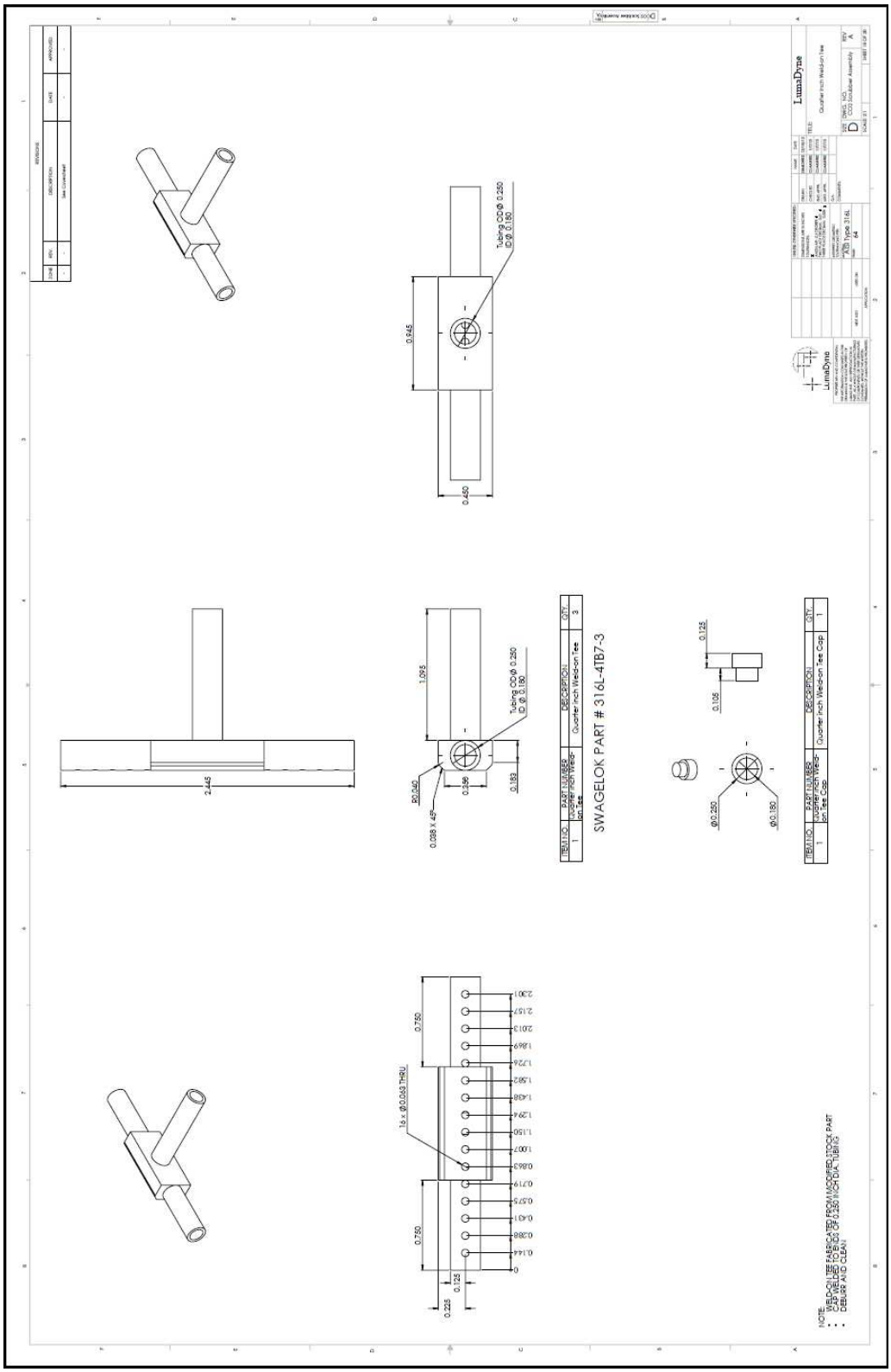
LumaDyne
Quarter Inch Weldon Tee
CCD Scrubber Assembly
Type 316L
SWAGELOK PART # 316L-4TB7-3
ITEM NO. | PART NUMBER | DESCRIPTION | QTY.
1 | SWAGELOK PART # 316L-4TB7-3 | Quarter Inch Weldon Tee | 3
ITEM NO. | PART NUMBER | DESCRIPTION | QTY.
1 | SWAGELOK PART # SS-400-C | Quarter Inch Weldon Tee Cap | 1
NOTE
WELD ONLY BE FABRICATED FROM MACHINED STOCK PART
DEBURR AND CLEAN

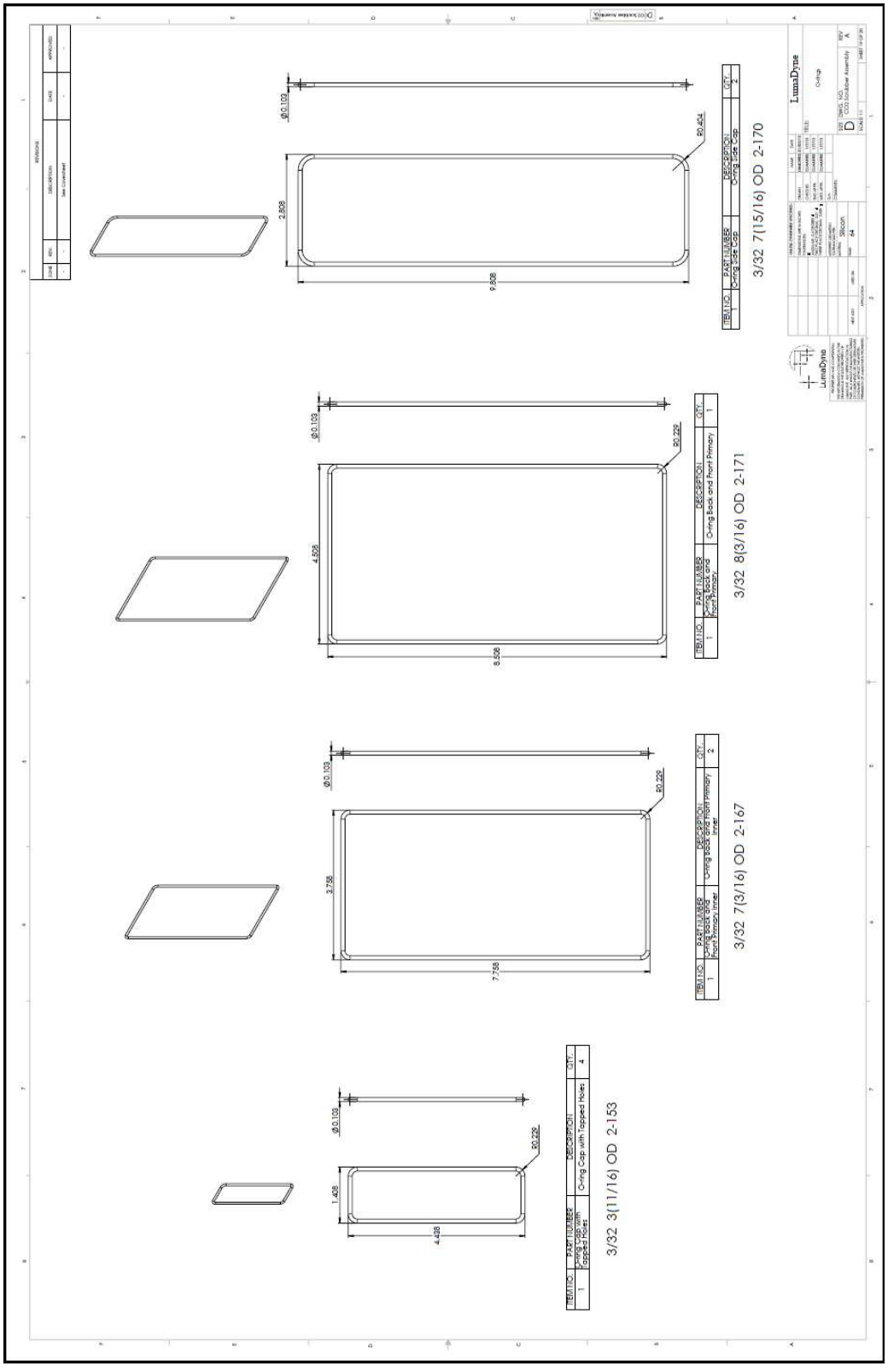
3/32 3(11/16) OD 2-153
3/32 7(3/16) OD 2-167
3/32 8(3/16) OD 2-171
3/32 7(15/16) OD 2-170
LumaDyne

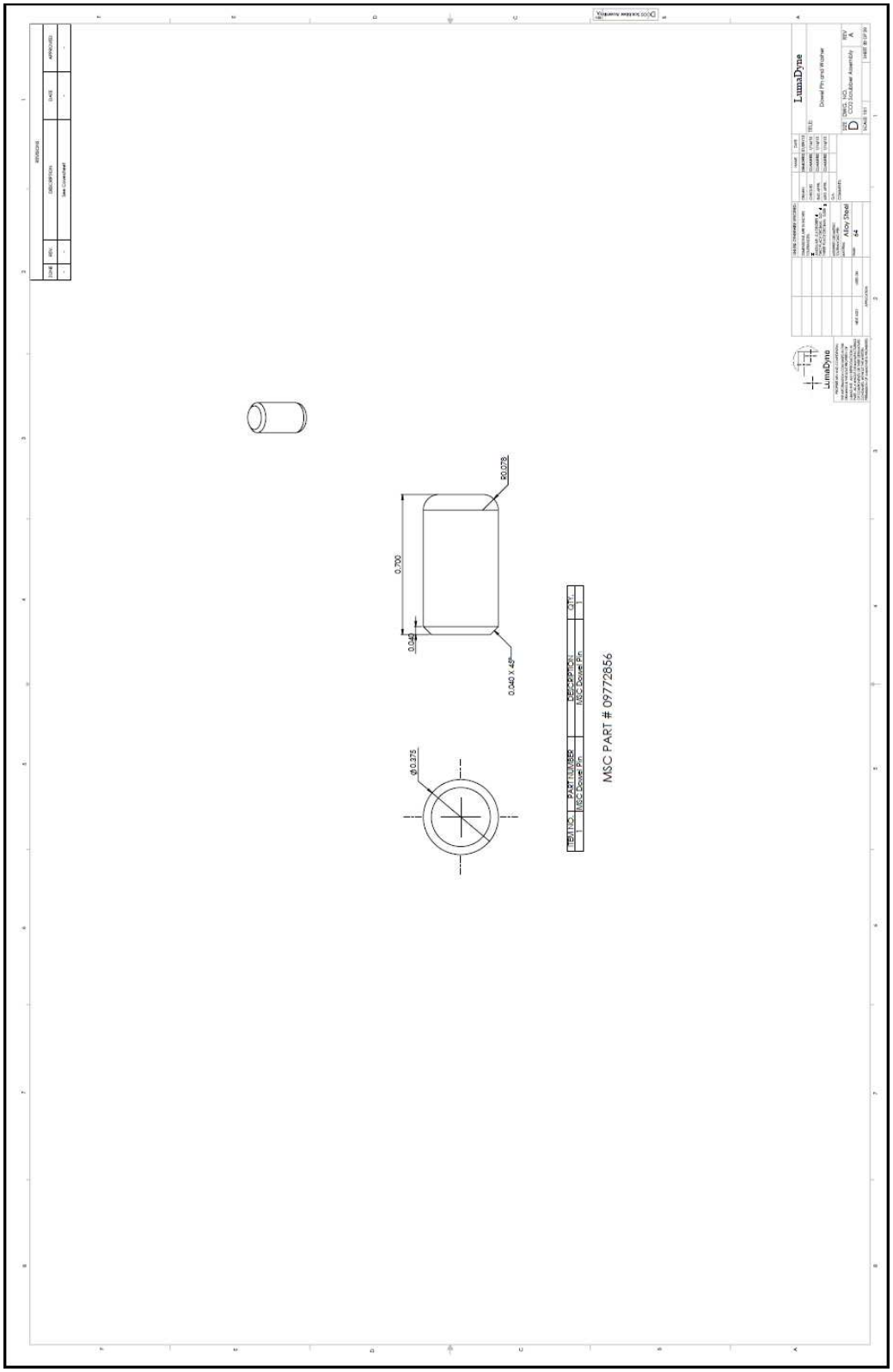
LumaDyne
Dowel Pin and Washer
D
CCD Sidelooker Assembly
A
Alloy Steel
64
0.700
0.040
Ø0.078
0.040 X 45°
Ø0.375
ITEM NO.
PART NUMBER
DESCRIPTION
QTY.
MSC Dowel Pin
MSC PART # 09772656

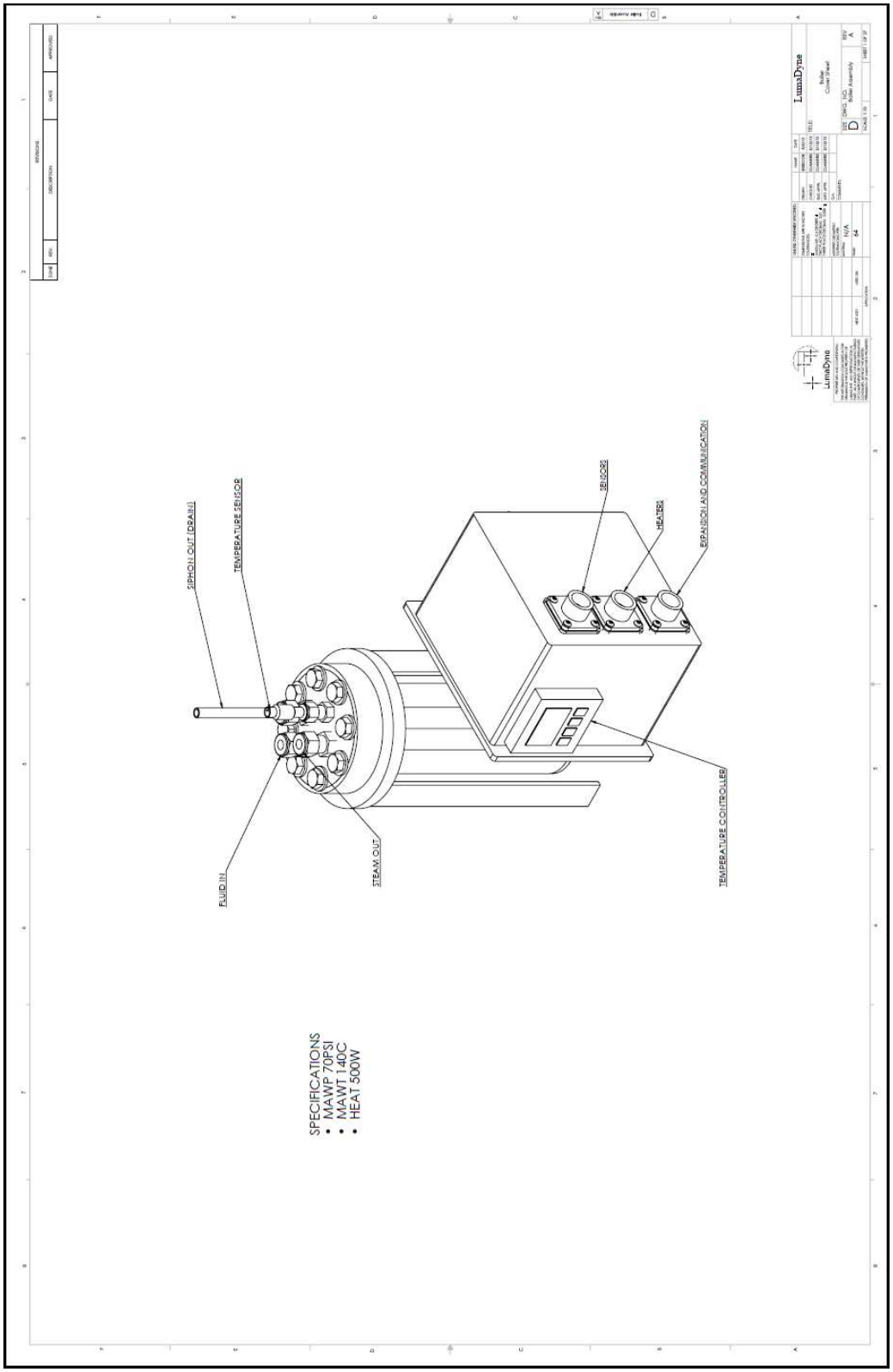
SIPHON OUT (DRAIN)
TEMPERATURE SENSOR
SENSORS
HEATERS
EXPANSION AND COMMUNICATION
FLUID IN
STEAM OUT
TEMPERATURE CONTROLLER
SPECIFICATIONS
• MAWP 70PSI
• MAWT 140C
• HEAT 500W
LumaDyne
Boiler
Cover Sheet
Boiler Assembly

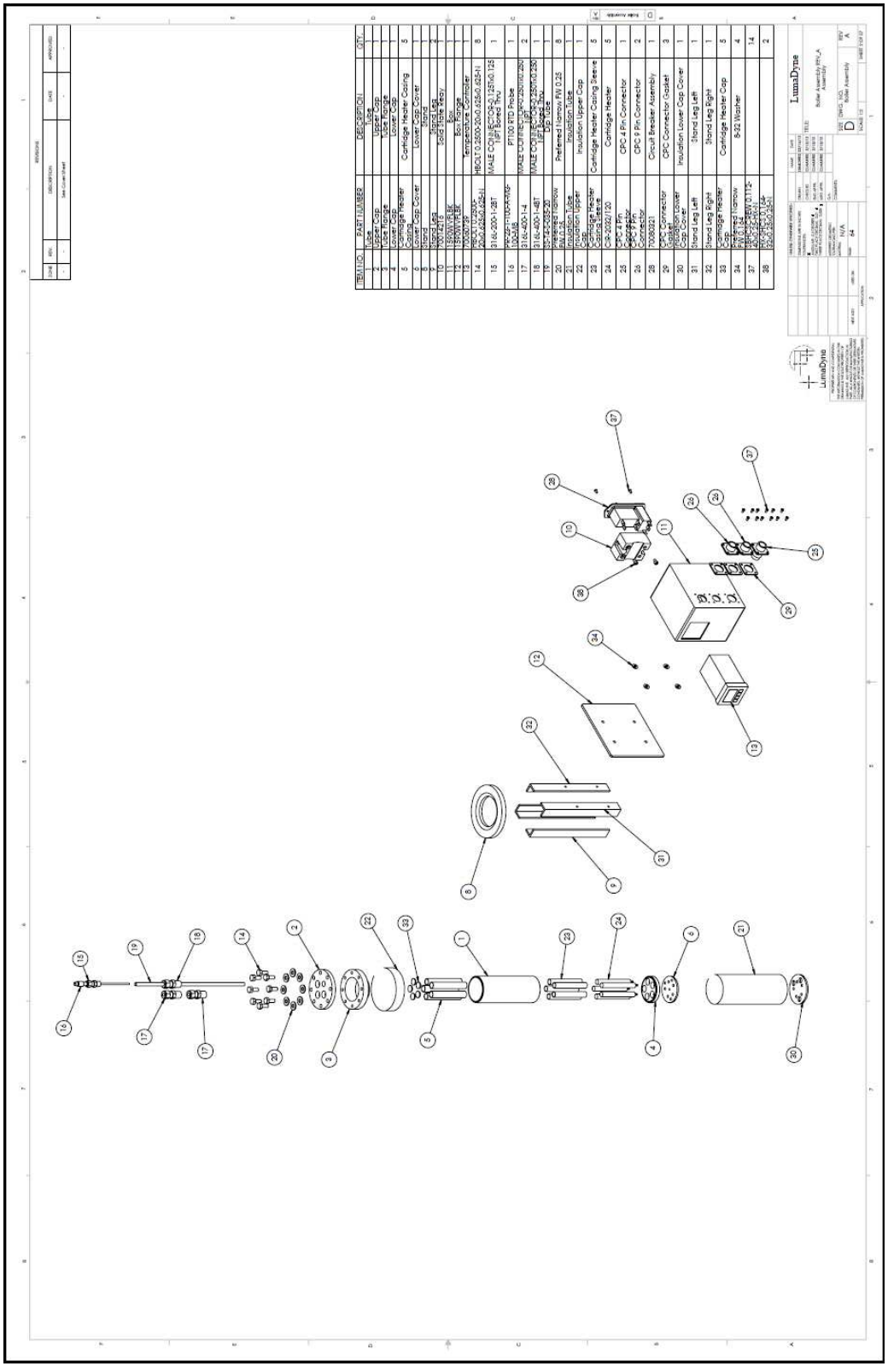
REVISIONS
ZONE
REV.
DESCRIPTION
DATE
APPROVED
See Current Sheet
Boiler Assembly
ITEM NO.
PART NUMBER
DESCRIPTION
QTY.
Tube
Upper Cap
Tube Flange
Lower Cap
Cartridge Heater Casing
Lower Cap Cover
Stand Leg
Solid State Relay
Fuse
Solid State Relay
Temperature Controller
HEXBOLT 0.3500-20x0.625x0.625-H
MALE CONNECTOR-2,1.25TA0.125 NPT Boxed Thru
PT100 RTD Probe
MALE CONNECTOR-1/4NPT
MALE CONNECTOR-1/4NPT Boxed 3/32ID Dip Tube
Preferred Harmony PW 0.25
Insulation Side
Insulation Upper Cap
Cartridge Heater Casing Sleeve
Cartridge Heater
CPC 4 Pin Connector
CPC 5 Pin Connector
Socket
Circuit Breaker Assembly
CPC Connector Gasket
Insulation Lower Cap Cover
Stand Leg Left
Stand Leg Right
Cartridge Heater Cap
Flanged Harmony PW 0.134
6-32 Washer
Base
LumaDyne
Boiler Assembly
SIZE
D
DWG. NO.
Boiler Assembly
REV
A
SCALE: 1:2
WEIGHT:
SHEET 1 OF 2
DO NOT SCALE DRAWING
UNLESS OTHERWISE SPECIFIED:
DIMENSIONS ARE IN INCHES
TOLERANCES:
FRACTIONAL ±
ANGULAR: MACH ± BEND ±
TWO PLACE DECIMAL ±
THREE PLACE DECIMAL ±
INTERPRET GEOMETRIC TOLERANCING PER:
MATERIAL
FINISH
NEXT ASSY
USED ON
APPLICATION
PROPRIETARY AND CONFIDENTIAL
THE INFORMATION CONTAINED IN THIS DRAWING IS THE SOLE PROPERTY OF LUMADYNE. ANY REPRODUCTION IN PART OR AS A WHOLE WITHOUT THE WRITTEN PERMISSION OF LUMADYNE IS PROHIBITED.
DRAWN
CHECKED
ENG APPR.
MFG APPR.
Q.A.
COMMENTS:
LumaDyne

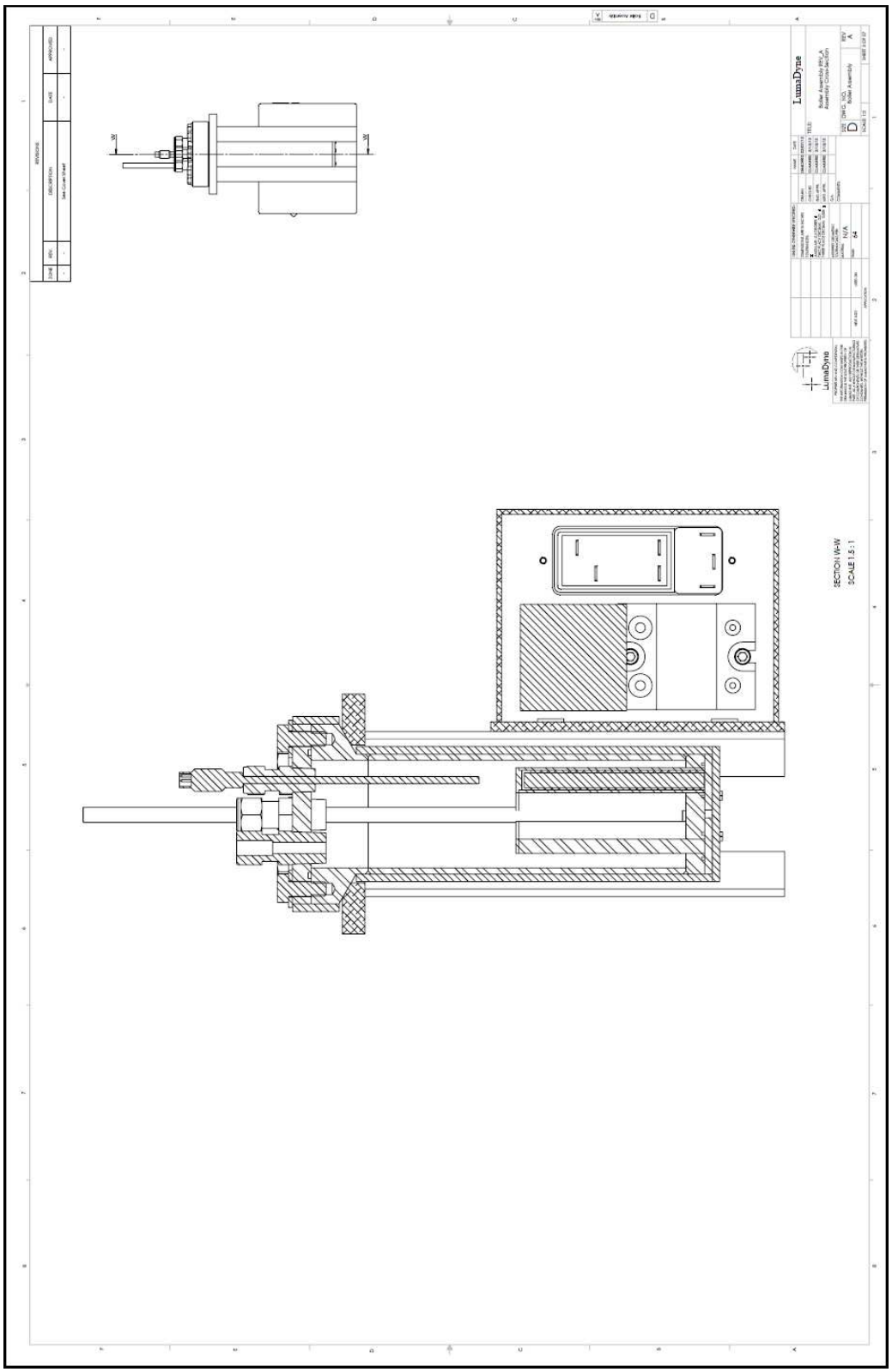
W
W
SECTION W-W
SCALE 1.5 : 1
LumaDyne
Boiler Assembly
Boiler Assembly REV. A
Assembly Cross-Section
DWG. NO.
Boiler Assembly
REV
A
SIZE
D
SCALE 1:2
SHEET 2 OF 2

Bibliography

[1] British Petroleum, "Statistical Review of World Energy, June 2011", 2012.

[2] A. Neftel, H. Friedli, E. Moor, H. Lötscher, H. Oeschger, U. Siegenthaler, and B. Stauffer, "Historical Carbon Dioxide Record from the Siple Station Ice Core", *Trends 93: A Compendium of Data on Global Change. ORNL/CDIAC-65. Carbon Dioxide Information Analysis Center, Oak Ridge National Laboratory, Oak Ridge, Tenn*, pp. 11–14, 1994.

[3] J.M. Barnola, D. Raynaud, C. Lorius, and N.I. Barkov, "Historical Carbon Dioxide Record from the Vostok Ice Core", *Nature*, vol. 329, pp. 408–414, 1987.

[4] National Oceanic and Atmospheric Administration (NOAA), "Global Surface Temperature Anomalies", 2013.

[5] P. Enkvist, T. Nauclér, and J. Rosander, "A Cost Curve for Greenhouse Gas Reduction", *McKinsey Quarterly*, vol. 1, pp. 34, 2007.

[6] Image Courtesy of California CCS Coalition, "CCS Primer: Introduction to CCS", 2013.

[7] Image Courtesy of Cooperative Research Center for Greenhouse Gas Technologies (CO2CRC), "CO2CRC: Images & Videos", 2013.

[8] Image Courtesy of Wikimedia Foundation, "Amine Gas Treating", 2013.

[9] A.L. Kohl and R.B. Nielsen, *Gas Purification*, Gulf Professional Publishing, 1997.

[10] R. Sakwattanapong, A. Aroonwilas, and A. Veawab, "Behavior of Reboiler Heat Duty for Carbon Dioxide (CO_2) Capture Plants using Regenerable Single and Blended Alkanolamines", *Industrial & engineering chemistry research*, vol. 44, no. 12, pp. 4465–4473, 2005.

[11] E. Alper, "Kinetics of Reactions of Carbon Dioxide with Diglycolamine and Morpholine", *The Chemical Engineering Journal*, vol. 44, no. 2, pp. 107–111, 1990.

[12] P.D. Vaidya and E.Y. Kenig, "CO_2 - Alkanolamine Reaction Kinetics: A Review of Recent Studies", *Chemical Engineering & Technology*, vol. 30, no. 11, pp. 1467–1474, 2007.

[13] E.Y. Kenig, R. Schneider, and A. Górak, "Reactive Absorption: Optimal Process Design via Optimal Modelling", *Chemical engineering science*, vol. 56, no. 2, pp. 343–350, 2001.

[14] Image Courtesy of Dong Suh Machinery Co., "Product Info: Steam Jet Vacuum

Ejector", 2013.

[15] M. Scheffler and P. Colombo, *Cellular Ceramics*, Wiley-Vch, 2006.

[16] M.S. DuPart, T.R. Bacon, and D.J. Edwards, "Understanding Corrosion in Alkanolamine Gas Treating Plants", *Hydrocarbon Processing*, vol. 72, no. 5, pp. 89–94, 1993.

[17] H. Spliethoff, *Power Generation from Solid Fuels*, Springer Verlag, 2010.

[18] Foucher J.C. Hestermann R. Hilton B. Keegan B. Stephen D. Bartley, P., "Maximizing Economic and Environmental Performance of Existing Coal-fired Assets", 2007.

[19] D. Singh, E. Croiset, P.L. Douglas, and M.A. Douglas, "Techno-economic Study of CO_2 Capture from an Existing Coal–fired Power Plant: MEA scrubbing vs. O_2/CO_2 Recycle Combustion", *Energy Conversion and Management*, vol. 44, no. 19, pp. 3073–3091, 2003.

[20] H.Z. Kister, *Distillation Design*, vol. 1, McGraw-Hill New York, 1992.

[21] R. Safruddin, "Twenty Year Experience in Controlling Corrosion in Amine Unit of Badak LNG Plant", *Corrosion (Paper: 00497*, 2000.

[22] M. Nouri and D.R. Clarida, "Interaction of Process Design, Operating Conditions and Corrosion in Amine Systems", *Corrosion Conference and Expo (Paper: 07398)*, 2007.

[23] N. Raut, R.M. Chaudhari, and V.S. Naik, "Failure of Amine Regenerating Column of Amine Treatment Unit", *Corrosion Conference and Expo (Paper: 09334)*, 2009.

[24] J. Conti and P. Holtberg, "International Energy Outlook 2011", *Department of Energy, US Energy Information Administration, Washington, DC*, 2011.

[25] National Oceanic and Atmospheric Administration (NOAA), "Trends in Carbon Dioxide", 2013.

[26] D.J. Griggs and M. Noguer, "Climate Change 2001: The Scientific Basis. Contribution of Working Group I to the Third Assessment Report of the Intergovernmental Panel on Climate Change", *Weather*, vol. 57, no. 8, 2002.

[27] S. Pacala and R. Socolow, "Stabilization Wedges: Solving the Climate Problem for the Next 50 Years with Current Technologies", *Science*, vol. 305, no. 5686, pp. 968–972, 2004.

[28] International Energy Agency, "CO_2 Emissions from Fuel Combustion: Highlights", 2013.

[29] B. Metz, *IPCC Special Report on Carbon Dioxide Capture and Storage*, Cambridge University Press, 2005.

[30] National Energy Technology Laboratory, "Carbon Sequestration Atlas of the United States and Canada: Third Edition (Atlas III)", 2013.

[31] H. Herzog, "What Future for Carbon Capture and Sequestration?", *Environmental Science and Technology*, vol. 35, no. 7, pp. 148, 2001.

[32] D. Aaron and C. Tsouris, "Separation of Carbon Dioxide (CO_2) from Flue Gas: A Review", *Separation Science and Technology*, vol. 40, no. 1, pp. 321, 2005.

[33] S.S. Warudkar, K.R. Cox, M.S. Wong, and G.J Hirasaki, "Influence of Stripper Operating Parameters on the Performance of Amine Absorption Systems for Post-combustion Carbon Capture: Part I. High Pressure Strippers (In Press)", *International Journal of Greenhouse Gas Control*, 2013.

[34] S.S. Warudkar, K.R. Cox, M.S. Wong, and G.J Hirasaki, "Influence of Stripper Operating Parameters on the Performance of Amine Absorption Systems for Post-combustion Carbon Capture: Part II. Vacuum Strippers (In Press)", *International Journal of Greenhouse Gas Control*, 2013.

[35] S.S. Warudkar, K.R. Cox, M.S. Wong, G.J Hirasaki, and J.C. Forsythe, "Provisional patent: Improved Absorbents for Carbon Dioxide Separation", 2012.

[36] United Nations, "Millenium Development Goals Indicators: Global Carbon Dioxide Emissions", 2013.

[37] N. Shakhova, I. Semiletov, A. Salyuk, and D. Kosmach, "Anomalies of Methane in the Atmosphere over the East Siberian Shelf: Is there any sign of Methane Leakage from Shallow Shelf Hydrates?", in *Geophysical Research Abstracts*, 2008, vol. 10, p. A01526.

[38] A. Chakma, A.K. Mehrotra, and B. Nielsen, "Comparison of Chemical Solvents for Mitigating Carbon Dioxide (CO_2) Emissions from Coal-fired Power Plants", *Heat Recovery Systems and CHP*, vol. 15, no. 2, pp. 231, 1995.

[39] C. Alie, L. Backham, E. Croiset, and P.L. Douglas, "Simulation of Carbon Dioxide (CO_2) Capture using MEA Scrubbing: A Flowsheet Decomposition method", *Energy Conversion and Management*, vol. 46, no. 3, pp. 475, 2005.

[40] J.P. Ciferno, P. DiPietro, and T. Tarka, "An Economic Scoping Study for Carbon Dioxide (CO_2) Capture using Aqueous Ammonia", *US DOE Final report*, 2005.

[41] H. Yang, Z. Xu, M. Fan, R. Gupta, R.B. Slimane, A.E. Bland, and I. Wright, "Progress in Carbon Dioxide Separation and Capture: A Review", *Journal of Environmental Sciences*, vol. 20, no. 1, pp. 14–27, 2008.

[42] E.S. Rubin, C. Chen, and A.B. Rao, "Cost and Performance of Fossil Fuel Power Plants with Carbon Dioxide (CO_2) Capture and Storage", *Energy Policy*, vol. 35, no. 9, pp. 4444–4454, 2007.

[43] Mitsubishi Heavy Industries, "Mitsubishi's Carbon Capture Technology: Ks-1, hindered amine", 2013.

[44] S. Bishnoi and G.T. Rochelle, "Absorption of Carbon Dioxide into Aqueous Piperazine: Reaction Kinetics, Mass Transfer and Solubility", *Chemical Engineering Science*, vol. 55, no. 22, pp. 5531–5543, 2000.

[45] J.T. Cullinane and G.T. Rochelle, "Carbon Dioxide Absorption with Aqueous Potassium Carbonate Promoted by Piperazine", *Chemical Engineering Science*, vol. 59, no. 17, pp. 3619–3630, 2004.

[46] J.T. Cullinane and G.T. Rochelle, "Kinetics of Carbon Dioxide Absorption into Aqueous Potassium Carbonate and Piperazine", *Industrial & Engineering Chemistry Research*, vol. 45, no. 8, pp. 2531–2545, 2006.

[47] S.A. Freeman, R. Dugas, D.H. Van Wagener, T. Nguyen, and G.T. Rochelle, "Carbon Dioxide Capture with Concentrated, Aqueous Piperazine", *International Journal of Greenhouse Gas Control*, vol. 4, no. 2, pp. 119–124, 2010.

[48] R.E. Baltus, R.M. Counce, B.H. Culbertson, H. Luo, D.W. DePaoli, S. Dai, and D.C. Duckworth, "Examination of the Potential of Ionic Liquids for Gas Separations", *Separation Science and Technology*, vol. 40, no. 1-3, pp. 525–541, 2005.

[49] P.G. Jessop, D.J. Heldebrant, X. Li, C.A. Eckert, and C.L. Liotta, "Green Chemistry: Reversible Nonpolar-to-Polar Solvent", *Nature*, vol. 436, no. 7054, pp. 1102–1102, 2005.

[50] F. Karadas, M. Atilhan, and S. Aparicio, "Review on the use of Ionic Liquids (ILs) as Alternative Fluids for CO_2 Capture and Natural gas Sweetening", *Energy & Fuels*, vol. 24, no. 11, pp. 5817–5828, 2010.

[51] B.A. Oyenekan, *Doctoral Dissertation: Modeling of Strippers for Carbon Dioxide Capture by Aqueous Amines*, ProQuest, 2007.

[52] B.A. Oyenekan and G.T. Rochelle, "Energy Performance of Stripper Configurations for Carbon Dioxide (CO_2) Capture by Aqueous Amines", *Industrial & Engineering Chemistry Research*, vol. 45, no. 8, pp. 2457–2464, 2006.

[53] M.S. Jassim and G.T. Rochelle, "Innovative Absorber/Stripper Configurations for Carbon Dioxide (CO_2) Capture by Aqueous Monoethanolamine", *Industrial & Engineering Chemistry Research*, vol. 45, no. 8, pp. 2465–2472, 2006.

[54] V. Darde, K. Thomsen, W.J.M. van Well, and E.H. Stenby, "Chilled Ammonia Process for CO_2 Capture", *Energy Procedia*, vol. 1, no. 1, pp. 1035–1042, 2009.

[55] F. Kozak, A. Petig, E. Morris, R. Rhudy, and D. Thimsen, "Chilled Ammonia Process for CO_2 Capture", *Energy Procedia*, vol. 1, no. 1, pp. 1419–1426, 2009.

[56] K. Okabe, H. Mano, and Y. Fujioka, "Separation and Recovery of Carbon Dioxide by a Membrane Flash Process", *International Journal of Greenhouse Gas Control*, vol. 2, no. 4, pp. 485–491, 2008.

[57] K. Okabe, S. Kodama, H. Mano, and Y. Fujioka, "Separation andRrecovery of Carbon Dioxide by a Membrane Flash Process Utilizing Waste Thermal Energy", *Energy Procedia*, vol. 1, no. 1, pp. 1281–1288, 2009.

[58] E. Chen, *Doctoral Dissertation: Carbon Dioxide Absorption into Piperazine*

promoted Potassium Carbonate using Structured packing, ProQuest, 2007.

[59] P. Jackson and M. Attalla, "Environmental Impacts of Post-combustion Capture–New Insights", *Energy Procedia*, vol. 4, pp. 2277–2284, 2011.

[60] P.M. Mathias, S. Reddy, and J.P. OConnell, "Quantitative Evaluation of the Chilled–Ammonia Process for CO_2 Capture using Thermodynamic Analysis and Process Simulation", *International Journal of Greenhouse Gas Control*, vol. 4, no. 2, pp. 174–179, 2010.

[61] E. Kenig and P. Seferlis, "Modeling Reactive Absorption", *Chemical Engineering Progress (CEP)*, vol. 1, pp. 65–73, 2009.

[62] R. Taylor and R. Krishna, "Modelling Reactive Distillation", *Chemical Engineering Science*, vol. 55, no. 22, pp. 5183–5229, 2000.

[63] E. Alfadala and E. Al-Musleh, "Simulation of an Acid Gas Removal Process Using Methyldiethanolamine; an Equilibrium Approach", in *Proceedings of the 1st Annual Gas Processing Symposium*, 2009, pp. 10–12.

[64] X. Luo, J.N. Knudsen, D. De Montigny, T. Sanpasertparnich, R. Idem, D. Gelowitz, R. Notz, S. Hoch, H. Hasse, E. Lemaire, P. Alix, F.A. Tobiesen, O. Juliussen, M. Köpcke, and H.F. Svendsen, "Comparison and Validation of Simulation Codes against Sixteen Sets of Data from Four Different Pilot Plants", *Energy Procedia*, vol. 1, no. 1, pp. 1249–1256, 2009.

[65] J. Polasek and J. Bullin, "Selecting Amines for Sweetening units.", *Energy Progress.*, vol. 4, no. 3, pp. 146–149, 1984.

[66] K.S. Sajwan, I. Twardowska, T. Punshon, and A.K. Alva, "Coal Combustion Byproducts and Environmental Issues", 2006.

[67] S. Reddy, D. Johnson, and J. Gilmartin, "Fluor's Econamine FG Plus Technology for CO_2 Capture at Coal-fired Power Plants", in *Power Plant Air Pollutant Control Mega Symposium*, 2008, pp. 25–28.

[68] R.H. Perry and D.W. Green, *Perry's Chemical Engineers' Handbook*, McGraw-Hill New York, 2008.

[69] V. Ganapathy, *Steam Plant Calculations Manual, Revised and Expanded*, vol. 87, CRC, 1993.

[70] J. Katzer et al., "The Future of Coal: Options for a Carbon–Constrained World", *Massachusetts Institute of Technology*, 2007.

[71] J.D. Figueroa, T. Fout, S. Plasynski, H. McIlvried, and R.D. Srivastava, "Advances in CO_2 Capture TechnologyThe US Department of Energy's Carbon Sequestration Program", *International Journal of Greenhouse Gas Control*, vol. 2, no. 1, pp. 9–20, 2008.

[72] Y.K. Salkuyeh and M. Mofarahi, "Reduction of CO_2 Capture Plant Energy Requirement by Selecting a Suitable Solvent and Analyzing the Operating Pa-

rameters", *International Journal of Energy Research (Available Online)*, 2012.

[73] M.O. Schach, R. Schneider, H. Schramm, and J.U. Repke, "Techno-economic Analysis of Post-combustion Processes for the Capture of Carbon Dioxide from Power Plant Flue Gas", *Industrial & Engineering Chemistry Research*, vol. 49, no. 5, pp. 2363–2370, 2010.

[74] M.R.M. Abu-Zahra, L.H.J. Schneiders, J.P.M. Niederer, P.H.M. Feron, and G.F. Versteeg, "CO_2 Capture from Power Plants: Part I. A Parametric Study of the Technical Performance based on Monoethanolamine", *International Journal of Greenhouse Gas Control*, vol. 1, no. 1, pp. 37–46, 2007.

[75] J. Klemeš, I. Bulatov, and T. Cockerill, "Techno-economic Modelling and Cost Functions of CO_2 Capture Processes", *Computers & chemical engineering*, vol. 31, no. 5, pp. 445–455, 2007.

[76] A. Cousins, L.T. Wardhaugh, and P.H.M. Feron, "A Survey of Rrocess Flow sheet Modifications for Energy Efficient CO_2 Capture from Flue Gases using Chemical Absorption", *International Journal of Greenhouse Gas Control*, vol. 5, no. 4, pp. 605–619, 2011.

[77] M.S. Peters, K.D. Timmerhaus, and R.E West, *Plant Design and Economics for Chemical Engineers*, vol. 5, McGraw-Hill NY, 2003.

[78] Bryan Research and Engineering, "Promax User Manual", 2013.

[79] J. Wagner, *GPSA Engineering Data Book Revitalization and Maintenance: Water-hydrocarbon Mutual Solubility Data*, Gas Processors Association, 1999.

[80] W.Y. Svrcek and W.D. Monnery, "Design Two-phase Separators within the Right Limits", *Chemical Engineering Progress*, vol. 89, no. 10, pp. 53–60, 1993.

[81] F.S. Manning and R.E. Thompson, *Oilfield Processing of Petroleum: Crude Oil*, vol. 2, Pennwell Corporation, 1995.

[82] M. Souders and G.G. Brown, "Design of Fractionating Columns I. Entrainment and Capacity", *Industrial & Engineering Chemistry*, vol. 26, no. 1, pp. 98–103, 1934.

[83] L. Theodore, *Heat Transfer Applications for the Practicing Engineer*, vol. 4, Wiley, 2011.

[84] R.R Bottoms, "Process for Separating Acidic Gases", Dec. 2 1930, US Patent 1,783,901.

[85] J. Oexmann and A. Kather, "Minimising the Regeneration Heat Duty of Post-combustion CO_2 Capture by Wet Chemical Absorption: The Misguided Focus on Low Heat of Absorption Solvents", *International Journal of Greenhouse Gas Control*, vol. 4, no. 1, pp. 36–43, 2010.

[86] F.Y Jou, F.D. Otto, and A.E. Mather, "Vapor-liquid Equilibrium of Carbon dioxide in Aqueous Mixtures of Monoethanolamine and

Methyldiethanolamine", *Industrial & Engineering Chemistry Research*, vol. 33, no. 8, pp. 2002–2005, 1994.

[87] J.D. Lawson and A.W. Garst, "Gas sweetening data: Equilibrium Solubility of Hydrogen Sulfide and Carbon Dioxide in Aqueous Monoethanolamine and Aqueous Diethanolamine Solutions", *Journal of Chemical and Engineering Data*, vol. 21, no. 1, pp. 20–30, 1976.

[88] M.L. Kennard and A. Meisen, "Solubility of Carbon Dioxide in Aqueous Diethanolamine Solutions at Elevated Temperatures and Pressures", *Journal of Chemical and Engineering Data*, vol. 29, no. 3, pp. 309–312, 1984.

[89] J.L. Martin, F.D. Otto, and A.E. Mather, "Solubility of Hydrogen Sulfide and Carbon Dioxide in a Diglycolamine Solution", *Journal of Chemical and Engineering Data*.

[90] S. Horstmann, P. Mougin, F. Lecomte, K. Fischer, and J. Gmehling, "Phase Equilibrium and Excess Enthalpy Data for the System Methanol + 2, 2'-Diethanolamine + water", *Journal of Chemical & Engineering Data*, vol. 47, no. 6, pp. 1496–1501, 2002.

[91] A. Archane, L. Gicquel, E. Provost, and W. Fürst, "Effect of Methanol Addition on Water–CO_2–Diethanolamine System: Influence on CO_2 Solubility and on Liquid Phase Speciation", *Chemical Engineering Research and Design*, vol. 86, no. 6, pp. 592–599, 2008.

[92] R.L. Kent and B. Eisenberg, "Better Data for Amine Treating", *Hydrocarbon Processing*, vol. 55, no. 2, pp. 87–90, 1976.

[93] K.N. Habchi Tounsi, A. Barreau, E. Le Corre, P. Mougin, and E. Neau, "Measurement of Carbon Dioxide Solubility in a Solution of Diethanolamine Mixed with Methanol", *Industrial & Engineering Chemistry Research*, vol. 44, no. 24, pp. 9239–9243, 2005.

[94] J.I. Lee, F.D. Otto, and A.E. Mather, "Solubility of Carbon Dioxide in Aqueous Diethanolamine Solutions at High Pressures", *Journal of Chemical and Engineering Data*, vol. 17, no. 4, pp. 465–468, 1972.

[95] A. Wakisaka, H. Abdoul-Carime, Y. Yamamoto, and Y. Kiyozumi, "Nonideality of Binary Mixtures Water/ Methanol and Water/Acetonitrile from the Viewpoint of Clustering Structure", *Journal of the Chemical Society, Faraday Transactions*, vol. 94, no. 3, pp. 369–374, 1998.

[96] A.R. Studart, U.T. Gonzenbach, E. Tervoort, and L.J. Gauckler, "Processing Routes to Macroporous Ceramics: A Review", *Journal of the American Ceramic Society*, vol. 89, no. 6, pp. 1771–1789, 2006.

[97] M.V. Twigg and J.T. Richardson, "Theory and Applications of Ceramic Foam Catalysts", *Chemical Engineering Research and Design*, vol. 80, no. 2, pp. 183–189, 2002.

[98] M.H. De Brito, U. Von Stockar, A.M Bangerter, P. Bomio, and M. Laso, "Effective Mass Transfer Area in a Pilot Plant Column Equipped with Structured Packings and with Ceramic Rings", *Industrial & Engineering Chemistry Research*, vol. 33, no. 3, pp. 647–656, 1994.

[99] Data Courtesy of AceChemPack Tower Packing Co Ltd, "Geometric Surface Areas of Common Tower Packing", 2013.

[100] S.L. Sah, *Encyclopaedia of Petroleum Science and Engineering*, vol. 1, Gyan Publishing House, 2010.

[101] C.P. Stemmet, J.N. Jongmans, J. Van der Schaaf, B.F.M. Kuster, and J.C. Schouten, "Hydrodynamics of Gas–Liquid Counter-current Flow in Solid Foam Packings", *Chemical Engineering Science*, vol. 60, no. 22, pp. 6422–6429, 2005.

[102] Sterlitech Corporation, "Chemical Compatibility Chart for General Laboratory Filtration Products (available online)", 2013.

[103] L.K. Wang, J.P. Chen, Y. Hung, and N.K. Shammas, *Membrane and Desalination Technologies*, Humana Press, 2010.

[104] A.L. Cummings, S.W. Waite, and D.K. Nelsen, "Corrosion and Corrosion Enhancers in Amine Systems", in *Brimstone Sulfur Conference. Banff, AB, Canada*, 2005.

[105] R. Haws, "Contaminants in Amine Gas Treating", in *Gas Processors Association Houston Regional Meeting*, 2001, pp. 1–13.

[106] H. Lepaumier, D. Picq, and P.L. Carrette, "New Amines for CO_2 Capture. I. Mechanisms of Amine Degradation in the Presence of CO_2", *Industrial & Engineering Chemistry Research*, vol. 48, no. 20, pp. 9061–9067, 2009.